SEISMIC RESPONSE - FOUNDATIONS IN SOFT SOILS

WA-RD 264.1

Final Technical Report
July 1993

Washington State Department of Transportation

Washington State Transportation Commission
Transit, Research, and Intermodal Planning (TRIP) Division
in cooperation with the U.S. Department of Transportation
Federal Highway Administration

TECHNICAL REPORT STANDARD TITLE PAGE

1. REPORT NO.	2. GOVERNMENT ACCESSION NO.	3. RECIPIENT'S CATALOG NO.
WA-RD 264.1		

4. TITLE AND SUBTITLE	5. REPORT DATE
SEISMIC RESPONSE — FOUNDATIONS IN SOFT SOILS	July 1993
	6. PERFORMING ORGANIZATION CODE
7. AUTHOR(S)	8. PERFORMING ORGANIZATION REPORT NO.
Steven L. Kramer	
9. PERFORMING ORGANIZATION NAME AND ADDRESS	10. WORK UNIT NO.
Washington State Transportation Center (TRAC) University of Washington, JD-10 The University District Building, Suite 535; 1107 N.E. 45th St. Seattle, Washington 98105-4631	11. CONTRACT OR GRANT NO. GC8719, Task 25
12. SPONSORING AGENCY NAME AND ADDRESS	13. TYPE OF REPORT AND PERIOD COVERED
Washington State Department of Transportation Transportation Building, MS 7370 Olympia, Washington 98504-7370	Final technical report
	14. SPONSORING AGENCY CODE

15. SUPPLEMENTARY NOTES

This study was conducted in cooperation with the U.S. Department of Transportation, Federal Highway Administration.

16. ABSTRACT

A geotechnical investigation was performed to develop information needed for an evaluation of the seismic vulnerability of a series of interstate highway bridges that cross a thick peat deposit in Washington. The research focused on estimation of dynamic pile stiffness, characterization of dynamic properties of peat, and prediction of ground motions.

A series of free vibration and forced vibration tests were performed on an 8-in. diameter pipe pile installed in the peat. The results of these tests were used to develop methods for estimation of the dynamic stiffness of other piles. A three-phase laboratory testing program was undertaken to investigate the dynamic properties of the peat. Ground response analyses were performed to investigate the influence of the peat on seismic ground motions.

The results of the analyses indicated that the ground response would be expected to vary along the alignment of the bridges in accordance with the variation in peat thickness. The peat exhibited very low stiffness in the field and laboratory tests, and is not expected to transmit large accelerations, particularly in the central portions of the bridges where it is thick.

The investigation has improved understanding of the dynamic response of peat and its implications with respect to seismic ground motions, but has also revealed the need for further research in this area.

17. KEY WORDS	18. DISTRIBUTION STATEMENT
Piles, seismic responses, peat, dynamic load testing, bender elements.	No restrictions. This document is available to the public through the National Technical Information Service, Springfield, VA 22616

19. SECURITY CLASSIF. (of this report)	20. SECURITY CLASSIF. (of this page)	21. NO. OF PAGES	22. PRICE
None	None	180	

Final Technical Report

Research Project GC 8719, Task 25
Seismic Soft Soils

SEISMIC RESPONSE — FOUNDATIONS IN SOFT SOILS

by

Steven L. Kramer
Associate Professor of Civil Engineering
University of Washington

Washington State Transportation Center (TRAC)
University of Washington, JE-10
The University District Building, Suite 535
1107 N.E. 45th Street
Seattle, Washington 98105-4631

Washington State Department of Transportation
Technical Monitors

E. H. Henley
Bridge Planning Engineer

A. P. Kilian
Chief Geotechnical Engineer

Prepared for

Washington State Transportation Commission
Department of Transportation
and in cooperation with
U.S. Department of Transportation
Federal Highway Administration

July 1993

DISCLAIMER

The contents of this report reflect the views of the authors, who are responsible for the facts and the accuracy of the data presented herein. The contents do not necessarily reflect the official views or policies of the Washington State Transportation Commission, Department of Transportation, or the Federal Highway Administration. This report does not constitute a standard, specification, or regulation.

TABLE OF CONTENTS

LIST OF FIGURES

LIST OF TABLES

INTRODUCTION

The Puget Sound area of Washington State is well known as a seismically active area that is likely to be subjected to both small and possibly very large earthquakes in the near future. The Washington State Department of Transportation (WSDOT) is responsible for a large number of critical bridge structures, some of which may be at risk during a major earthquake. Many of these bridges represent lifelines whose successful performance during and after earthquakes will be critical to rescue, repair, and rehabilitation efforts, as well as to the economic recovery of the surrounding area.

Many bridges cross, and have foundations extending through, deposits of soft to very soft soil. Typical soft clay and silt soils have been known to frequently amplify the effects of earthquake ground shaking while providing little lateral resistance to lateral bridge movement. Examples of damage to bridges and other structures supported on such soils are common following significant earthquakes.

A number of bridges cross the extremely soft soil deposits found in sloughs. Sloughs are generally filled with peat, an organic material in varying stages of decomposition, to some depth. However, virtually no information is available on the seismic response of peat deposits or on the dynamic response of foundations extending through them.

Recently, increasing interest in the dynamic response of highly organic deposits such as peat has developed. The origin of much of this interest stems from the need to evaluate the seismic stability of pile-supported highway bridges crossing substantial peat deposits. The recent failure of the Struve Slough bridge [1] near Watsonville, California, in the 1989 Loma Prieta earthquake illustrated the potential vulnerability of such bridges to earthquake-induced damage. An example of a very similar site is the location shown in Figure 1, where Interstate 90 (I-90) crosses Mercer Slough in south Bellevue, Washington. Mercer Slough is filled with a very soft, thick peat deposit. In the area

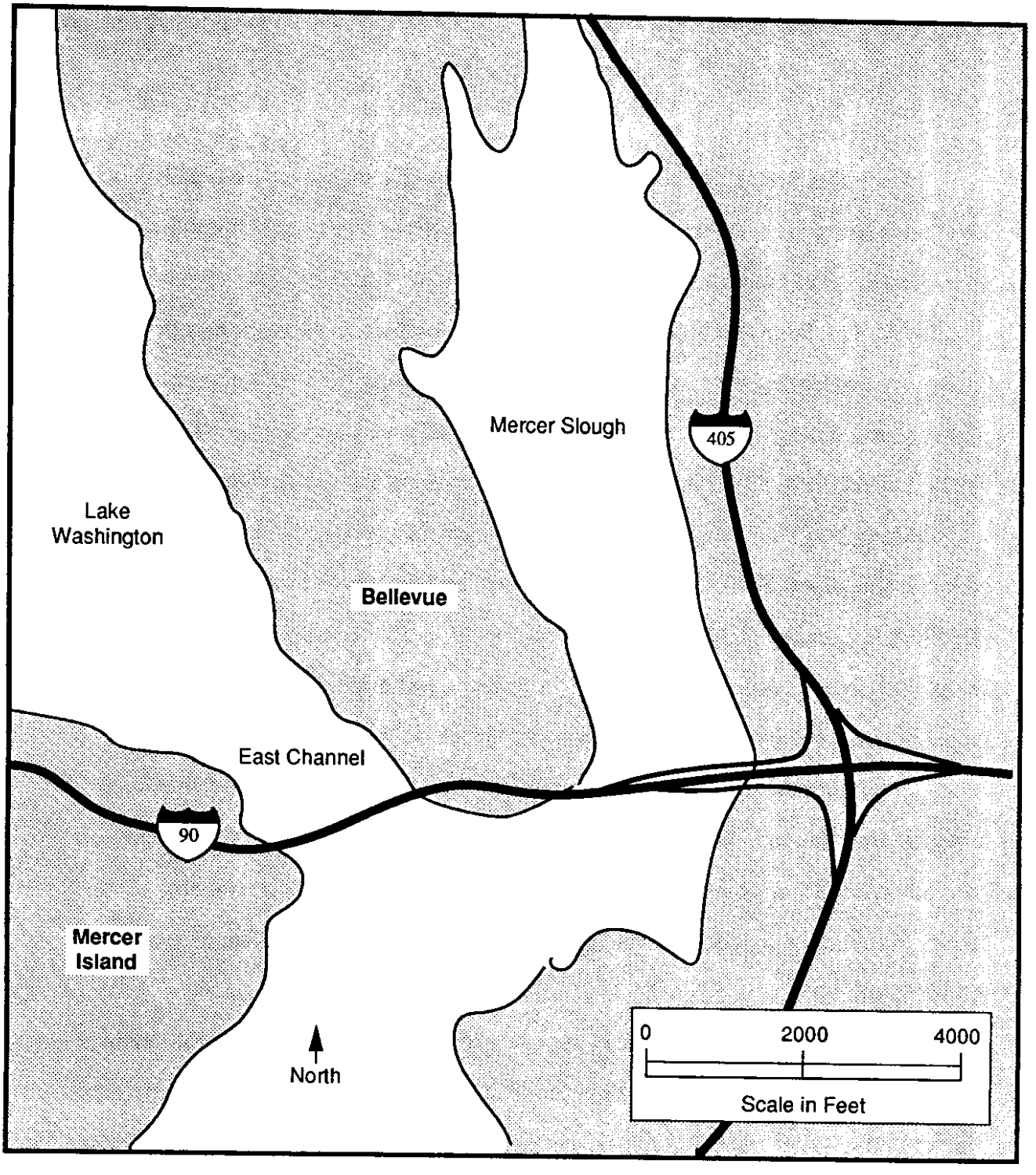

Figure 1. Location of Mercer Slough in Bellevue, Washington

where I-90 crosses Mercer Slough in Bellevue, the soft, peaty soils are known from previous research to provide little resistance to static lateral bridge movement. However, little is currently known about the behavior of such soils during earthquakes. To evaluate the response of the I-90 bridge structures in this area, and to develop seismic rehabilitation alternatives, WSDOT needed to evaluate the seismic response of bridge foundations in the on-site soils.

OBJECTIVES

The objective of this project was to evaluate the seismic behavior of the I-90 bridge foundations in the area where I-90 crosses Mercer Slough for the purpose of providing geotechnical input for a detailed, dynamic structural analysis of the existing bridge structure. As the project progressed, the need for an evaluation of the anticipated seismic ground response of the Mercer Slough site became apparent. The scope of the research project was modified to include this activity as a second main objective.

PREVIOUS RESEARCH

Little research has been performed on the dynamic response of peat or on the response of foundations in or on peat deposits. The only previous work identified in the literature was associated with the foundation investigation for a proposed (but never constructed) highway tunnel in the Union Bay area of Seattle, Washington [2]. The Union Bay site, also located on Lake Washington, but about 6.8 miles northwest of Mercer Slough, consisted of up to 60 feet of peat underlain by up to 80 feet of soft to medium stiff clay. Under the clay was a heavily overconsolidated, dense glacial till. In 1966, water contents in the Union Bay peat ranged from 700 percent to 1,500 percent at the surface with a trend of slightly decreasing water content with increasing depth. Saturated unit weights ranged from 62.6 pcf to 66.0 pcf and averaged 63.7 pcf. Atterberg limits tests showed liquid limits of 700 to 1,000 and plasticity indices of 200 to 600. The

Union Bay and Mercer Slough peats were deposited under very similar conditions, and many of their important geotechnical characteristics are expected to be similar.

The 1967 foundation investigation, conducted under the direction of Stanley D. Wilson, included a number of interesting and innovative laboratory and field experiments. In the laboratory, samples of the Union Bay peat were subjected to repeated load triaxial tests. Loading was apparently applied pneumatically through a solenoid-controlled valve, resulting in a loading pattern that was characterized as a triangular wave with a period of 0.5 seconds. In the field experiments, various dynamic tests were conducted near a set of three seismometers installed in a boring in Union Bay. The upper seismometer was located about 3.3 m below the surface of the 17.4-m thick Union Bay peat deposit. The second seismometer was located at a depth of 18.6 m in the 12.5-m thick silty clay layer immediately below the peat. The lowest seismometer was installed 32 m below the surface in the very dense glacial till beneath the clay. The water level at the location of the seismometers was approximately 1 to 2 m above the surface of the peat. In the dynamic tests, accelerations were measured in response to a number of sources of dynamic loading. These included forced and free lateral vibrations of adjacent piles, driving of a nearby pile into the till, blasting with dynamite at different distances from the seismometers, natural microtremors, a distant nuclear blast, and a magnitude 4.5 earthquake at an epicentral distance of about 25 miles and focal depth of 15 to 20 miles. Each of these loading sources produced motions of different amplitude, frequency content, and duration.

On the basis of the results of these laboratory and field tests, Shannon and Wilson [2] concluded that "the damping factor in the peat is quite high, of the order of 20% or more, particularly in shear. Qualitative tests in the laboratory indicate even higher damping factors ..."

Tsai [3] used the recorded motions from the magnitude 4.5 earthquake in an early study of the influence of local soil conditions on earthquake ground motions. The

recording of the seismometer in the peat deposit, however, was neglected in this approximate analysis. The explanation was that "with the unusually high water content ... the peat media would behave essentially like a viscous fluid and can hardly sustain shear wave motions."

Seed and Idriss [4] analyzed the recorded earthquake motions with an equivalent linear, lumped mass technique. The motion measured in the glacial till was applied as a rigid base motion [5] at the clay/till interface. Shear moduli were obtained from shear wave velocity measurements and repeated loading tests. Damping ratios were estimated with the reasoning that "because of its fibrous and less cohesive characteristics, damping for peat would be expected to be higher than for clay." The damping ratios used in the analyses were approximately three times as large as those used at the time for clay, ranging from approximately 8 percent at a cyclic shear strain of 0.00005 percent to approximately 19 percent at a cyclic shear strain of 0.03 percent. With these damping ratios, reasonable agreement was obtained between the measured accelerations and the accelerations predicted by the rigid base model.

PEAT

The term "peat" has been used both correctly and incorrectly to describe many different materials. The most common classification systems use ash content to identify peat. The ash content is generally obtained by firing an oven-dried sample in a muffle furnace until the soil has been reduced to an inorganic ash. The temperature and duration of firing vary, but ASTM D2974 recommends that a temperature of 550° C be held until the soil has been completely ashed [6]. Generally, soils with ash contents of less than 25 percent are classified as peat [7], though others have suggested that an ash content of 20 percent be used [8].

Peat has long been recognized by geotechnical engineers as a problematic material. It is usually noted for its very low unit weight, very low shear strength, and very high compressibility [9]. Of particular note is the viscous nature of peat behavior,

which gives rise to time- and rate-dependent phenomena such as secondary compression, creep, and stress relaxation. This aspect of peat behavior leads to its frequent characterization as a viscous fluid for problems in which long-term deformation is important.

MERCER SLOUGH PEAT

Mercer Slough is a peat-filled extension of Lake Washington that covers several square miles in Bellevue, Washington. The surface of the slough is flat and heavily overgrown with horsetails, grasses, and small trees. Lake Washington water levels are maintained at a nearly constant level at the Hiram Chittenden Locks in Seattle; consequently, the groundwater level in Mercer Slough is generally within 1 foot of the ground surface.

The thickness of the Mercer Slough peat is variable across the slough, with a maximum thickness of approximately 60 feet along the alignment of Interstate 90, which crosses Mercer Slough by means of four pile-supported bridge structures. While some of the deepest peat has been dated at more than 13,000 years old, most was deposited after Lake Washington was isolated from Puget Sound by the Cedar River alluvial fan some 7,000 years ago [10]. Since that time, the peat appears to have accumulated at an average rate of approximately 0.07 in/year. The peat is underlain by very soft to medium stiff silty clay and occasional loose to dense sand, which is in turn underlain by heavily overconsolidated, dense glacial till. Tertiary bedrock in the area is about 1,000 feet down. A subsurface profile of Mercer Slough along the I-90 alignment is shown in Figure 2.

The Mercer Slough peat is fibrous at shallow depths and becomes less fibrous and more highly decomposed with increasing depth. In recent subsurface investigations, water contents were generally between approximately 500 percent and 1,200 percent, with no apparent trend with depth. A limited number of vane shear tests indicated peak undrained strengths ranging from 15 psf to 160 psf. Piezocone penetration tests showed a

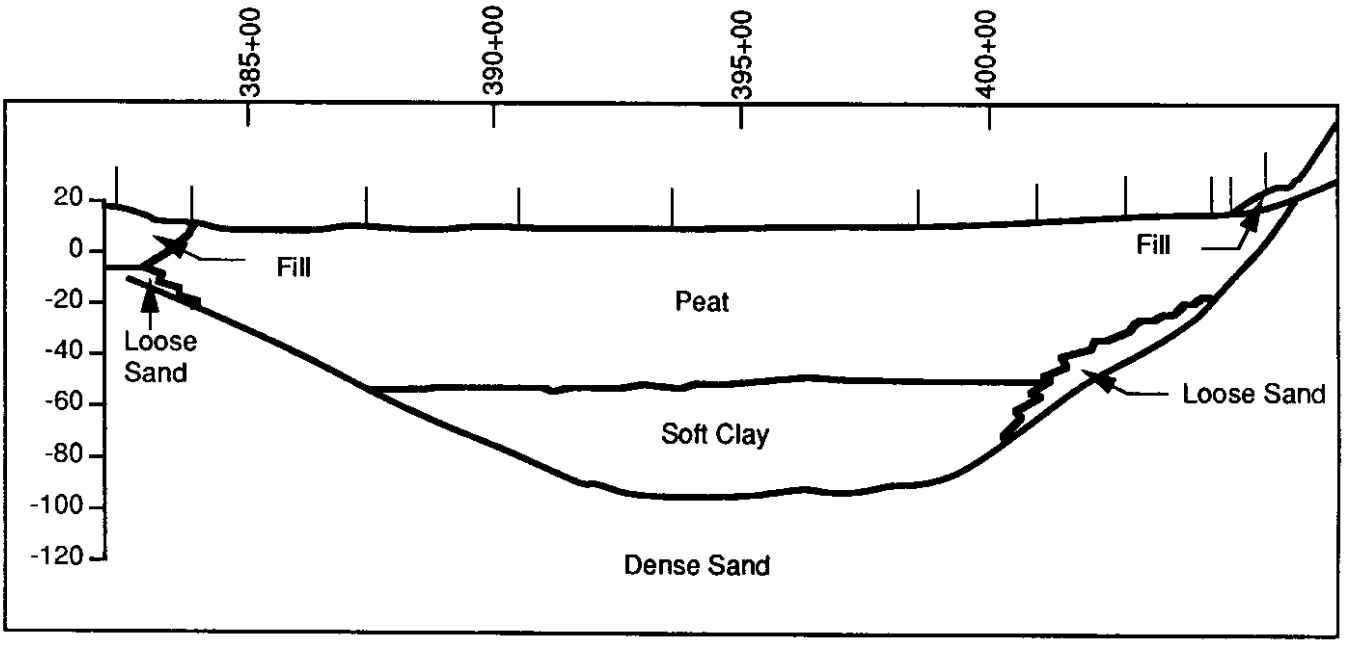

Figure 2. Subsurface Profile through Mercer Slough along I-90 Alignment

uniform tip resistance of approximately 340 psf, with a friction ratio of 1.5 percent to 6.0 percent. Pore pressures during penetration were essentially hydrostatic. However, interpretation of small-scale, in-situ tests such as the vane shear test and cone penetration test has been recognized to be very difficult in peat [11]. A small number of UU triaxial tests produced undrained strengths of 50 psf to 175 psf; very large strains were required for full strength mobilization. Interpretation of the results of a large-scale, lateral pile load test inferred a cohesive strength of approximately 200 psf [12]. Significant time-dependent response, in the form of creep and stress relaxation, was observed during the performance of these tests.

The existing bridges across Mercer Slough are supported on vertical piles driven to depths sufficient to resist design loads of 20 to 70 tons each. In general, these piles do not extend far beneath the bottom of the peat. Piling consists of timber piles and 14- to 18-inch cast-in-place concrete piles. A distant landslide along Lake Washington Boulevard caused lateral movement of the bridge and, presumably, the pile foundations supporting the bridge. Previous research conducted by the principal investigator [13] indicated that the soils of Mercer Slough offer very little resistance to lateral movement of laterally loaded piles.

RESEARCH APPROACH

DYNAMIC PILE LOADING TESTS

Analysis and prediction of the dynamic response of piles is a complicated problem, even in soil deposits whose dynamic characteristics are well defined. For this reason, dynamic load tests are conducted when possible, and a modest database of such tests now exists for dynamic load tests on piles in clays and sands. However, the results of these tests provide little guidance for predicting the dynamic response of piles in peat. Consequently, a dynamic pile loading test program was undertaken. The dynamic loading tests were conducted under the supervision of Dr. C. B. Crouse of Dames and Moore, Seattle.

An 8-inch diameter pipe pile with a wall thickness of 0.25 in. (0.64 cm) was pushed through the peat and slightly into the underlying medium dense sand at the location shown in Figure 3 during the spring of 1989. Static load tests were conducted on the pile, and another, identical pile was located nearby shortly after installation [13]. The response of the pile to static lateral loading is shown in Figure 4. This response was similar to that exhibited by the other pile in the previous research project. To prepare the pile for the forced-harmonic load tests that were conducted in September 1990, a steel plate was welded to the top of the pile to serve as the mounting platform for an eccentric mass shaker. The eccentric mass shaker consisted of two aluminum buckets, which rotated about a common axis at the same speed but in opposite directions. The speed of the buckets could be varied to change the frequency of loading, and lead weights could be added to the buckets to increase the amplitude of loading at a given frequency. A photograph of the eccentric mass shaker is shown in Figure 5. Four triangular steel plates were welded to connect the platform to the pile in order to increase the stiffness of the pile/shaker connection. The assembly is shown in Figure 6; its total above-ground

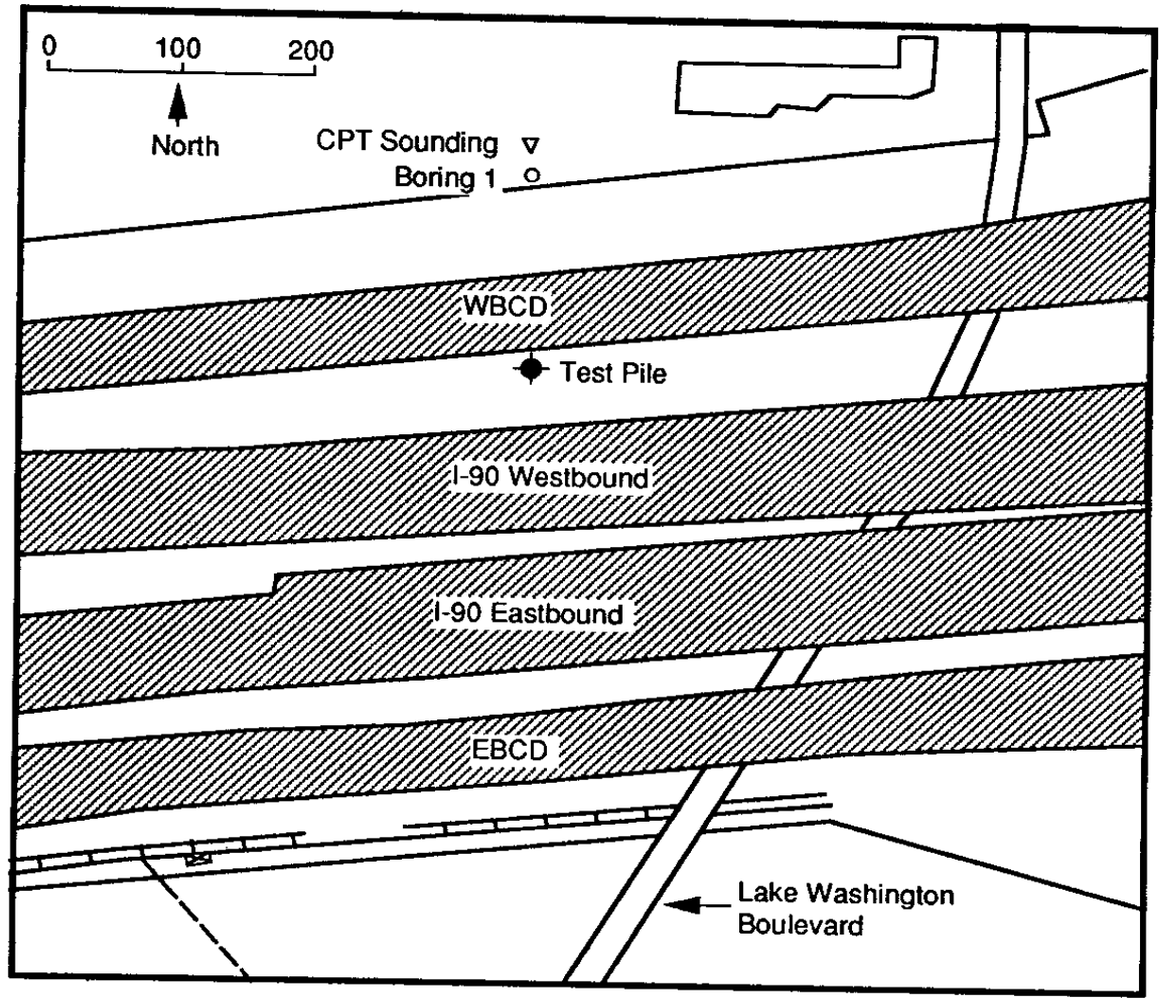

Figure 3. Location of Test Pile, Boring 1 and CPT Sounding

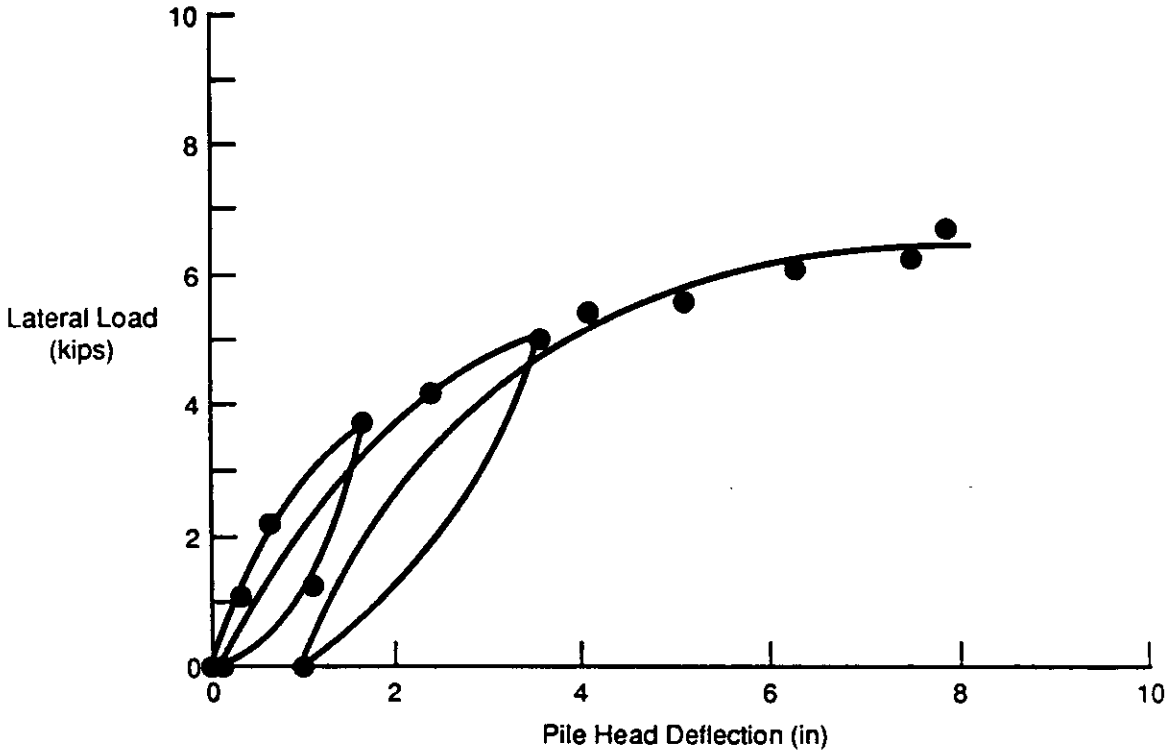

Figure 4. Load Deflection Curve for Previous Static Load Test on Test Pile

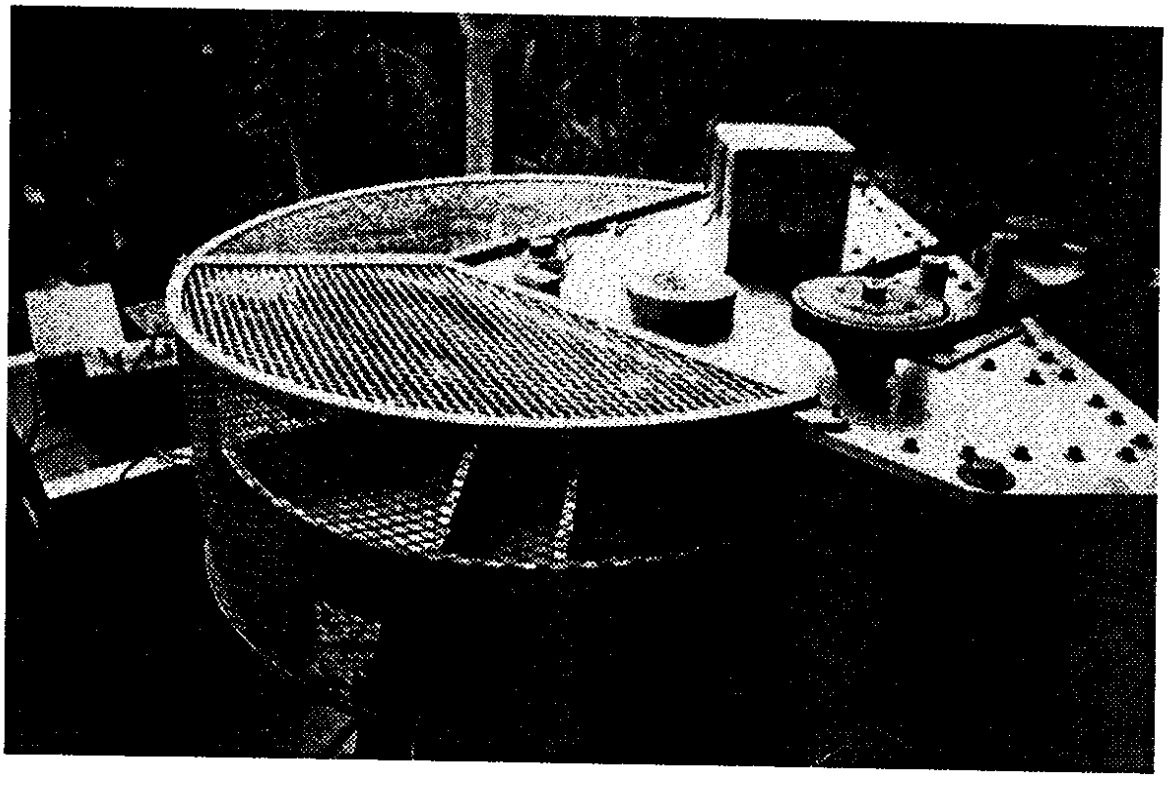

Figure 5. Eccentric Mass Shaker Used in Forced Vibration Tests

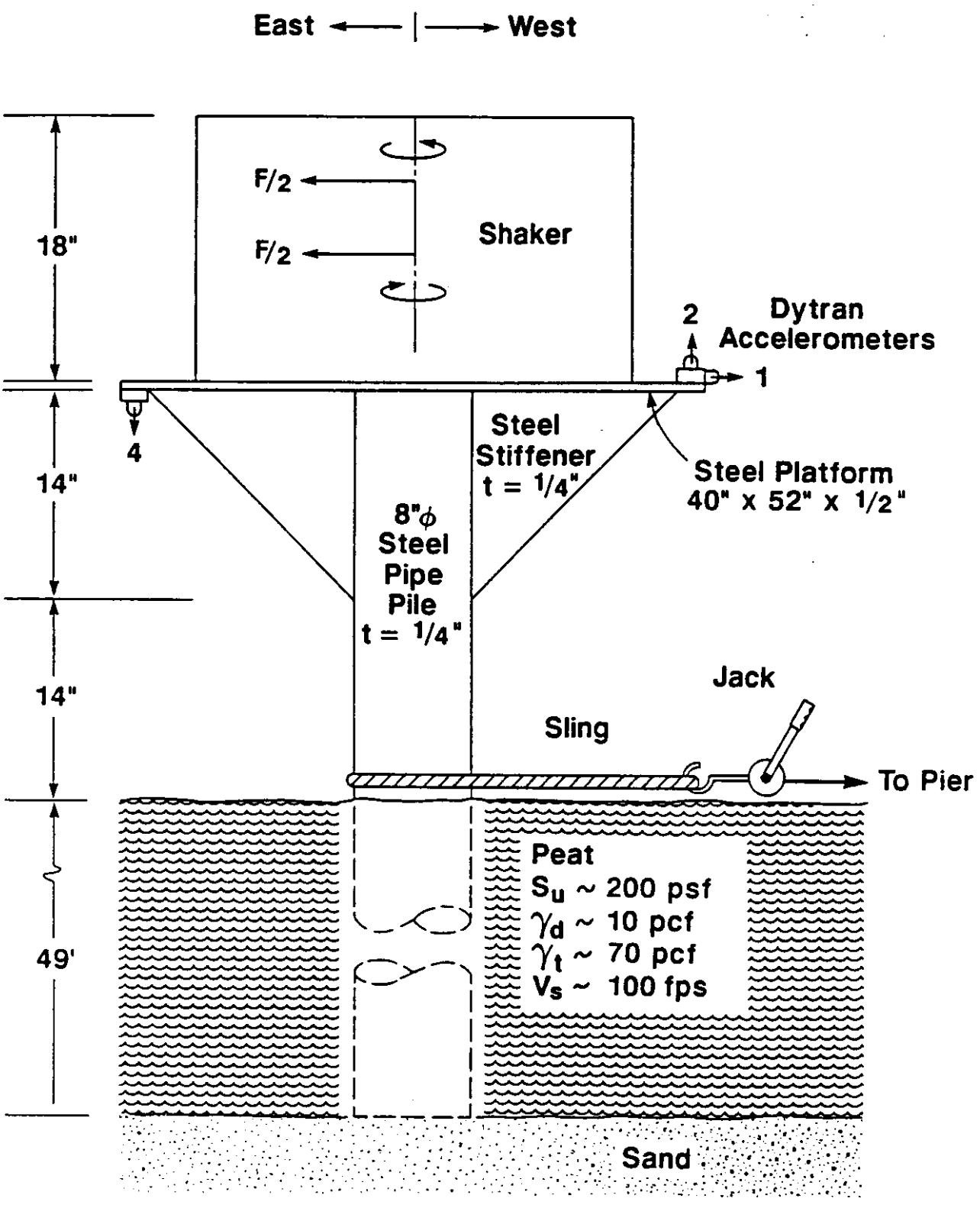

Figure 6. Schematic Illustration of Shaker Platform and Shaker Configuration

weight was estimated to be 902 lb. (4.01 kN) with no weights in the buckets or on the platform.

During the period of September 11-13, 1990, a series of dynamic tests were performed. The tests included impact tests, free vibration tests, and forced vibration tests. In the impact tests, the pile was struck lightly with a hammer. The free vibration tests involved quickly releasing the pile from some imposed, initial lateral displacement. The forced vibration tests were performed with the eccentric mass shaker and were conducted in two directions. In one set of tests, the dynamic load was applied in a direction parallel to that in which loads were applied during the previous static load tests and the free vibration tests, i.e., in the direction of a line passing through the centers of the pile and nearby bridge pier. In the other tests, the dynamic load was applied in the perpendicular direction.

Accelerations of the mounting platform during the impact, free vibration, and forced-vibration tests were measured in the horizontal and vertical directions with Dytran accelerometers that were fixed to the platform, as shown in Figure 6. Another accelerometer (Kinemetrics FBA-11) was placed next to the horizontal Dytran accelerometer for redundancy. Dytran and Kinemetrics power supply units were used to drive the respective accelerometers.

During all tests, voltage signals from the accelerometers were processed with a Dytran 4126 Amplifier and Krohn-Hite Model 3750 band pass filter. The processed signals passed through an A/D converter and were recorded at 200 samples/sec for the free vibration and 2,000 samples/sec for the forced vibration tests on a Compaq portable computer equipped with an RC Electronics Computerscope board and software. Power to this recording system was provided by a Honda EM2200 generator.

Impact Tests

To evaluate the low strain stiffness of the pile/soil system, a series of low amplitude impact tests were performed at various intervals during the test program.

While an impact test is not, strictly speaking, a free vibration test, the duration of loading was so short that the measured response was dominated by the free vibration characteristics of the pile. For this reason, the results of the impact tests will be combined with those of the free vibration tests in subsequent discussions.

Free Vibration Tests

The loading equipment for the quick-release, free vibration tests consisted of two rope slings and a come-along jack. The slings were tied around the pile and the nearby bridge pier just above ground level. The ends of the slings were attached to each end of the jack. The jack was operated manually and was used to apply a lateral force, producing a measured initial offset of the platform. The jack was then quickly released (by hand), thereby inducing free vibrations in the pile assembly.

Seven quick-release tests were performed during the first day, and six tests were performed at the end of the third day. Since considerable nonlinearity of pile resistance was observed in the previous static lateral load tests, the quick release tests were performed at several initial displacements of the pile-assembly to observe possible nonlinear or strain-rate effects. Quick-release tests were also performed with different weights in the eccentric mass shaker buckets.

Forced Vibration Tests

The loading equipment for the forced vibration tests was supplied under subcontract by the California Institute of Technology and consisted of (1) a Kinemetrics Vibration Generator or eccentric mass shaker (Serial No. 102), (2) a Kinemetrics Generator System and frequency control unit (Model VG-1), (3) a Kinemetrics VG-1 Applied Force Monitor, (4) a Monsanto frequency-time counter (Model 100A), and (5) an Onon K5000 generator, which powered the shaker.

The forced-harmonic vibration tests began during the second day of the test program with several trial tests. These tests were followed by tests at 2.0 and 2.5 Hz in which the applied loads were in the parallel direction. During the morning of the third

day, these two harmonic tests were repeated in the perpendicular, horizontal direction. These tests were followed by a frequency sweep test in the perpendicular direction in which the induced accelerations were measured at 18 different frequencies between 1.8 and 2.9 Hz.

These harmonic shaking tests were conducted with no lead weights in the counter rotating buckets. On the basis of the mass of the empty buckets, the shaker forces generated during the tests were $F = 53.0\ f^2$, where F is the force in lbs and f is the frequency of loading in Hz. After these tests had been completed, several more were attempted at frequencies of 1.0 and 1.5 Hz with lead weights in the buckets. The amount of weight added was such that the applied dynamic forces at these lower frequencies were approximately equal to the dynamic forces generated at 2.0 and 2.5 Hz with no weights in the buckets.

DYNAMIC PEAT PROPERTIES TESTING

To evaluate the anticipated ground response at Mercer Slough during a design-level earthquake, a program of field and laboratory testing was undertaken. This testing program was not anticipated in the original research proposal and represented a significant extension of the scope of the research.

Field Testing

To estimate the low-strain stiffness of the peat materials, a seismic cone sounding was performed near the edge of a parking lot fill, at the location shown in Figure 3. The seismic cone work was conducted by ConeTec of Burnaby, British Columbia, on September 8, 1990. The seismic cone sounding involved advancing the cone penetrometer at the standard rate of 2 cm/sec. The cone penetration log is shown in Figure 7. The boundary between the bottom of the parking lot fill and the underlying peat is clearly shown in the figure by the dramatic reduction of tip resistance and sleeve friction, and the simultaneous increase in friction ratio, observed at a depth of approximately 19.7 feet.

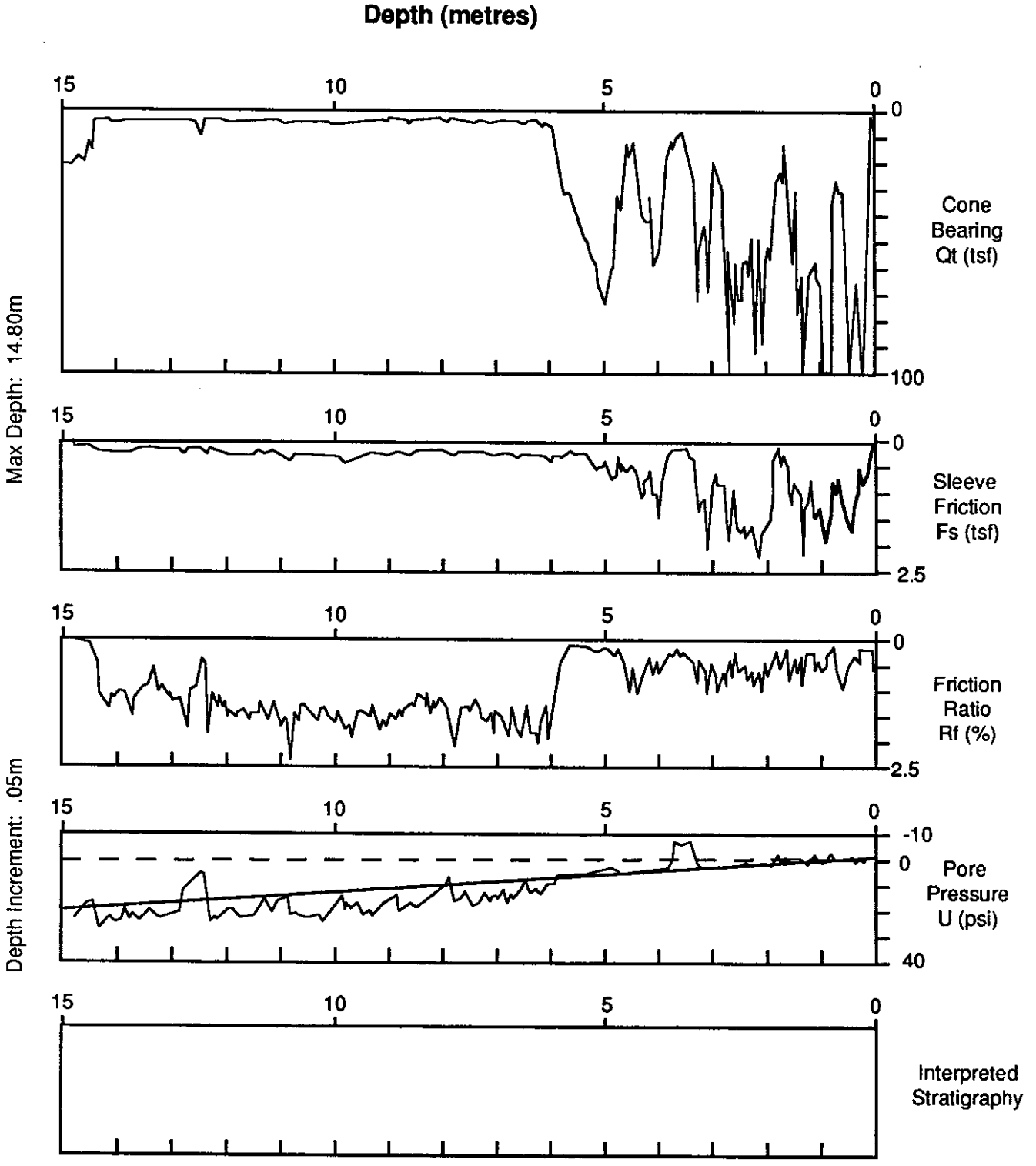

Figure 7. Cone Penetration Sounding

At 1-meter (3.28-ft) intervals, penetration of the cone was suspended to perform a seismic downhole shear wave velocity test. A shear wave was generated at the ground surface when the end of a horizontal reaction beam was struck with an instrumented hammer. The impact of the hammer on the reaction beam triggered a data acquisition system, which recorded the response of an accelerometer located about 12 inches above the tip of the cone. The process was repeated by striking the other end of the reaction beam to generate a shear wave of opposite polarity. A plot of typical results, shown in the form of accelerometer output for each of the opposite polarity waves at a given depth, is presented in Figure 8. Arrival times were interpreted from the direct arrival, first cross-over, and second cross-over arrivals. The difference in arrival times at adjacent test depths was used to determine the shear wave velocity for each depth interval. Shear wave velocity profiles based on direct arrival, first cross-over, and second cross-over are shown in Figures 9, 10, and 11, respectively. The velocities from each method of interpretation were consistent and clearly showed that the shear wave velocity of the peat was much lower than that of the overlying fill. The shear wave velocity of the peat appeared to be fairly uniform with depth, with an average value of approximately 100 ft/sec.

Laboratory Testing

A series of dynamic laboratory tests was performed to develop a preliminary estimate of the dynamic properties of the peat. The tests were conducted on undisturbed samples obtained by WSDOT Materials Laboratory personnel.

Testing of peats is a difficult task. By virtue of their fibrous nature and low strength and stiffness, sample preparation is difficult. Many of the Mercer Slough test specimens were barely able to stand under their own weight. The acts of cutting and trimming, mounting, membrane installation, cell assembly, and diameter measurement were difficult to accomplish without inducing at least some sample disturbance. While

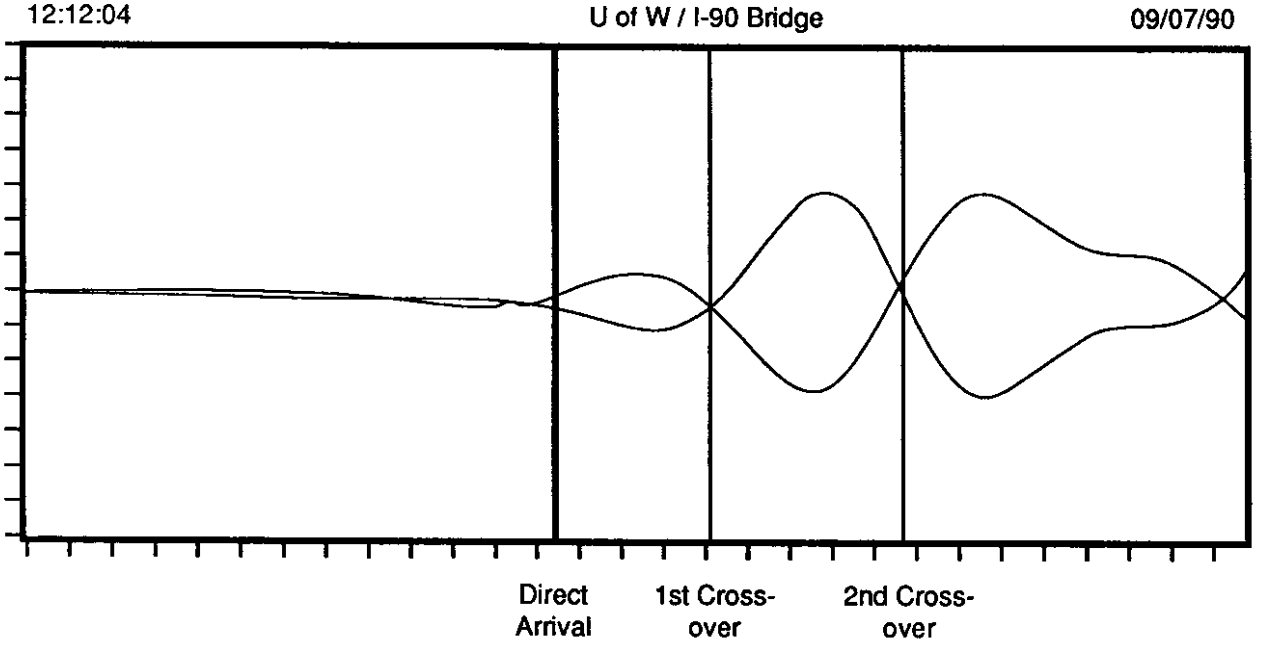

Figure 8. Typical Seismic Cone Acceleration Time Histories for Waves of Opposite Polarity. Times of direct arrival, 1st crossover and 2nd crossover are indicated.

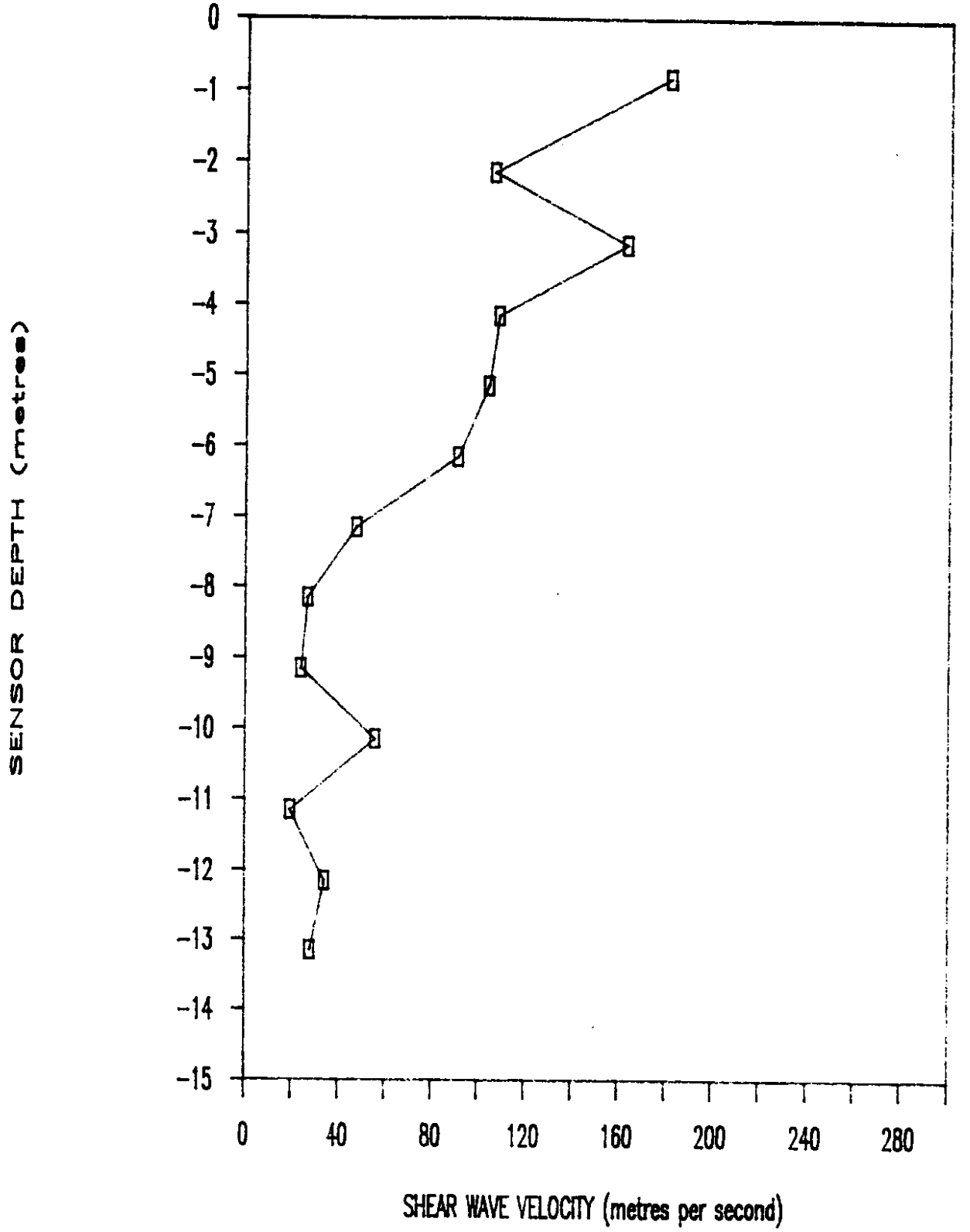

Figure 9. Shear Wave Velocity Profile Based on Direct Arrival Times

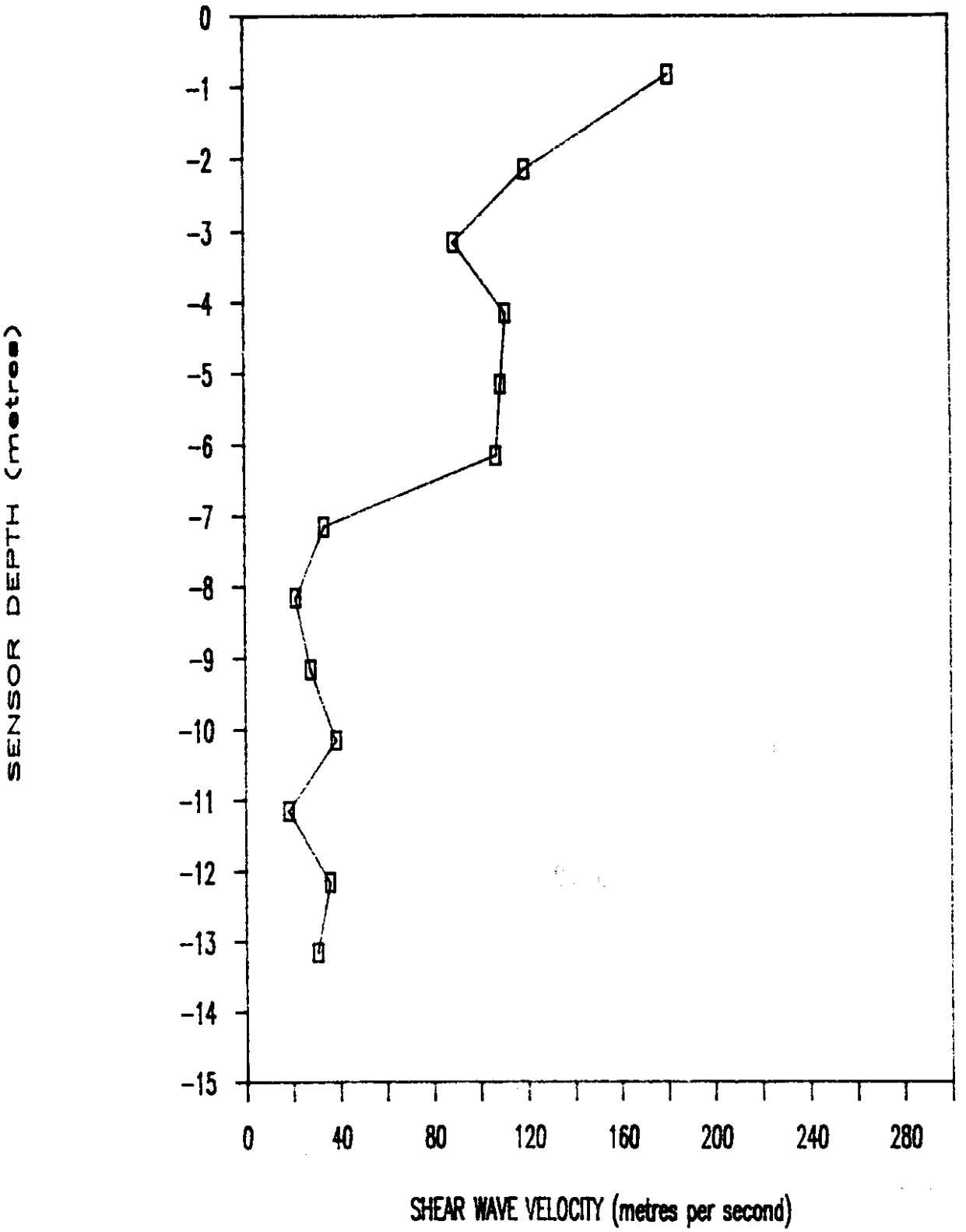

Figure 10. Shear Wave Velocity Profile Based on 1st Crossover Times

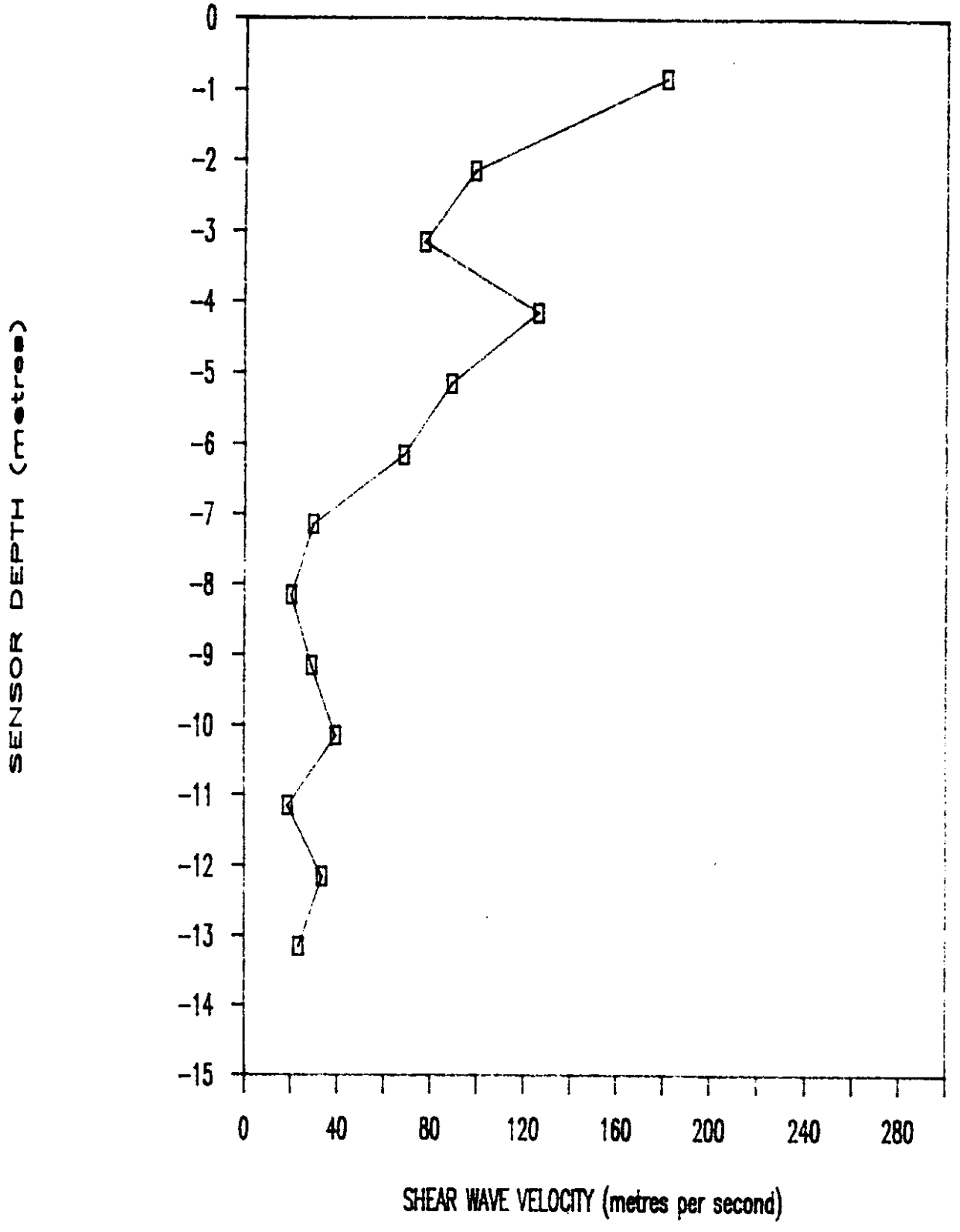

Figure 11. Shear Wave Velocity Profile Based on 2nd Crossover Times

all possible care was taken to minimize sample disturbance, some disturbance was inevitable, and the test results should be interpreted with this in mind.

Additional complications in the cyclic triaxial testing resulted from the peat's very low strength and stiffness. Because peat stiffness is so low, the forces resisting specimen deformation are very small. These difficulties are most pronounced at the low cyclic strain levels that are so important for proper characterization of dynamic soil behavior. To achieve sufficient resolution of piston load, the acquisition and use of a very sensitive load cell was required. To measure very small strains, a low-range LVDT was acquired and used. Finally, the development and fabrication of an entirely new cyclic loading system and piezoelectric bander element system was required.

Test Specimens

Undisturbed Shelby tube samples were obtained at two locations at two times. The first set of samples were obtained from Boring 1, located near the edge of the parking lot fill, as shown in Figure 3, on August 22, 1990. At this location, the boring encountered approximately 15 feet of fill consisting of loose sand and gravel with wood. The fill was underlain by very soft peat to a depth of 46 feet, and samples were obtained at depths of 15, 20, 25, 30, 40, and 45 feet.

The second set of samples was obtained from Boring 2, located near the center of Mercer Slough. Boring 2 encountered approximately 58 feet of peat, which was underlain by up to 43 feet of soft silty clay. The soft silty clay was underlain by dense sand.

Test Equipment and Procedures

Because the testing procedures and equipment evolved over the duration of the research project, the tests will be described in terms of three testing phases. Each successive phase reflected an incremental modification of the testing equipment and, consequently, the test procedures.

Phase I Tests. The Phase I tests were performed with the standard cyclic triaxial testing system available in the University of Washington Geotechnical Engineering Laboratory. Loading was applied pneumatically with a CKC electro-pneumatic loader [14, 15, 16] with a 4-inch diameter air piston. The CKC loader featured computer-based control and data acquisition and could be programmed to apply harmonic loads at frequencies of up to 1 Hz. Piston loads were measured with an Interface SM-250 load cell, which provided an output voltage of 7.2 mv per 100 lbs. The load cell output was conditioned (amplified and filtered) by a Sensotec SA-BII signal conditioner before being digitized by the interface process control unit connected to the loading system's Radio Shack Model 4 computer. Test data files were saved on floppy disks and converted to MS-DOS format for more convenient processing. Examination of the initial Phase I test results suggested that the peat was exhibiting a frequency-dependent response. To investigate the frequency dependence of the dynamic properties of the peat, the CKC loading system was disconnected from the Radio Shack computer and interface process control unit and connected to an analog function generator and PC-based data acquisition system (Metabyte DAS-16F A/D board and Labtech Notebook data acquisition software). The purpose of this equipment modification was to allow loading to be applied at frequencies greater than 1 Hz. Additional Phase I tests were performed with this loading/data acquisition system configuration.

Phase II Tests. During the latter part of Phase I testing (with the modified loading system) the loading amplitude from the electro-pneumatic transducer driven by the analog function generator was observed to vary at frequencies above about 2 Hz. To allow variation of loading frequency without significant fluctuation in loading amplitude, a new strain-controlled, variable frequency cyclic loading system was developed and fabricated [17]. The new mechanical loading system was used for the Phase II tests.

The mechanical cyclic loading system consisted of a variable speed driving system and a rotation/translation converter. The driving system consisted of a variable

speed electric motor that drove a gear reducer. The gear reducer decreased the rotational speed of the motor and also reduced the torque demand on the motor. The rotation/translation converter was a mechanical crank and crankshaft system that converted the rotational movement of the driving system to a harmonic translational movement of a loading rod. The system is shown schematically in Figure 12 and in a photograph in Figure 13.

The crank was designed so that its eccentricity, and consequently the strain amplitude imposed upon the specimen, could be continuously adjusted from 0 to 1.5 in. Manual eccentricity adjustments involved loosening the two screws on the sliding bar and adjusting its position as desired before tightening the screws. Because the sliding bar was machined to be flush with the outer edge of the crankwheel at zero eccentricity, the eccentricity could be conveniently measured with a micrometer during adjustment. The actual eccentricity could then be more accurately determined with the LVDT connected to the loading piston. The length of the crankshaft was 6.0 in.

In the Phase II tests, frequency sweeps were conducted at various strain levels. Starting at the smallest possible strain level, a hysteresis loop was first obtained at a very low frequency — usually approximately 0.007 Hz. The frequency was then increased by a small amount and another hysteresis loop was obtained. This process was repeated until the frequency had reached a value of at least 10 Hz.

Phase III Tests. The Phase II tests were useful for evaluating frequency dependent dynamic soil properties at shear strain levels above approximately 0.05 percent. However, to characterize the dynamic soil properties at lower strain levels, three additional modifications were made to the testing equipment.

1. An Interface SM-25 load cell, ten times more sensitive than the previously used SM-250, was installed in the system.

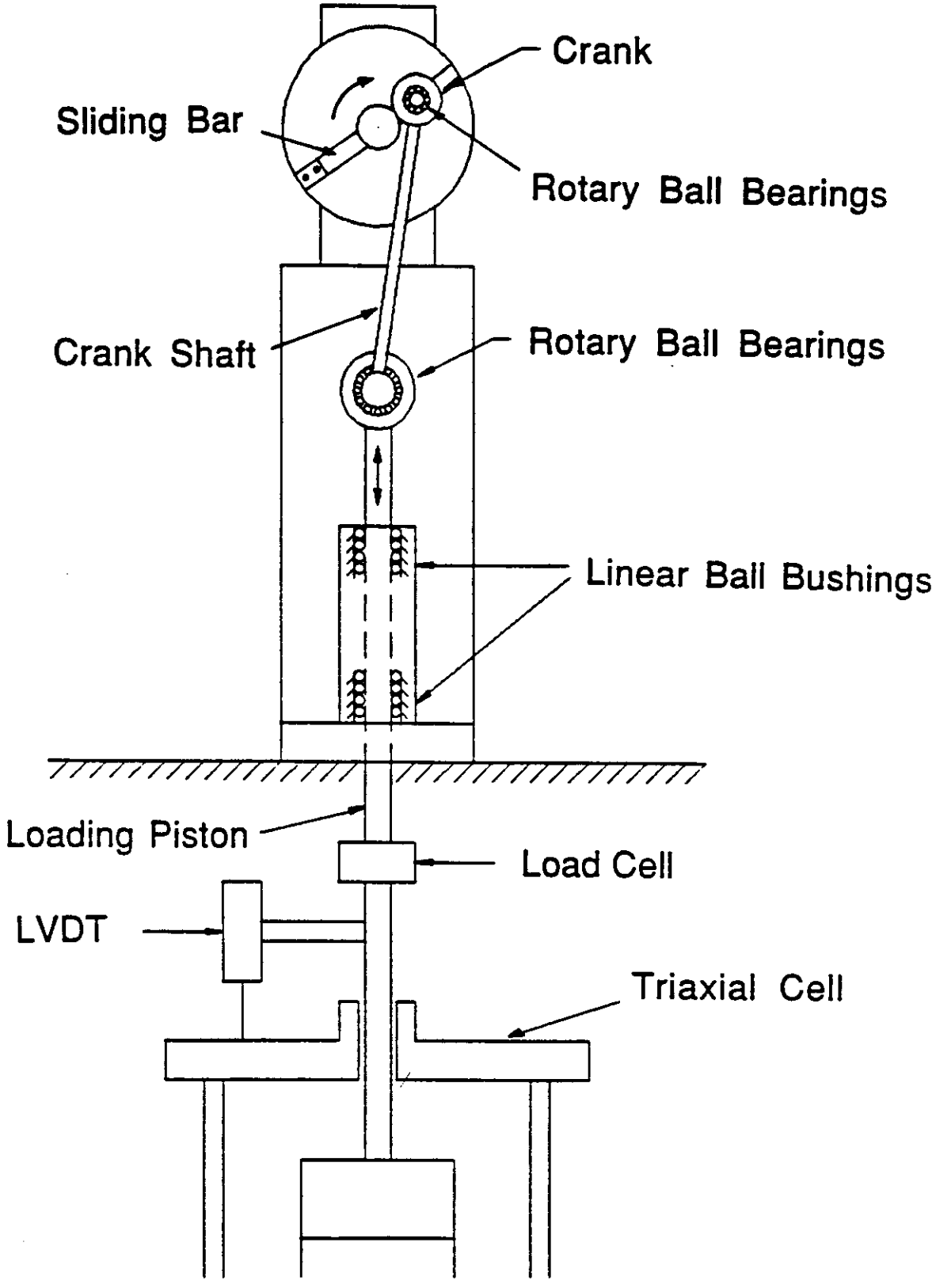

Figure 12. Schematic Illustration of Rotation/Translation Converter

Figure 13. Rotation/Translation Converter

2. To produce lower strain amplitudes, a soft cantilever spring was developed and inserted between the loading rod of the strain-controlled loader and the triaxial cell loading piston.

3. To determine the stiffness of the peat at very low strain levels, a piezoelectric bender element system was developed and installed in the system.

The use of piezoelectric bender elements was introduced into soil dynamics testing in 1975 by Shirley and Anderson [18]. Since that time, bender elements have gained acceptance as a valuable tool for measuring shear wave velocity in laboratory samples. Piezoelectric bender elements are electromechanical transducers; i.e., they are capable of transforming electrical energy to mechanical energy and vice versa. They are typically formed by bonding two piezoceramic plates together, either with opposite polarity and series electrical connection for use as a receiver or with identical polarity and parallel electrical connection for use as a transmitter. When voltage is applied to a transmitting bender element, one of the piezoceramic plates lengthens while the other shortens, thus producing bending deformation, as shown in Figure 14. When a receiving element is deformed, as by the passage of a stress wave, one plate is placed in compression and the other in tension, each producing output voltage of the same polarity.

Bender elements have been used in different configurations for soil dynamics testing. In most cases, the bender elements are configured so that they protrude into the test specimen by some short distance. Dyvik and Madshus [19] installed bender elements in the top and bottom platens of a resonant column apparatus to investigate correlations between the values of G_{max} inferred from shear wave velocities that were measured by the bender elements and those measured by the resonant column test. Excellent agreement was obtained in their tests. Thomann and Hryciw [20] performed similar tests on two cohesionless soils and found that the shear wave velocity measured by the bender

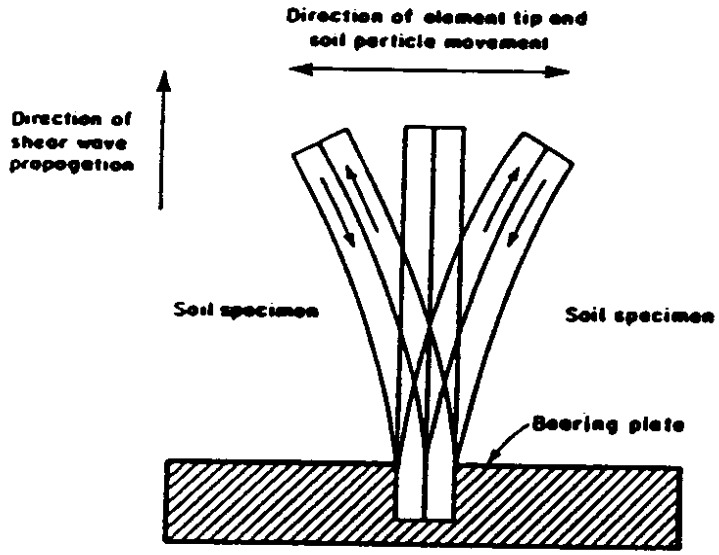

Figure 14. Operation of Transmitting Piezoelectric

elements was slightly greater than that inferred from the resonant column test. The difference was attributed to the lower strain level induced by the bender elements.

GROUND MOTION EVALUATION

To estimate the level of shaking at the surface of the Mercer Slough peat deposit, a series of one-dimensional ground response analyses were performed. These analyses were not anticipated in the original research proposal and represented an extension of the scope of the research. The ground response analyses produced time histories of ground surface acceleration and elastic response spectra for use in the dynamic structural analyses performed in a parallel investigation by Professor David McLean of Washington State University.

Analytical Method

The ground response analyses were performed with one-dimensional wave propagation analysis techniques. Though the soft soils in Mercer Slough varied in thickness, the variation appeared, from available subsurface information, to be fairly gradual with respect to horizontal distance. Consequently, the one-dimensional analyses should have provided a reasonable estimate of ground motion amplitudes.

Ground response analyses were performed with the complex response analysis program SHAKE, developed at the University of California at Berkeley [21]. SHAKE has been commonly used for one-dimensional ground response analysis for the past 20 years. In the complex response method implemented in SHAKE, the soil is represented as a system of horizontally layered, linear, visco-elastic materials. The base motion is transformed to the frequency domain, where the equations of motion for each layer are solved, and the result is transformed back to the time domain. To work in the frequency domain, the soil layers must be assumed to be linear. The effects of soil nonlinearity are approximated by iterating toward strain-compatible shear moduli and damping ratios for each soil layer. Though these equivalent linear properties are clearly an approximation of

actual soil behavior, they have been shown to represent the actual behavior with reasonable accuracy.

Soil Profiles

The subsurface soil conditions varied significantly across Mercer Slough. The thickness of the peat varied, as shown in Figure 2, from zero at the margins of the slough to over 60 feet near the center. Near the east end of the slough, the peat was underlain by loose to dense sand. In the central portion of the slough the peat was underlain by up to 40 feet of soft clay. In the western portion of the slough, dense sands were encountered beneath the peat. For purposes of ground response analysis, the subsurface materials were divided into five units: fill, peat, soft clay, loose sand, and dense sand.

To characterize the range of ground motions that could be produced at the surface of Mercer Slough, 11 different soil profiles were investigated. The locations of the various soil profiles are shown in Figure 15. The thicknesses (in feet) of the various materials in each profile are indicated in Table 1 below:

Table 1. Soil Profiles Used in Ground Response Analysis

Layer	A	B	C	D	E	F	G	H	I	J	K
Fill	8	0	0	0	0	0	0	0	0	23	0
Peat	11	30	44	60	60	60	60	60	32	0	25
Soft Clay	0	0	0	0	40	43	26	0	0	0	0
Loose Sand	0	0	11	13	0	0	0	0	0	0	0
Dense Sand	981	970	945	927	900	897	914	940	968	977	975

As indicated by the total thicknesses of each soil profile, the depth to bedrock was assumed to be 1,000 feet [22].

Material Properties

Because of the time requirements for providing ground motion information for the dynamic structural analyses that were being conducted in parallel with this investigation by Dr. David McLean of Washington State University, an initial series of ground

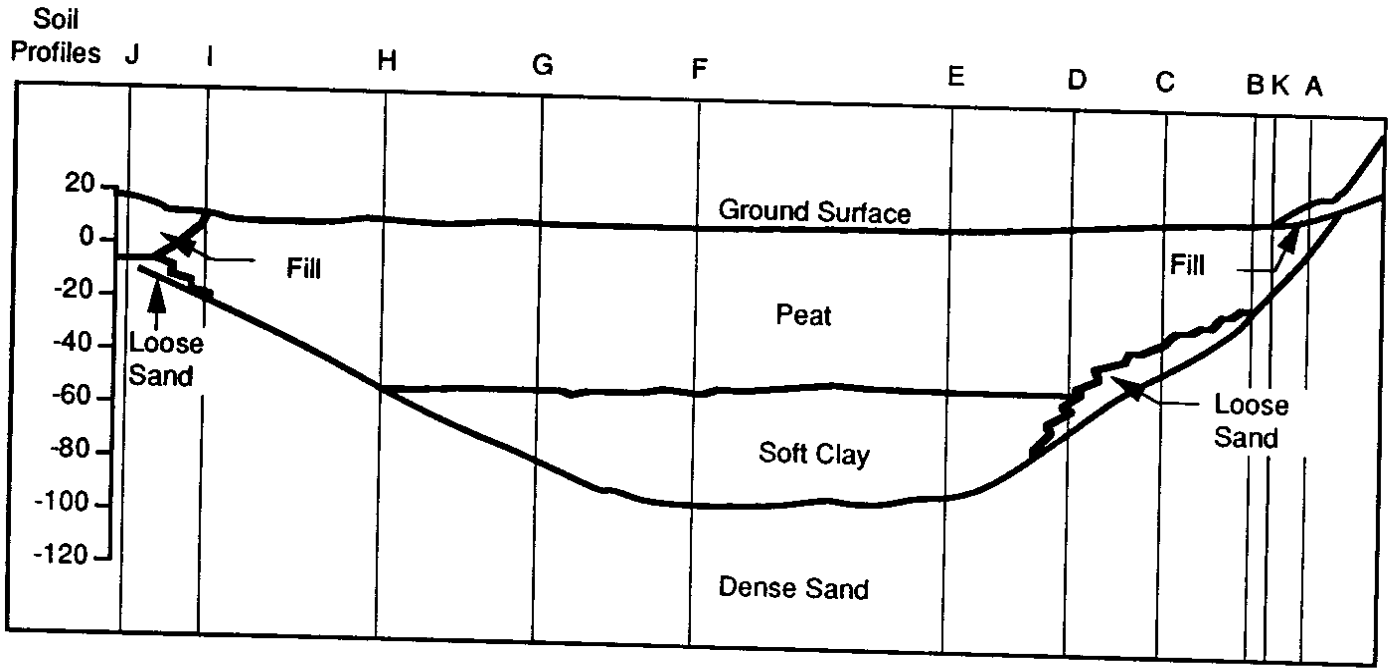

Figure 15. Locations of Soil Profiles

response analyses, hereafter referred to as the Stage 1 analyses, was initially performed. The Stage 1 analyses were conducted with the best estimate of the peat properties that could be made at the end of the Phase I laboratory testing program. After completion of the Phase III laboratory tests, in which sample-specific shear wave velocities were measured, a series of Stage 2 ground response analyses were performed. These analyses were based on a greatly improved estimate of the dynamic peat properties. The properties of all other materials were the same in both series of analyses.

During Phase I of the laboratory testing program, test results indicated low damping ratios in the peat at frequencies near 1 Hz. Because the conventional formulation of SHAKE assumes frequency independence of all soil properties, the SHAKE program was modified to allow representation of the effects of frequency dependent dynamic soil properties in the Stage 1 analyses. The dynamic properties of the other materials at the site were evaluated with information from previous subsurface investigations [23, 24, 25].

The fill materials were generally described as very loose to medium dense silty sands with variable amounts of gravel, wood, and concrete debris. A moist unit weight of 100 pcf and K_{2max} value of 52 was assumed for the fill materials. The modulus degradation curve was that recommended for sands by Seed and Idriss [26].

The properties assigned to the peat were those available at the end of the Phase I laboratory testing program. The maximum shear modulus was assumed to be 21,120 psf, based on an average shear wave velocity of 100 ft/sec and a saturated unit weight of 69 pcf. The modulus degradation curve was as indicated below:

Effective Shear Strain (%)	0.0001	0.001	0.00316	0.01	0.0316	0.1	0.316	1.0	3.16	10
Shear Modulus (ksf)	21.2	21.12	21.12	21.12	20.91	20.7	17.3	13.7	7.4	5.0

This modulus degradation curve was based on the general shape of the plasticity-dependent modulus degradation curves of Vucetic and Dobry [27], extrapolated to a plasticity index greater than 200. While measurement of the plasticity index of peats is difficult, previous tests on a similar peat [2] and several tests on the Mercer Slough peat indicated plasticity indices in the range of 200 to 600. The damping ratio of the peat was assumed to be frequency dependent, with low values in the vicinity of 1 Hz. Note that subsequent testing revealed the effect of frequency to be less important than was assumed in these analyses; in particular, the actual damping ratios at frequencies near 1 Hz were higher than originally indicated.

The soft clay that underlay the peat in the central portion of the Mercer Slough was determined, from the results of previous subsurface investigations, to have an average saturated unit weight of approximately 107 pcf and an average plasticity index of about 20. With an assumed undrained shear strength of 300 psf, a modulus degradation curve was generated from the normalized curves of Vucetic and Dobry [27].

The loose and dense sands were found, in a limited number of tests, to have saturated unit weights of 129 pcf and 142 pcf, respectively. The modulus degradation behavior, determined in the same manner as for the fill materials, was based on K_{2max} values of 52 and 80 for the loose and dense sands, respectively.

Input Motions

The response of each soil profile was analyzed for three different earthquake input motions. Each input motion was scaled to a peak bedrock acceleration of 0.25 g and a predominant period of 0.36 sec; these values corresponded to the the range of input motion that might be expected from an M = 7.5 earthquake with an epicenter near the site. This level of shaking was determined in consultation with WSDOT personnel and was consistent with the criteria used for other important WSDOT structures in the area.

FINDINGS AND INTERPRETATION

This section describes the results of the various tests and analyses, their interpretation, and their implications for the dynamic structural analyses of the Mercer Slough bridge structures.

PILE LOAD TEST RESULTS

The data reduction and initial interpretation of the dynamic load tests were performed by Dr. C. B. Crouse and his staff under a subcontract between Dames and Moore and the University of Washington. All other activities were conducted under the supervision of the author.

Impact Tests

An example of typical impact test results, expressed in terms of time histories of acceleration and in terms of power spectra, is shown in Figure 16. This impact test was one of several conducted prior to the performance of any quick-release or forced vibration tests; hence the response corresponds to that produced by the low-strain stiffness of the undisturbed soil. For the test shown in Figure 16 (PILE 02), the power spectrum indicated a natural frequency of 5.27 Hz and a damping ratio, using the half-power bandwidth method, of 30 percent to 35 percent. This measured damping was primarily geometric (radiation damping) in origin; the material damping represented only a small portion of this amount. In the perpendicular direction, however, the center of gravity of the shaker assembly was offset from the centerline of the pile. Consequently, when an impact load was applied at the centerline in the perpendicular direction, a torsional component of response was induced, producing the response shown in Figure 17 (PILE 04). In still another test, the location and direction of the impact load and the FBA-11 accelerometer were arranged to isolate the torsional response. The natural frequency in torsion, shown in Figure 18, was approximately 9.8 Hz, which confirmed that the second, or higher, frequency peak in the power spectrum of Figure 17

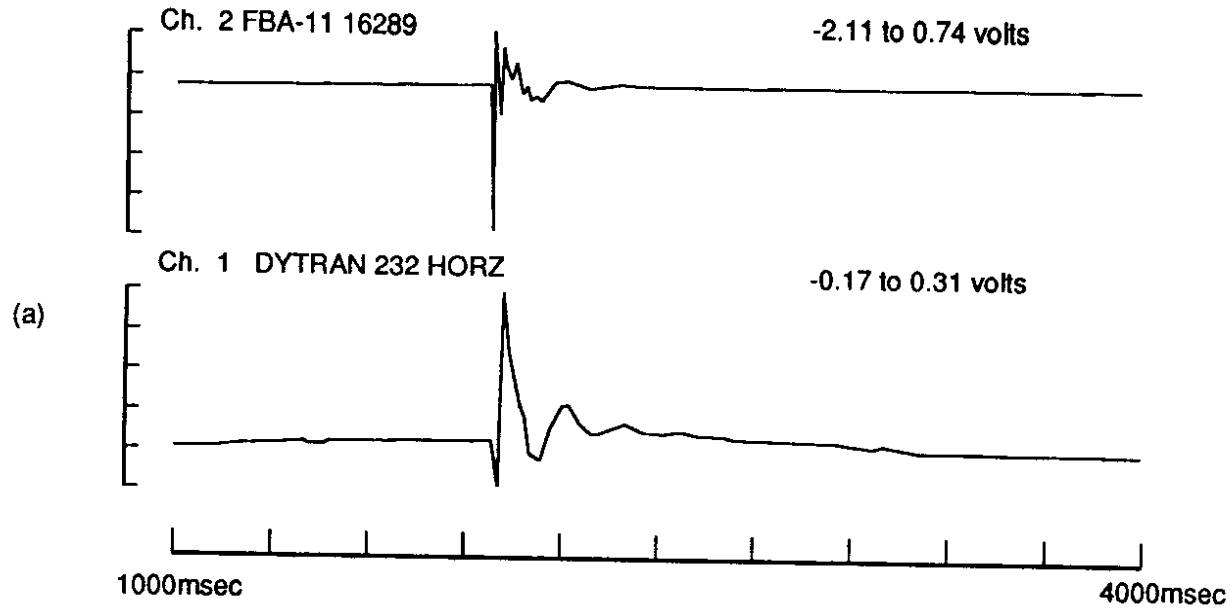

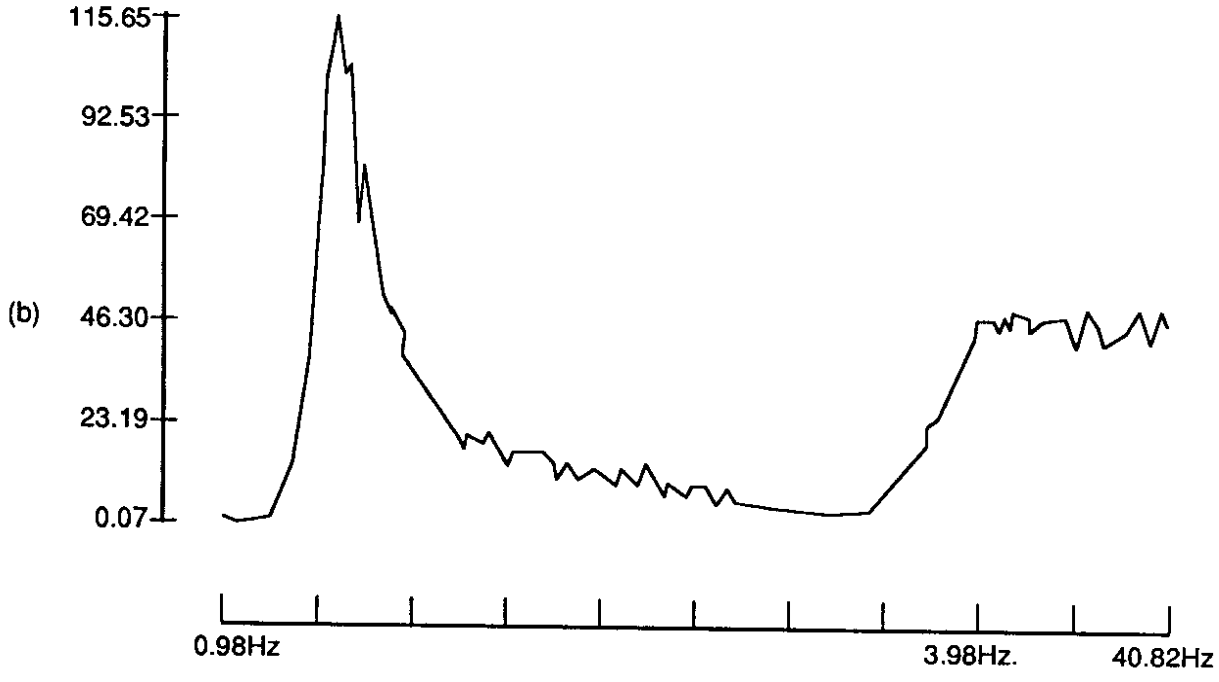

Figure 16. Response of Pile to Typical Impact Test in Parallel Direction (a) Time Histories of Acceleration, and (b) Power Spectrum

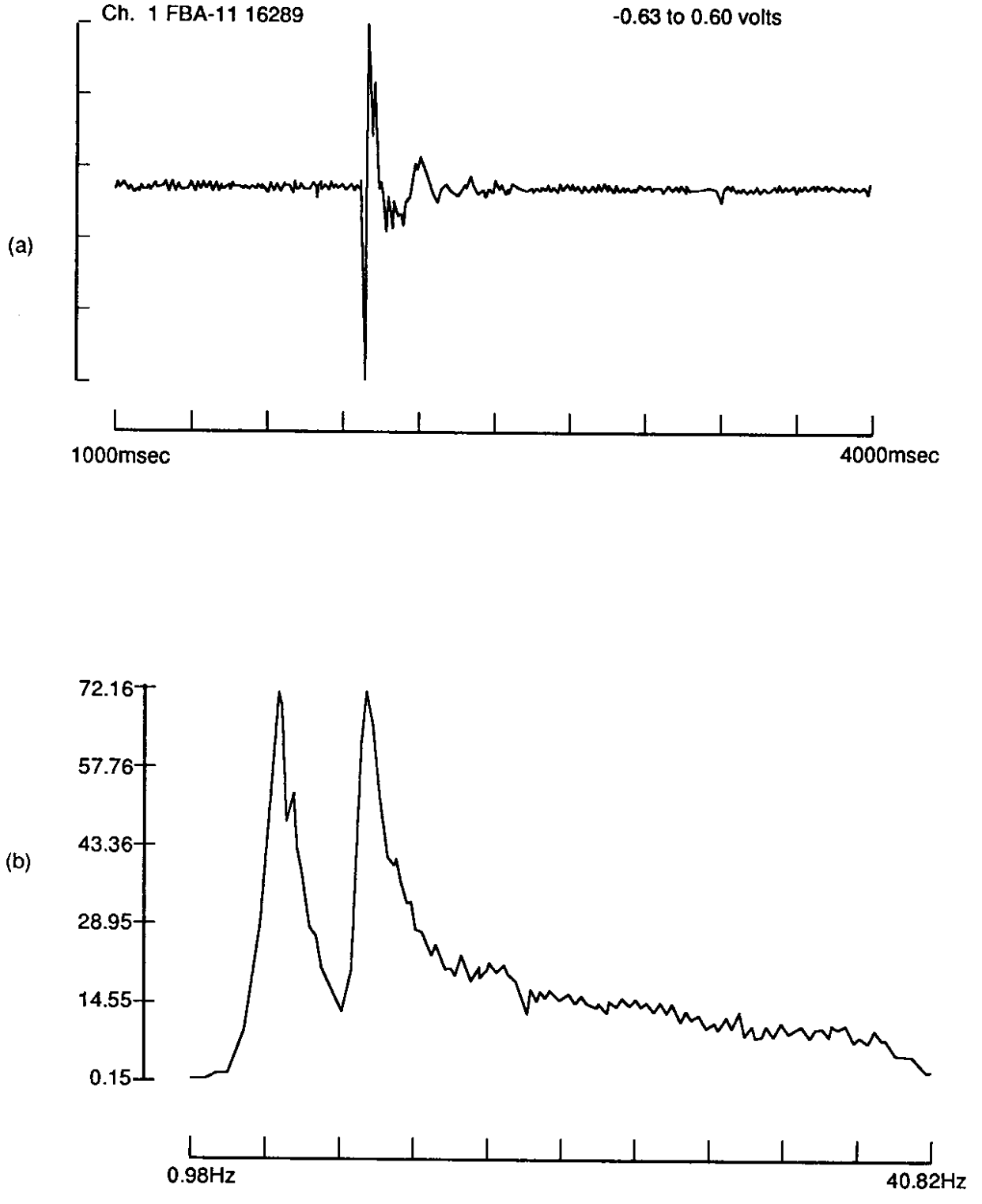

Figure 17. Response of Pile to Typical Impact Test in Perpendicular Direction (a) Time Histories of Acceleration, and (b) Power Spectrum

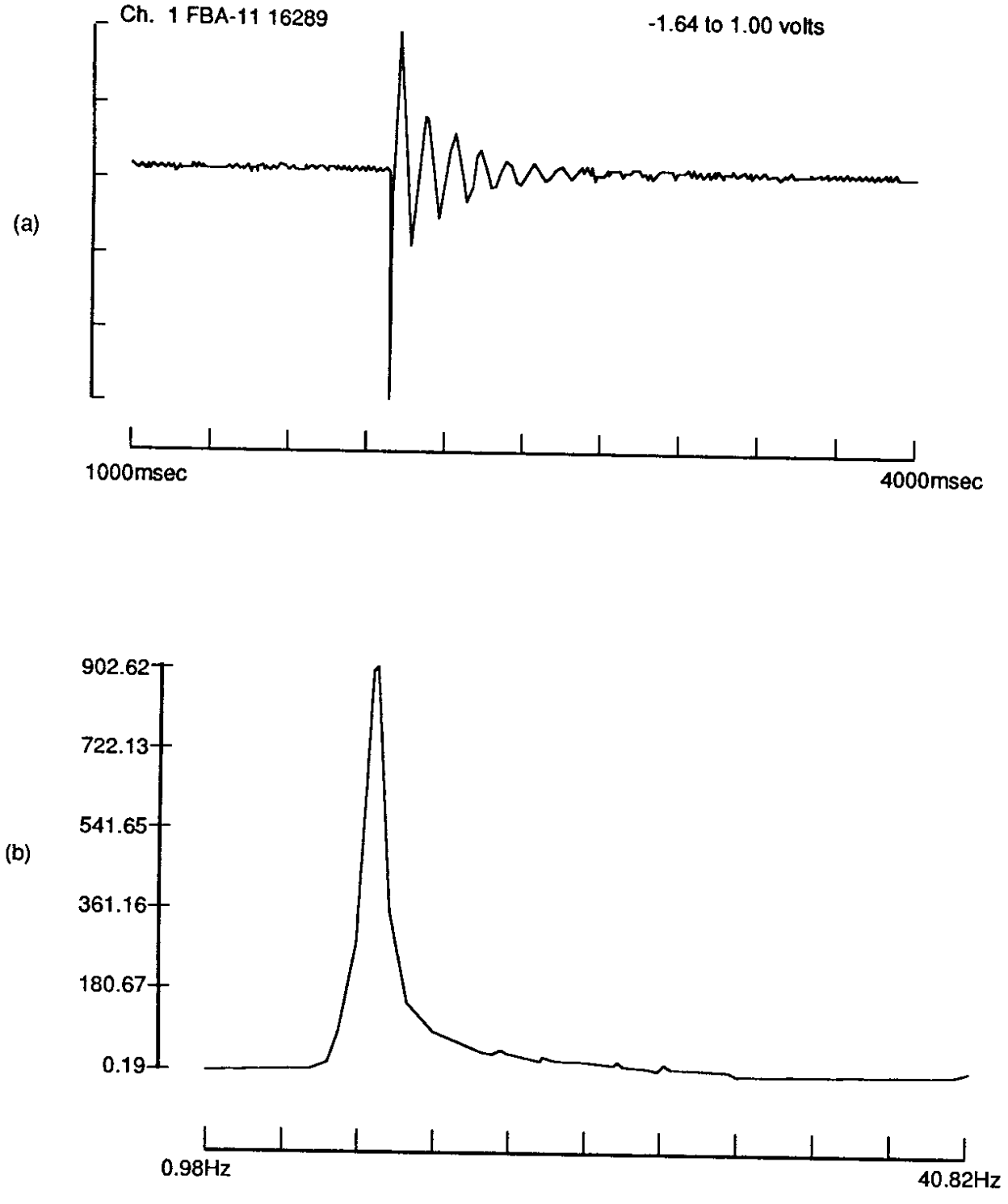

Figure 18. Response of Pile to Impact Test Designed to Isolate Torsional Mode of Vibration (a) Time Histories of Acceleration, and (b) Power Spectrum

corresponded to torsional response. The lower damping in the torsional mode of vibration was apparent from the slower decay of acceleration amplitude and the smaller bandwidth of the power spectrum.

Free Vibration Tests

A typical example of the measured accelerations in the parallel direction during a quick-release test is shown in Figure 19. The horizontal accelerations were generally observed to be about 5 to 10 times greater than the vertical accelerations, and the vertical accelerations recorded on the east side of the platform were about 1.5 times greater than the west-side accelerations. This latter characteristic was consistently observed during all parallel direction tests and was not the result of transducer miscalibration or incorrect amplifier gains, as initially suspected.

The accelerations recorded during the quick-release tests clearly indicated that the release of sling tension was not instantaneous but took approximately 0.1 sec., i.e., about one-half the low-strain natural period of vibration. The free vibrations induced during Test Nos. 5-9 (performed before the forced vibration tests) were similar to those of a simple linear oscillator, whereas the free vibrations generated during Test Nos. 54 and 55 (performed after the forced vibration tests), which had much larger initial displacements, exhibited natural periods that were amplitude dependent, reflecting the nonlinearity of the peat. For these tests the period of vibration of the first cycle (-0.5 sec.) was about 25 percent larger than the fairly constant periods of the subsequent cycles in which the displacement amplitudes were much smaller.

The Fourier Amplitude Spectra (FAS) were computed from the horizontal accelerations recorded during the quick-release tests. The peaks in the FAS were used to obtain the fundamental frequencies and associated damping ratios, which were again estimated by the half-power bandwidth method. The values of these two parameters are summarized in Table 2. The results generally indicated that, for a given pile assembly

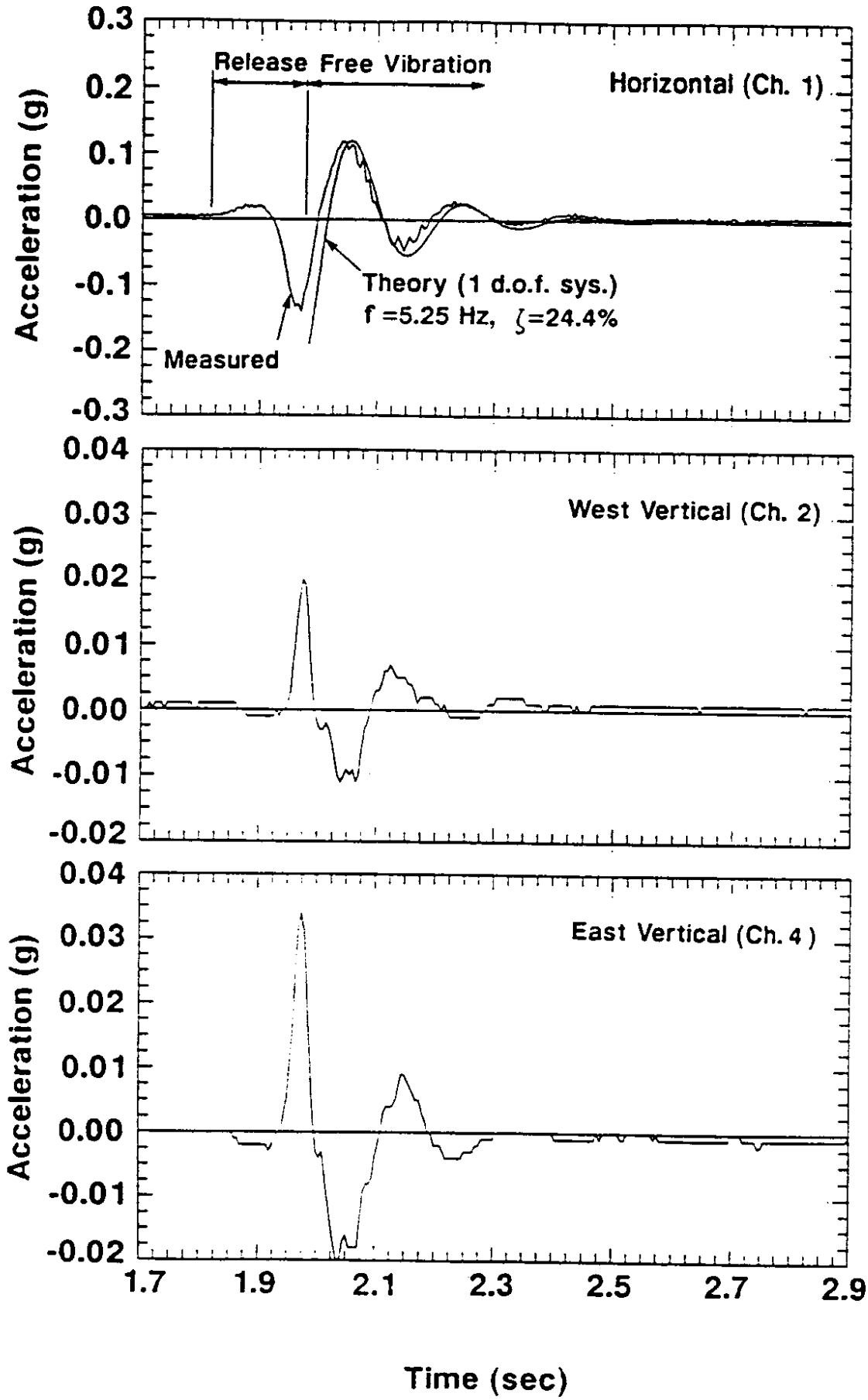

Figure 19. Typical Response to Quick Release Free Vibration Test

Table 2. Free Vibration Tests

Test No.	Additional Weight in Buckets (lbs)	Initial Displacement (in)	Fundamental Frequency (Hz)	Damping Ratio (%)
5	0	0.18	5.5	25.6
6	0	0.49	4.7	32.7
7	0	0.61	4.7	29.9
8	0	0.16	5.5	27.4
9	252*	0.18	4.7	25.6
54	404	1.81	2.3	28.5
55	404	2.36	2.3	31.3

*weight placed on shaker platform rather than in buckets

weight, the fundamental frequency decreased and the damping ratio increased as the initial platform displacement increased. This observation was consistent with the static-load deflection data, which revealed a softening of the peat with increased deflections similar to that observed during pile-load tests in sands and clays.

The unfiltered accelerations, a(t), and the shaker forces, F(t), recorded during the forced-harmonic tests were approximated by the simple harmonic functions $a(t) = a_o \sin(\omega t+\theta_1)$, and $F(t) = F_o \sin(\omega t+\theta_2)$, respectively, where ω is circular frequency in radians and t is time. The parameters a_o, F_o, θ_1 and θ_2 were determined by a least-squares fit between the data and the sine functions. Similar results were obtained with the same data after they were first processed with a low-pass filter. A comparison of the fitted response with the actual data confirmed the observation that load release did not occur instantaneously, as shown in Figure 19.

Forced Vibration Tests

A number of forced vibration tests were performed with loading in both the parallel direction and the perpendicular direction. Tests were performed, and data were acquired, at different loading frequencies and with different amounts of weight in the eccentric mass shaker buckets.

The first set of forced vibration tests imposed simple harmonic loading in the parallel direction. Tests were performed with no weight in the eccentric mass shaker buckets at frequencies of 1.0, 1.5, and 2.0 Hz. A number of individual tests were performed at each frequency with different signal conditioning parameters in an effort to obtain the best possible waveform. An example of a typical test result is shown in Figure 20 (PILE 16F2R). After completion of these tests, additional tests in the parallel direction were performed with different amounts of weight in the shaker buckets.

The gearing system of the eccentric mass shaker was then modified to allow simple harmonic loading in the perpendicular direction. Before forced vibration tests were begun in the perpendicular direction, a series of impact tests were performed in the perpendicular direction. These indicated that the forced vibration tests in the parallel direction had not softened the soil in the perpendicular direction. Forced vibration tests in the perpendicular direction were then performed at loading frequencies of 1.0, 1.5, 2.0, 2.5, and 2.9 Hz, with no weights in the shaker buckets, and then at 1.0 Hz with different weights in the buckets.

An example of accelerometer data from a test at a loading frequency of 1.0 Hz is shown in Figure 21. The data for tests at this frequency were contaminated with noise at a frequency close enough to 1.0 Hz that it could not be removed by signal processing techniques. Consequently, it was not possible to interpret the results of the 1.0-Hz tests.

Interpretation of Test Data

Because the center of gravity of the pile loading assembly was above the ground surface, the free vibration and forced vibration tests induced both horizontal and rotational movement of the pile at the ground surface. Therefore, the response of the system must be interpreted within the framework of a two-degree-of-freedom model.

The response of foundations to dynamic loading is often expressed in terms of impedance functions. An impedance function describes the resistance, both elastic and viscous, to foundation displacement provided by the soil.

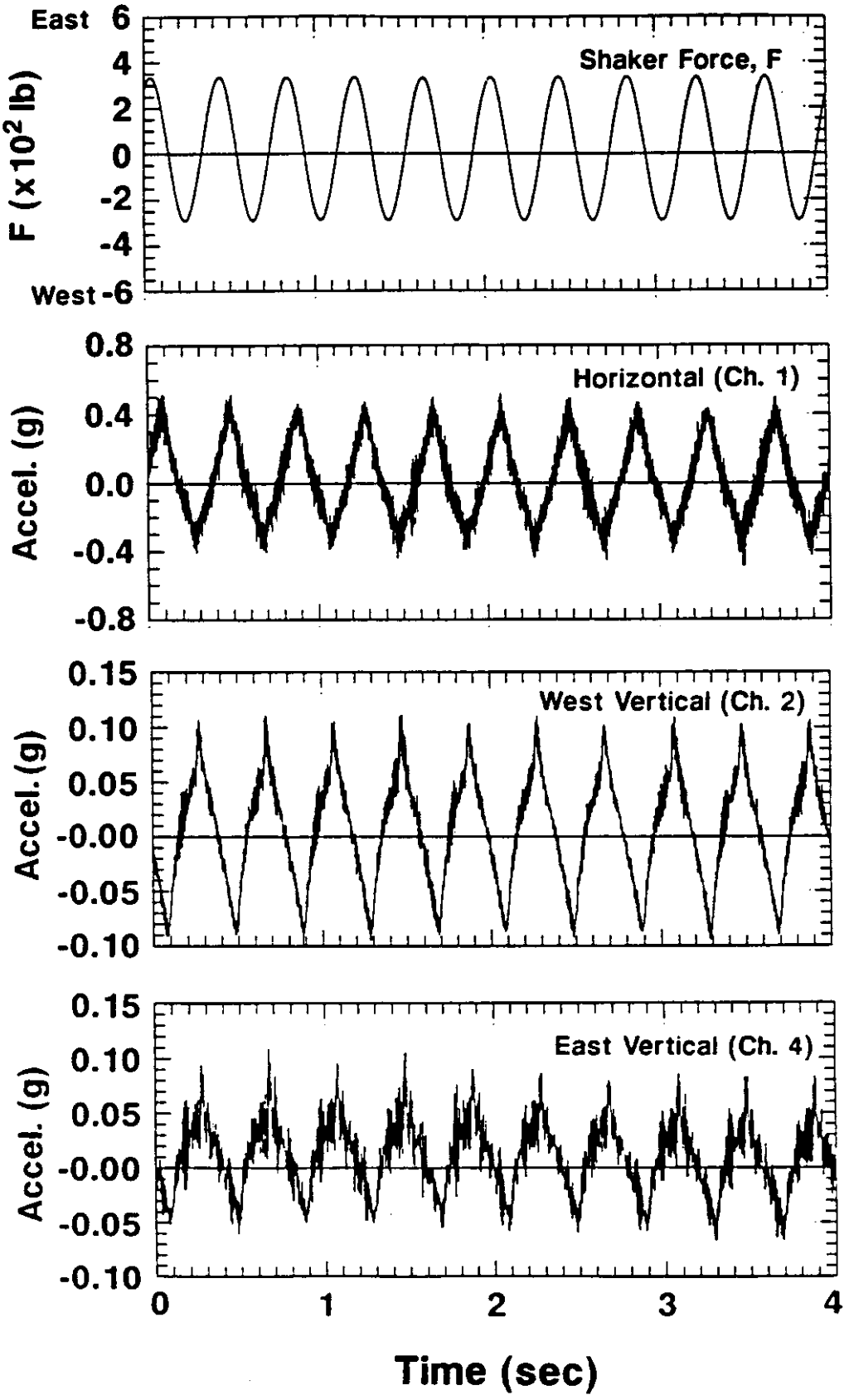

Figure 20. Typical Response to Forced Vibration Test

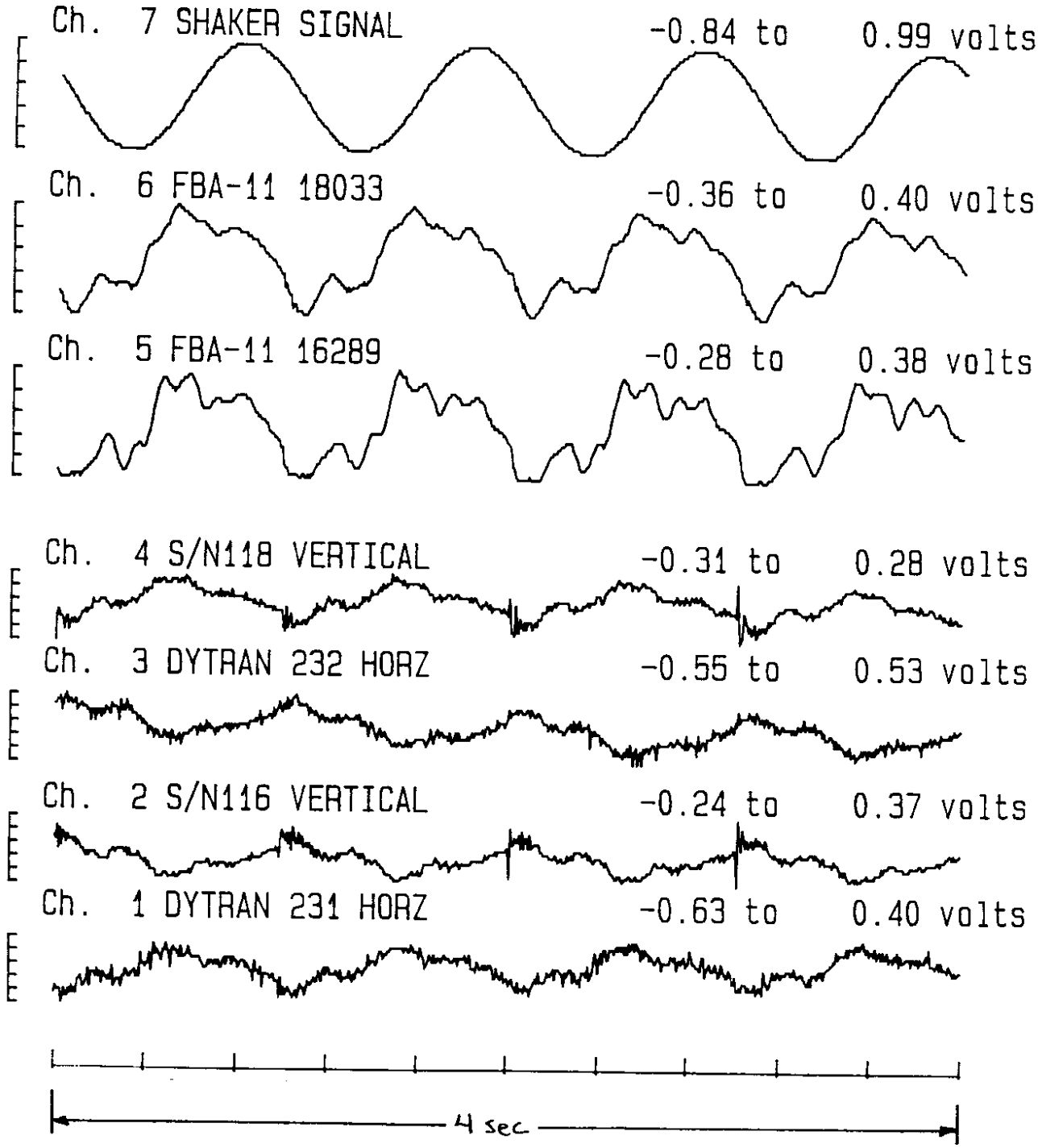

Figure 21. Typical Results from Forced Vibration Test at Frequency of 1 Hz. Low frequency noise (see Channels 5 and 6) rendered signal processing impossible.

Equations of Motion

The dynamic response characteristics of foundations are often expressed in terms of impedance functions, which describe the stiffness and damping of the pile/soil system as functions of frequency. Impedance functions are generally complex; the real part reflects the stiffness of the system, and the imaginary part reflects its damping characteristics. The researchers estimated the translational and rotational impedance functions (stiffness and damping) of the pile at the ground surface by solving the equations of motion for the quick-release and forced-vibration tests. Assuming linear response (and using bold face to denote vector quantities), the equations have the usual form

$$\mathbf{M}\ddot{\mathbf{v}} + \mathbf{K}^*\mathbf{v} = \mathbf{f} \tag{1}$$

where

M is the symmetric mass matrix,

K* is the complex stiffness matrix,

f is the external force vector, and

$\ddot{\mathbf{v}} = \{u, \theta\}^T$ is the displacement vector, which consists of the horizontal translation (u) and rotation (θ) of the pile at the ground surface.

The double dot over v indicates double differentiation with respect to time. The expressions for **M** and **K*** are as follows:

$$\mathbf{M} = \begin{bmatrix} (m + 2m_e) & (mh + m_e(h_1 + h_2)) \\ (mh + m_e(h_1 + h_2)) & (mh^2 + m_e(h_1^2 + h_2^2) + I_{yy}) \end{bmatrix} \tag{2a}$$

$$\mathbf{K}^* = \begin{bmatrix} K_u & 0 \\ 0 & K_\theta \end{bmatrix} \tag{2b}$$

where

m = the above-ground mass of the system minus the mass of the rotating buckets;

I_{yy} = the mass moment of inertia about the horizontal axis perpendicular to the direction of motion;

m_e = the mass of each rotating bucket;

h = the height above the ground of the center of gravity (c.g.) of m; and

h_1 and h_2 are the heights above ground of the centers of gravity of each rotating bucket.

The force vector for the harmonic vibration tests is

$$\mathbf{f} = \begin{bmatrix} 2m_e r\,\omega^2 \\ m_e\,(h_1 + h_2)\,\omega^2 \end{bmatrix} e^{i\omega t} \qquad (2c)$$

where

r = the eccentricity of the rotating buckets, and

i = -1.

The external force vector for the quick-release tests is the null vector $\mathbf{f} = \mathbf{0}$.

Free Vibration Tests

The solution of the equations of motion for the quick-release tests can be obtained in the frequency domain and expressed as follows:

$$K_u = \frac{\omega^2 (M_{11}\,F(\ddot{u}) + M_{12}\,F(\ddot{\theta}))}{(F(\ddot{u}) + \dot{u}(t=0) + i\omega u(t=0))} \qquad (3a)$$

$$K_\theta = \frac{\omega^2(M_{21}F(\ddot{u}) + M_{22}\,F(\ddot{\theta}))}{(F(\ddot{\theta}) + \dot{\theta}\,(t=0) + i\omega\theta\,(t=0))} \qquad (3b)$$

where

M_{ij} = elements of the mass matrix in Equation (2), and

the function F( ) denotes the Fourier Transform of the variable within the parentheses.

The initial conditions were denoted by u (t=0), $\dot{u}$ (t=0), θ(t=0), and $\dot{\theta}$(t=0), where the origin of the time was at the end of the sling release when the free vibrations actually began. The translational and rotational accelerations were estimated from the accelerations measured on the platform and assumed that the stiffened above-ground portion of the pile assembly behaved as a rigid body. The values for the initial conditions were estimated by integrating $\ddot{v}_o$ and $\ddot{\Theta}$ over the release time. The initial values of u and θ at the beginning of the release were estimated from the initial horizontal platform offset and an empirical relationship between u and θ based on the results of the earlier static load-deflection tests [12]. The initial values of translational and rotational velocity at the beginning of the release were assumed to be zero.

Forced Vibration Tests

The equations of motion for the forced vibration tests can be solved by expressing the response as harmonic functions:

$$u(t) = (u_1 + iu_2)\, e^{i\omega t} \tag{4a}$$

$$\theta(t) = (\theta_1 + i\theta_2)\, e^{i\omega t} \tag{4b}$$

Differentiating each twice, substituting them into the equation of motion (Equation 1), and separating the real and imaginary parts yields the following two systems of simultaneous equations:

$$\begin{bmatrix} u_1 & \theta_1 \\ u_2 & \theta_2 \end{bmatrix} \begin{Bmatrix} k_{11} \\ k_{12} \end{Bmatrix} = \begin{Bmatrix} f_1 + \omega^2 (m_{11} u_1 + m_{12} u_2) \\ \omega^2 (m_{11} u_2 + m_{12} \theta_2) \end{Bmatrix} \tag{5a}$$

$$\begin{bmatrix} u_1 & \theta_1 \\ u_2 & \theta_2 \end{bmatrix} \begin{Bmatrix} k_{21} \\ k_{22} \end{Bmatrix} = \begin{Bmatrix} f_2 + \omega^2 (m_{21} u_1 + m_{22} \theta_1) \\ \omega^2 (m_{21} u_2 + m_{22} \theta_2) \end{Bmatrix} \tag{5b}$$

which can easily be solved for the unknown stiffness coefficients.

Experimental Impedance Functions

Experimental impedances obtained from both the forced vibration and quick-release tests are shown in Figures 22 through 29. Estimates of Re (K_x or K_y) and Re (K_θ) from the forced vibration data are shown in Figures 22 and 24, respectively; estimates of the corresponding damping coefficients, $C = Im(K)/\omega$, are shown in Figures 23 and 25. In these figures, the circles represent the results of individual tests at 2.0 Hz and 2.5 Hz, and the diamonds represent the results of the frequency sweep in the perpendicular direction. The stiffness and damping values in Figures 22 through 25 exhibit some fluctuation with frequency, but in general these values were relatively insensitive to frequency. The values for the individual and frequency-sweep tests were similar, which suggests that prolonged vibration during the continuous frequency-sweep tests did not affect the system behavior any differently than the individual tests of much shorter duration.

Estimates of $Re(K_u)$ and $Re(K_\theta)$ from the quick-release data are shown as functions of the initial platform displacement in Figures 26 and 28, respectively; the corresponding damping coefficients are shown in Figures 27 and 29. These stiffness and damping values were estimated at the natural frequencies shown in Table 2. Although conceptually the stiffness and damping values can be computed at all frequencies, the calculation was best conditioned at the fundamental frequency, where the signal-to-noise ratio was highest. The test numbers from Table 1 are listed next to the data points. For comparison, the stiffness and damping values obtained from the parallel direction forced harmonic vibration data at 2.0 Hz and 2.5 Hz are shown as dashed lines in Figures 26 through 29. These values were plotted at low deflections similar to the 1/4-in. (5/8-cm) to 1/2-in. (1 1/4-cm) maximum harmonic platform displacements generated during the 2.0 and 2.5 Hz tests. Also shown in Figure 26 are the static tangent stiffnesses estimated from the aforementioned (Figure 4) static load-deflection test conducted by Kramer et al. [12]. The range of deflections over which these tangent stiffnesses are applicable are

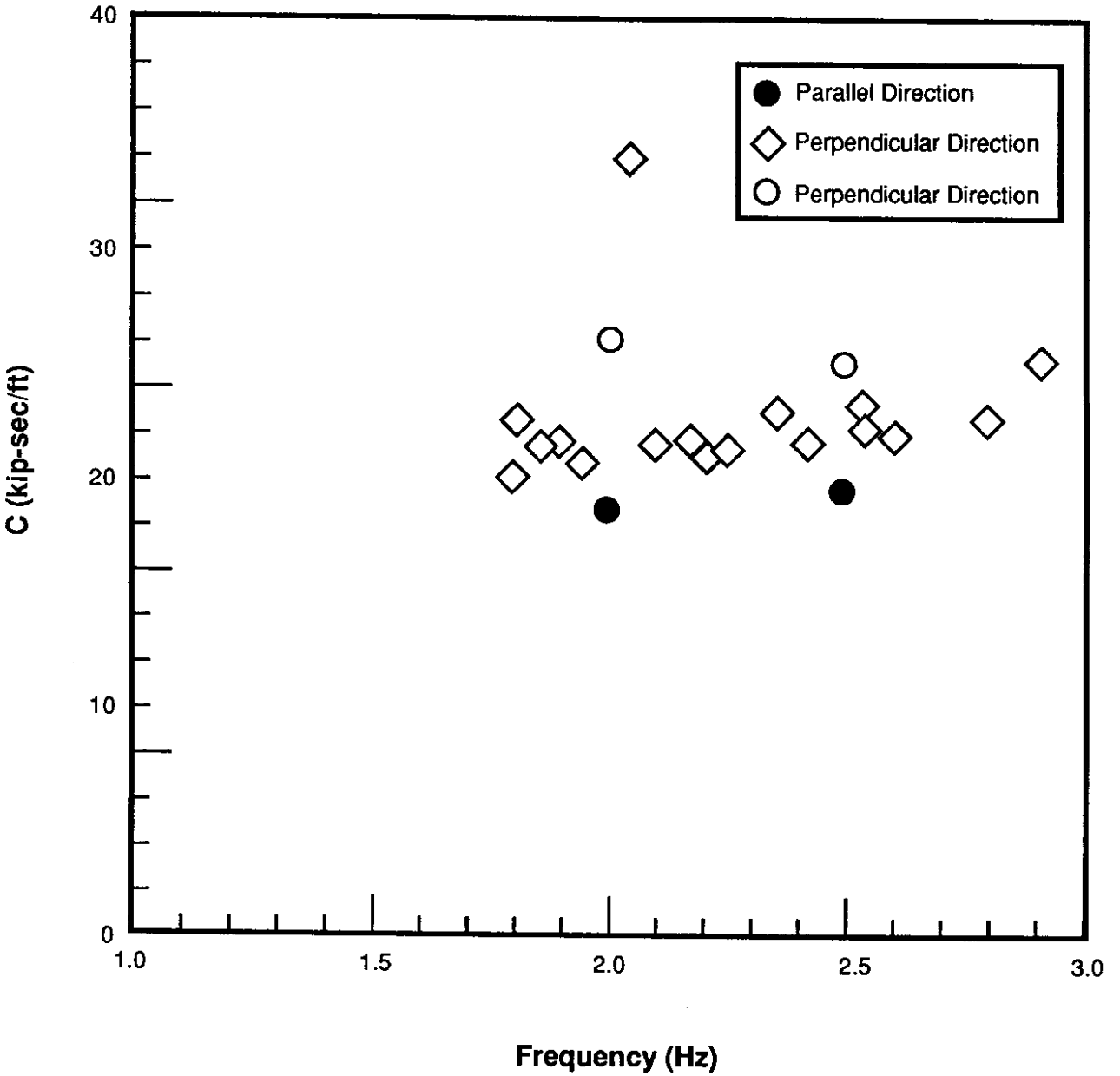

Figure 22. Computed Stiffness for Horizontal Translation Mode of Vibration in Forced Vibration Tests

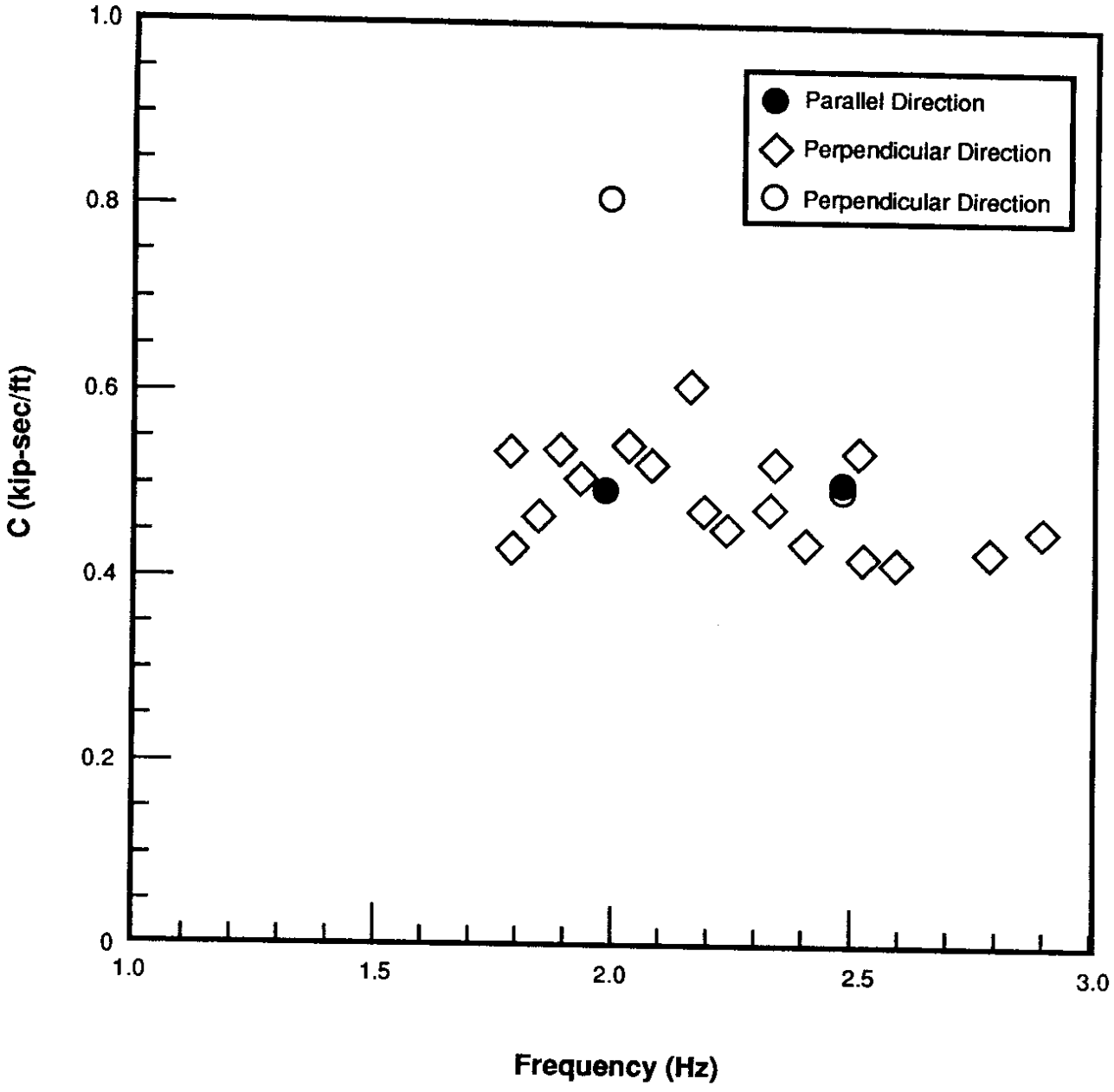

Figure 23. Computed Damping Coefficients for Horizontal Translation Mode of Vibration in Forced Vibration Tests

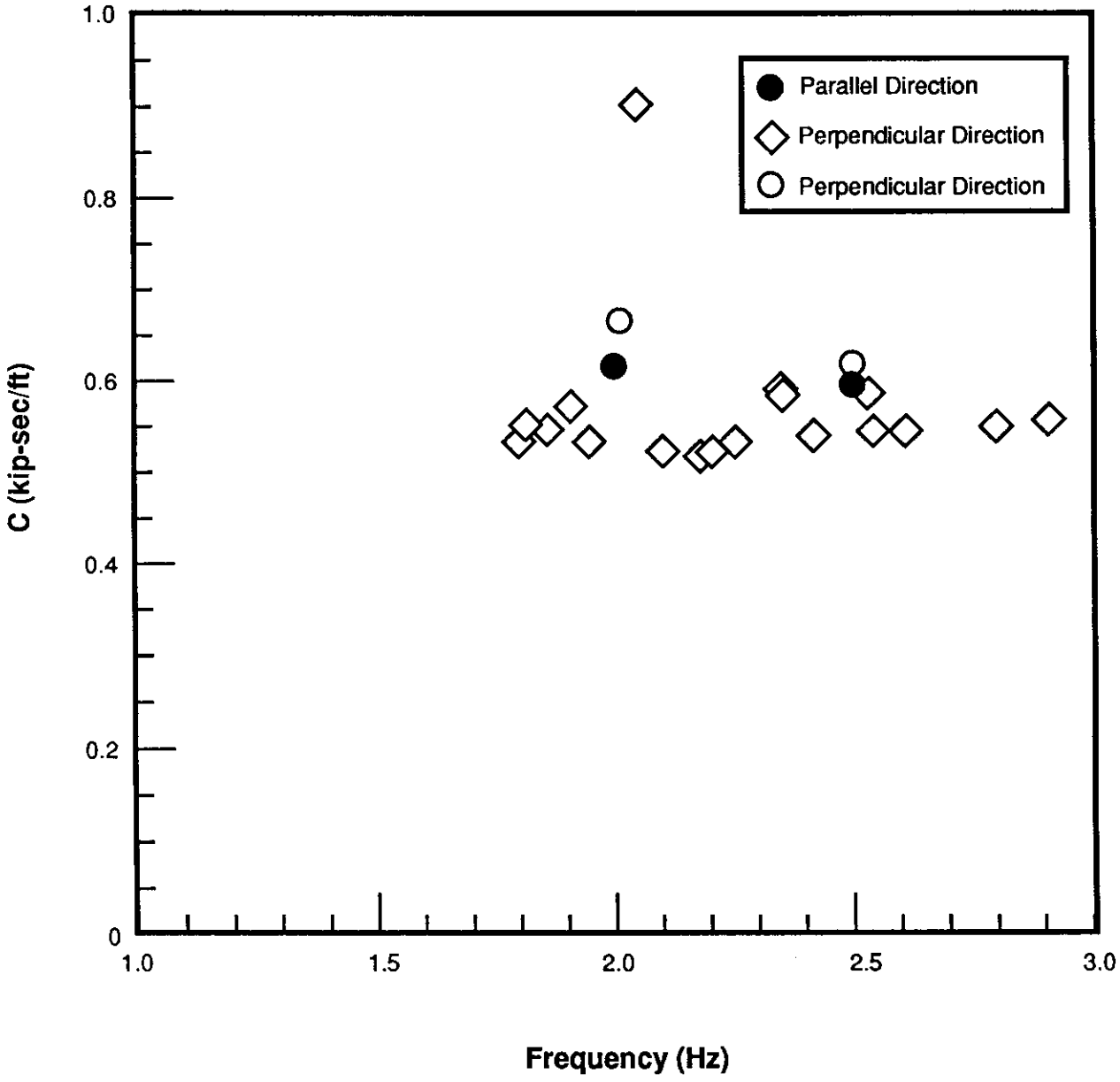

Figure 24. Computed Stiffness for Rotational Mode of Vibration in Forced Vibration Tests

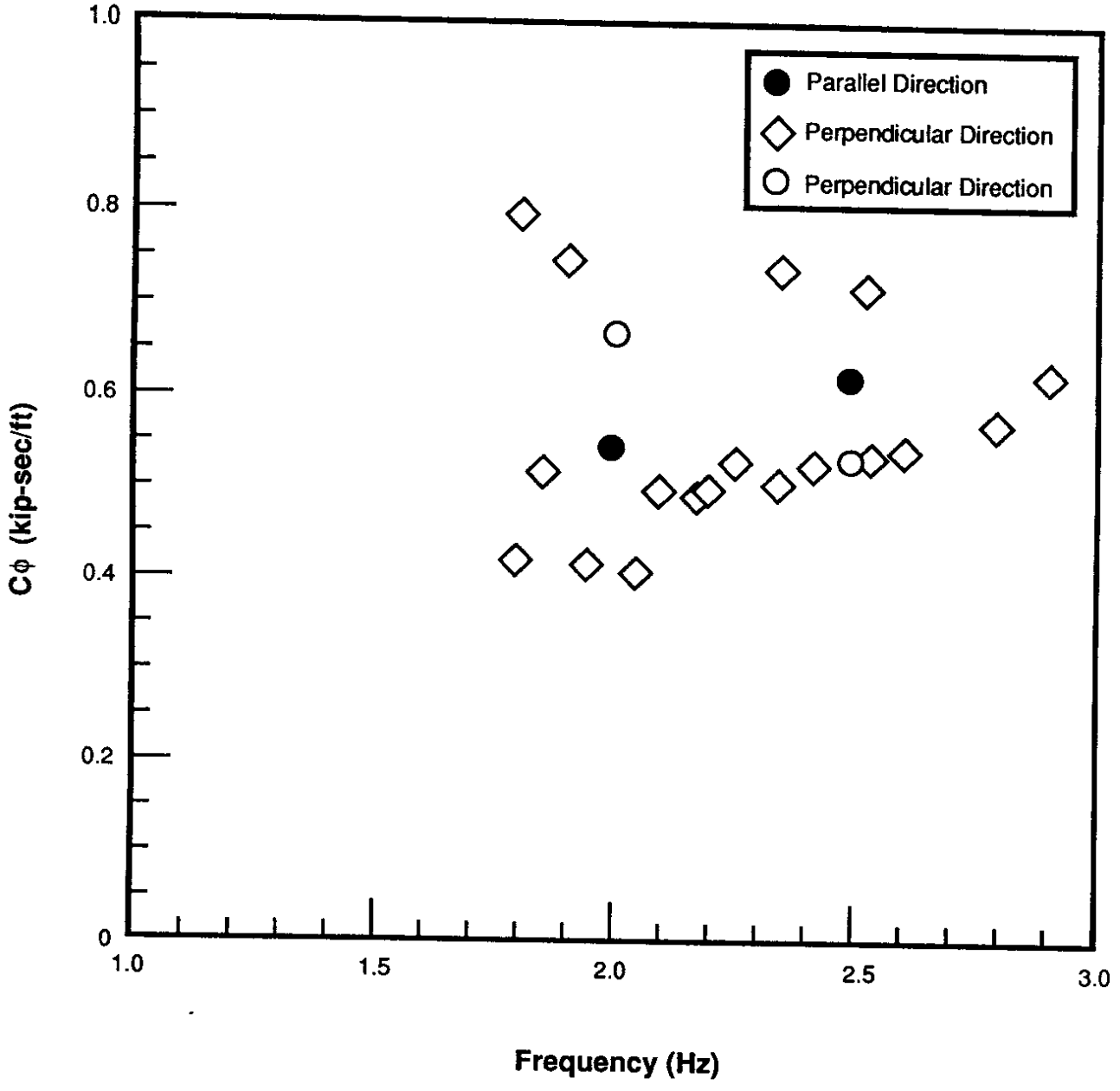

Figure 25. Computed Damping Coefficients for Rotational Mode of Vibration in Forced Vibration Tests

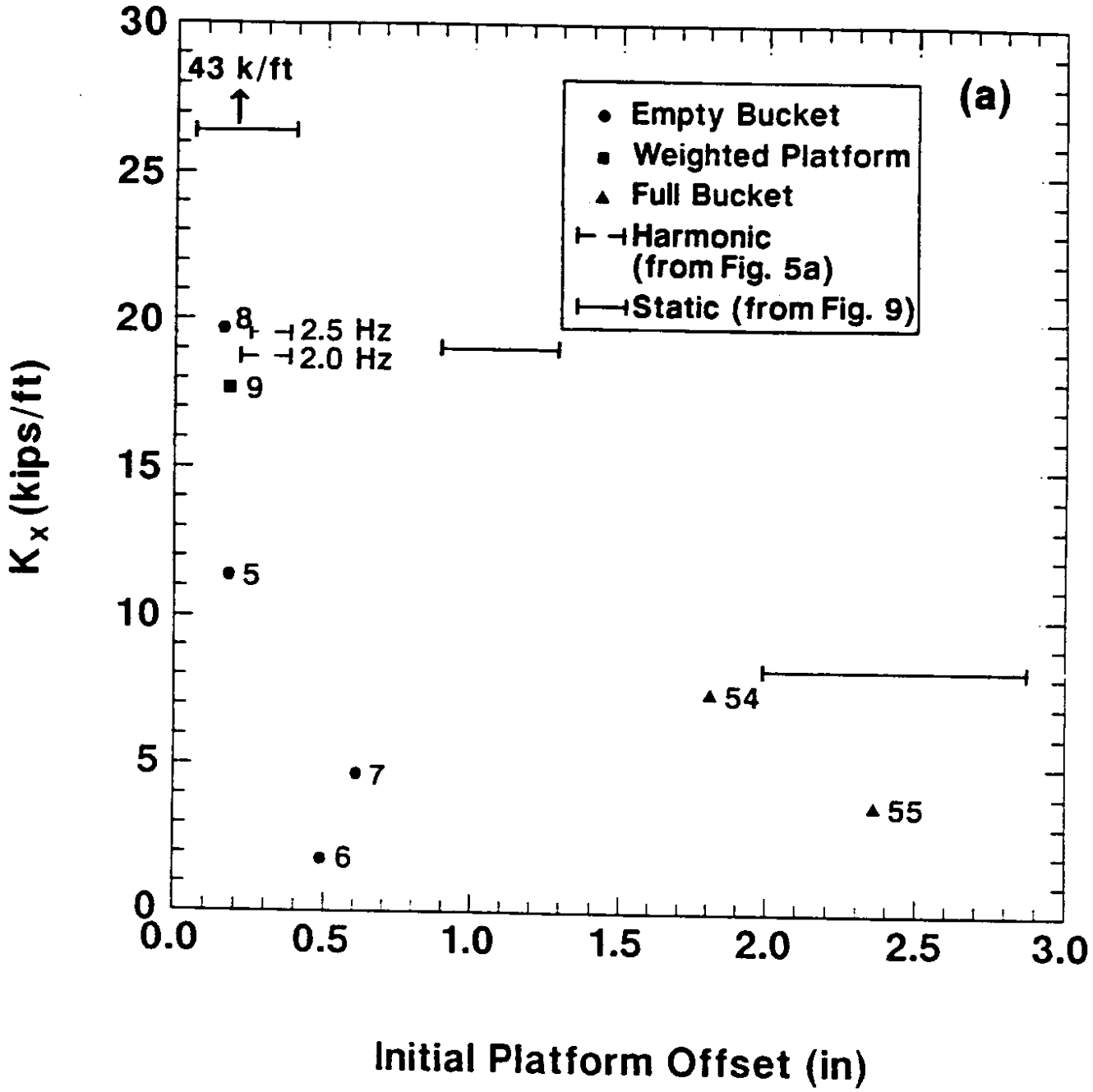

Figure 26. Computed Stiffness for Horizontal Translation Mode of Vibration in Quick Release Free Vibration Tests

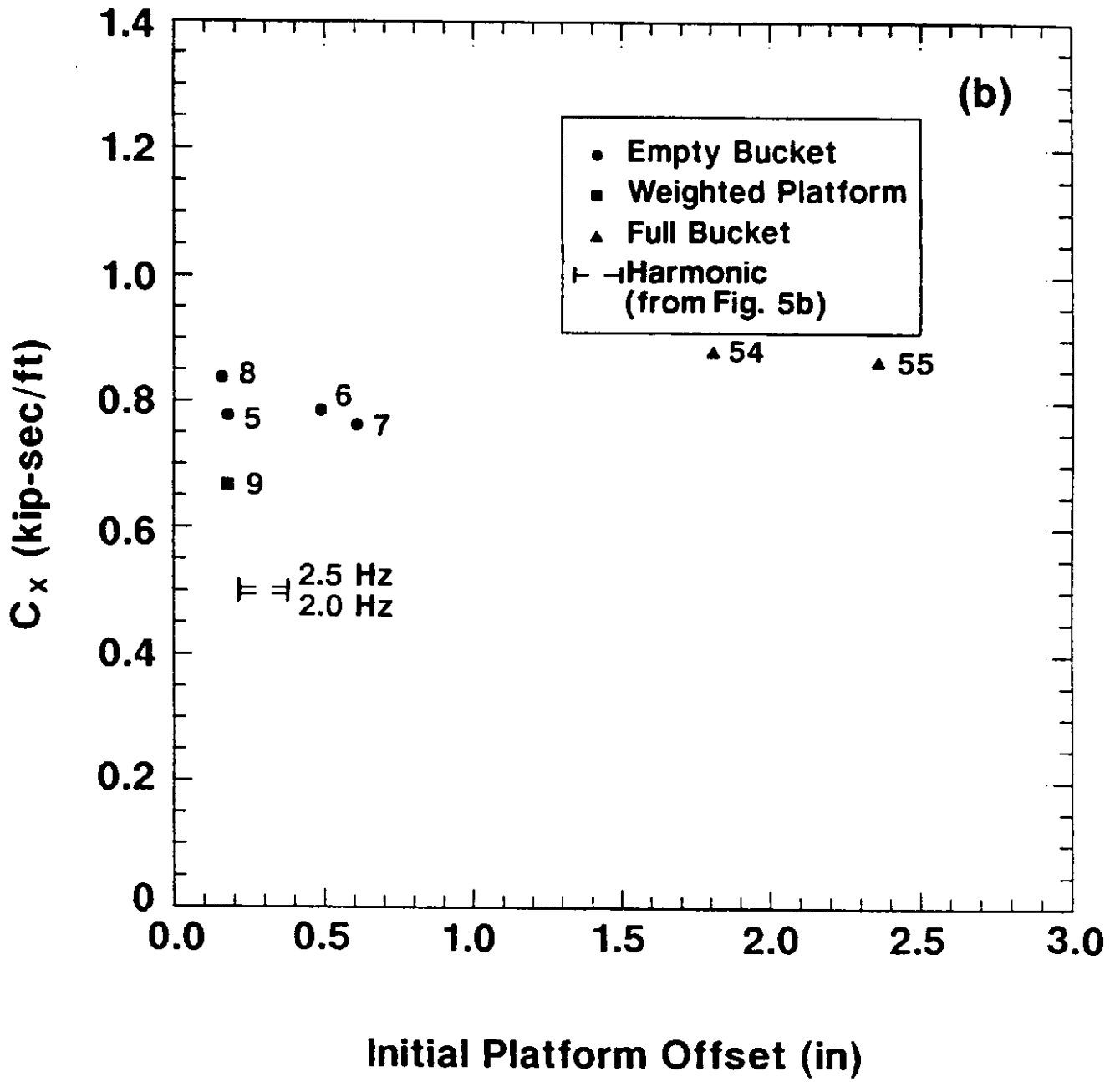

Figure 27. Computed Damping Coefficients for Horizontal Translation Mode of Vibration in Quick Release Free Vibration Tests

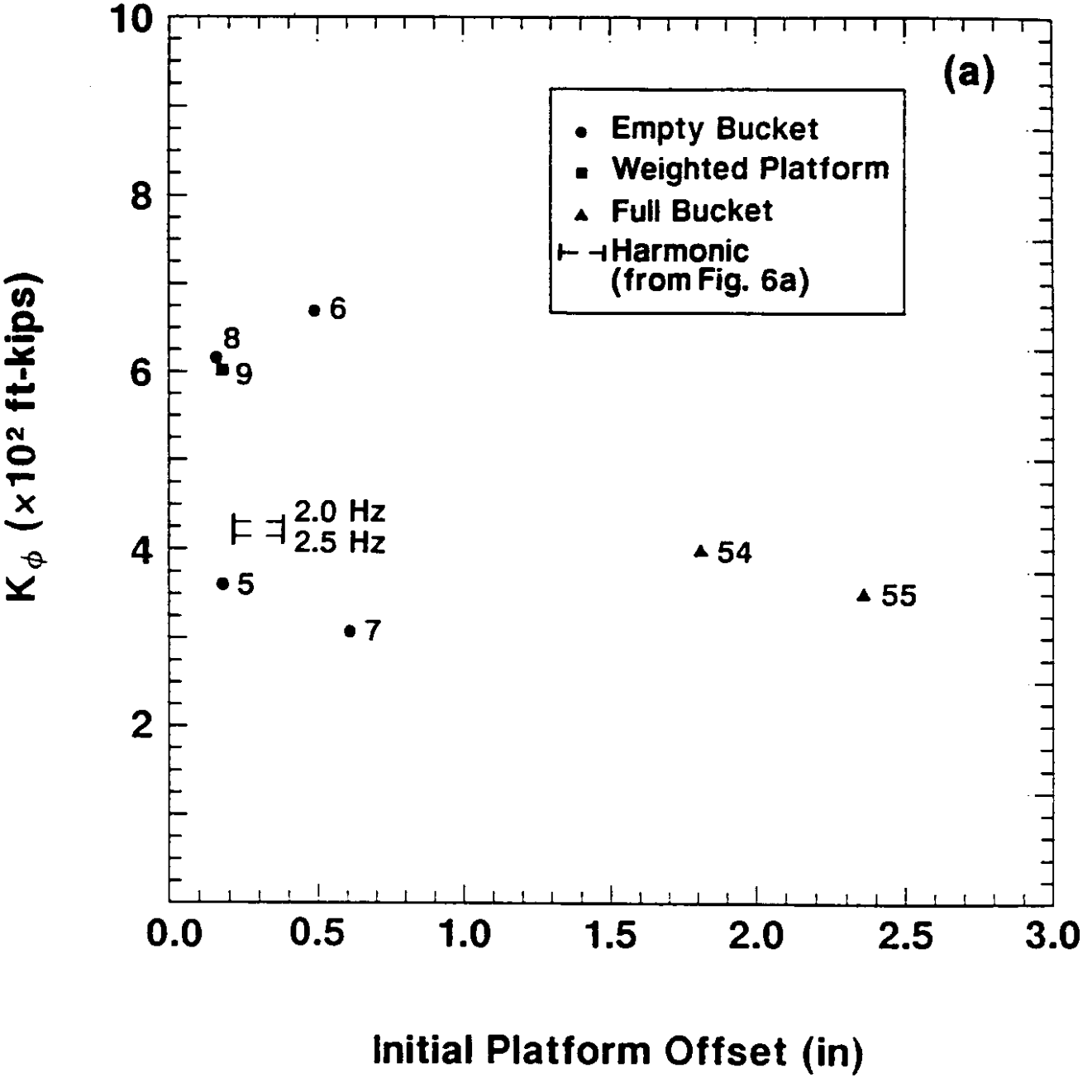

Figure 28. Computed Stiffness for Rotational Mode of Vibration in Quick Release Free Vibration Tests

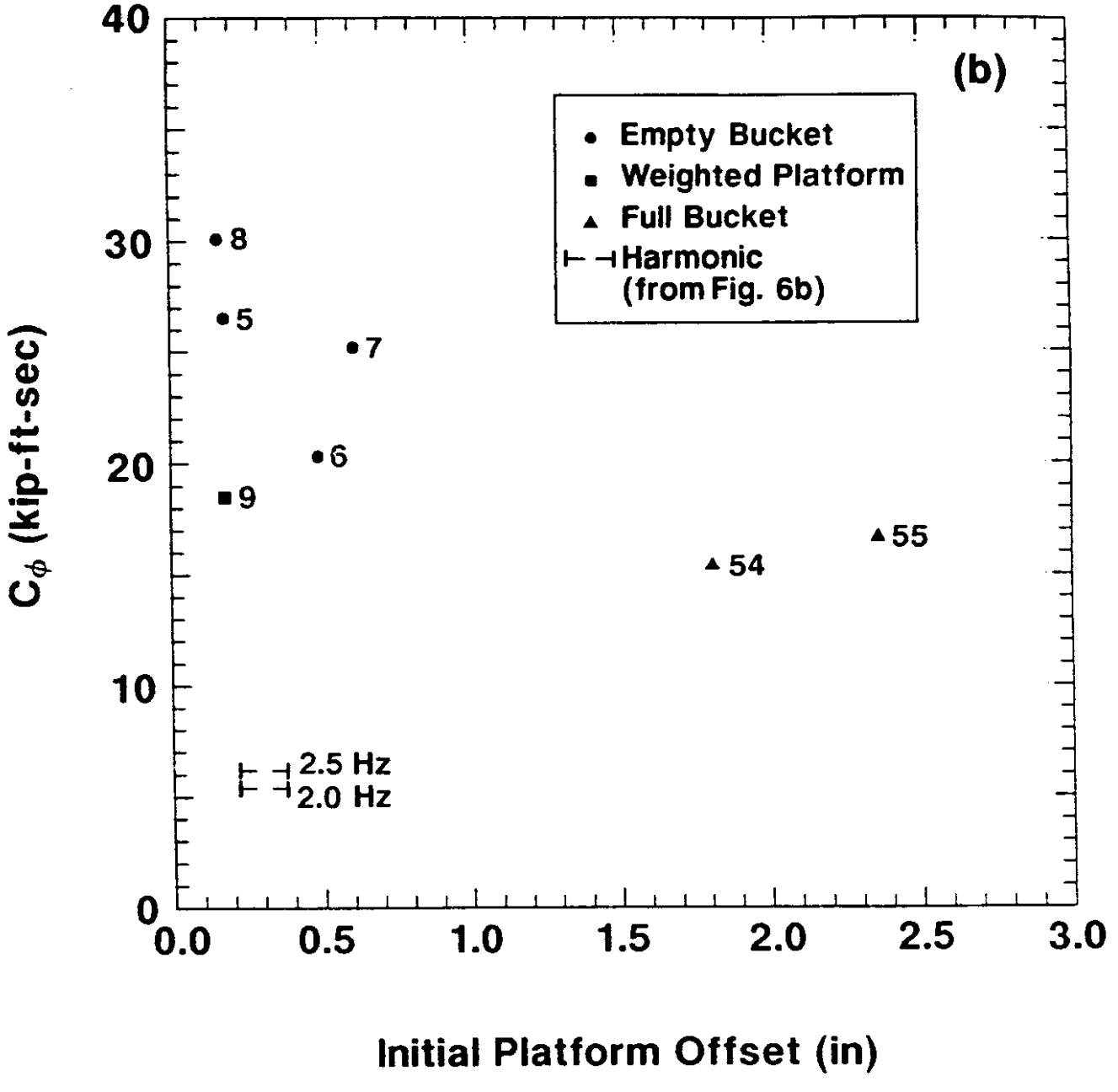

Figure 29. Computed Damping Coefficients for Rotational Mode of Vibration in Quick Release Free Vibration Tests

indicated in Figure 26. Several interesting observations are apparent in Figures 26 through 29. The stiffnesses, K_u and K_θ, for quick-release Test No. 5, conducted at an initial platform offset of 0.18 in (0.46 cm), are approximately 60 percent of the stiffnesses estimated for Test No. 8, conducted at a slightly lower initial platform offset of approximately 0.16 in (0.41 cm). The reasons for the differences in stiffnesses are not clear, but they believed to be more the result of experimental error and uncertainties in the initial conditions than the result of significant changes in the stiffness of the soil surrounding the pile. Intuitively, one would have expected that the stiffnesses for the first test (No. 5), when the soil was essentially undisturbed, would have been larger than or similar to the stiffnesses derived from a latter test at the same initial offset. The primary evidence suggesting that the stiffnesses were in fact similar is the identical fundamental frequency of 5.5 Hz measured for both tests (Table 2).

The computed stiffnesses from Tests 8 and 9, which had similar initial offsets but different assembly weights (and therefore different natural frequencies), were similar and within the experimental error. Consequently, the data did not indicate any rate or frequency-dependent effects over this limited frequency range.

Despite the inherent experimental error, there was a general trend of decreasing stiffness with increasing initial offset, which, for the translational stiffness, was consistent with the static load-deflection curve shown in Figure 4. Interestingly, the stiffnesses at small initial offsets were similar to the stiffnesses from the forced-harmonic vibration tests, whereas the static stiffnesses shown in Figure 4 are approximately two times greater. Such differences between static and dynamic foundation stiffnesses are usually explained in terms of cyclic degradation or the formation of a gap between the pile of soil [28]; however, this explanation may not be totally satisfactory for the first series of quick-release tests, which were conducted with relatively small offsets and for which the degradation was not expected to be significant. The natural frequency of 5.5 Hz for the first quick-release test (No. 5) was similar to the natural frequency (5.8 Hz) measured

during several impact tests conducted just before the quick-release tests. The displacements generated during the impact tests were much less than 0.1 in. (0.25 cm) and should not have degraded the soil surrounding the pile. A possible explanation for part of the discrepancy between the static and dynamic stiffness is experimental error associated with the static load-deflection tests on the pile. The static stiffnesses associated with small deflections from a test on the same size pile approximately 400 ft. (122 m) away [12] were only about 30 percent greater than the dynamic stiffness.

The translational damping values estimated from the quick-release test results (Figure 27) were similar and exhibited no obvious dependence on initial platform offset. The scatter in these damping values at low initial offsets was much less than the associated stiffness values in Figure 26. The quick-release damping values were roughly 50 percent greater than those estimated from the results of the forced-vibration test conducted at 2.0 Hz and 2.5 Hz.

The quick-release test results (Figure 29) exhibited a trend of decreasing rotational damping with increasing initial offset; this observation was inconsistent with the usual observation of increased damping with increased deflection. The quick-release damping values were much greater than those estimated from the forced-vibration data by factors between three and six. Whereas the corresponding differences noted in the translational damping could be attributed partly to experimental error, the large differences in the two sets of rotational damping values are difficult to ascribe to experimental error and suggest differences in soil behavior during the two tests. However, if this explanation is correct, then one would expect to see significant differences in the two sets of rotational stiffnesses. These are not observed in Figure 28.

Pile Stiffness Estimation

The purpose of the pile load testing program was to estimate the resistance of the peat to dynamic pile movement to estimate the stiffnesses of the full-scale pile groups supporting the existing bridge structures. The rotational stiffness and damping behavior

of the test pile were not significant because the existing bridges were supported on groups of piles, and the rotational stiffness of each pile group was controlled by the axial stiffnesses (in tension and compression) of the piles within each group.

Given the limited scope of the testing program and the level of uncertainty regarding existing soil/foundation conditions, the use of complex analytical or numerical approaches to the pile stiffness problem was not considered justified. Instead, a simple, rational procedure for using the results of the dynamic pile load tests for evaluation of pile group stiffness was used.

Horizontal Stiffness

The forced vibration tests in both the parallel and perpendicular directions indicated an average horizontal stiffness of 20,000 lb/ft for the test pile. For the frequency range used in these tests, previous research [29] has indicated that the dynamic stiffness of the pile should be equal to its static stiffness. Consequently, the effective dynamic stiffness of the soil surrounding the pile can be estimated from methods based on the static lateral load behavior of piles.

By using the simplified graphical procedure of Scott [30], which is based on the analytical, half-space solution of Poulos, the equivalent soil modulus can be obtained from the dynamic load test results. Letting $K_u = E_S L/C_{UT}$, the value of C_{UT} corresponding to $K_u = 20{,}000$ lb/ft is

$$C_{UT} = \frac{E_S L}{K_u} \tag{6}$$

Using the graph of Figure 30(a) with Equation (6) and

$$K_R = \frac{EI}{E_S L^4} \tag{7}$$

a value of $E_S \approx 4000$ psf is obtained by iteration. This value can be used with Equations (6) and (7) and Figure 30(a) (pinned head) or 30 (b) (fixed head) to estimate the horizontal stiffness of other piles.

(a)

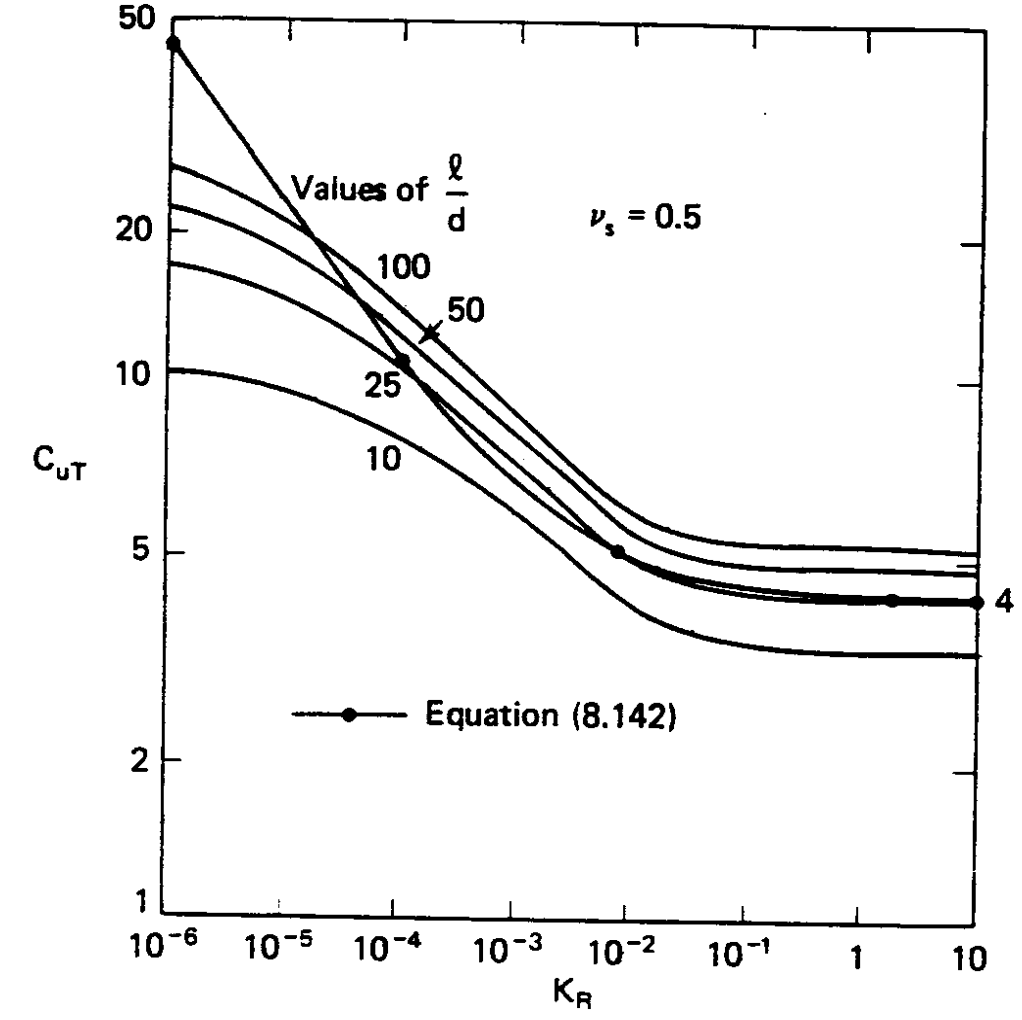

(b)

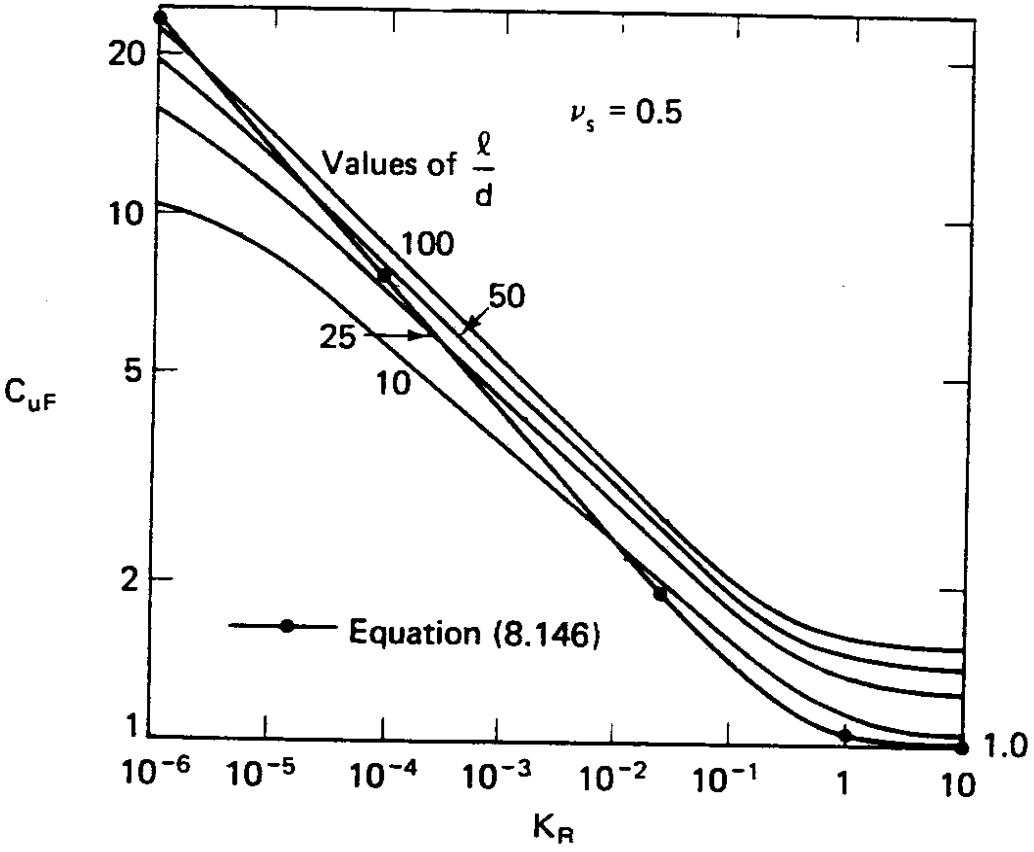

Figure 30. Dimensionless Stiffness Factors for (a) Free-Head Pile and (b) Fixed-Head Pile (after Scott, 1981)

For example, consider the horizontal stiffness of a 14-in. C.D., 13.25-in. I.D., 50-ft-long, steel pile filled with 4,000 psi concrete and restrained against rotation at its head. Then

$$K_r = \frac{EI}{E_s L^4} = \frac{E_{steel} I_{steel} + E_{concrete} I_{concrete}}{E_s L^4}$$

$$= \frac{\left[(29 \times 10^6 \text{psi}) \frac{\pi}{4} \left((7 \text{ in})^4 - (6.625 \text{ in})^4\right) + 57000 \sqrt{4000} \frac{\pi}{4} (6.625 \text{ in})^4\right] \frac{1 \text{ ft}^2}{144 \text{ in}^2}}{(4000 \text{ psf}) (50 \text{ ft})^4}$$

$$= 0.00452$$

From Figure DD (b) with L/D = (50 ft) (12 in/ft) / (14 in) = 42.9, $C_{UF} \approx 4$. Then

$$K_u = \frac{E_s L}{C_{UF}} = \frac{(4000 \text{ psf})(50 \text{ ft})}{4} = 50{,}000 \text{ lb/ft}$$

Pile Group Effects

The response of pile groups to dynamic lateral loading is a complicated and poorly understood problem, even for pile groups in soils whose properties are better known than those of the Mercer Slough peat. In view of this, it is common in current geotechnical engineering practice to assume that the lateral stiffness of a group of piles is equal to the sum of the lateral stiffnesses of the individual piles, unless specific data to suggest otherwise are available. Because no such data are available, the pile group lateral stiffness may be estimated this way.

DYNAMIC PEAT PROPERTIES

A series of cyclic triaxial tests was performed on undisturbed samples of the Mercer Slough peat. In addition to the dynamic properties measured during the cyclic triaxial tests, other important properties of the peat, including density, water content, and ash content, were also measured. A summary of these properties is presented in Table 3.

As previously discussed, the laboratory testing program for evaluation of dynamic peat properties was conducted in three phases. Test conditions are summarized in Table 3. Each phase represented an incremental improvement in testing equipment and

Table 3. Laboratory Test Conditions

Sample	Boring	Depth (ft.)	γ_{sat} (pcf)	w(%)	Ash Content (%)	$\sigma_3'_c$ (psf)	v_s (ft./sec)
I-1	1	41	80.5	90.2	83.9		
I-2	1	16	65.5	641	23.5		
I-3	1	22	66.1	501	27.4		
II-1	2	38	62.4	558	19.7	312	
II-2	2	62	71.8	280	75.0	458	
II-3	2	61	70.5	281	76.0	437	
II-4	2	60	71.1	285	77.8	458	
III-1	2	57	68.0	602	41.3	395	105
III-2	2	35	62.4	632	27.0	250	90
III-3	2	31	62.4	501	27.4	229	106
III-4	2	31	62.4	501	27.4	624	150
III-5	2	26	65.0	785		208	96
			65.1	739		312	104
			65.2	706		416	106
			65.2	687		520	108
			65.4	648		1040	136
			66.5	457		2080	200

testing procedures, and was based on the results of the previous testing phase. As a result, the level of understanding of the dynamic properties of the Mercer Slough peat evolved over the duration of the project. Because of time and budgetary constraints, the total amount of laboratory testing was limited, and further testing of the Mercer Slough peat will be necessary to more reliably characterize its dynamic properties. The current understanding of these properties, and its evolution over time, is described in the following sections.

Phase I Tests

The Phase I tests were performed on samples from Boring 1 with the standard CKC cyclic triaxial testing system. Limitations of the data acquisition system imposed a lower shear strain limit of approximately 0.05 percent. Early Phase I tests, performed at the standard loading frequency of 1 Hz, showed nearly elastic stress-strain behavior, as evidenced by hysteresis loops that were extremely narrow. The unexpectedly low damping values implied by these hysteresis loops prompted additional testing at different loading frequencies. At lower loading frequencies, the areas of the hysteresis loops were larger, indicating greater damping at lower frequencies. At higher loading frequencies the hysteresis loops were also larger, though the CKC electro-pneumatic loader was unable to maintain constant load amplitude at higher frequencies. In these tests, the shear moduli appeared to be insensitive to loading frequency at all strain levels. The results of the Phase I tests suggested that the damping characteristics of the Mercer Slough peat were strongly frequency dependent, with high damping at low and high frequencies and lower damping at intermediate frequencies. Damping ratios at all strain levels fell within the shaded region shown in Figure 31.

The strain-dependent variation of shear modulus and damping ratio from the Phase I tests are shown in Figures 32 through 37. The shear modulus values are expressed in terms of a normalized shear modulus, as is commonly done in soil dynamics. The normalized shear modulus is usually defined as the shear modulus at the

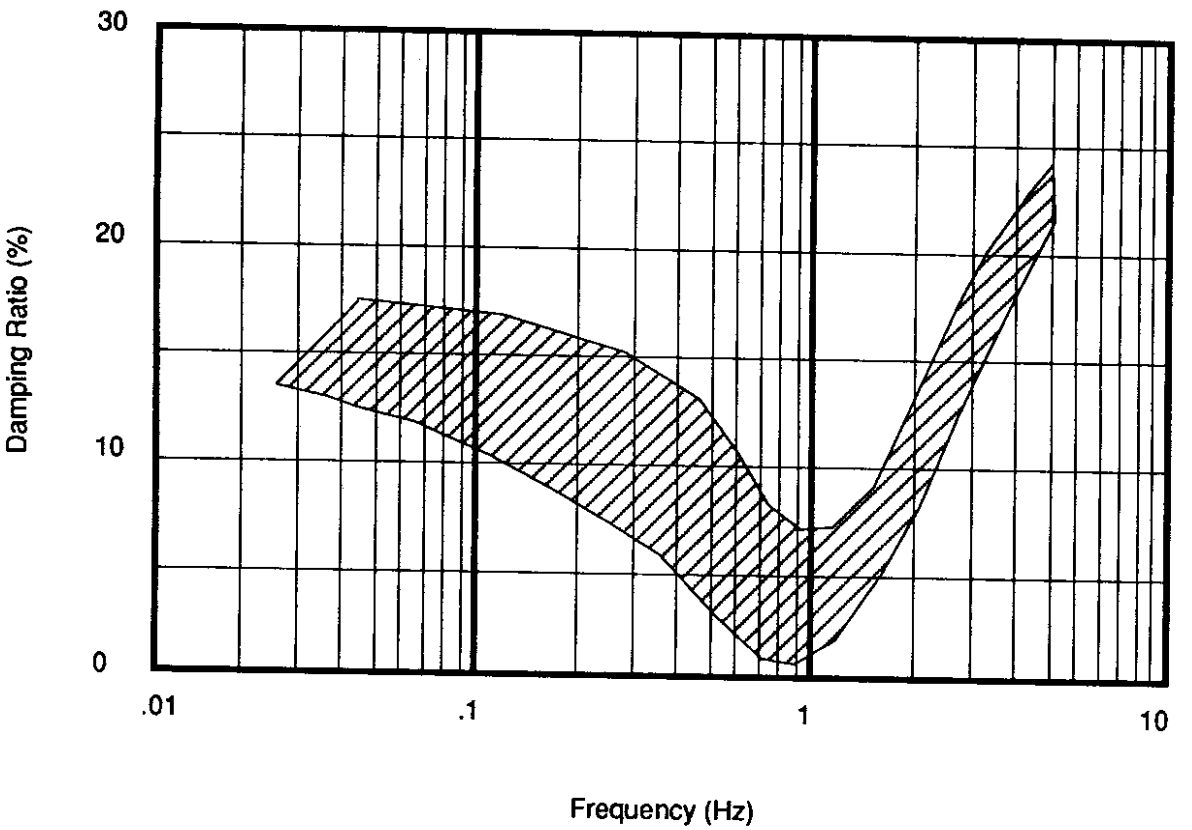

Figure 31. Observed Variation of Damping Ratio with Loading Frequency in Phase I Tests

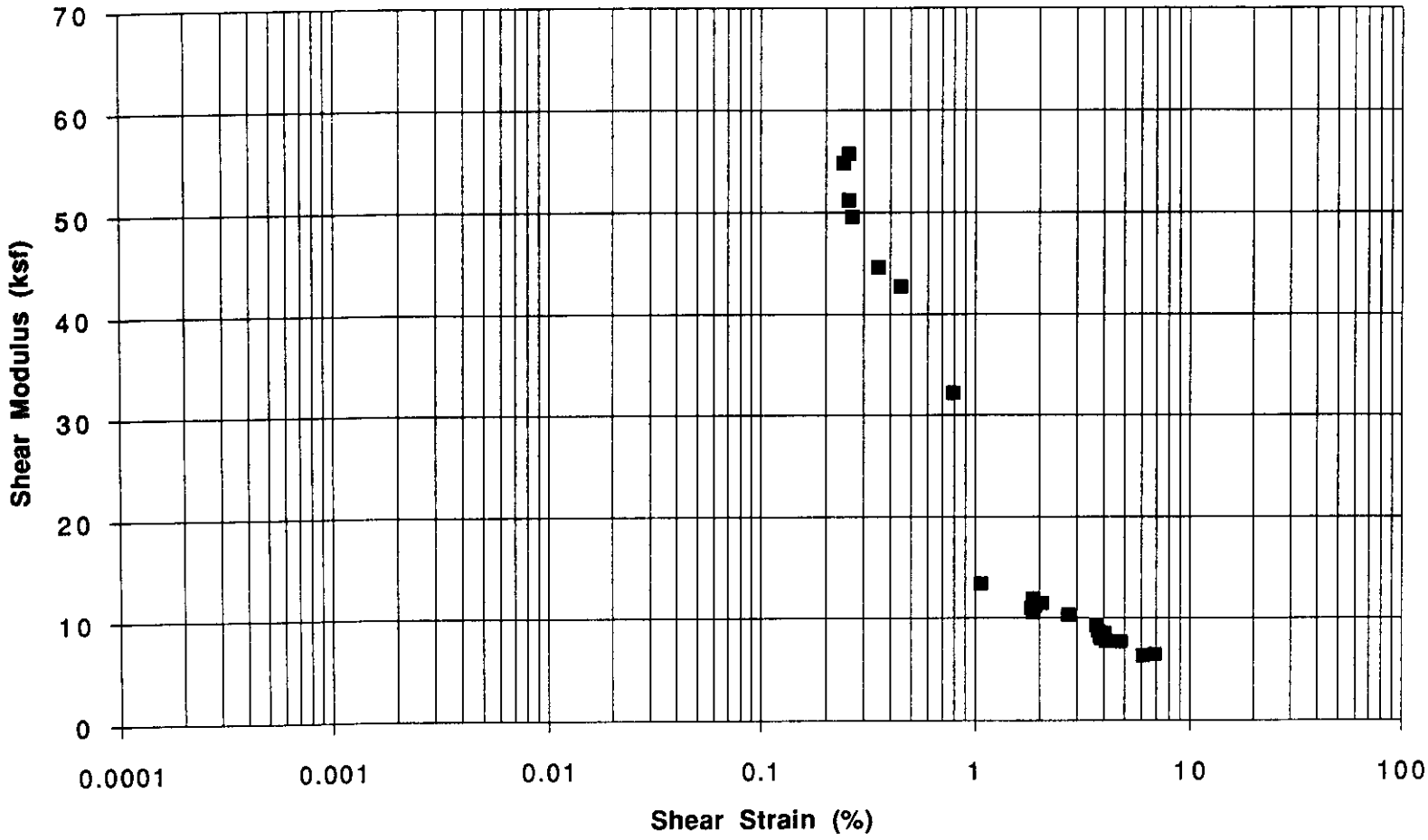

Figure 32. Strain-Dependent Variation of Shear Modulus for Sample I-1

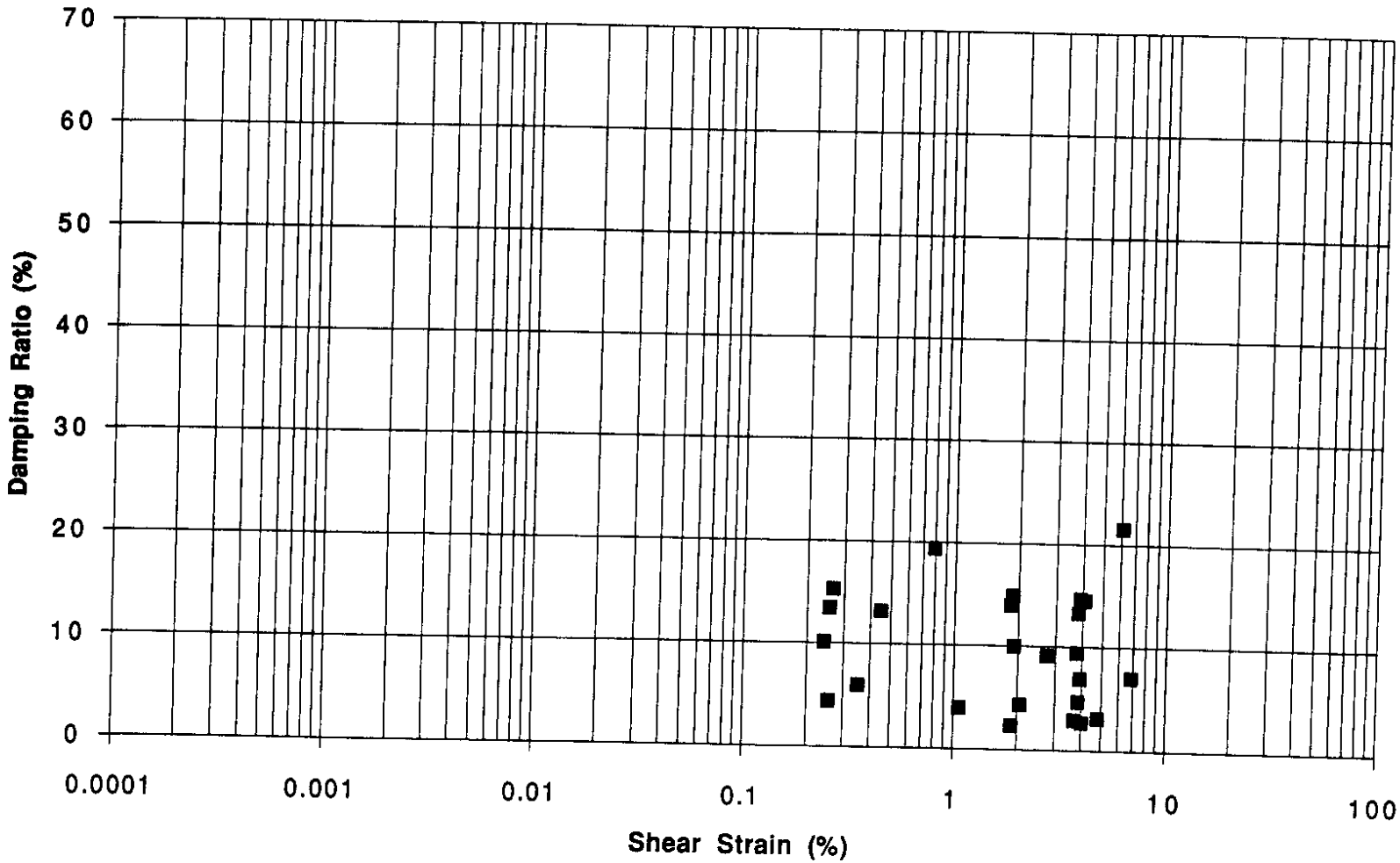

Figure 33. Strain-Dependent Variation of Damping Ratio for Sample I-1

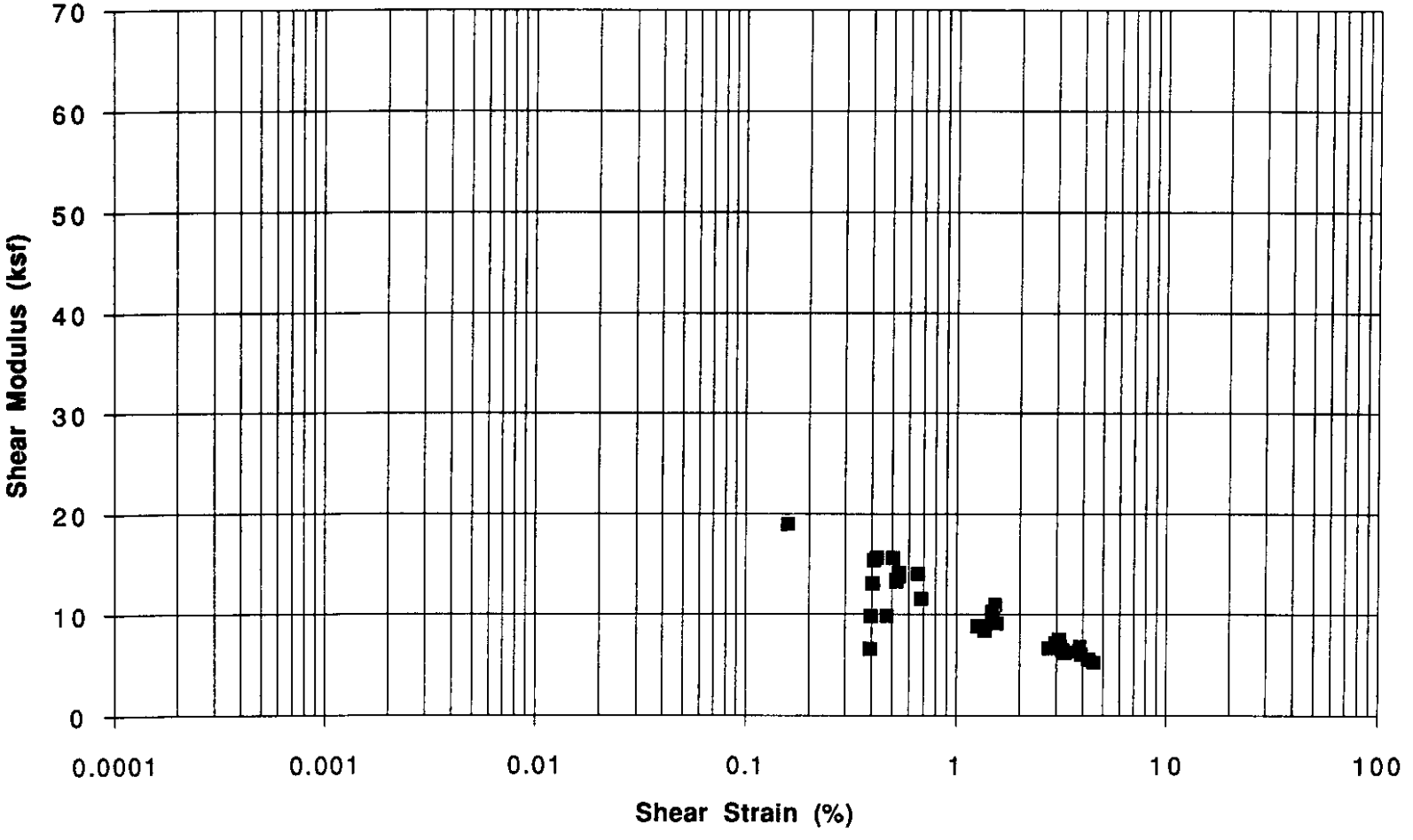

Figure 34. Strain-Dependent Variation of Shear Modulus for Sample I-2

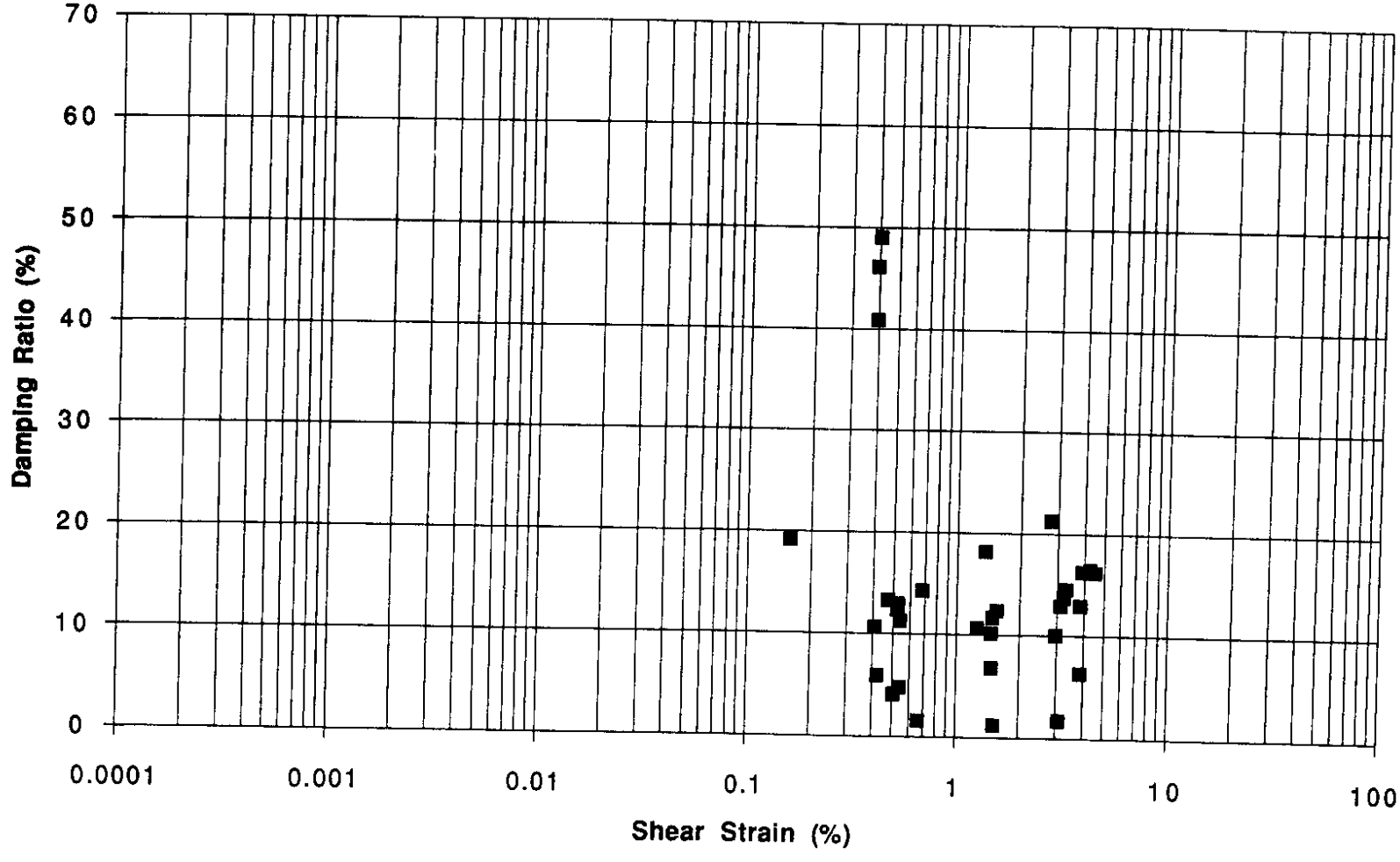

Figure 35. Strain-Dependent Variation of Damping Ratio for Sample I-2

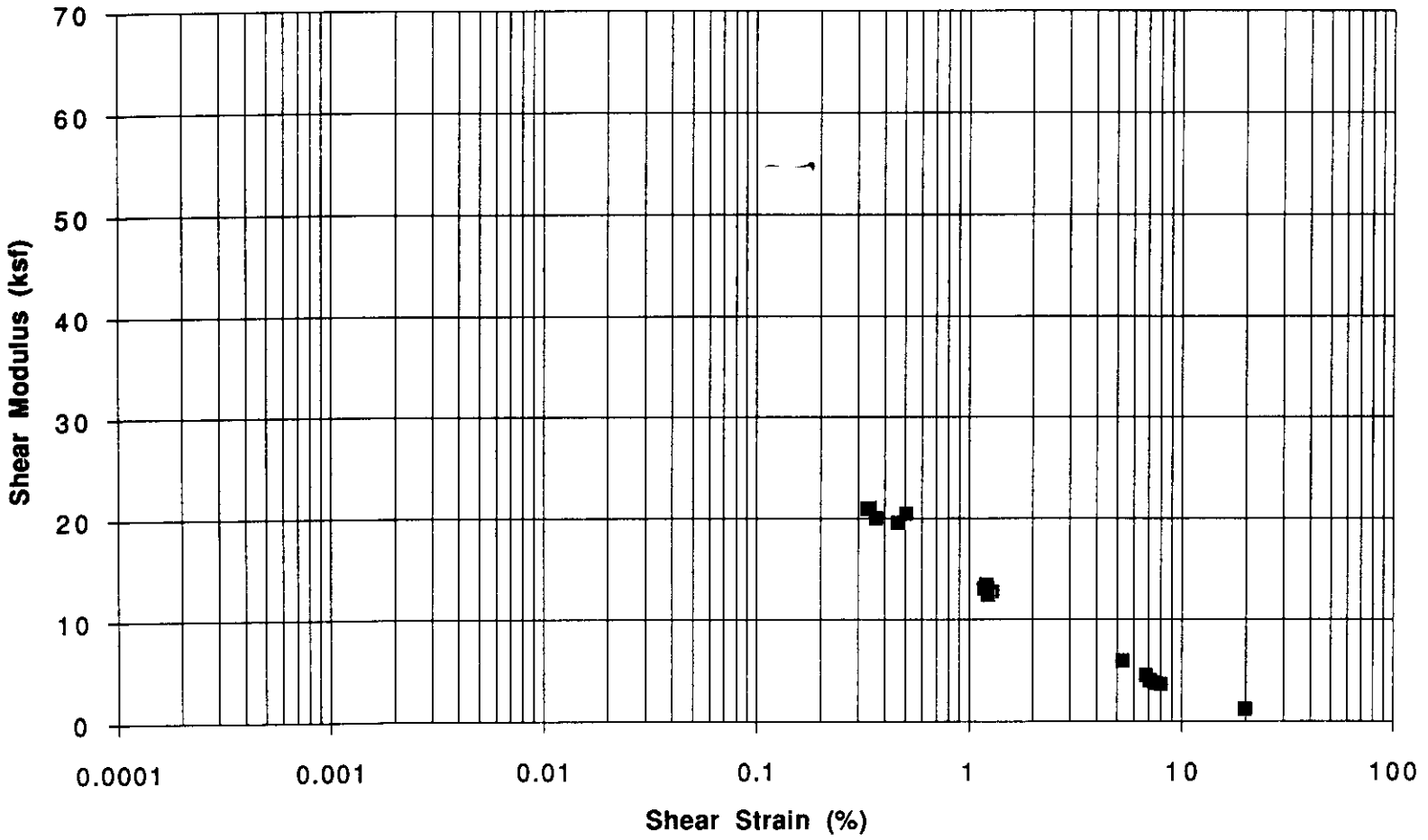

Figure 36. Strain-Dependent Variation of Shear Modulus for Sample I-3

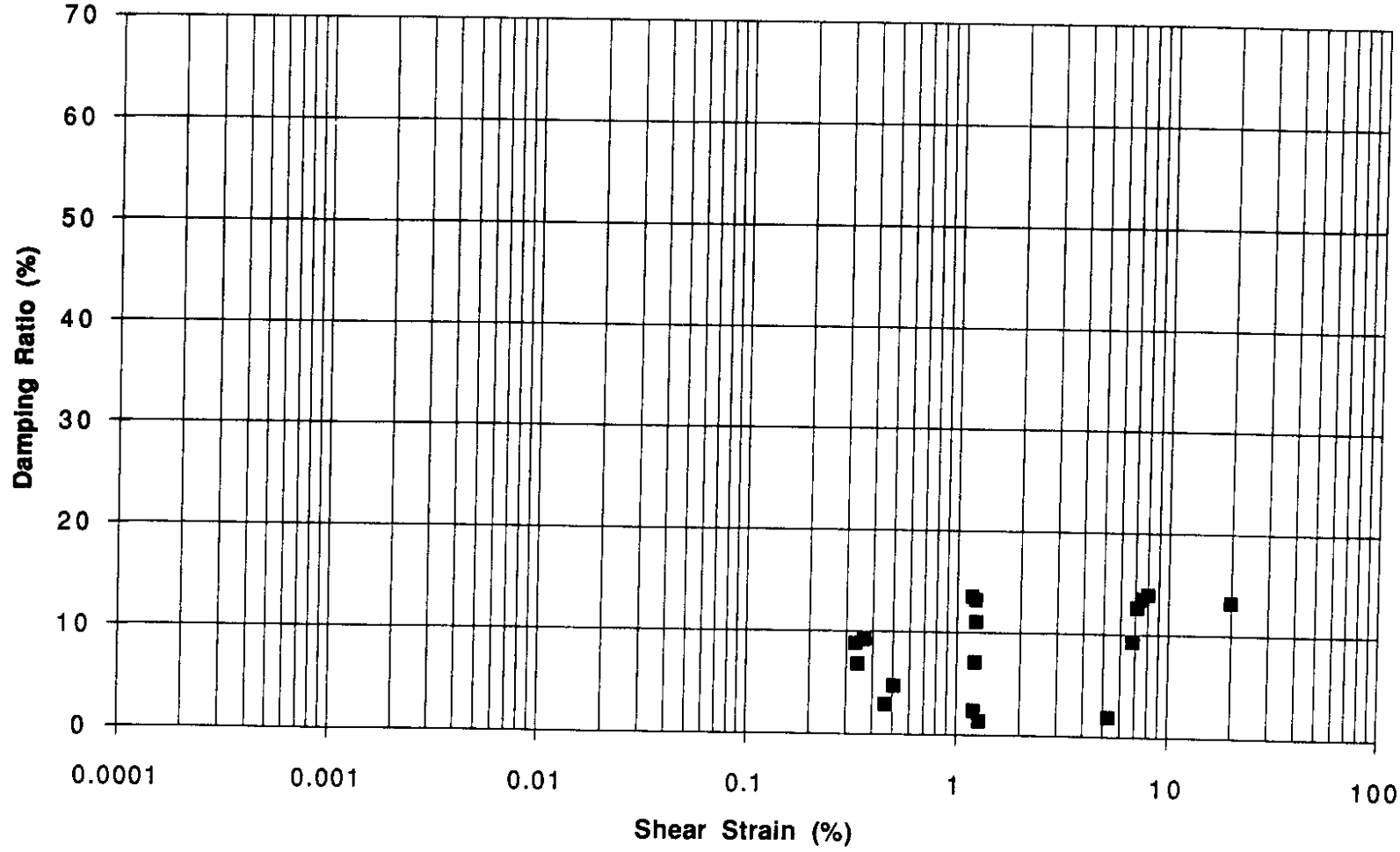

Figure 37. Strain-Dependent Variation of Damping Ratio for Sample I-3

strain level of interest divided by the maximum shear modulus, G_{max}, which is mobilized only at very low strains. In the Phase I tests, however, the G_{max} values computed from the in-situ shear wave velocities were inconsistent with those from the cyclic triaxial tests. The source of the inconsistency could not be determined; however use of the field G_{max} values to normalize the laboratory moduli appeared to be inappropriate. The laboratory shear moduli were then normalized by the shear modulus at a different reference strain level, one that could be attained in the laboratory tests. The shear moduli for samples I-1 through I-3, normalized with a reference shear strain of 0.3 percent, are shown in Figures 38, 39, and 40. These figures indicate consistent behavior at shear strain levels greater than about 0.2 percent.

When the standard CKC loading system was modified with an external analog function generator to drive the electro-pneumatic loader and a PC-based data acquisition system to acquire the test data, the hysteretic behavior of the samples could be monitored during testing. At low frequencies, the hysteresis loops looked as expected, with the peak shear stress reached before the peak shear strain (positive phase angle, consequently positive damping). As the loading frequency approached 1 Hz, the response of the sample appeared to be virtually linearly elastic (nearly zero phase angle, consequently very little damping). However, when the loading frequency increased above 1 Hz, the peak shear strain appeared to be reached before the peak shear stress, i.e., the hysteresis loops were being generated in the counter-clockwise direction (negative phase angle, implying negative damping). Because a negative phase angle is not possible for real materials, these results suggested that the recorded data from Phase I tests were in error. Isolating and testing each component in the instrumentation and data acquisition systems revealed that the signal conditioning module for the load cell output, which essentially consisted of an amplifier and filter circuit, was introducing a nearly constant time delay of 32 msec into the load cell readings. At low loading frequencies, the effect of this time delay was minimal, but at higher loading frequencies, it introduced a substantial, though

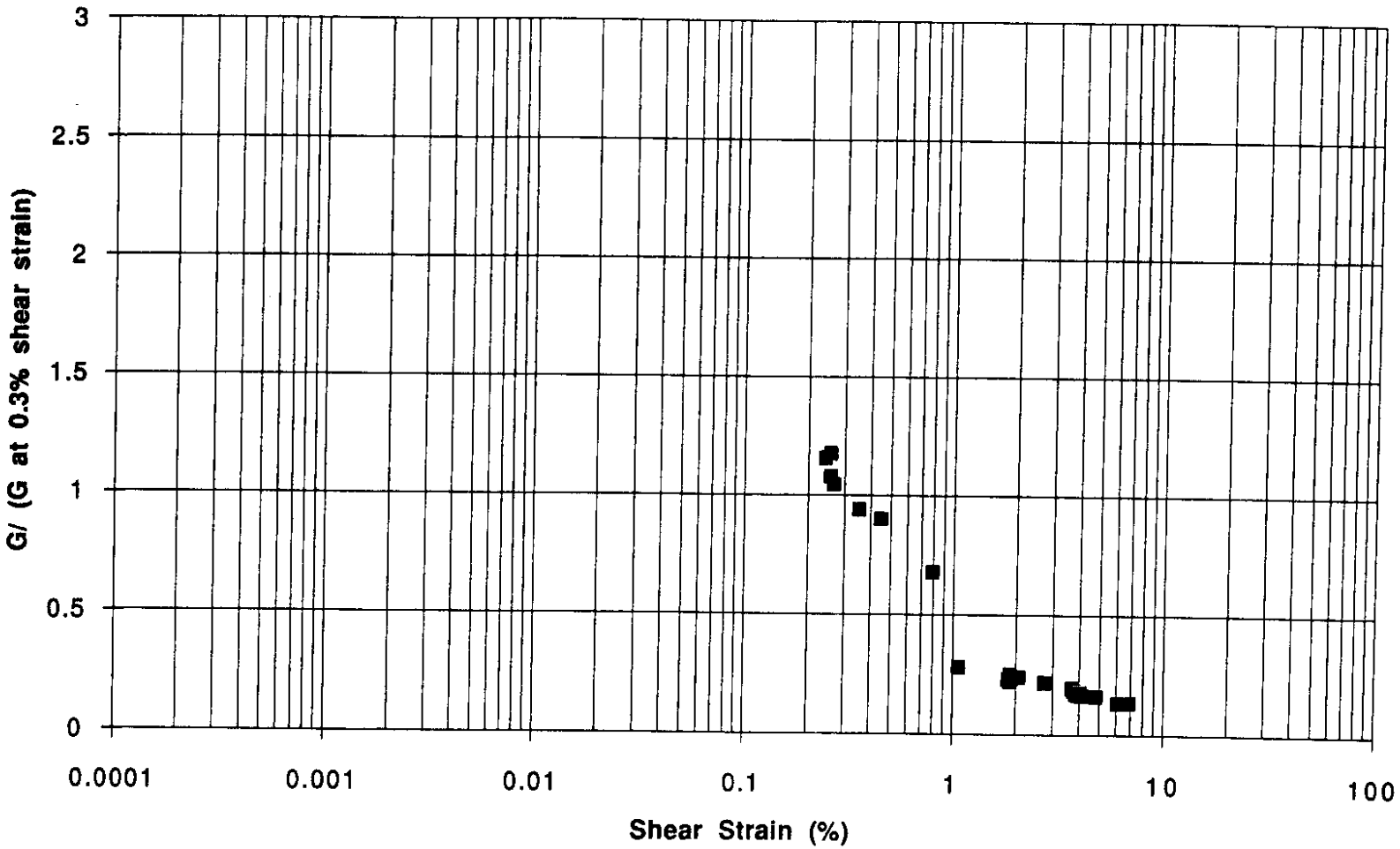

Figure 38. Strain-Dependent Variation of Normalized Shear Modulus for Sample I-1

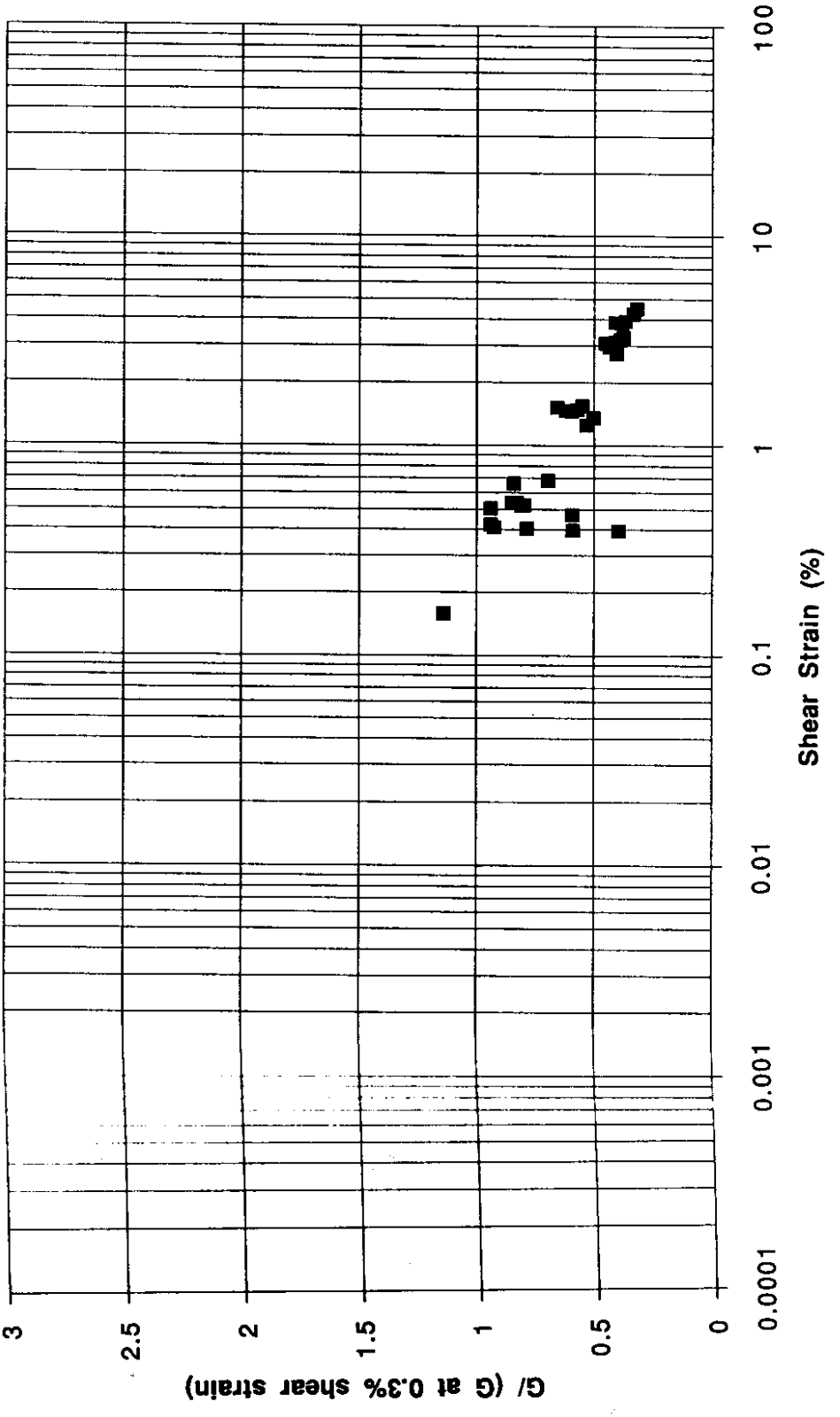

Figure 39. Strain-Dependent Variation of Normalized Shear Modulus for Sample I-2

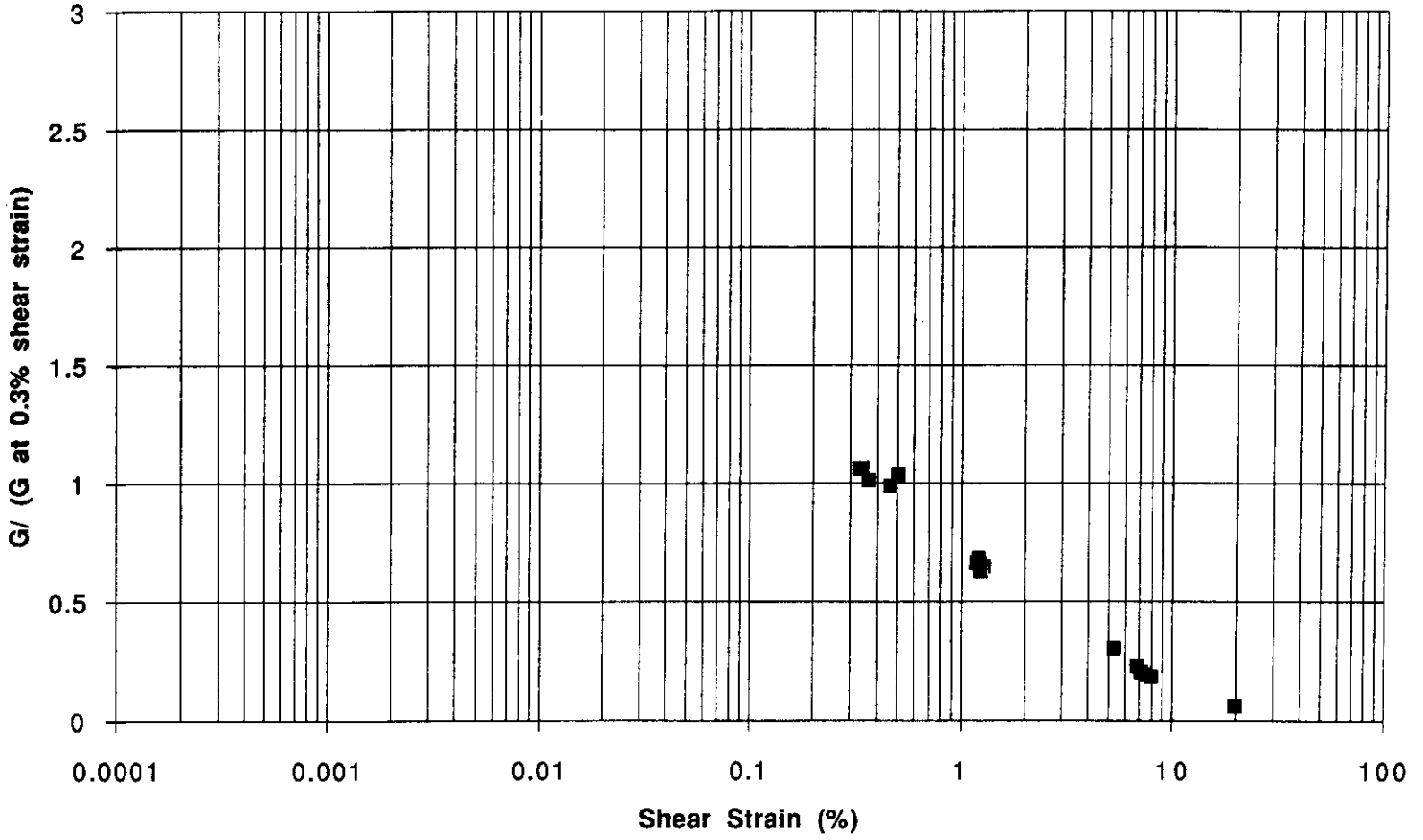

Figure 40. Strain-Dependent Variation of Normalized Shear Modulus for Sample I-3

artificial, negative phase angle into the data. The strong frequency dependence of damping observed in the earlier Phase I tests was at this point questioned. On the other hand, the stiffness data from the Phase I tests were not significantly affected by the instrumentation error.

Phase II Tests

The Phase II tests were performed on samples from Boring 2 with the variable frequency, strain-controlled cyclic loading system. A new load cell signal conditioning module was acquired, tested, and installed in the instrumentation system. Limitations of the loading system imposed a lower shear strain limit of approximately 0.07 percent and, because in-situ shear wave velocities were not measured at the location of Boring 2, shear moduli at lower strain levels could not be estimated.

The shear modulus and damping ratio of the Mercer Slough peat varied in the Phase II tests, as shown in Figures 41 through 48. The tests showed similar degradation of shear modulus with increasing shear strain, although the results could not be normalized with respect to G_{max}, since G_{max} was not measured. However, normalizing the shear moduli with respect to the shear modulus at the 0.3 percent reference strain level allowed comparison of the Phase I and Phase II stiffnesses. The results, shown in Figure 49, indicated that the moduli from the Phase I and Phase II test degraded at similar rates over the range of shear strains greater than about 0.1 percent. The variation of damping ratio with loading frequency was still evident, but it was much less pronounced than that observed in the Phase I tests. The damping ratios, however, appeared to decrease with increasing strain amplitude.

Phase III Tests

The Phase III tests were intended to provide data on the variation of shear modulus over the entire range of strains from very small to large. The piezoelectric bender elements were used to measure the shear wave velocity of each sample before cyclic testing. This sample-specific shear wave velocity was used to evaluate the shear

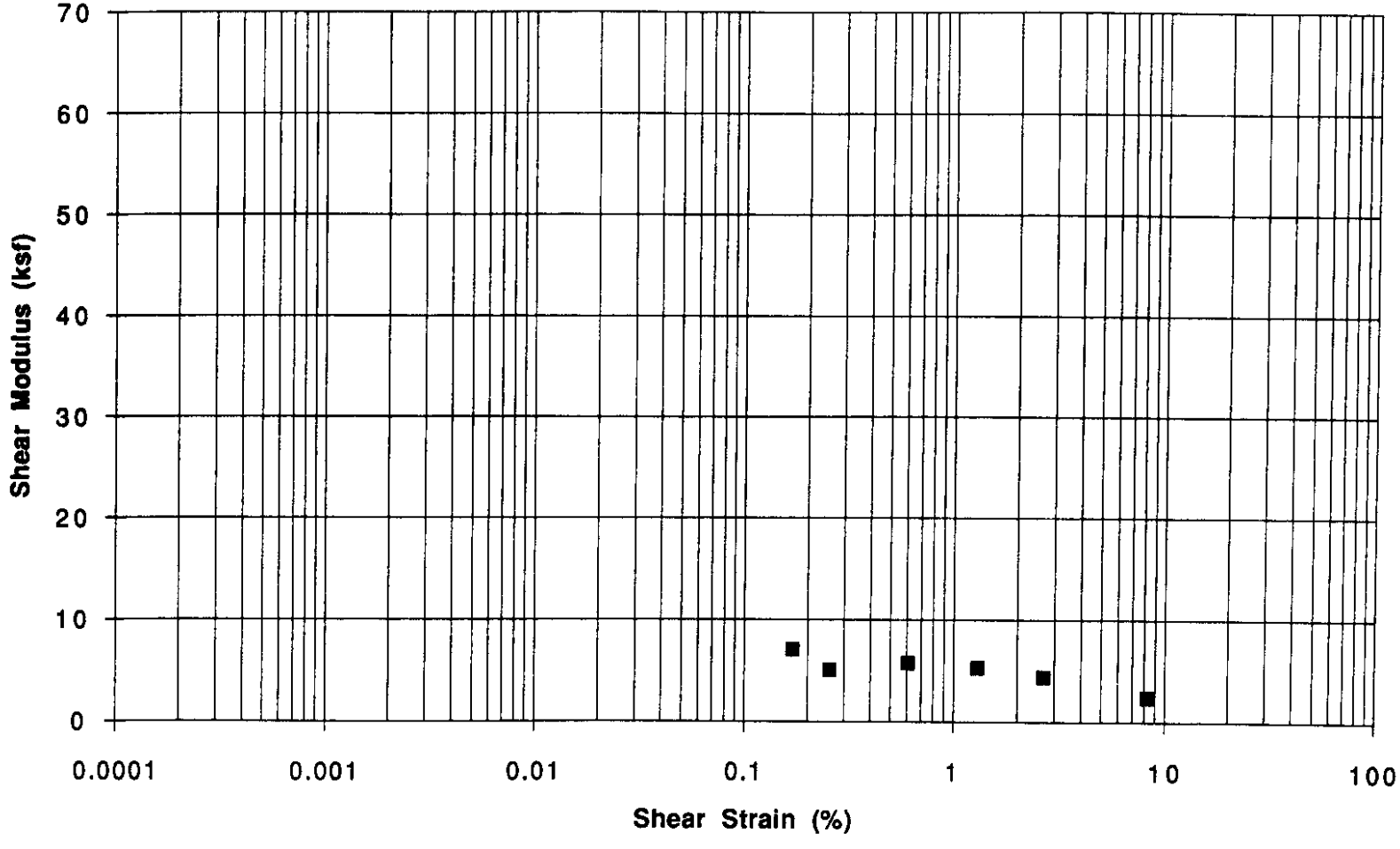

Figure 41. Strain-Dependent Variation of Shear Modulus for Sample II-1

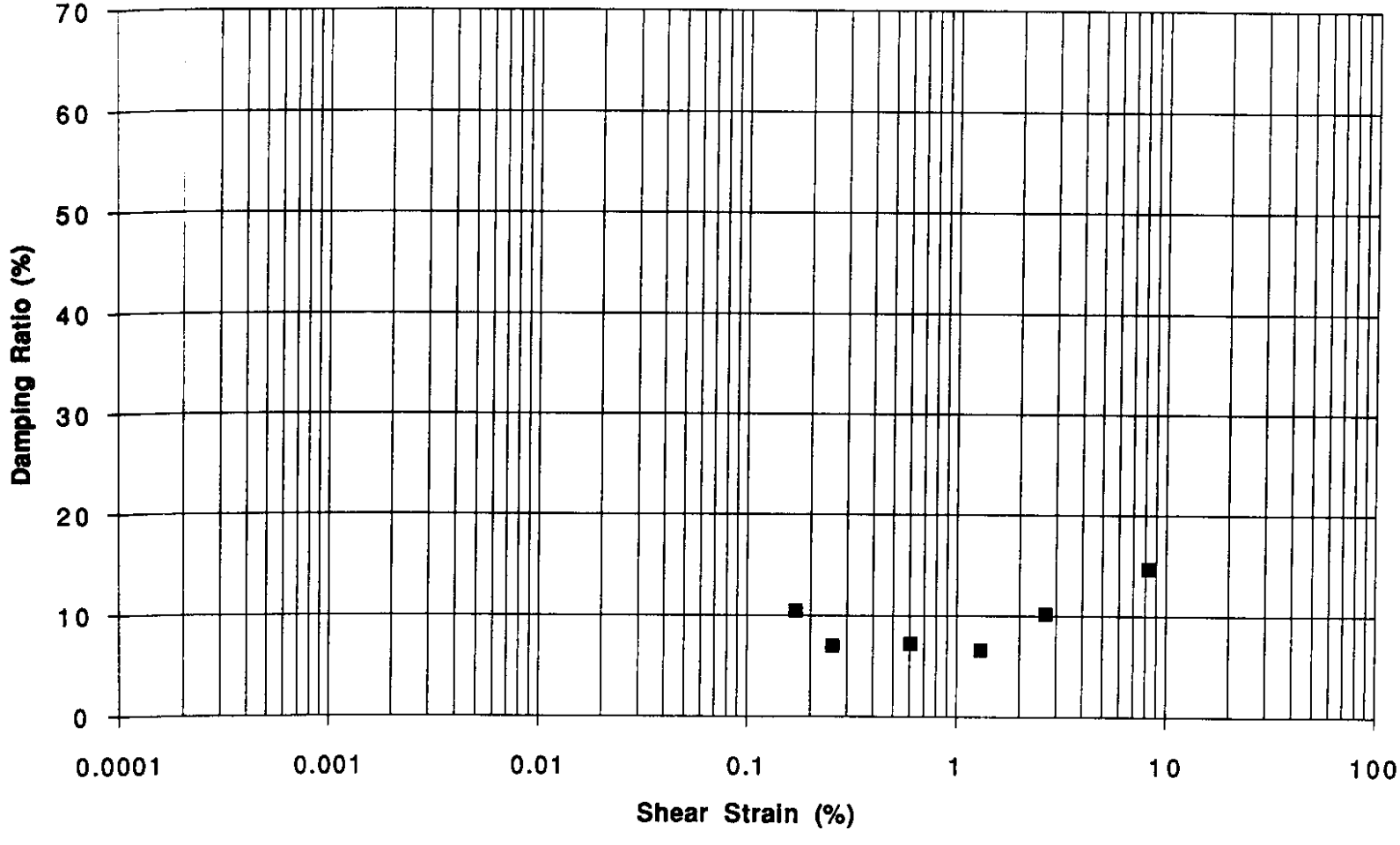

Figure 42. Strain-Dependent Variation of Damping Ratio for Sample II-1

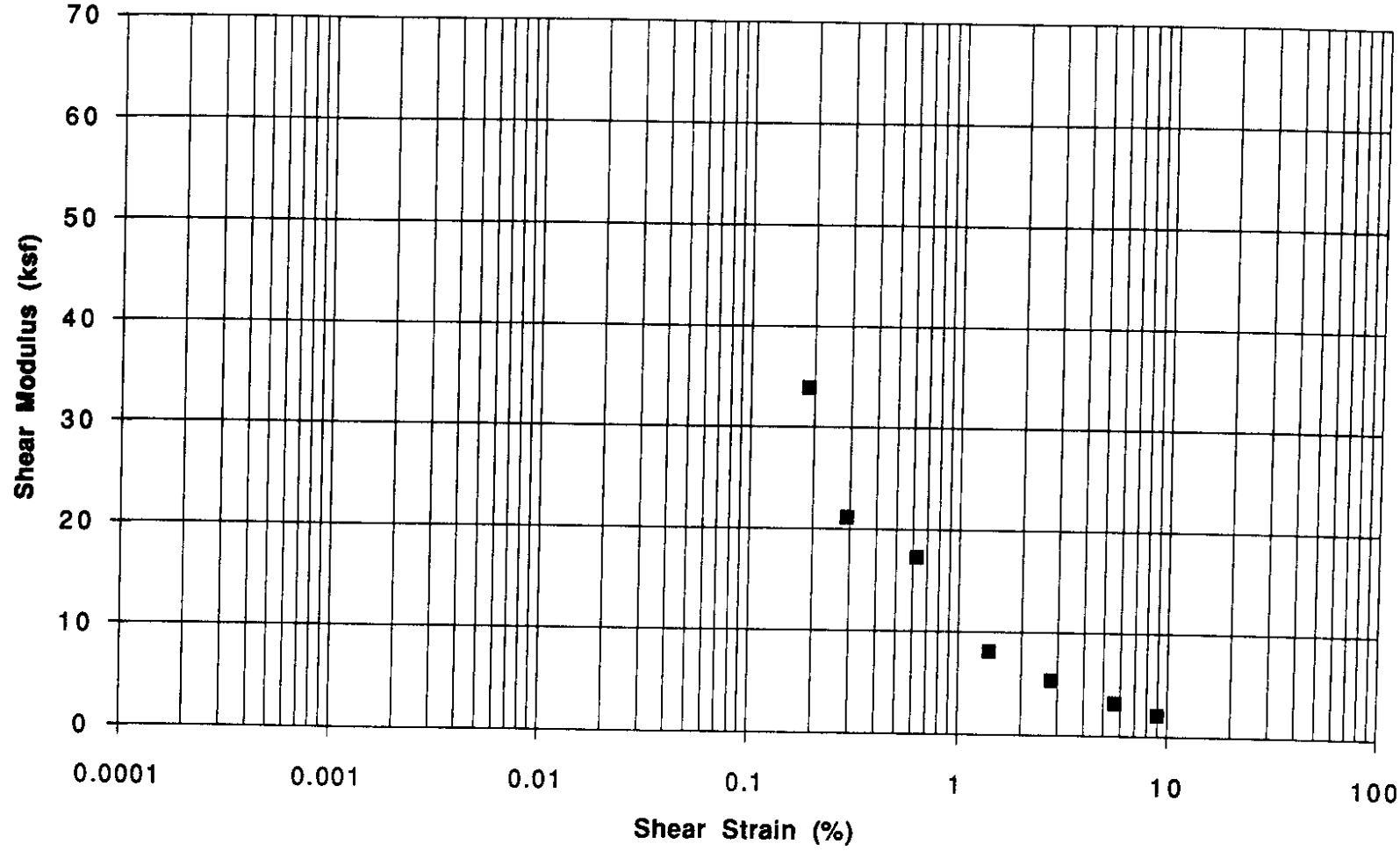

Figure 43. Strain-Dependent Variation of Shear Modulus for Sample II-2

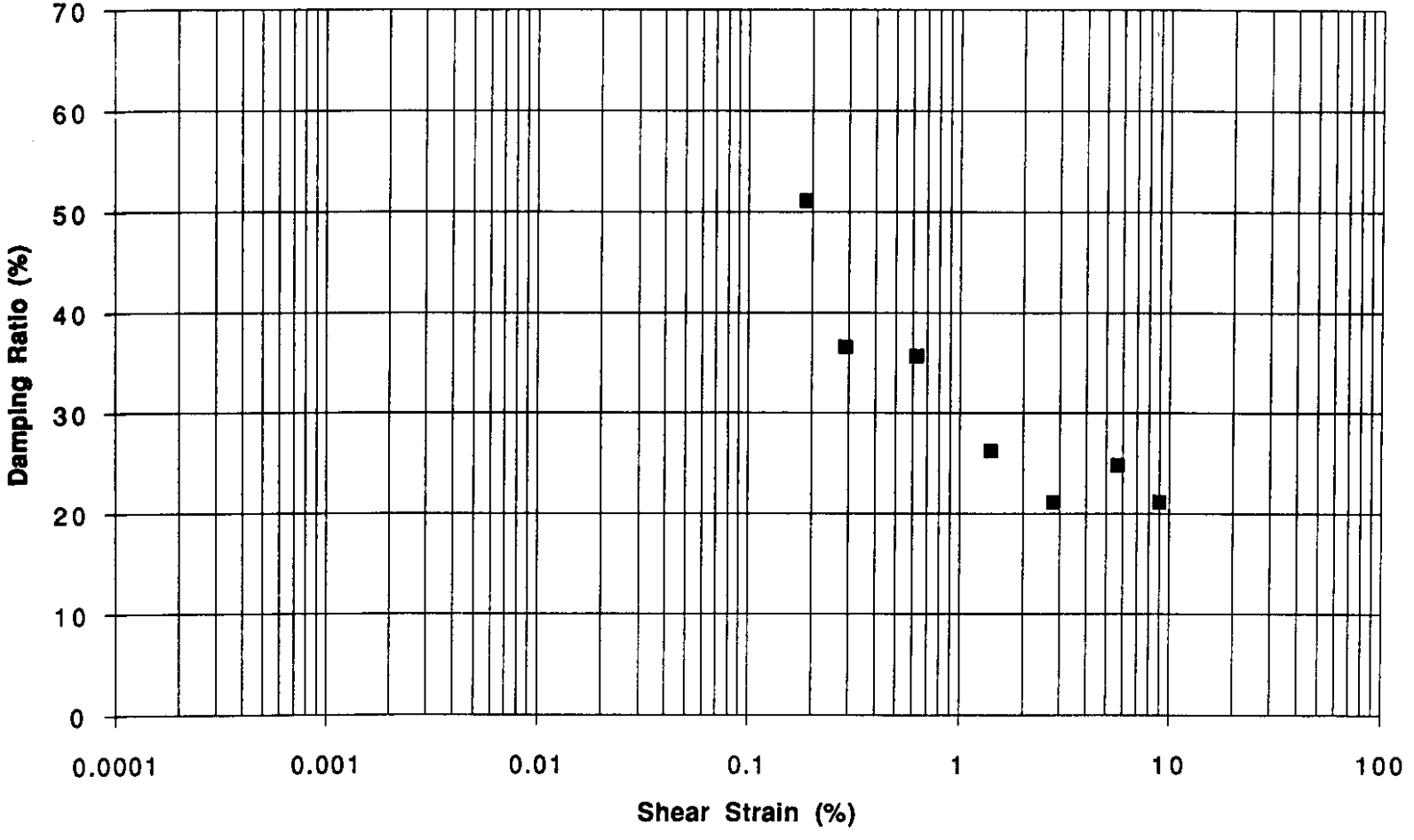

Figure 44. Strain-Dependent Variation of Damping Ratio for Sample II-2

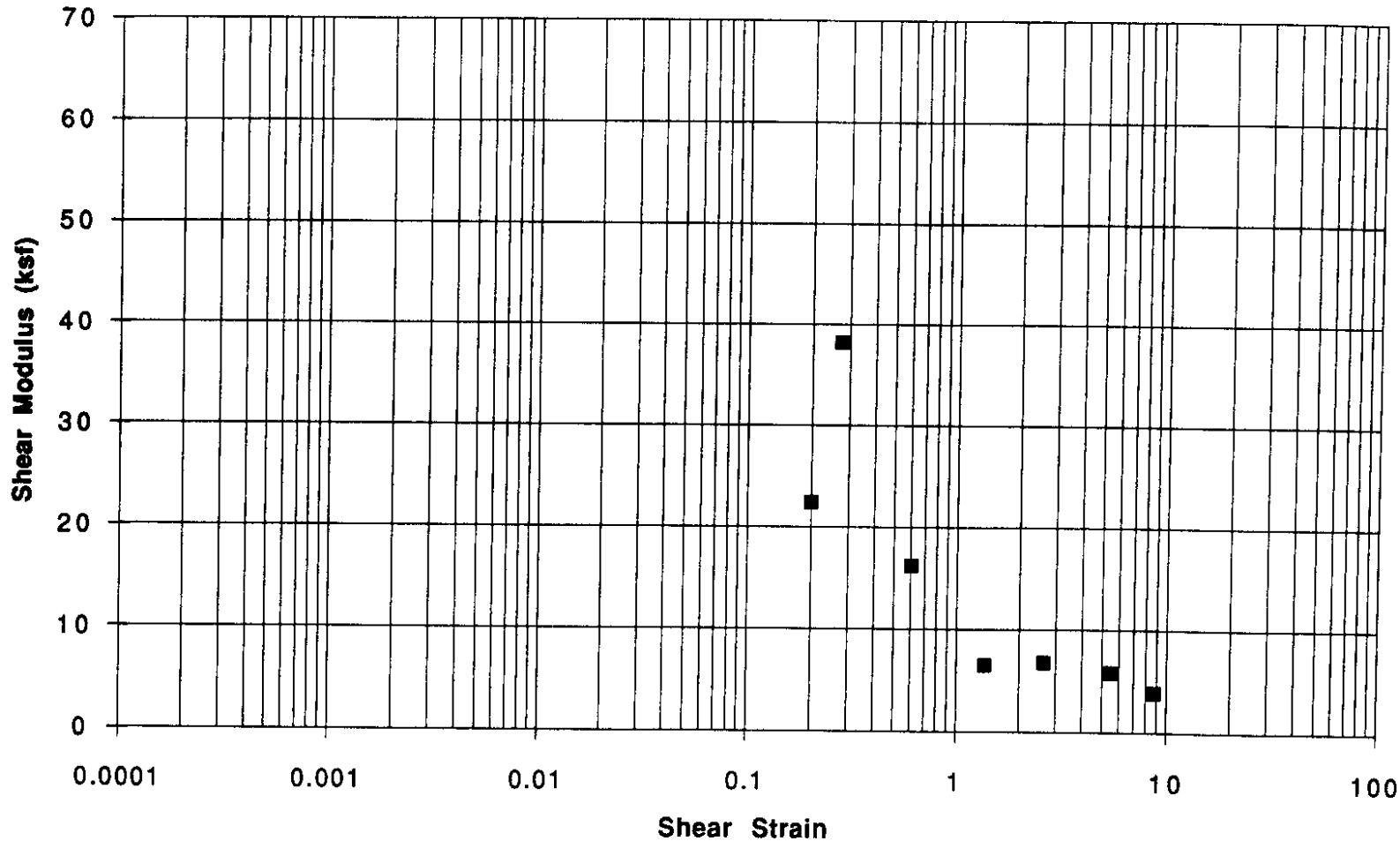

Figure 45. Strain-Dependent Variation of Shear Modulus for Sample II-3

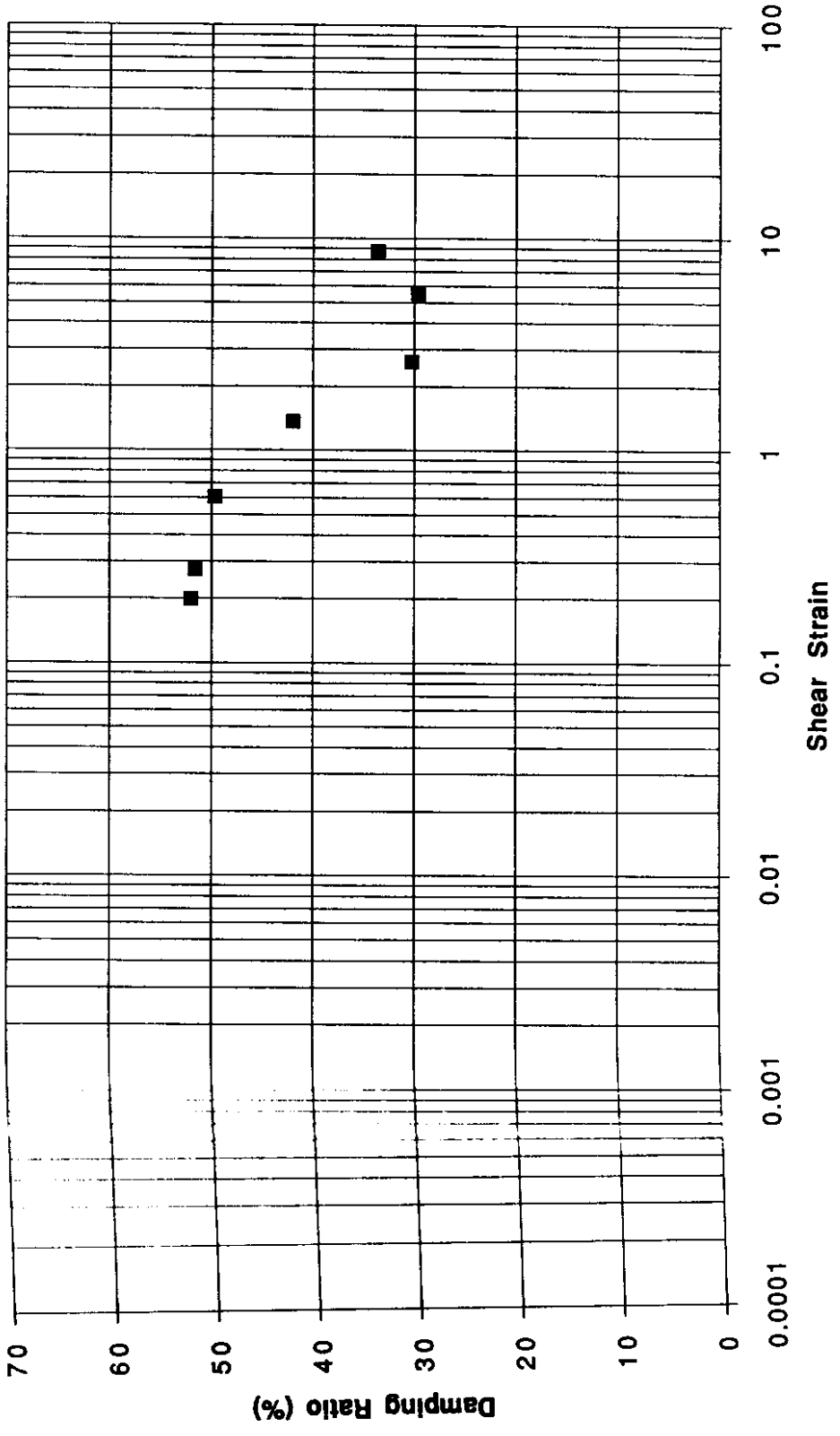

Figure 46. Strain-Dependent Variation of Damping Ratio for Sample II-3

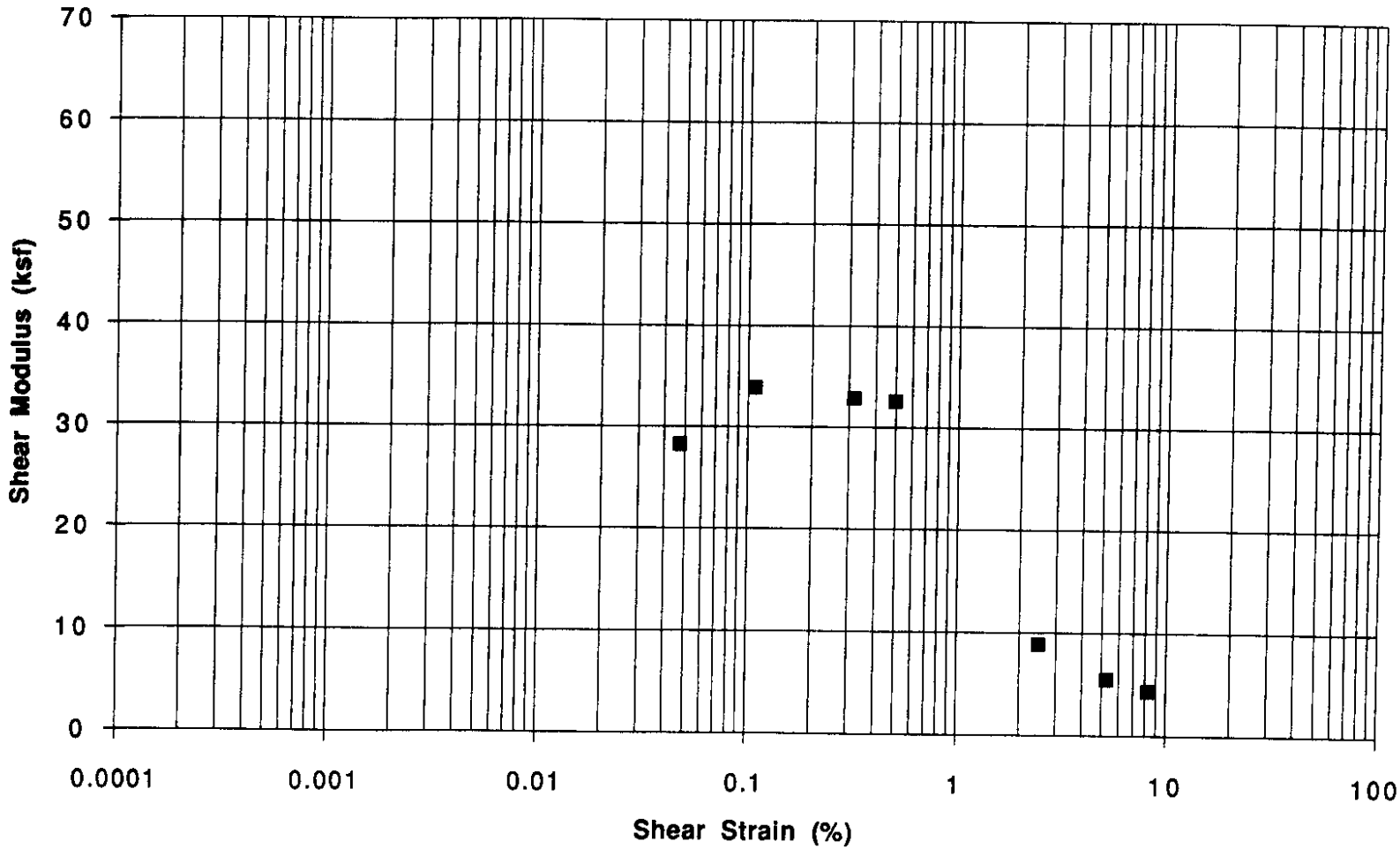

Figure 47. Strain-Dependent Variation of Shear Modulus for Sample II-4

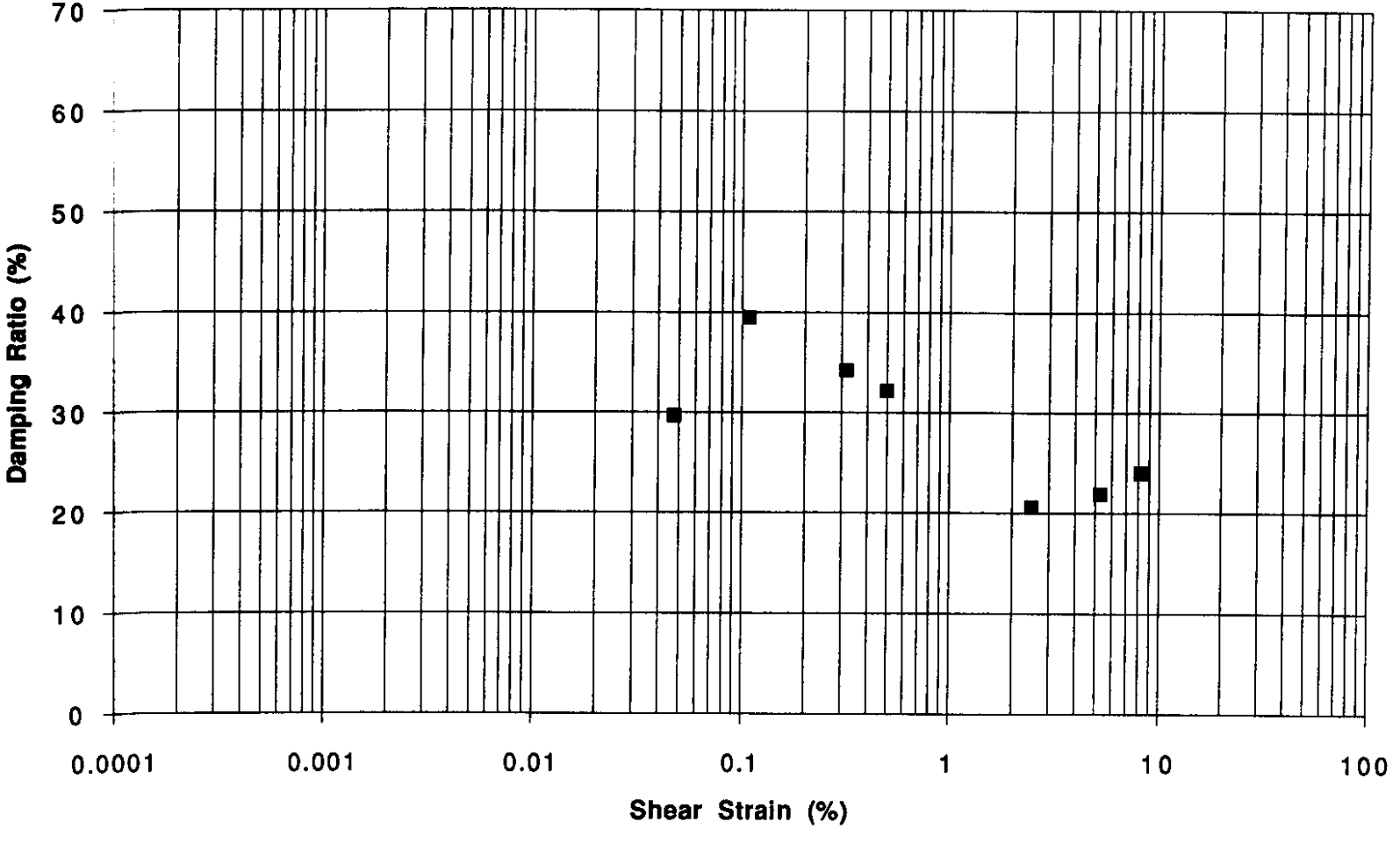

Figure 48. Strain-Dependent Variation of Damping Ratio for Sample II-4

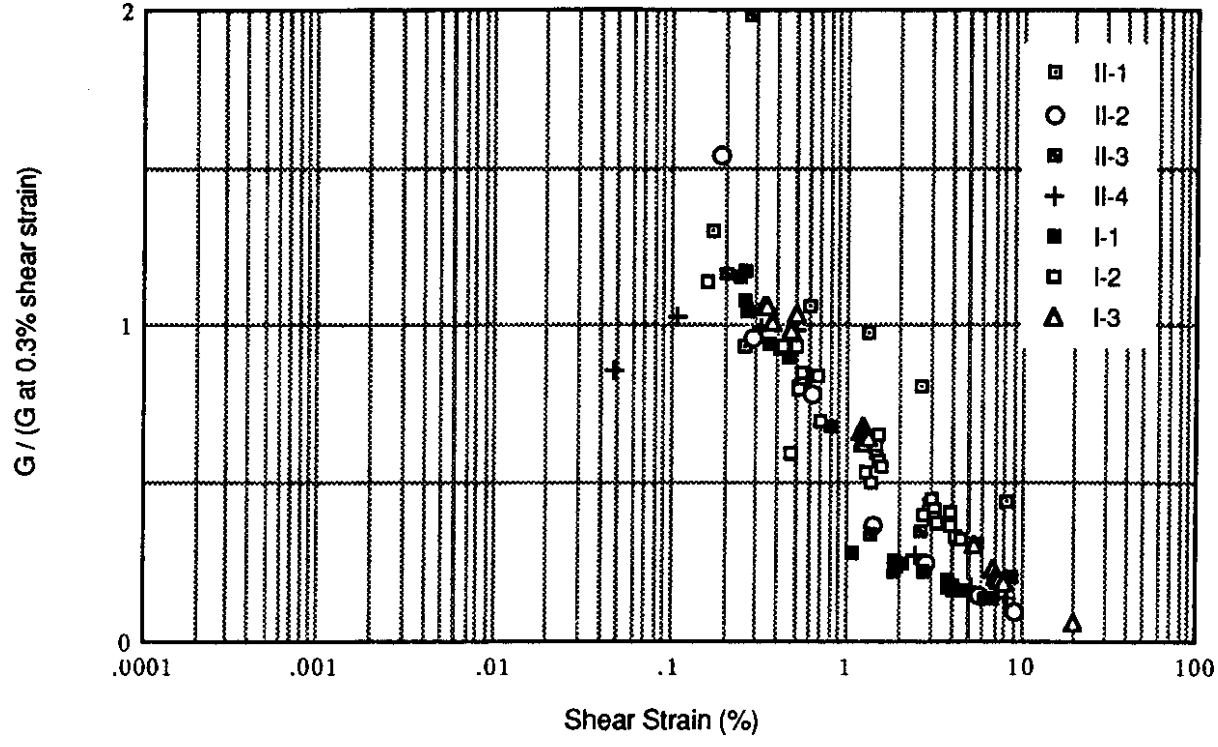

Figure 49. Strain-Dependent Normalized Shear Modulus for all Phase I and Phase II Tests

modulus at very low strains. When this information is combined with the results of the cyclic triaxial tests that correspond to higher strain levels, the stiffness behavior can be properly characterized.

The variation of shear modulus and damping ratio with cyclic shear strain from the Phase III tests is shown in Figures 50 through 57. The results indicated that the shear modulus was nearly constant at very low cyclic shear strains, perhaps up to 0.01 percent. The data from Samples III-1 and III-2 suggested that the shear modulus at intermediate strain (0.01 percent to 0.1 percent) might be slightly larger than those at very low strains. Whether this effect represented the actual behavior of the peat or was a result of experimental uncertainty/incompatibility was not known. At any rate, the effect did not appear to be large. The results also indicated a consistent trend of decreasing damping ratio with increasing shear strain amplitude.

Summary of Dynamic Soil Properties

Dynamic soil properties were measured in a limited number of tests in a three-phase testing program. Though each successive phase of testing represented an improvement in testing capability, many of the data from the early tests remained useful for evaluation of dynamic properties. In the following sections, the data from all tests are combined to provide the best estimate of the dynamic properties of the Mercer Slough peat.

Shear Modulus

The shear modulus of the Mercer Slough peat samples decreased with increasing cyclic shear strain amplitude. The shear modulus at very low strains, G_{max}, was measured on a sample-specific basis only in the Phase III tests. In these tests, however, G_{max} appeared to be approximately 1.6 to 2.7 times the shear modulus at a cyclic shear strain amplitude of 0.3 percent. When the normalized (with respect to $G_{0.3\%}$) shear moduli from all tests were plotted as a function of cyclic shear strain amplitude, as in Figure 58, the general rate of shear modulus degradation could be seen. Figure 59 shows

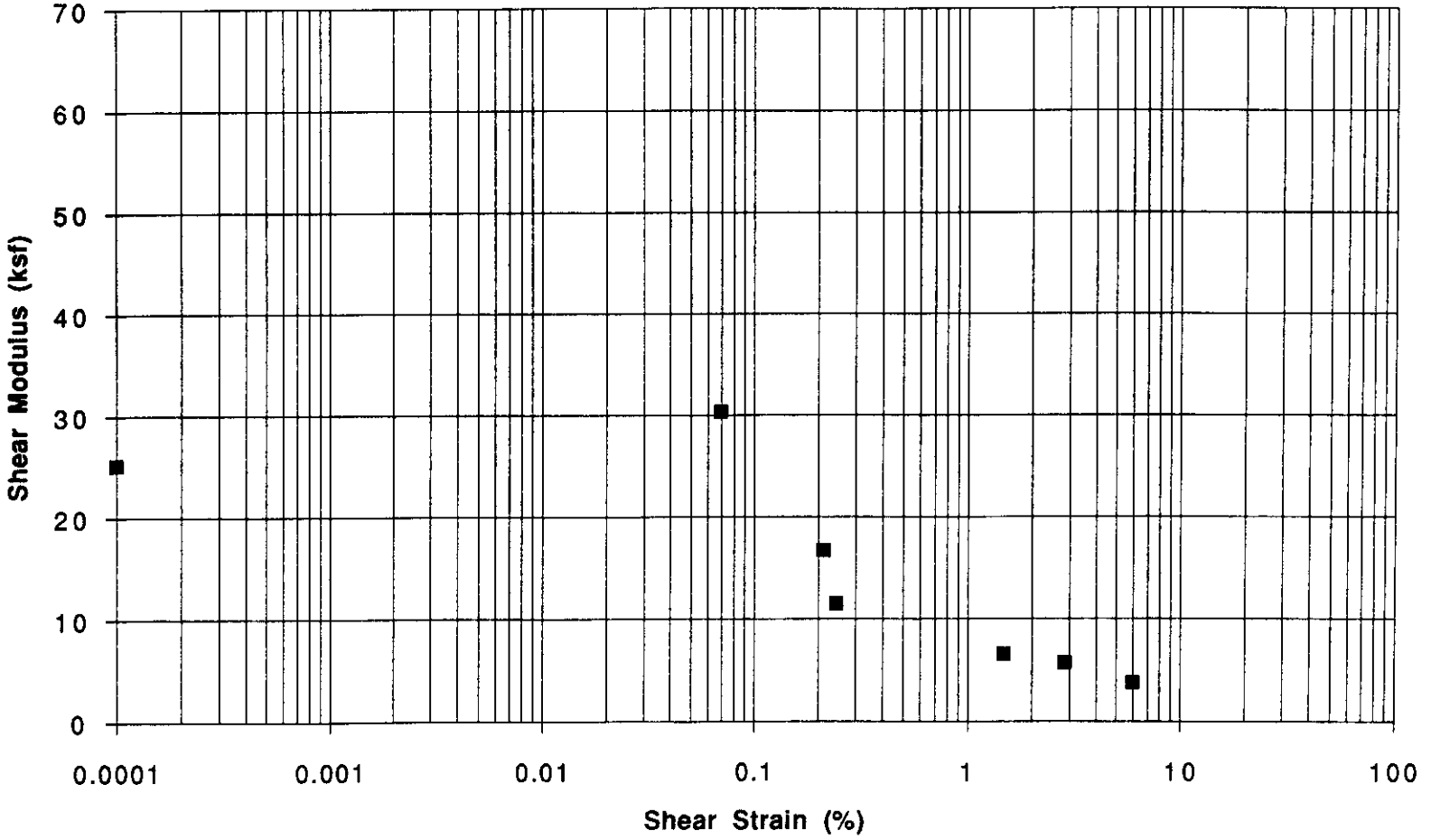

Figure 50. Strain-Dependent Variation of Shear Modulus for Sample III-1

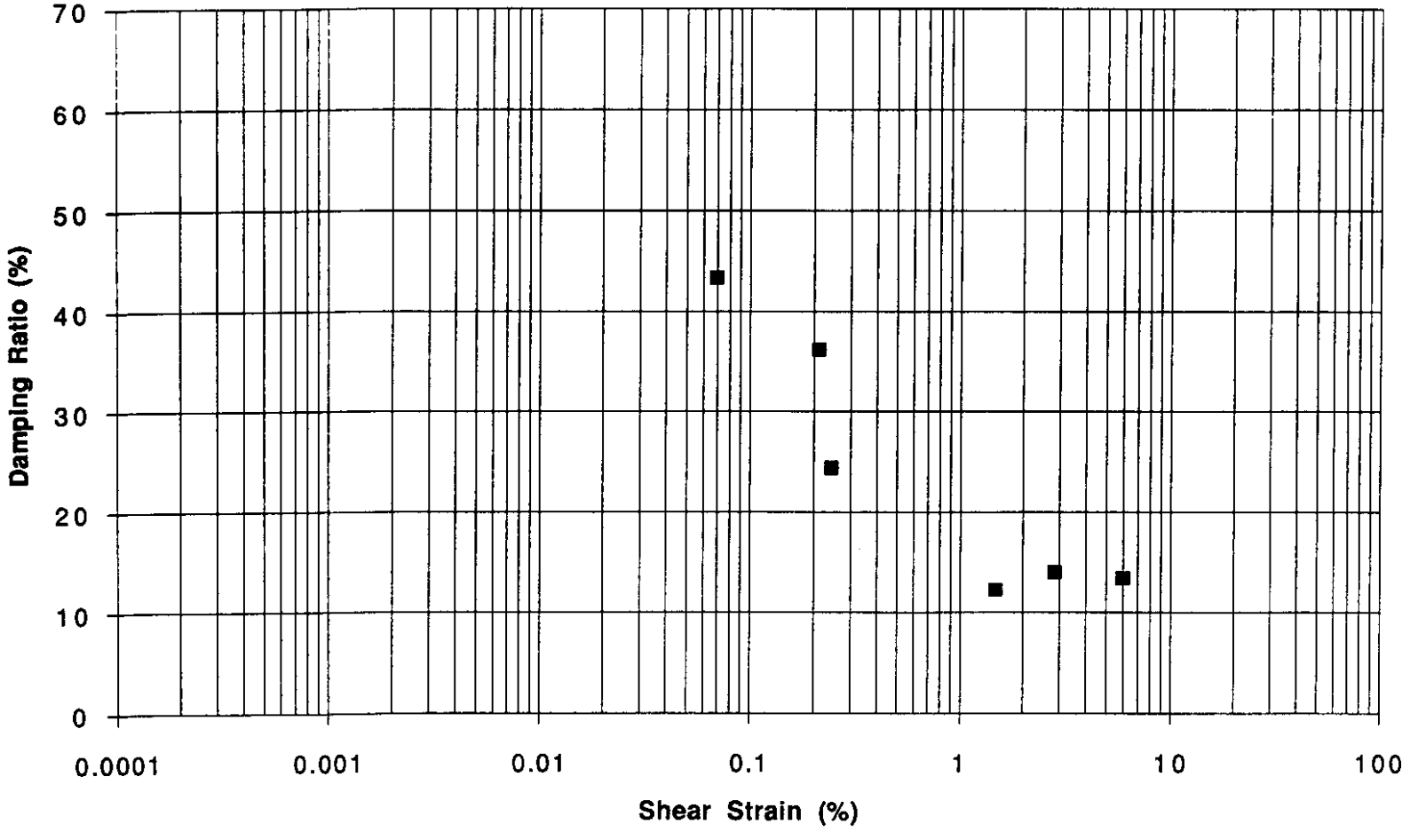

Figure 51. Strain-Dependent Variation of Damping Ratio for Sample III-1

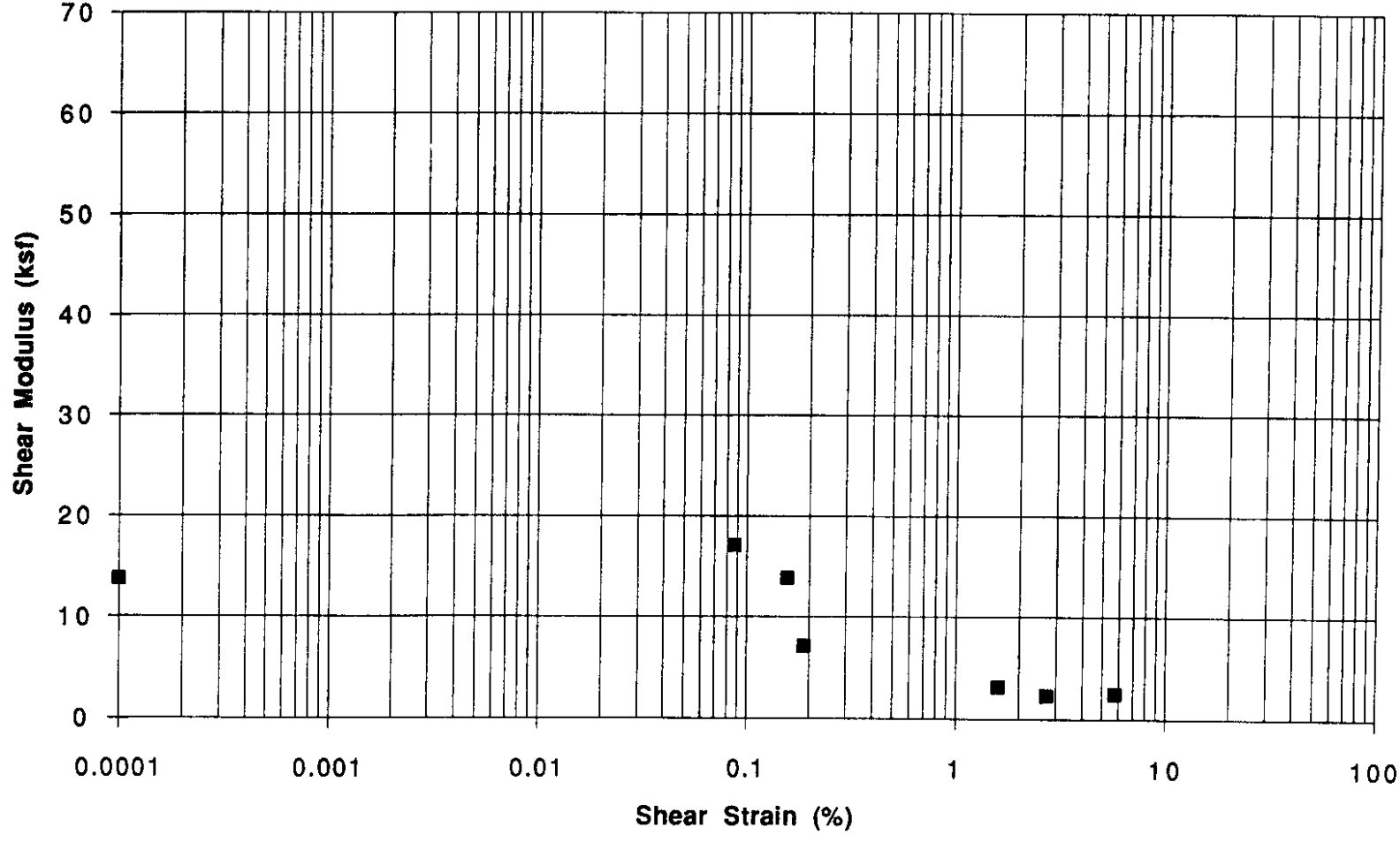

Figure 52. Strain-Dependent Variation of Shear Modulus for Sample III-2

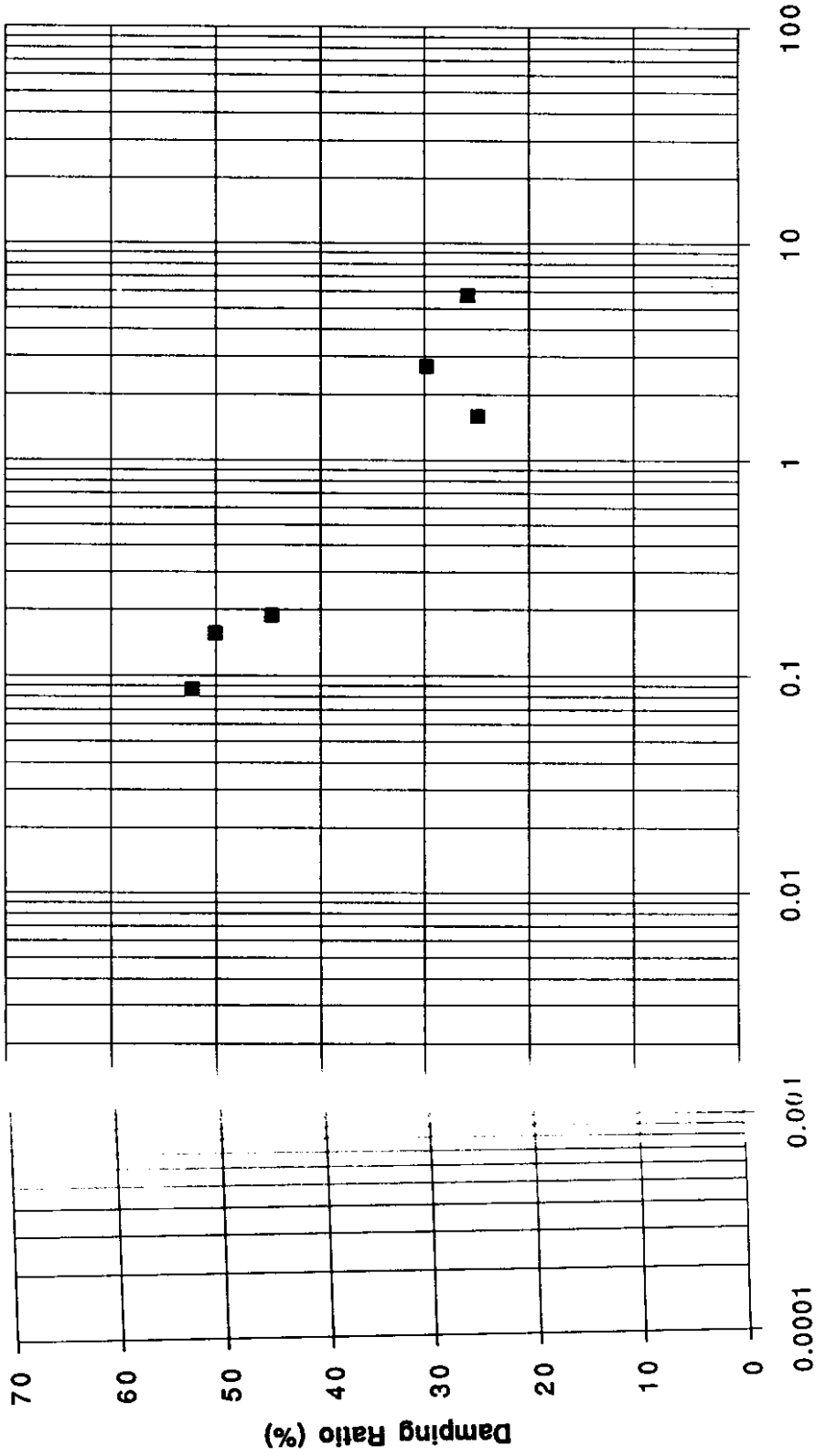

Figure 53. Strain-Dependent Variation of Damping Ratio for Sample III-2

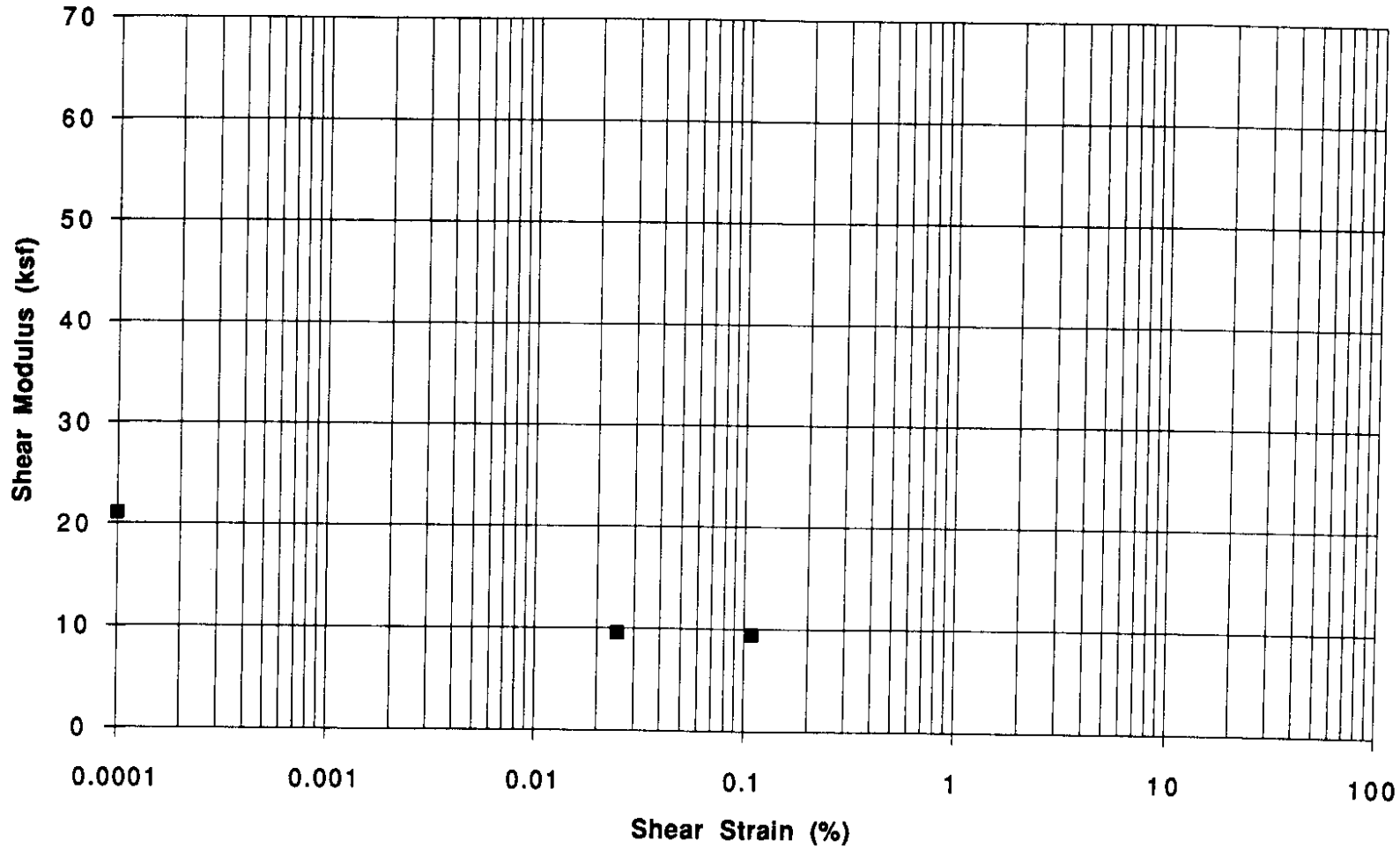

Figure 54. Strain-Dependent Variation of Shear Modulus for Sample III-3

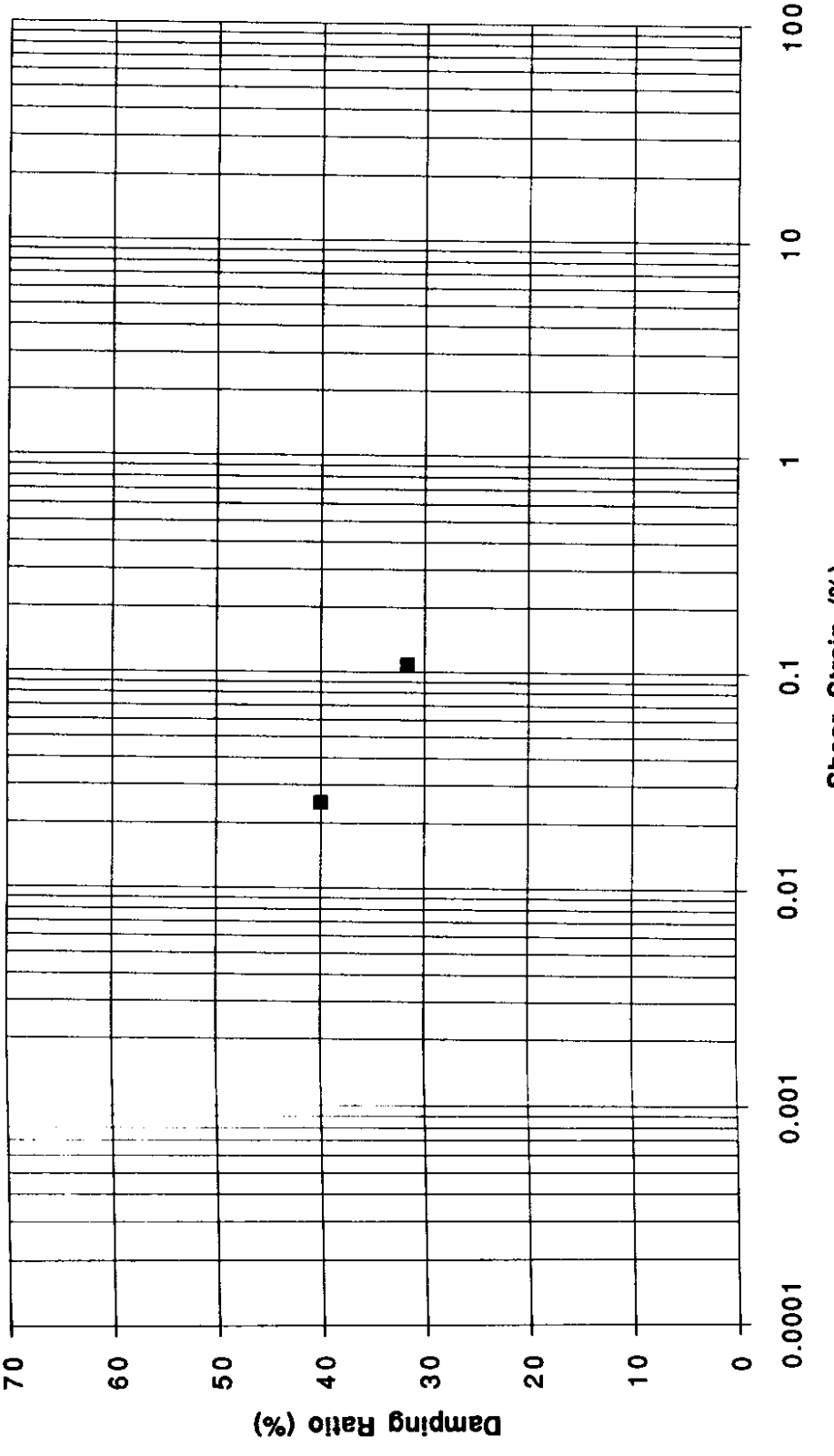

Figure 55. Strain-Dependent Variation of Damping Ratio for Sample III-3

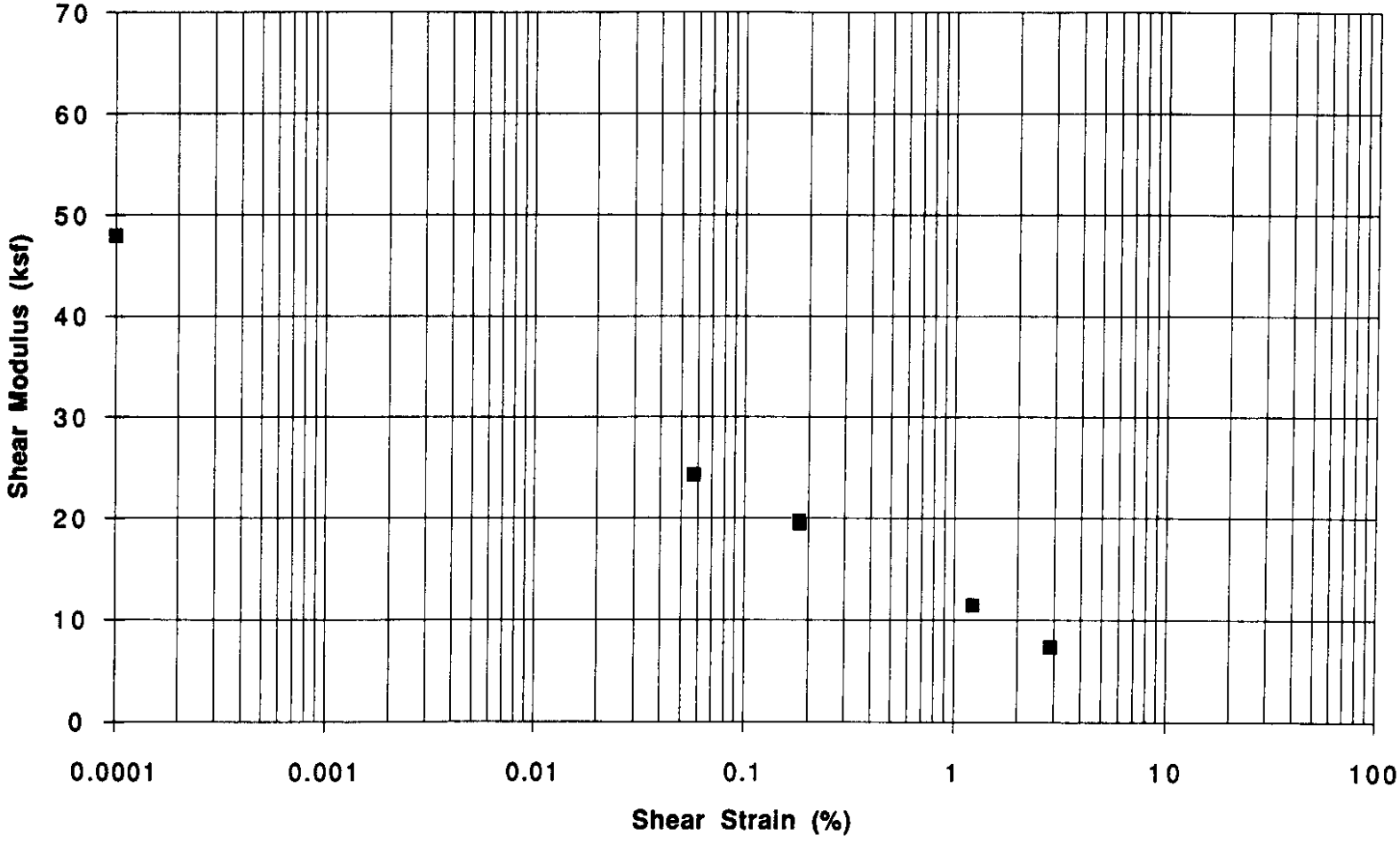

Figure 56. Strain Dependent Variation of Shear Modulus for Sample III-4

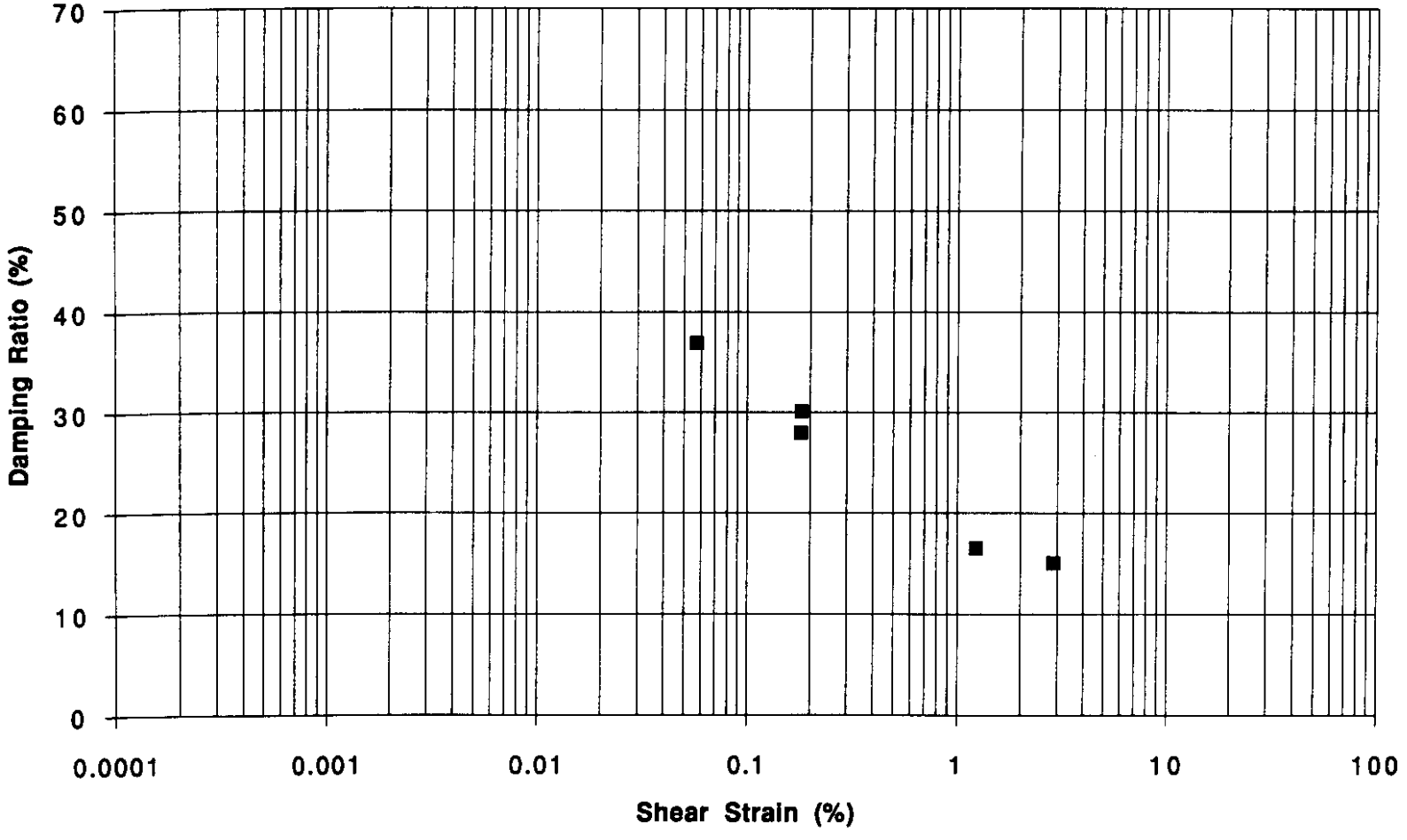

Figure 57. Strain Dependent Variation of Damping Ratio for Sample III-4

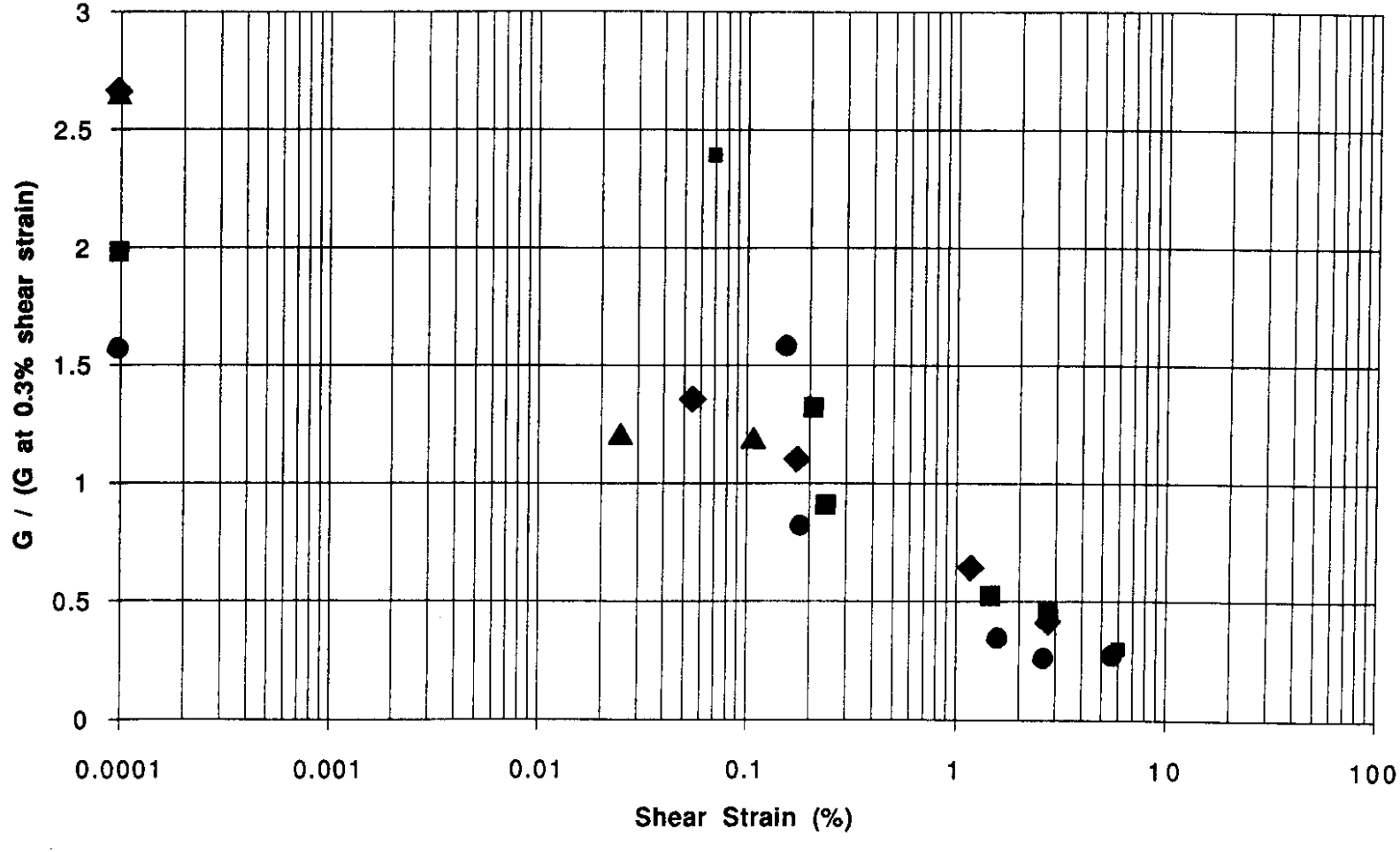

Figure 58. Strain-Dependent Normalized Shear Modulus for all Phase III Tests

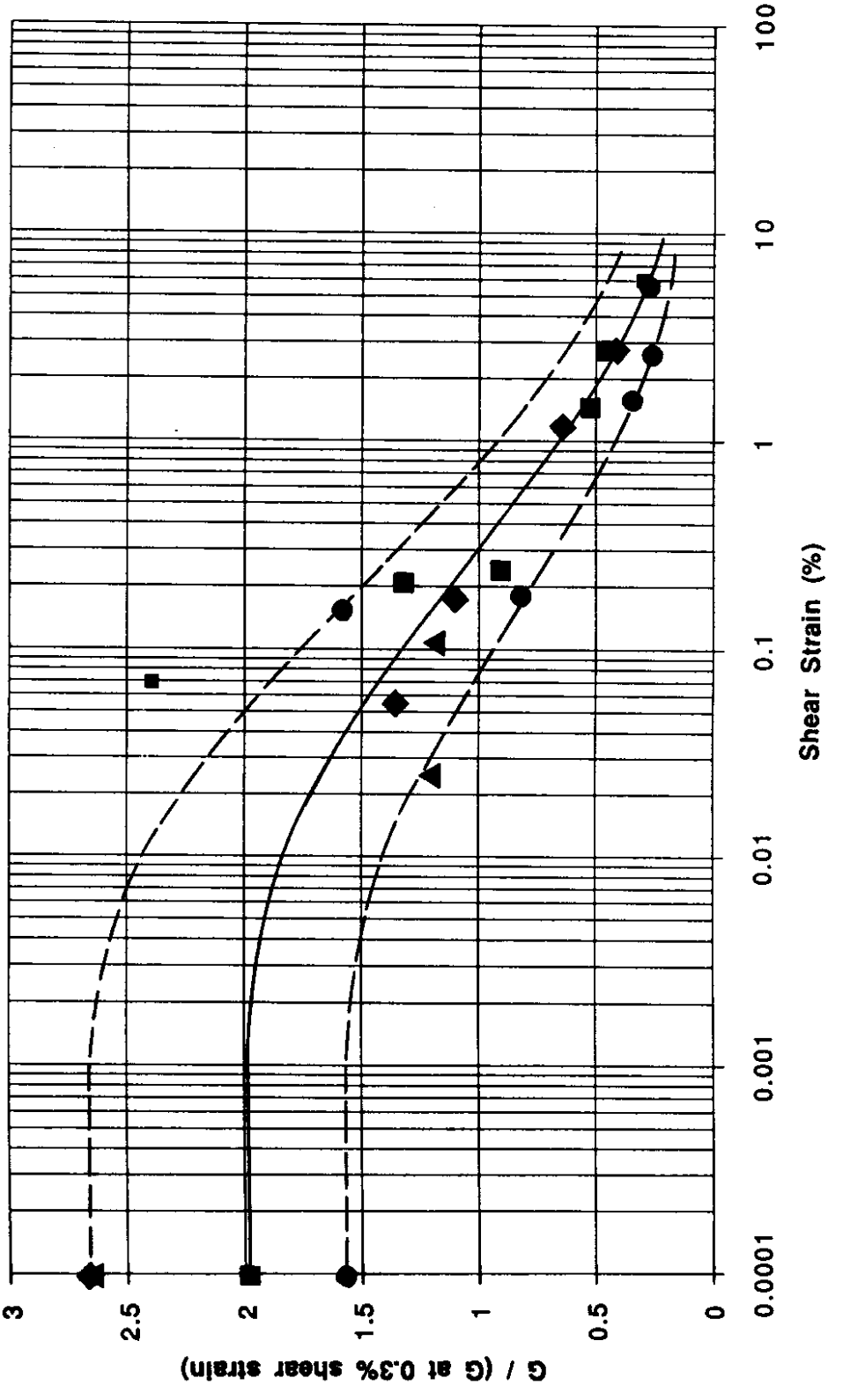

Figure 59. Estimated Range of Normalized Shear Modulus Degradation for Phase III Tests

the average rate of degradation, along with estimated upper and lower limits to the degradation curve. If the degradation curves of Figure 59 were re-normalized with respect to G_{max}, the inferred degradation curve could be compared with similar curves for inorganic soils. Figure 63 shows the degradation curves for cohesive soils published by Vucetic and Dobry [27]. The results indicate that the degradation behavior of Mercer Slough peat was similar to that of an inorganic clay of PI ≈ 30 at strains below about 0.02 percent but that it behaved like a clay of higher plasticity at larger strain levels. At very large strain levels, the Mercer Slough peat retained a much greater proportion of its low strain stiffness than most inorganic clays, probably because of the mobilization of tensile resistance in the fibers of the peat.

To use the normalized shear modulus curve of Figure 60, it was necessary to estimate G_{max} at different depths within the peat. The in-situ shear wave velocity profiles of Figures 9, 10, and 11 suggest that the shear wave velocity was uniform throughout the thickness of the peat. However, at the location of the in-situ measurements, the peat had been consolidated under the weight of the overlying parking lot fill. Because the buoyant unit weight of the fill materials was much larger than that of the peat, the effective stress in the peat was likely to be nearly constant. In the Phase III tests, samples were consolidated to different effective confining pressures. Because the tests on samples III-1 through III-4 were all conducted at different effective confining pressures, their respective shear wave velocities could be used to estimate G_{max}. To supplement the results of these tests, another sample (III-5) was prepared and consolidated for 24 hours at several increasing effective confining pressures. Shear wave velocity measurements were made at the end of each consolidation period. Figure 61 illustrates the variation of G_{max} with effective confining pressure for the Phase III tests.

Damping Ratio

As indicated in Figures 51, 53, 55, and 57, the damping ratio decreased with increasing shear strain amplitude, though it could not be measured at shear strains lower

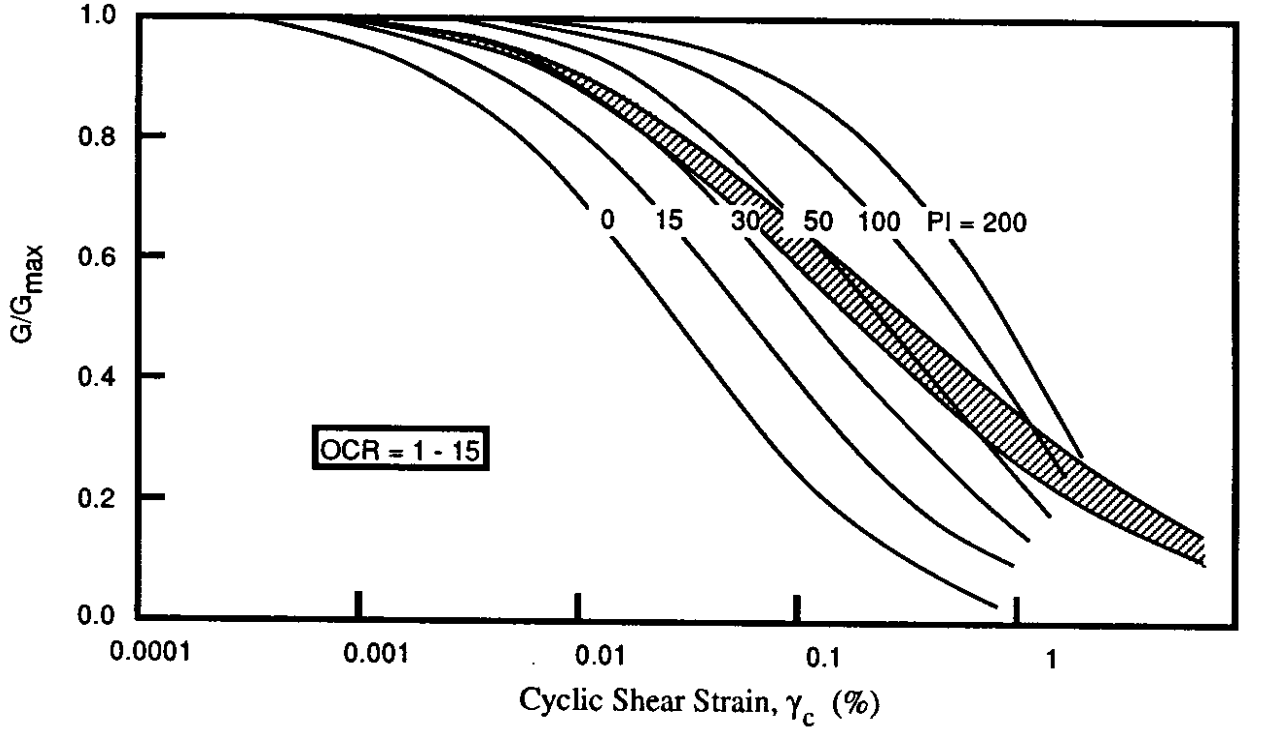

Figure 60. Comparison of Normalized Modulus Degradation Curve for Mercer Slough Peat (shaded) with Normalized Modulus Degradation Curves of Inorganic Clays

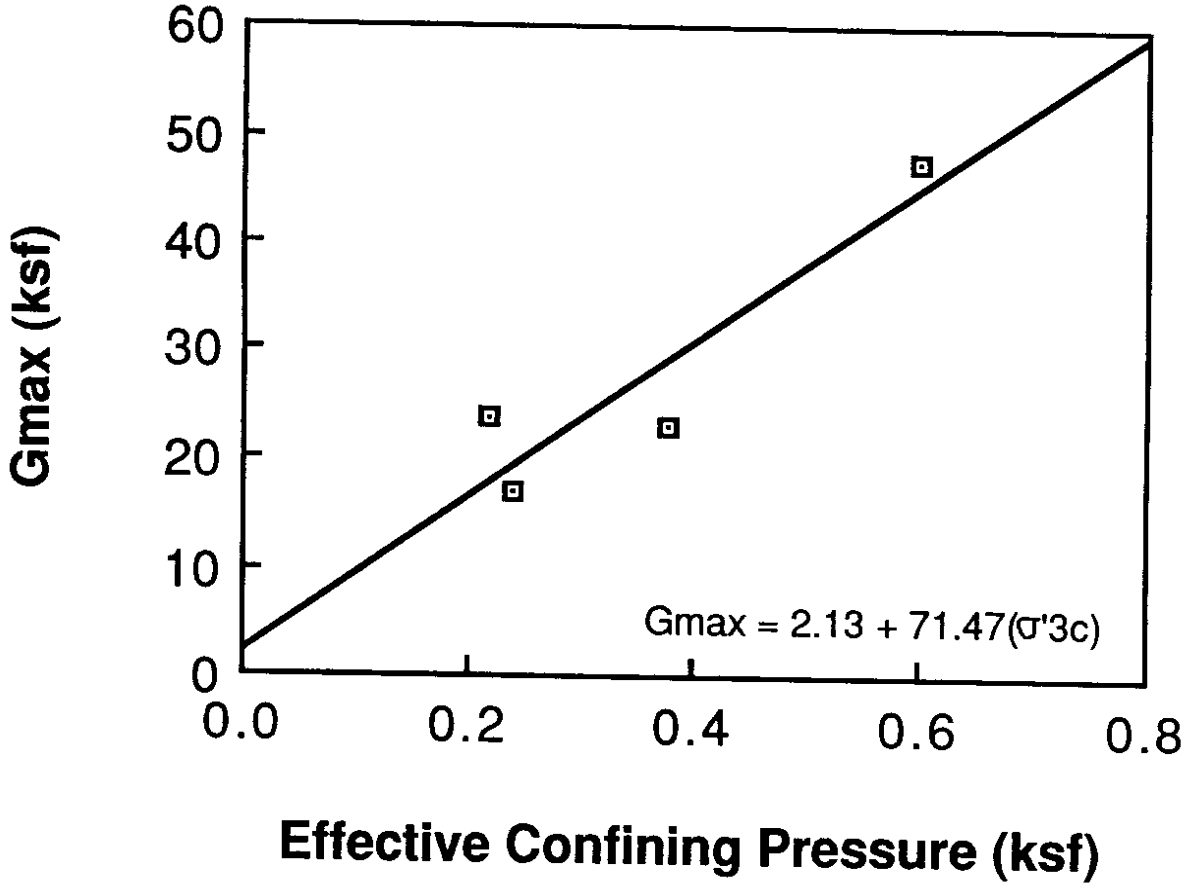

Figure 61. Variation of G_{max} with Effective Confining Pressure from Phase III Tests

than about 0.025 percent in the cyclic triaxial tests. The overall variation of damping ratio with shear strain is shown in Figure 62.

GROUND RESPONSE ANALYSES

The Stage 1 ground response analyses were performed at the end of the Phase I laboratory testing program to provide information required for the dynamic structural analyses within the time frame of the parallel structural investigation. These analyses were performed with a frequency-dependent damping model that was later found to underpredict the anticipated level of damping at frequencies near 1 Hz. The Stage 2 ground response analyses were performed with the peat properties determined at the end of the Phase III laboratory testing program.

Computed Ground Response

Ground response levels were computed for each of the 11 soil profiles for two scaled input motions. The acceleration time histories were scaled to the same peak acceleration (0.25 g) and predominant period (0.36 sec). Because several of the soil profiles were similar and consequently produced similar ground motions, the ground response across Mercer Slough can be divided into the five ground response zones shown in Figure 63.

Stage 1 Analyses

The ground surface response computed in the Stage 1 analyses was expressed in terms of time histories of ground surface acceleration and elastic response spectra. The El Centro and Lake Hughes accelerograms were used for all Stage I ground response analyses. Acceleration time histories are presented in Figures A-1 through A-10 of Appendix A. Elastic response spectra for 2 percent, 5 percent and 10 percent damping are presented in Figures A-11 through A-20. The time histories and response spectra show significant amplification, particularly at frequencies in the range of 1 Hz where the damping ratio was assigned a very low value.

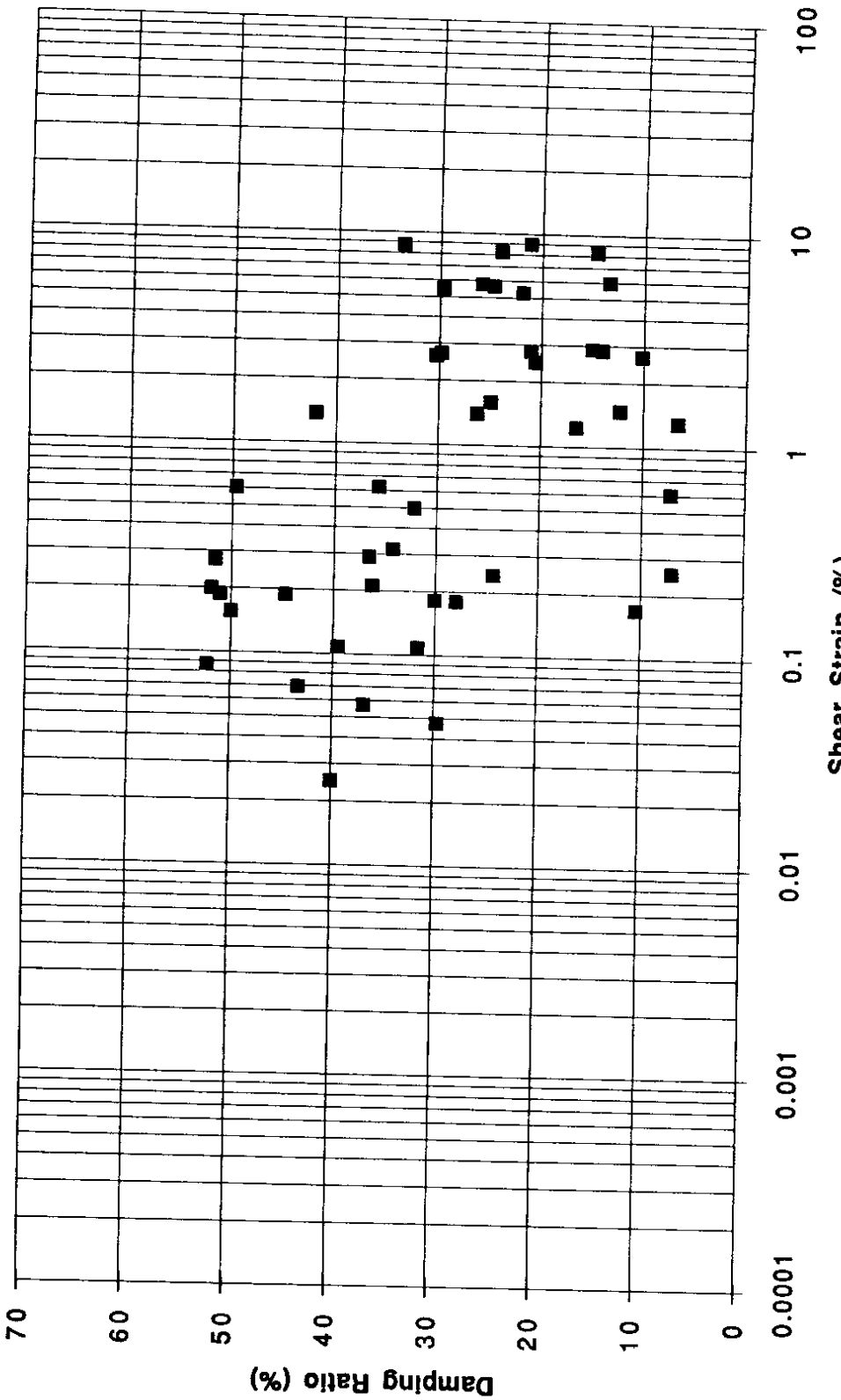

Figure 62. Strain-Dependent Damping Ratios

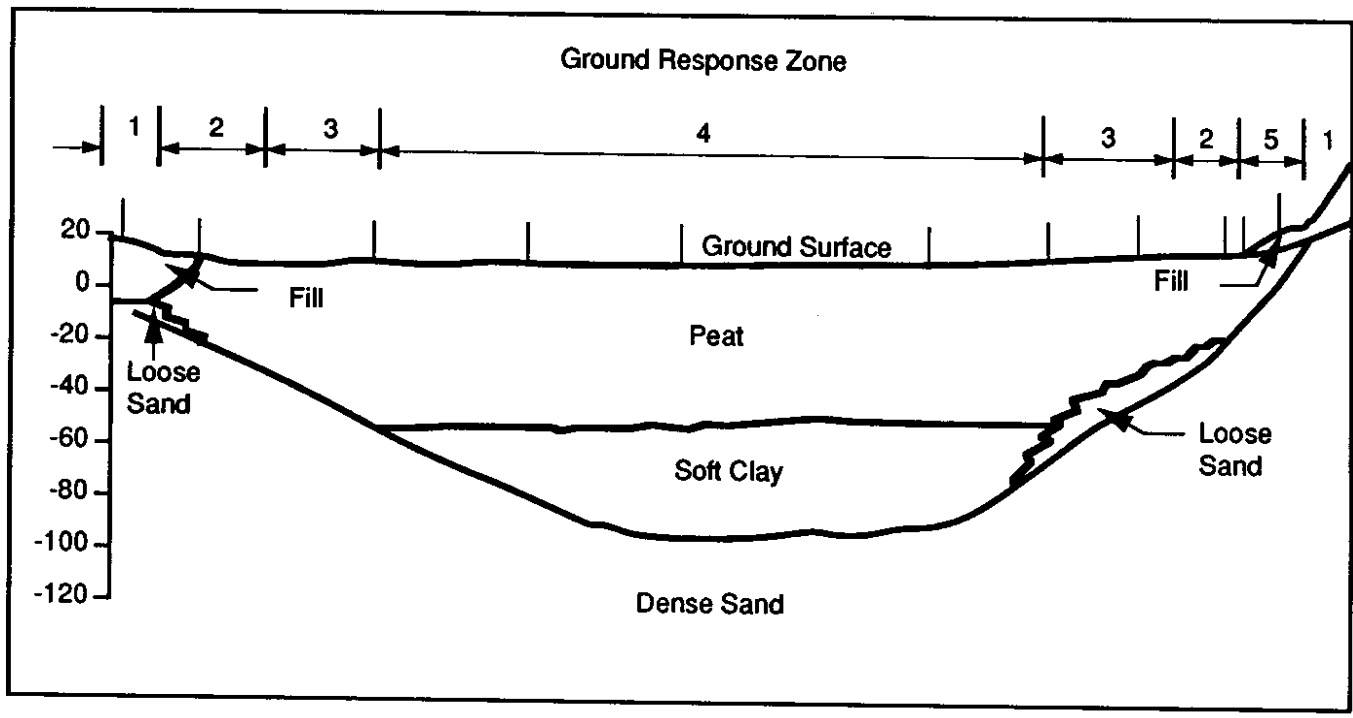

Figure 63. Ground Response Zones

Stage 2 Analyses

The results of the Stage 2 ground response analyses are presented in Appendix B in the form of ground motion time histories and elastic response spectra. Time histories of ground surface acceleration, velocity, and displacement, computed for the scaled El Centro and Lake Hughes earthquake motions, are presented in Figures B-1 through B-10. Response spectra for 2 percent, 5 percent and 10 percent damping are presented in Figures B-11 through B-20. The computed motions show the strong influence of subsurface soil conditions on the amplitude and frequency content of the ground surface motions. Ground surface accelerations are de-amplified by amounts which vary with the thickness of the soft soils. The predominant period of the motions increases with increasing soft soil thickness, however, which leads to significant ground surface displacements. In order to estimate the potential lateral loading on the pile foundations, the relative displacement (the difference between the ground surface displacement and the displacement at the top of the dense sand layer) was also computed for each zone. Maximum relative displacements are shown in Table 4.

Table 4. Computed Maximum Relative Displacements

	Zone 1	Zone 2	Zone 3	Zone 4	Zone 5
Lake Hughes	0.01 ft.	0.95 ft.	0.72 ft.	1.08 ft.	0.48 ft.
El Centro	0.01 ft.	0.87 ft.	4.04 ft.	3.73 ft.	0.58 ft.

Interpretation

The results of the two stages of ground response analyses were very different, as evidenced by the time histories and response spectra of Appendices A and B. The reason for the differences is that different dynamic properties were assigned to the peat in each set of analyses. Figure 64 shows the modulus degradation curves used in both the Stage 1 and Stage 2 analyses. At a cyclic shear strain of 0.1 percent, for example, the shear

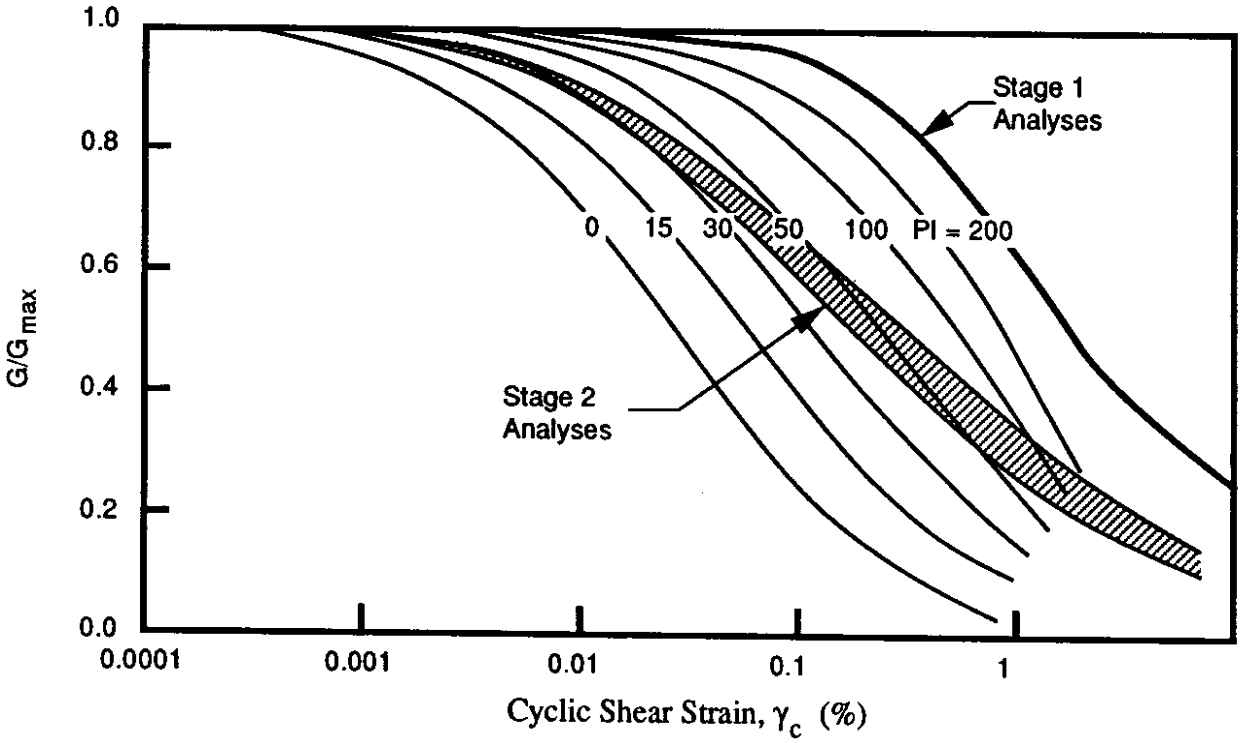

Figure 64. Comparison of Shear Modulus Degradation Curves Used in Stage 1 and Stage 2 Ground Response Analyses

modulus in the Stage 1 analyses was assumed to have decreased from its maximum value by only about 2 percent, compared with a 40 percent reduction in the Stage 2 analyses. Differences in damping characteristics also contributed to the differences between the response spectra. The Stage 1 analyses assumed frequency-dependent, but not strain-dependent, damping. At frequencies below about 5 Hz, these damping ratios were lower than 20 percent. In the range of about 1 Hz, the Stage 1 analyses tests showed much larger strain-dependent damping values. A comparison of the Stage 1 and Stage 2 damping characteristics is shown in Figure 65.

Examination of the computed acceleration time histories and response spectra revealed that, as anticipated, the amplitude and frequency content of ground surface motion varied across the slough. Though the magnitudes of the peak spectral accelerations were different for the different input motions, they were relatively uniform across the central portion of the slough and became more variable near the margins.

Examination of the computed response spectra also shows significant differences in the Stage 1 and Stage 2 analyses. The very soft nature of the Mercer Slough peat is expected to induce relatively low accelerations in short-period structures, but may cause unusually large accelerations in long-period structures. It is known that the shape of response spectra depends on soil characteristics. In fact, the design spectra recommended for buildings and bridges by the Applied Technology Council [31, 32] are specified according to soil type, as illustrated in Figure 66. These spectra show spectral accelerations decreasing for periods greater than 1 second, even for the softest (S3) soil conditions.

The influence of the Mercer Slough peat on ground surface motions can be seen by comparing smoothed, normalized, average response spectra (5 percent damping) for the different zones to normalized response spectra recommended for use in building codes, as illustrated in Figures 67 through 71. For Zone 1, which contained no peat, the computed normalized spectra are consistent with those proposed by the Applied

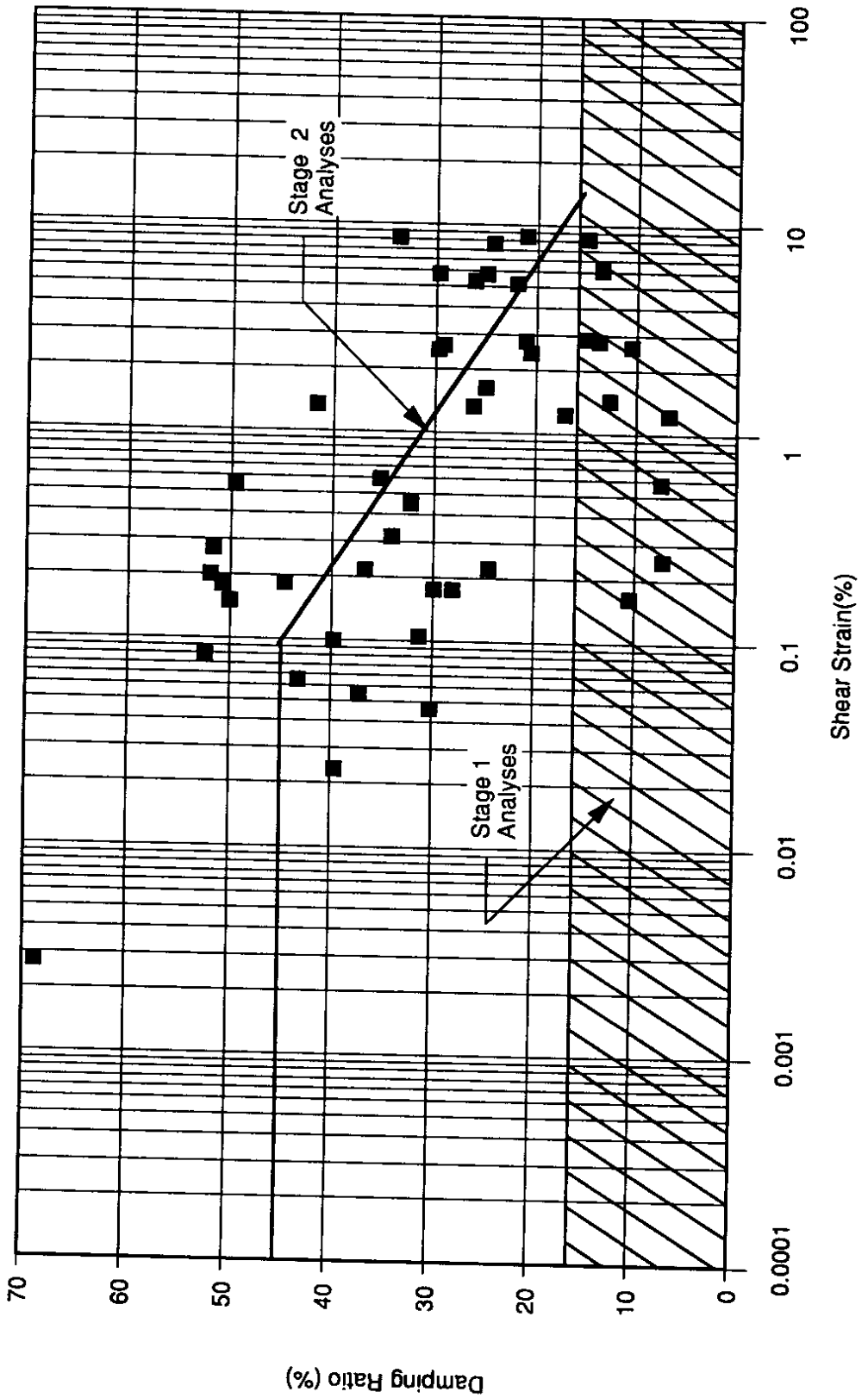

Figure 65. Comparison of Damping Ratios Used in Stage 1 and Stage 2 Ground Response Analyses

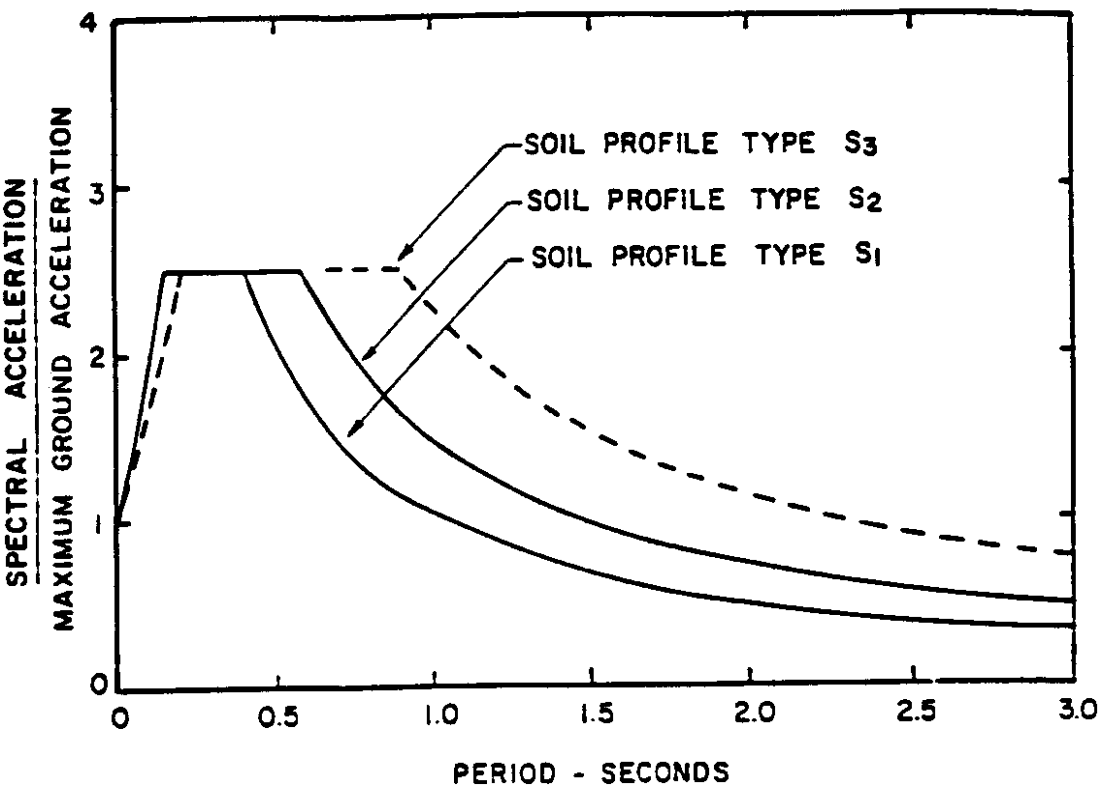

Soil Profile Type S_1: Rock of any characteristic, either shale-like or crystalline in nature (such material may be characterized by a shear wave velocity greater than 2500 feet per second); or stiff soil conditions where the soil depth is less than 200 feet and the soil types overlying rock are stable deposits of sands, gravels, or stiffer clays.

Soil Profile Type S_2: Deep cohesionless or stiff clay soil conditions, including sites where the soil depth exceeds 200 feet and the soil types overlying rock are stable deposits of sands, gravels, or stiff clays.

Soil Profile Type S_3: Soft- to medium-stiff clays and sands, characterized by 30 feet or more of soft- to medium-stiff clay with or without intervening layers of sand or other cohesionless soils.

Figure 66. Normalized Response Spectra for Various Soil Conditions [31, 32]

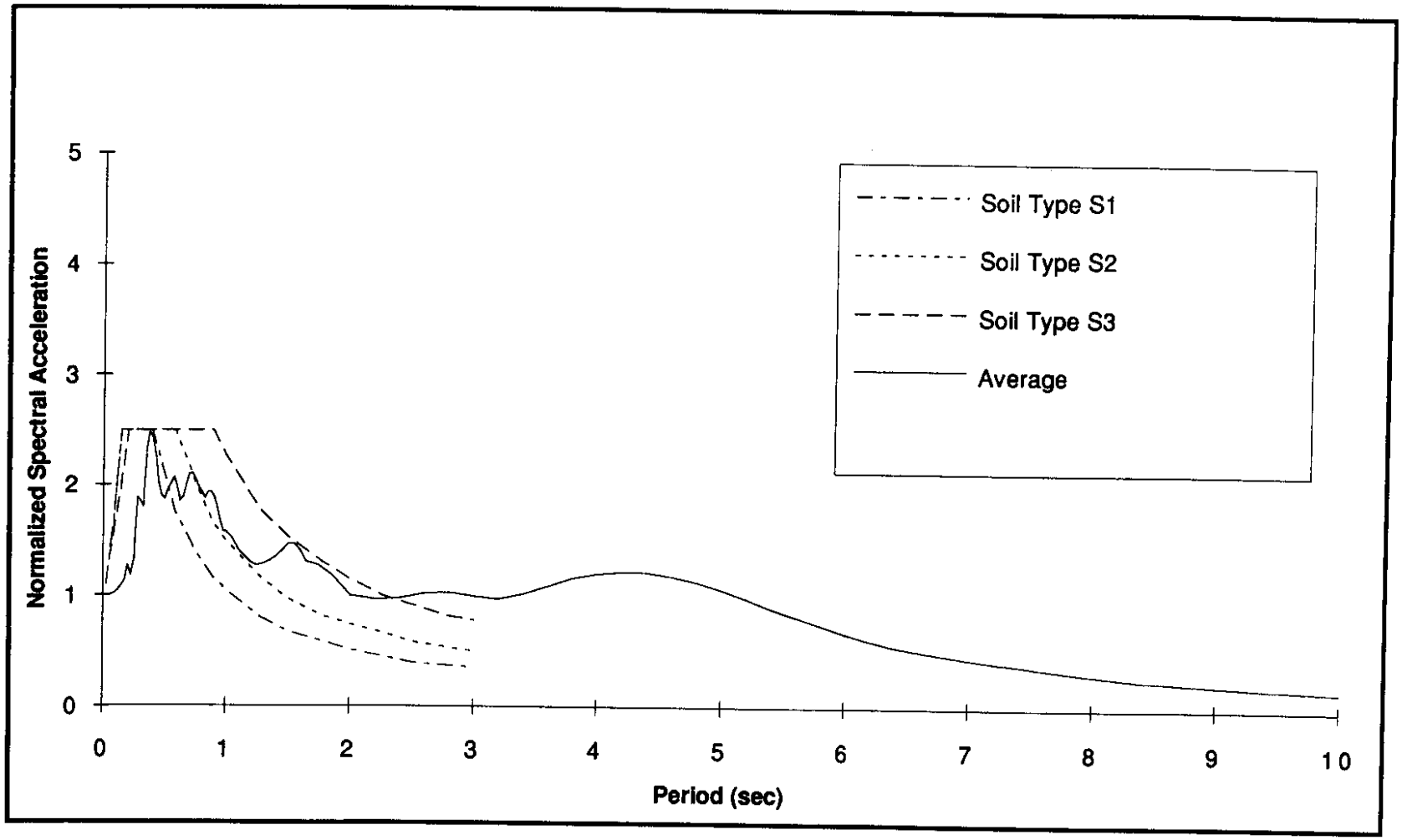

Figure 67. Comparison of Average Mercer Slough Spectra and ATC Spectra for Zone 1 (5 percent damping)

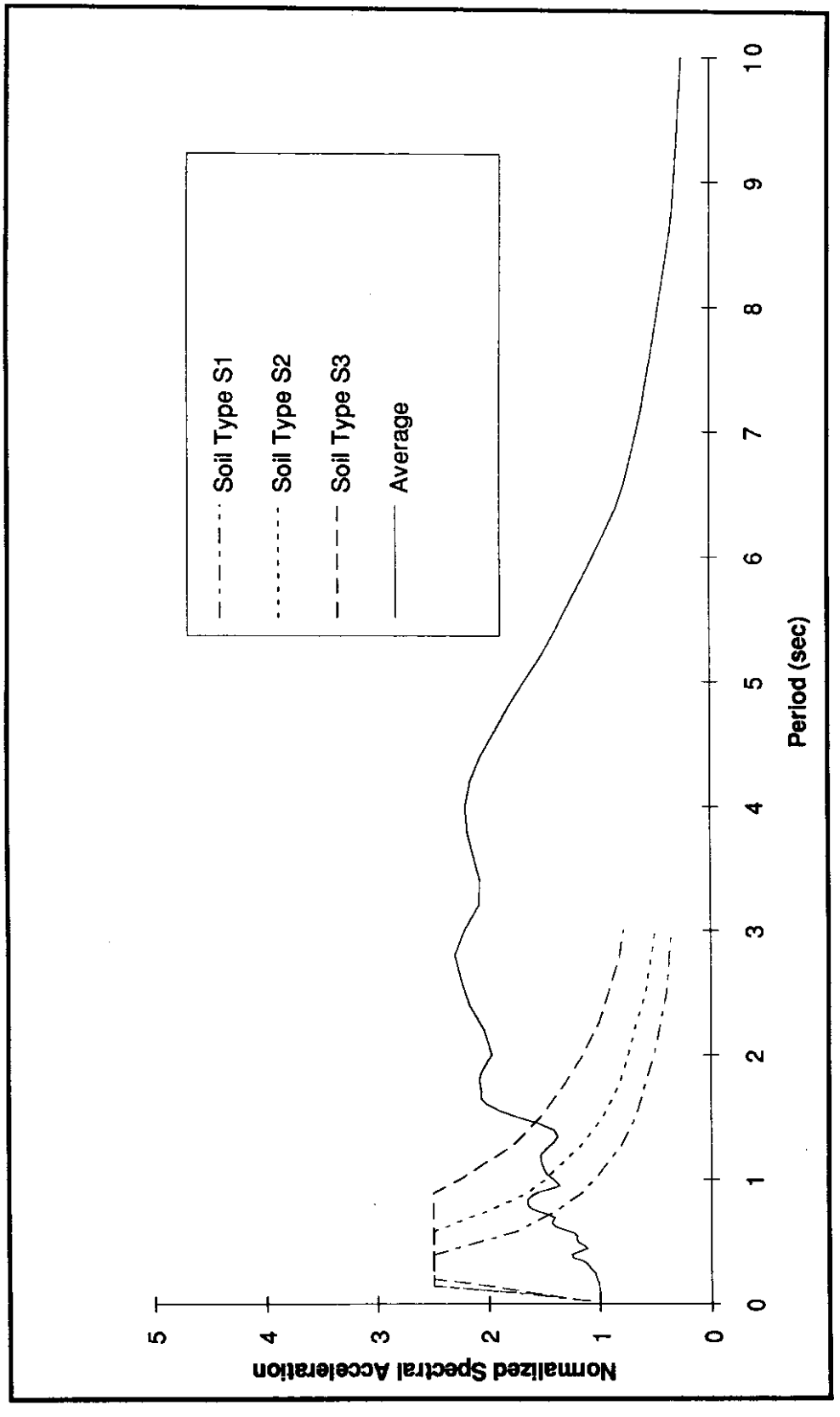

Figure 68. Comparison of Average Mercer Slough Spectra and ATC Spectra for Zone 2 (5 percent damping)

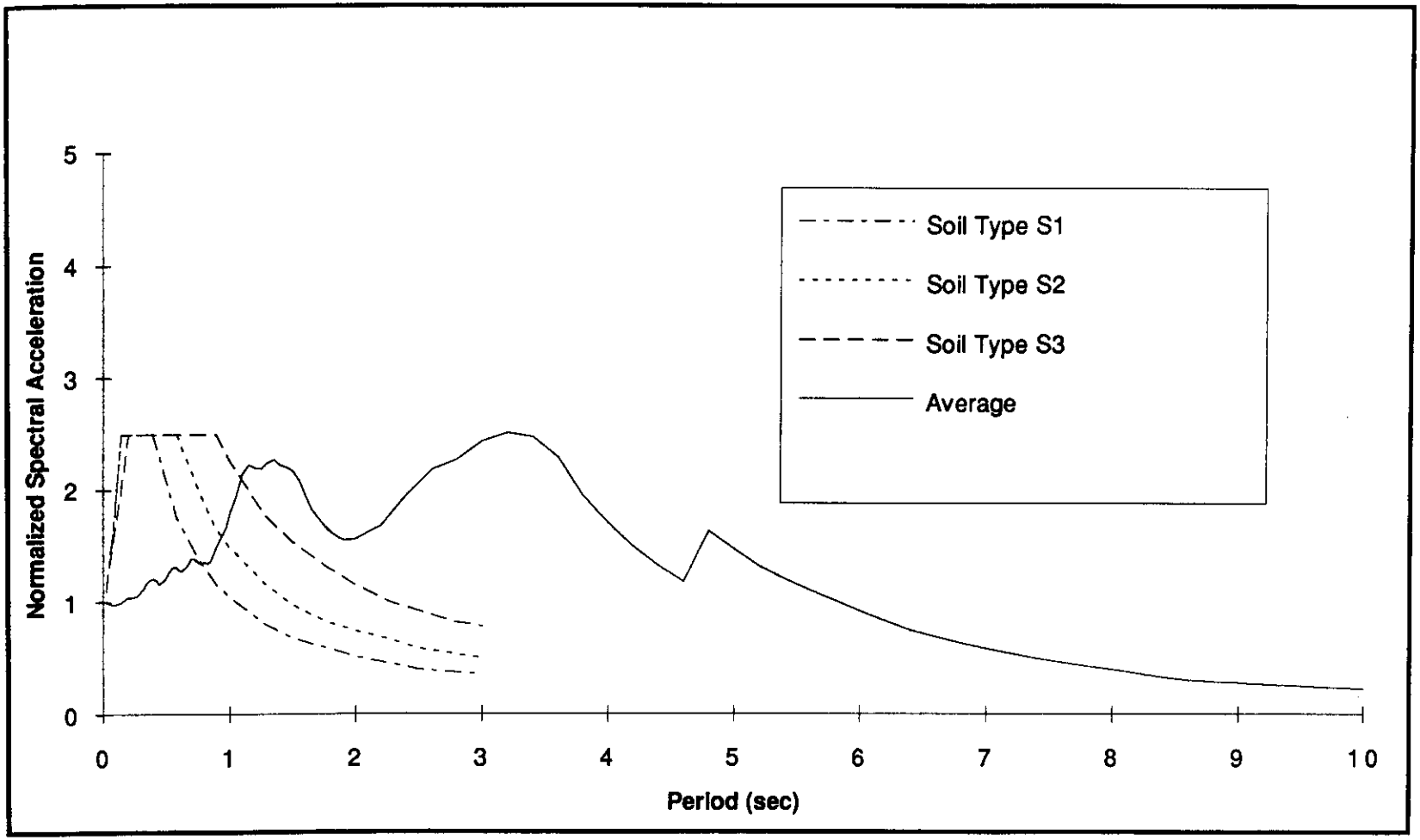

Figure 69. Comparison of Average Mercer Slough Spectra and ATC Spectra for Zone 3 (5 percent damping)

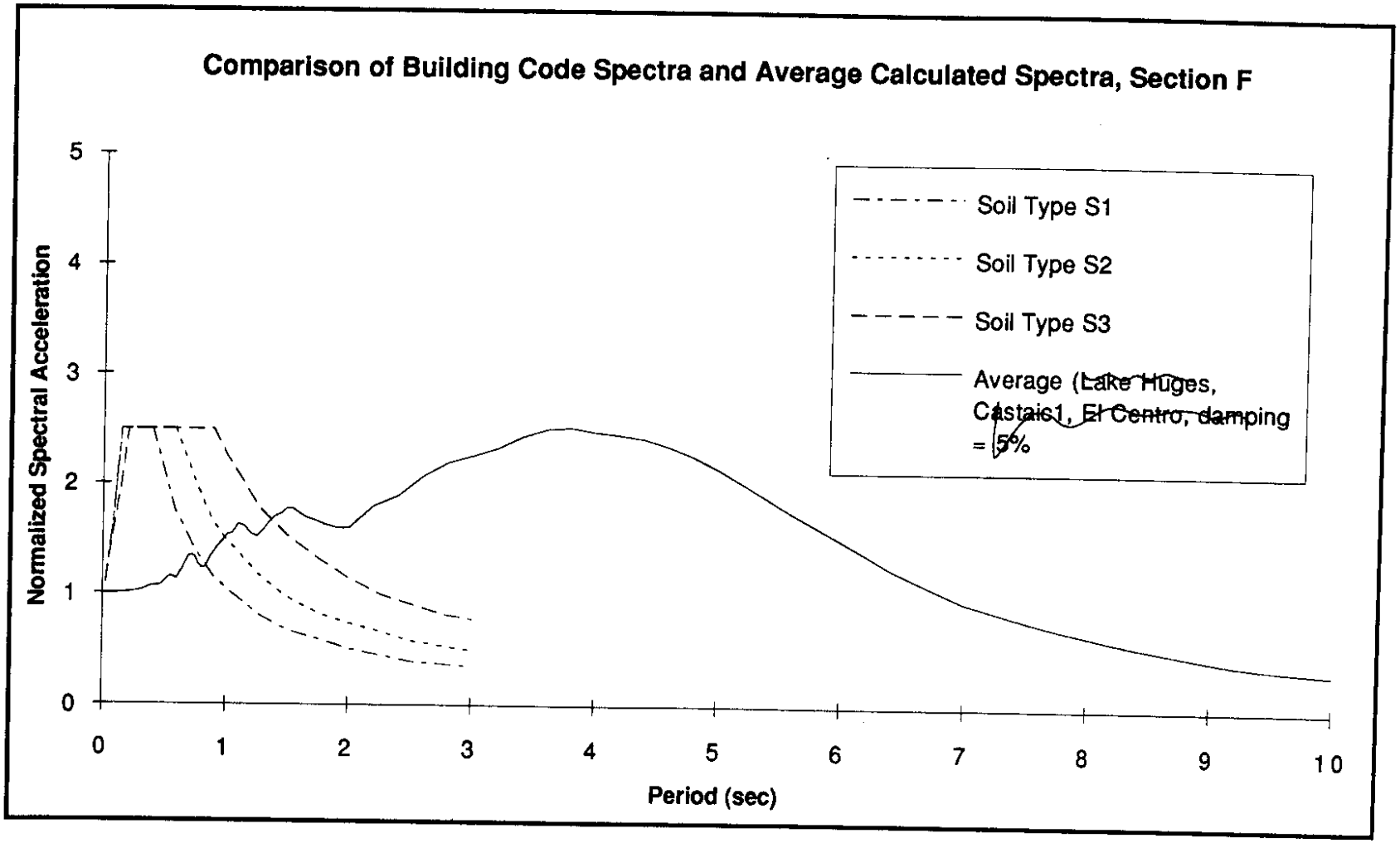

Figure 70. Comparison of Average Mercer Slough Spectra and ATC Spectra for Zone 4 (5 percent damping)

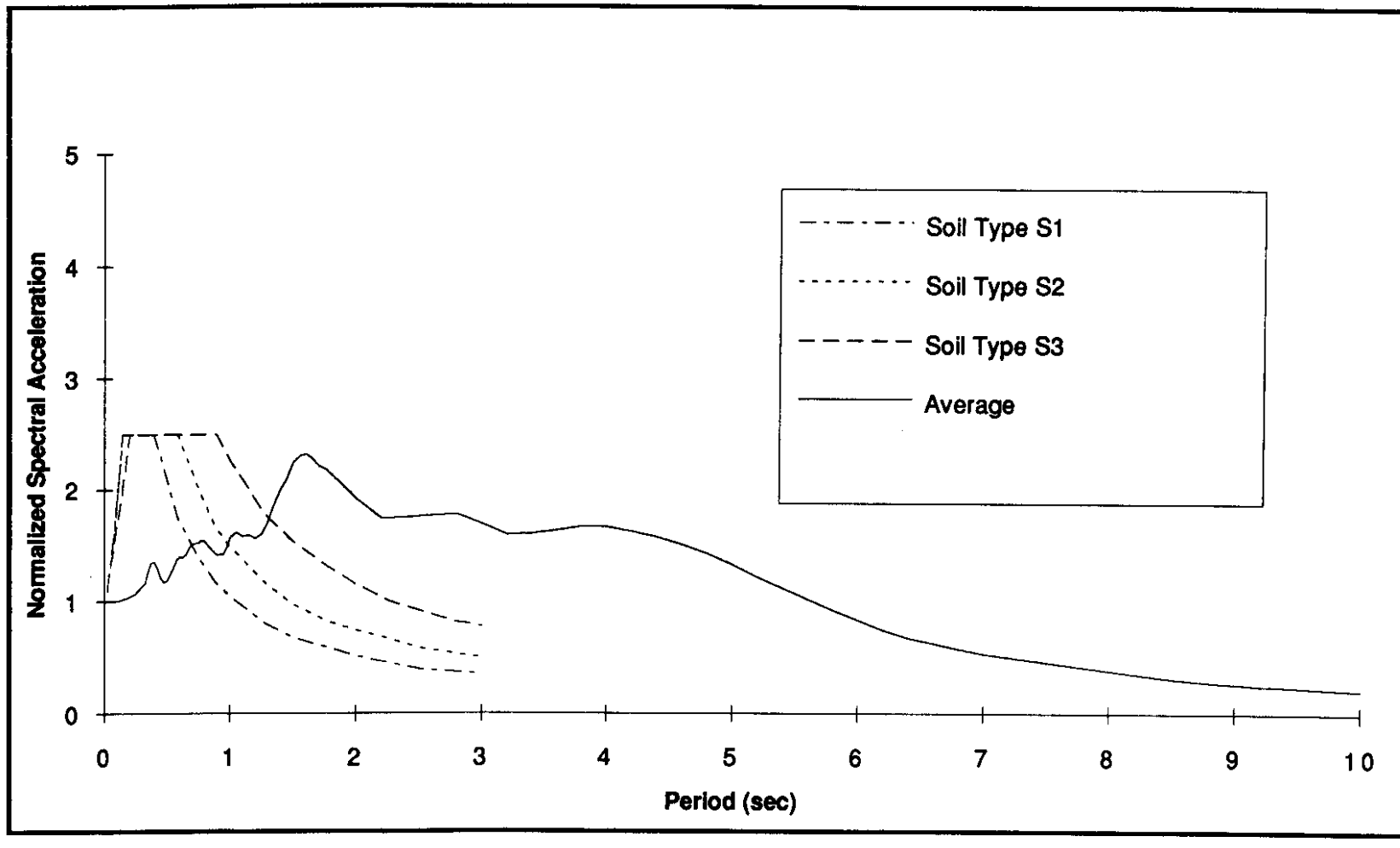

Figure 71. Comparison of Average Mercer Slough Spectra and ATC Spectra for Zone 5 (5 percent damping)

Technology Council in the design of buildings and bridges [31, 32]. For the other zones, however, the shapes of the computed normalized spectra are clearly different than the standard design spectra. At periods less than about 1 second, the computed spectral accelerations are generally lower than the design values, exhibiting the inability of the soft, weak peat to transmit higher frequency waves to the ground surface. However, the computed spectral accelerations may be considerably larger than the design spectral accelerations for greater periods, particularly for periods in the range of 3-4 seconds. These large, long-period accelerations can produce very large displacements at the ground surface. When the top and bottom of the peat layer are 180° out of phase, the relative displacement can become very large, as indicated in Table 4. These very large relative displacements can induce very large bending moments in the existing pile foundations.

The Stage 2 ground response analyses were based on laboratory test results that provided better definition of the dynamic properties of the peat than was available at the time of the Stage 1 analyses. The ground response computed in the Stage 2 analyses was therefore considered to be more representative of the motions that would be expected in a design level earthquake. It is important to recognize, however, that even the Stage 2 analyses were based on a small number of laboratory test data, and that significant uncertainty in the dynamic peat behavior still exists.

Pile Bending

Earthquake-induced ground shaking causes vertical and horizontal displacements of soil at and below the ground surface. The nature of the deformations depends on the geometry and the material properties of the various soil and underlying rock units at the site and on the characteristics of the seismic waves that reach the site. Ground displacement amplitudes are typically small for small or distant earthquakes, or for very stiff or dense soil profiles; however, these amplitudes may become quite large in soft soil

deposits. Displacement amplitudes are generally largest at the ground surface and tend to decrease with depth below the ground surface.

In soft soil areas, significant transportation structures such as highway bridges are often supported on deep foundations. These deep foundations may be subjected to lateral loading at their heads from traffic, thermal expansion, and other sources; methods for evaluating their response to such loads are now well established [33-36]. When deep foundation elements extend through soft soils in seismically active areas, however, they may be subjected to a different form of lateral loading—a lateral loading that is imposed by earthquake-induced displacement of the surrounding soils. Because earthquake-induced soil displacements are not uniform with depth, the soil displacement profile will be curved, thereby inducing bending moments in the piles. Soil profile curvatures are generally greatest at boundaries between materials of different stiffness. Damage to pile foundations for highway bridges has been observed in a number of earthquakes [37-39].

Until recently, designers commonly assumed that the mass and stiffness of piles were small enough to allow the piles to move with the surrounding soil during earthquakes [31,40]. As a result, the curvature demand for piles was considered to be equal to the maximum computed free-field soil profile curvature. Margason and Holloway [40] used numerical analyses to predict the curvature profile for a soft soil site in the San Francisco Bay area. The soil curvature profile was far from constant; it displayed large pile curvatures occurring over relatively short vertical distances. The largest computed curvature was located at the boundary between soft bay mud and an underlying layer of stiff clay at which the small strain impedance ratio was approximately 1.6. This computed soil curvature, approximately 4.0×10^{-4} cm^{-1} (1.6×10^{-4} cm^{-1}), corresponded to a radius of curvature of about 208 ft (63.4 m), which exceeds the elastic limit of many piles. Margason and Holloway [40] indicated that maximum pile curvatures of $2.0 - 4.0 \times 10^{-4}$ in^{-1} ($0.8 - 1.6 \times 10^{-4}$ cm^{-1}) could be expected for magnitude

7.0 earthquakes, and 8.0 x 10^{-4} in^{-1} (3.2 x 10^{-4} cm^{-1}) could be expected for magnitude 8.0 earthquakes in the San Francisco Bay area.

Banerjee et al. [41] repeated the analysis of the San Francisco Bay area profile for which Margason and Holloway had obtained a maximum curvature of 4.0 x 10^{-4} in^{-1} (1.6 x 10^{-4} cm^{-1}). However, Banerjee et al. performed a two-dimensional, soil-structure interaction analysis with a 12-in (30.5 cm) precast, prestressed concrete pile embedded in the soil profile. They found that the maximum computed pile curvature was only 2.2 x 10^{-4} in^{-1} (0.9 x 10^{-4} cm^{-1}) or slightly more than half of the free-field soil profile curvature. These analyses showed that the flexural stiffness of the pile was sufficient to span short distances of high soil profile curvature with significantly lower pile curvature. Other methods for analysis of seismic pile-soil interaction have also been developed.

Soil-Pile Interaction

The existence of locally high curvatures suggests that the free field soil displacement profile exhibits "kinks" at the depths corresponding to high curvature. The assumption that the concrete-filled steel pipe piles and timber piles supporting the I-90 bridges will move with the soil and assume the same kinked shape is clearly inappropriate, particularly in light of the very low stiffness and strength of the Mercer Slough peat.

A simple, but perhaps somewhat conservative, method of estimating pile bending would be to assume pile fixity at the ground surface and at the top of the dense sand. The maximum curvatures could then be estimated from

$$\phi_{max} = \frac{M_{max}}{EI} = \frac{6\Delta}{L^2}$$

which, for the relative displacements of Table 4, yields the curvatures shown in Table 5.

Table 5. Conservatively Estimated Maximum Pile Curvatures

	Zone 1	Zone 2	Zone 3	Zone 4	Zone 5
Lake Hughes	0.00011 ft^{-1}	0.0063 ft^{-1}	0.0014 ft^{-1}	0.00061 ft^{-1}	0.0080 ft^{-1}
El Centro	0.00011 ft^{-1}	0.0058 ft^{-1}	0.0080 ft^{-1}	0.0021 ft^{-1}	0.0096 ft^{-1}

The minimum radius of curvature, given by the reciprocal of the ϕ_{max} values listed in Table 5, are quite small at a number of locations.

To obtain an improved estimate of the curvature demand on the piles, approximate soil-pile interaction analyses were performed using a three-dimensional finite element model of a column of soil containing a pile. The meshes used in the analyses are shown in Figure 72 and 73. To minimize potential boundary effects, all boundaries were located at least 10 pile diameters from the center of the pile. For these analyses, all soils were considered linear, elastic and virtually incompressible ($\nu = 0.49$). The peat was assigned a Young's Modulus of 8,000 psf and the loose and dense sands were assigned moduli consistent with coefficients of subgrade reaction of 30 pci and 100 pci, respectively. The soil deformation patterns used in the interaction analyses corresponded to the times at which the maximum soil profile curvatures had developed. The soil deformations were applied statically and inertial forces transmitted to the pile by the superstructure were not considered.

The actual analyses were performed in the following manner:

1. With the pile elements assigned the same properties as the surrounding soil at the same depth, the finite element mesh was deformed such that the lateral displacements of the nodal points along the centerline of the pile were equal to the computed free-field soil profile displacements at the time of maximum soil curvature.

2. The nodal point forces required to deform the mesh into this configuration were computed and stored.

3. The pile elements were then assigned properties that produced the flexural stiffnesses of the various piles being considered.

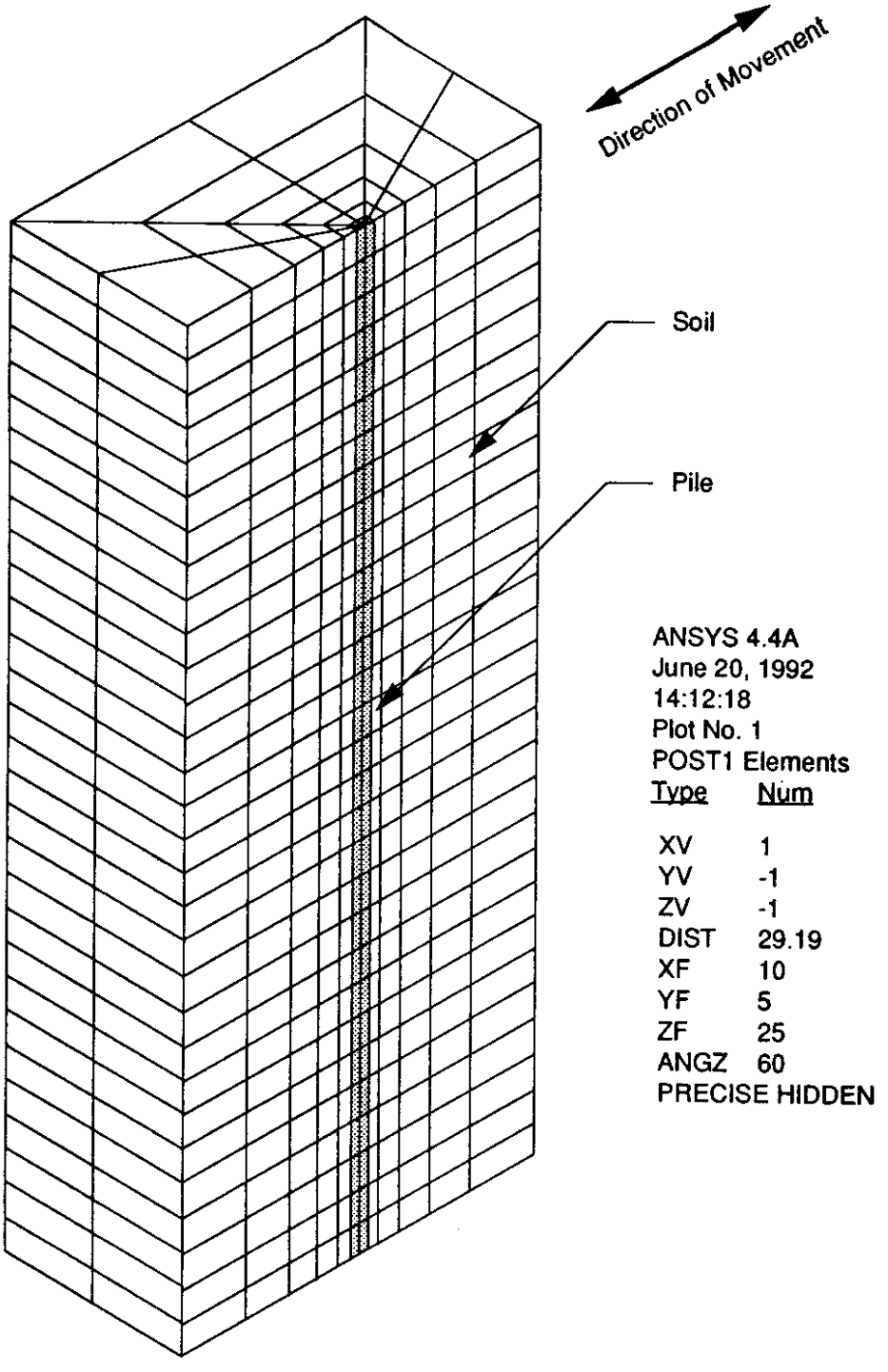

Figure 72. Finite Element Mesh for Analysis of Pile Bending Due to Soil Deformation: Ground Response Zone 2 with Lake Hughes Motion

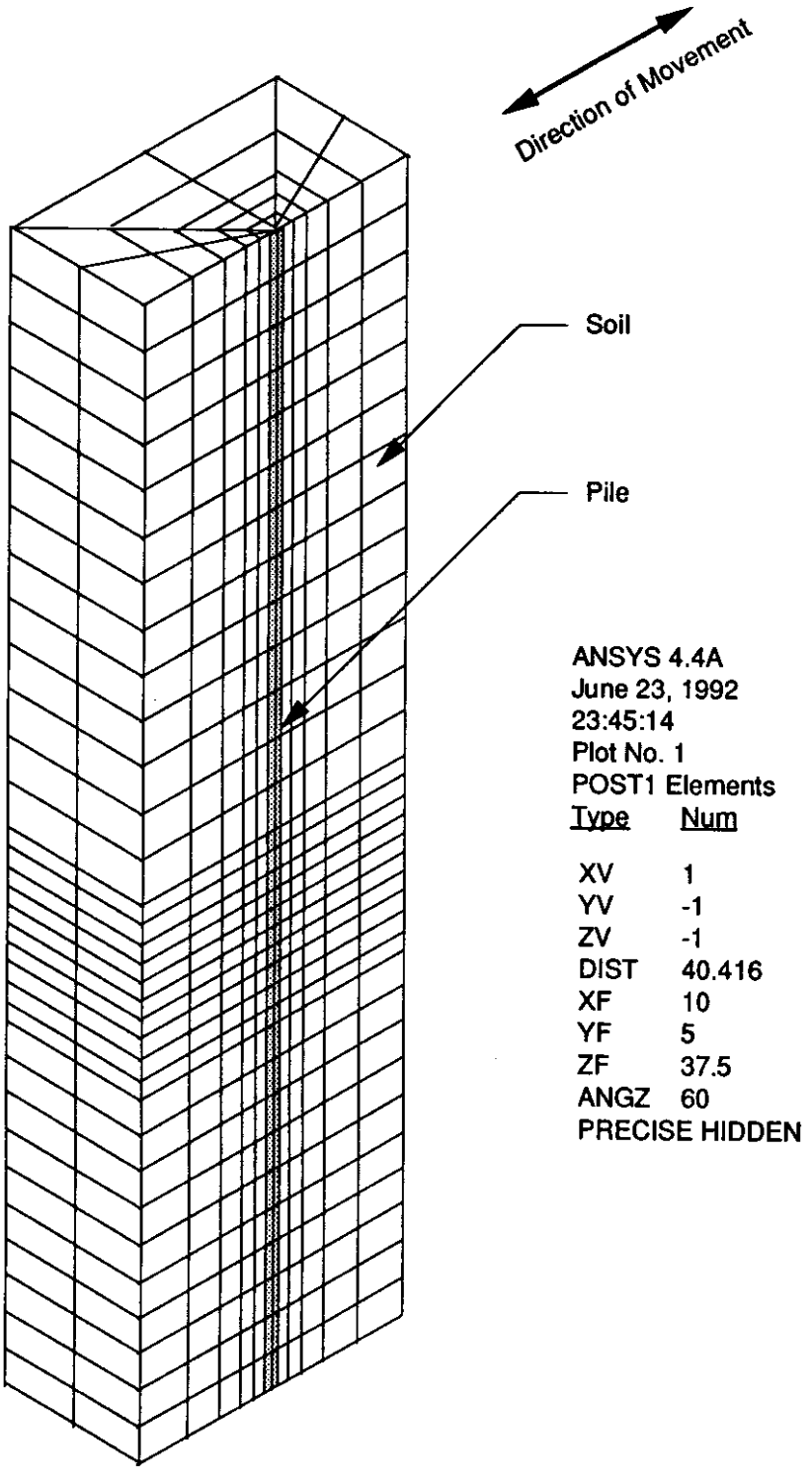

Figure 73. Finite Element Mesh for Analysis of Pile Bending Due to Soil Deformation: Ground Response Zone 3 with El Centro Motion

4. The modified finite element model was subjected to the nodal point forces computed in Step 2. The resulting lateral displacements of the nodal points along the centerline of the pile were then used to compute the curvature demand on the piles.

Assumptions and Justification

This approximate method of interaction analysis involved a number of simplifying assumptions. First, the interaction analysis was static, not dynamic. Second, inertial forces at the pile heads resulting from the mass of the superstructure were not modelled. Third, the P-Δ effect associated with large lateral deflections was not modelled.

Though the interaction analysis itself was performed statically, the displacements imposed upon the piles were obtained by dynamic analysis. At the time of maximum curvature for each ground response zone, accelerations were small, particularly at the depth of maximum curvature; consequently, the error involved in the static interaction analysis was assumed to be small. Because accelerations were low, inertial forces at the pile head were not large. Those forces that would develop would be resisted by the soil near the ground surface rather than the soil at the depth of maximum curvature; consequently, the error associated with neglecting these inertial forces was assumed to be small. Because the vertical loads were relatively small, bending moments attributable to the P-Δ effect were estimated to be much smaller that those caused by seismically-induced curvature of the surrounding soil profile.

Results

Two cases were evaluated: Ground Response Zone 2 with the Lake Hughes input motion and Ground Response Zone 3 with the El Centro input motion. The approximate interaction analyses indicated that the curvatures induced in the piles would be considerably lower than the free-field soil profile curvatures. The influence of the flexural stiffness of the piles is most easily illustrated by comparing the deflected shape of the piles and the free-filed soil profile at the times of maximum curvature, as shown in

Figures 74 and 75. Figures 74 and 75 show that the flexural stiffness of the piles allows the kink in the free-field soil profile to be bridged with considerably smaller pile curvatures. The reduction in maximum curvature for the various pile types is shown in Table 6. Obviously, the maximum computed pile curvatures are considerably smaller than the maximum computed free-field soil profile curvatures. The curvature reduction clearly varies with the flexural stiffness of the pile; greater curvature reduction is associated with greater flexural stiffness. However, the computed pile curvatures are still very large.

Table 6. Maximum Computed Pile and Free-Field Soil Curvatures

	Ground Response Zone 2			Ground Response Zone 3		
	14" Pipe	18" Pipe	Timber	14" Pipe	18" Pipe	Timber
ϕmax, pile	0.0018 ft^{-1}	0.0013 ft^{-1}	0.0043 ft^{-1}	0.0350 ft^{-1}	0.0308 ft^{-1}	0.0509 ft^{-1}
ϕmax, soil	0.0174 ft^{-1}	0.0174 ft^{-1}	0.0174 ft^{-1}	0.1800 ft^{-1}	0.1800 ft^{-1}	0.1800 ft^{-1}
$\frac{\phi\text{max pile}}{\phi\text{max soil}}$	0.103	0.075	0.247	0.194	0.171	0.283

Note that the researchers who performed these analyses assumed that the piles extended well into the soils underlying the peat. For piles that do not extend far beyond the bottom of the peat, tip rotation may reduce the computed pile curvatures considerably. Sufficient information to investigate the extent and effects of such conditions was not available.

Coherence

It should be noted that actual ground surface motions will be incoherent, i.e., the motions will be of different amplitudes and out of phase at different locations across the slough. Such incoherence may tend to reduce the response of the structure in some of the lowest modes of vibration, but may increase the response of some higher modes.

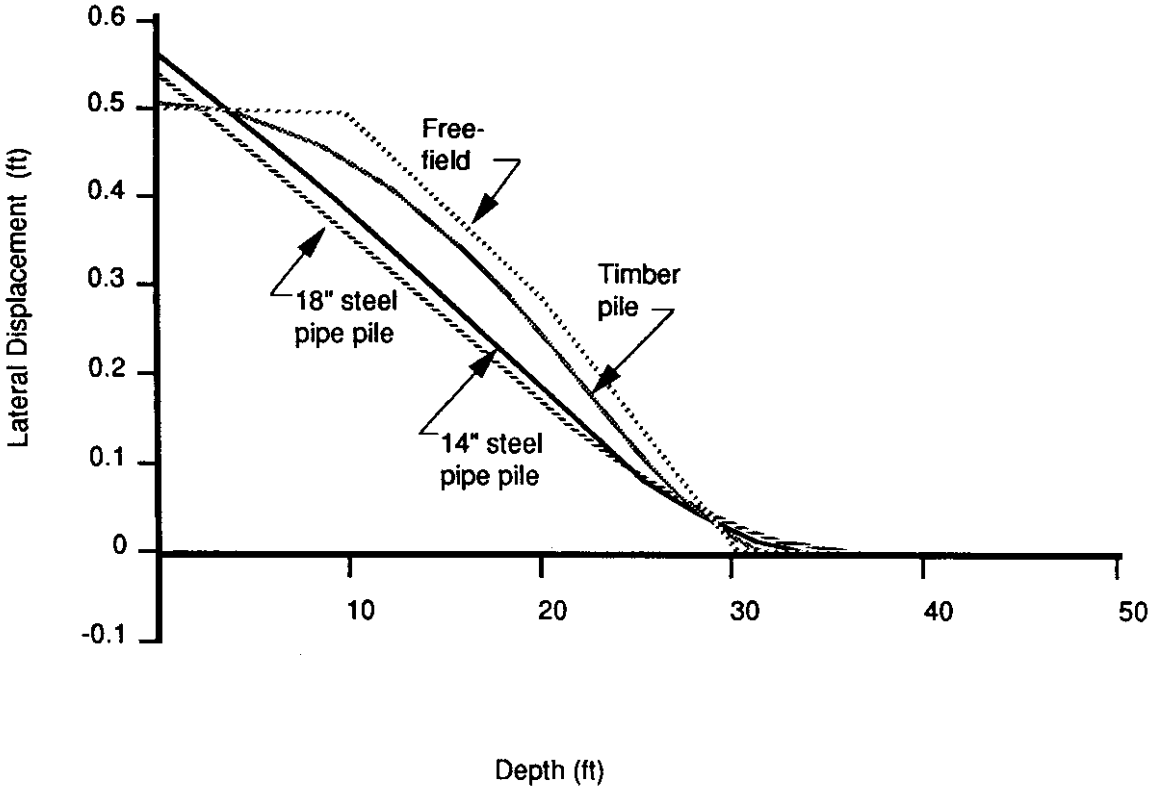

Figure 74. Computed Free-Field and Pile Deflection Profiles at Time of Maximum Free-Field Curvature for Ground Response Zone 2.

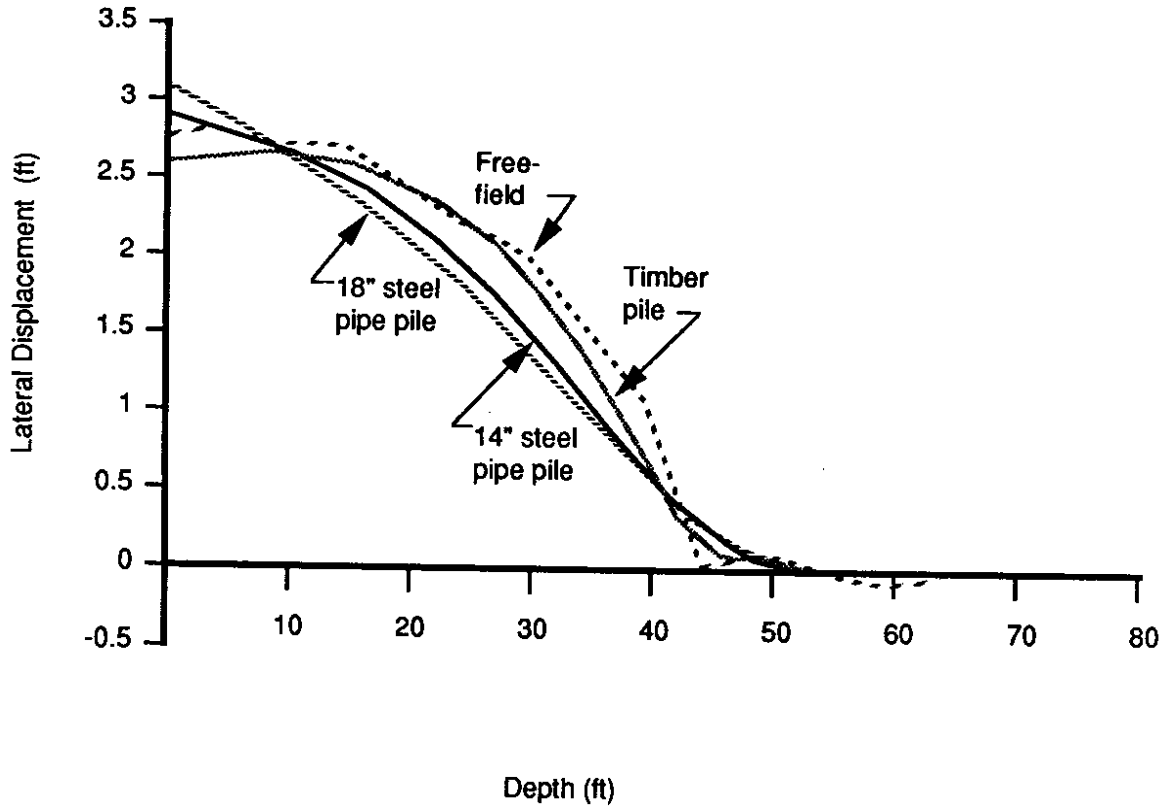

Figure 75. Computed Free-Field and Pile Deflection Profiles at Time of Maximum Free-Field Curvature for Ground Response Zone 3.

CONCLUSIONS AND RECOMMENDATIONS

The purpose of the research was to estimate the dynamic stiffnesses of pile groups supporting the four I-90 bridge structures that cross Mercer Slough. Through careful interpretation of the results of impact, free vibration, and forced vibration tests on an 8-inch pile at the site, these estimates were developed. During the course of the research, it became apparent that an investigation of the dynamic properties of the Mercer Slough peat would be necessary to produce a reasonable estimate of ground motion characteristics. A limited laboratory and field testing program was performed to determine these properties, and the results were used to estimate anticipated ground motion characteristics.

PILE STIFFNESS

The Mercer Slough peat is obviously soft and very weak. It provides, as observed in field loading tests conducted during this and a previous investigation, very little resistance to lateral pile deflection. Consequently, the translational stiffnesses of piles extending through the Mercer Slough peak are expected to be low.

The significant difference between the observed static and dynamic translational stiffnesses at small pile-head deflections may be partly the result of experimental error. However, this difference suggests that both static and dynamic tests should be conducted at sites on similar soils in seismic regions where critical structures exist or will be constructed. Although forced-harmonic and quick-release vibration tests are preferred, the similarity in the translational stiffness and damping values obtained from both tests suggest that the less expensive, quick-release test can yield reasonable results, provided it is carefully conducted with high quality data acquisition equipment.

The relatively low soil modulus and low hysteretic damping over the upper portion of the pile where the deflection was large support the observation that a water-filled gap between the peat and the pile may have formed during the testing. Such gaps

have been observed during lateral load testing of piles in cohesive soils, and were observed at large displacements during the quick-release tests in this investigation and at smaller displacements during the quick-release tests in this investigation and at smaller displacements during the previous static tests at the site. However, the gaps were impossible to observe during the forced vibration tests because of the small displacements and disturbed nature of the saturated peats adjacent to the test pile.

To estimate the translational stiffness of full-scale single piles in Mercer Slough, the use of Equations (6) and (7), along with Figure 30, is recommended. The translational stiffness of pile groups can be estimated as the sum of the translational stiffnesses of the piles within the group.

GROUND MOTION

The soft and weak nature of the Mercer Slough peat will also influence the characteristics of earthquake-induced ground shaking at the site. The combination of low shear modulus, nonlinear stress-strain behavior, and significant thickness of the peat will serve to de-amplify bedrock acceleration at the frequencies of primary interest in a large earthquake. The use of standard response spectrum shapes may produce an overconservative estimate of the response of the Mercer Slough bridges. The soil conditions will also modify the frequency content of the motion, resulting in a ground surface motion with a considerably greater long-period content than the bedrock motion.

Though the Mercer Slough peat may not tolerate large accelerations at its surface, the significant long-period content of the computed ground surface motions suggest that large displacements may be generated. Large strains can be expected in the peat near its contact with underlying soils. The effect of large displacements, as well as the effects of acceleration-induced forces, must be considered when evaluating the structural performance of the bridges and their foundations.

FOUNDATION PERFORMANCE

Horizontal ground displacements associated with earthquake shaking will induce bending moments in the pile foundations, particularly in the vicinity of the interface between the peat and the underlying materials. At some locations, the surface and subsurface deformations may be quite large. Procedures were developed for estimation of pile curvatures induced by horizontal soil displacement for design-level earthquakes. These procedures assumed that the piles extended well into the stiffer soils underlying the peat; the accuracy of the assumption should be checked. Additional bending moments that may develop due to P-Δ effects may be estimated with the aid of Table 4. These procedures may be used for preliminary evaluation of the structural capacity of the existing piles.

LIQUEFACTION

A review of subsurface conditions disclosed a zone of loose sand and silt, between the peat and underlying dense sands, near the eastern border of the slough. These loose sands appear from the available information to be potentially liquefiable; the extent to which the bridge foundations rely upon them for support is not known. If the pile foundations bear directly on these loose sands, and if the loose sands are indeed liquefiable, a large earthquake could cause a devastating foundation failure. Though evaluation of this condition is beyond the scope of this research project, prompt determination of the potential for liquefaction-induced foundation failure here is strongly recommended.

OTHER CONSIDERATIONS

It is important that the limitations of the present study be understood, particularly with respect to the anticipated ground motions. Even under the best conditions, prediction of earthquake ground motions is a difficult task. The most accurate predictions of anticipated ground motions are made when the following conditions exist:

(a) material properties are well-defined, (b) site geometry is well-known and accurately modeled, and (c) input motions are well-defined. For various reasons, some of these conditions were not met completely in this investigation.

The ground response of the Mercer Slough site is dominated by the dynamic properties of the Mercer Slough peat. While the properties of the Mercer Slough peat were investigated in a laboratory testing program, the testing program was limited by time, budget, and equipment constraints and did not fully define the dynamic properties of the peat. (A detailed investigation of the dynamic response of peats is currently underway in a new WSDOT research project.) Ground motions were predicted using one-dimensional ground response analyses. Recent research indicates that two- or even three-dimensional effects may increase ground motion amplitudes near the edges of the slough.

Consideration should be given to installing strong motion instrumentation at the site. A local array in Seismic Zone 4 could provide invaluable information on soil and structural response during small and moderate earthquakes that are likely to occur before a large, design-level event. Such an array could consist of downhole instruments at the top of the dense sand and soft clay layers, an instrument on the surface of the peat (in the free field), and instruments on the pile cap and bridge deck. Ground motion records from such an array would go far towards eliminating the uncertainty in the current predictions of soil and structural behavior.

Despite these limitations, the researchers believe that the ground response analyses captured the essential characteristics of the Mercer Slough site and are considered adequate for preliminary analysis of the structural integrity of the I-90 bridges.

IMPLEMENTATION

The results of this research may be implemented by using the recommendations for pile stiffness calculation and dynamic peat properties described in the section titled "Conclusions and Recommendations."

ACKNOWLEDGMENTS

The research described in this report was funded by the Washington State Department of Transportation. Valuable assistance was provided by Al Kilian and Todd Harrison of the Materials Laboratory and Ed Henley, Dick Stoddard, and Al Walley of the Bridge and Structures Office.

The research was conducted by the University of Washington Department of Engineering. Associate Professor Steven L. Kramer was the Principal Investigator. Graduate and undergraduate students Matt Craig, Fan-Yie von Laun, N. Sivaneswaran, Jun Xu, Jerry Wu, Peter Sajer, Terry Martin, and Kuan Sian Go assisted in various field testing, laboratory testing, and analytical aspects of the research.

The field pile load tests were performed by subcontractors Dames and Moore and the California Institute of Technology. C. B. Crouse and Robert Mitchell of Dames and Moore, and Benham Hushmand, Raul Relles, and Bill Iwan of CalTech were involved in the tests.

Dr. David McLean of Washington State University, principal investigator of a parallel project investigating the dynamic response of the I-90 bridge structures, provided valuable input to the researchers.

REFERENCES

1. Board of Inquiry (1990) "Competing Against Time," C. C. Thiel, ed., Office of Planning and Research, State of California, May, 264 pp.

2. Shannon and Wilson (1967). "Thomson Way crossing of Union Bay, Seattle, Washington," *Foundation Engineering Report Technical Supplement*, November, 108 pp.

3. Tsai, N.-C. (1969). "Influence of local geology on earthquake ground motion," Earthquak Engrg. Res. Lab., Calif. Inst. Tech.

4. Seed, H. B. and Idriss, I. M. (1970). "Analyses of ground motions at Union Bay, Seattle during earthquakes and distant nuclear blasts, " *Bull. Seism. Soc. Am.*, 60(1), 125-136.

5. Idriss, I. M. (1991). *Personal communication.*

6. ASTM (1991). "Test for Moisture, Ash, and Organic Matter of Peat Materials," *Annual Book of ASTM Standards*, Part 19, pp.

7. Andrejko, M. J., Fiene, F., and Cohen, A. D. (1983). "Comparison of ashing techniques for determination of the inorganic content of peats," *Testing of Peats and Organic Soils*, ASTM STP 820, 5-20.

8. Landva, A., Korpijaakko, E. O., and Pheeney, P. E. (1983). "Geotechnical classification of peats and organic soils," *Testing of Peat and Orgnaic Soils*, ASTM STP 820. 37-54.

9. Landva, A. and LaRochelle, P. (1983). "Compressibility and Shear Characteristics of Radforth Peats," ASTM STP 820, pp. 141-156.

10. Newman, D. E. (1983). "A 13,500 year pollen record from Mercer Slough, King County, Washington," M. S. Thesis, University of Washington.

11. Landva, A. (1986). "In-Situ Testing of Peat," *Proceedings*, ASCE Conference on Use of In Situ Tests in Geotechnical Engineering, Blacksburg, Virginia, pp. 191-205.

12. Kramer, S. L., Satari, R., and Kilian, A. P. (1990). "Evaluation of insitu strength of a peat deposit from laterally loaded pile test results," *Transportation Research Record No. 1278*, Transportation Research Board, Washington, D. C., 103-109.

13. Kramer, Steven L. (1991). "Behavior of Piles in Full-Scale, Field Lateral Loading Tests," Washington State Transportation Center, Seattle, Washington, October, 79 pp.

14. Chan, C. K. and Mulilis, J. P. (1976). "Pneumatic Sinusoidal Loading System," *Journal of the Geotechnical Engineering Division*, ASCE, Vol. 102, No. GT3, pp. 277-282.

15. Chan, C. K. (1982). "An Electropneumatic Cyclic Loading System," *Geotechnical Testing Journal*, ASTM, pp. 183-187.

16. Li, X. S., Chan, C. K., and Shen, C. K. (1988). "An Automated Triaxial Tesing System," Advanced Triaxial Testing of Soil and Rock, ASTM STP 977, pp. 95-106.

17. Kramer, S. L., Von Laun, F.-Y., and Sivaneswaran, N. (1992). "Strain-controlled, variable frequency cyclic loading system for soft soils, " submitted for review to *ASTM Geotechnical Testing Journal*, July.

18. Shirley, D. J. and Anderson, A. L. (1975). "Acoustic and Engineering Properties of Sediments," Applied Research Laboratory, University of Texas at Austin, Report No. ARL-TR-75-58.

19. Dyvik, R. and Madshus, C. (1985). "Lab Measurements of G_{max} Using Bender Elements," Advances in the Art of Testing Soils Under Cyclic Conditions, ASCE, V. Khosla, ed., pp. 186-196.

20. Thomann, T. G. and Hryciw, R. D. (1990). "Laboratory Measurement of Small Strain Shear Modulus Under K_0 Conditions," Geotechnical Testing Journal, ASTM, Vol. 13, No. 2, pp. 97-105.

21. Schnabel, P. B., Lysmen, J., and Seed, H. B. (1972). "SHAKE: A Computer Program for Earthquake Response Analysis of Horizontally Layered Sites," Earthquake Engineering Research Center Report No. EERC 72-12, December, 88 pp.

22. Galster, R. W. and Laprade, W. T. (1991). "Geology of Seattle, Washington, United States of America," Bulletin of the Association of Engineering Geologists, Vol. 28, No. 3, pp. 235-302.

23. Rittenhouse-Zeman and Associates (1989). "Bellevue Transit Access, EBDC & WBCD Ramp Movement, SR-90, King County, Washington, " 40 pp.

24. GeoEngineers, Inc. (1989). "Report of Geotechnical Services, SB-HOV Ramp, WB Ramp Widening, and S-WB Ramp, Bellevue Transit Access, SR-90, Bellevue, Washington," July, 50 pp.

25. GeoEngineers, Inc. (1989). "Report of Geotechnical Services, EB-N/S Ramp and EBCD Widening, Bellevue Transit Access, SR-90, Bellevue, Washington," February, 36 pp.

26. Seed, H. B. and Idriss, I. M. (1970). "Soil Moduli and Damping Factors for Dynamic Response Analysis," Report No. EERC 70-10, Earthquake Engineering, Research Center, University of California, Berkeley, California, September, 37 pp.

27. Vucetic, M. and Dobry, R. (1991).. "Effect of soil plasticity on cyclic response," *J. Geotech. Engrg.*, ASCE, 117(1), 89-107.

28. Novak, M. (1991). "Piles Under Dynamic Loads," Proceedings, Second International Conference on Recent Advances in Geotechnical Engineering and Soil Dynamics, St. Louis, Missouri, Vol. III, pp. 247-273.

29. Gazetas, G. and Dobry, R. (1984). "Horizontal Response of Piles in Layered Soils," Journal of the Geotechnical Engineering Division, ASCE, Vol. 101, No. 1, pp. 20-40.

30. Scott, R. F. (1981). *Foundation Analysis*, Prentice Hall, Inc., Englewood Cliffs, N.J., 545 pp.

31. Applied Technology Council (1984). "Tentative Provisions for the Development of Seismic Regulations for Buildings," Report ATC-3-06, Palo Alto, California, 599 pp.

32. Applied Technology Council (1986). "Seismic Design Guidelines for Highway Bridges," Report ATC-6, Redwood City, California, 204 pp.

33. Matlock, H. and Reeses, L.C. (1960). "Generalized Solution for Laterally Loaded Piles," *Journal of the Soil Mechanics and Foundations Division*, ASCE, Vol. 86, No. SM5, pp. 63-91.

34. Matlock, H. (1970). "Correlations for design of laterally pile in soft clays," *Paper No. OTC 1204*, Second Annual Offshore Technology Conference, Houston, Texas, Vol. 1, pp. 577-594.

35. Nogami, T. and Novak, M. (1977). "Resistance of Soil to a Horizontally Vibrating Pile," *Journal of Earthquake Engineering and Structural Dynamics*, Vol. 5, pp. 249-261.

36. Blaney, G.W. and O'Neill, M.W. (1983). "Lateral Response of a Single Pile in Overconsolidated Clay to Relatively Low-Frequency Pile-Head Loads and Harmonic Ground Surface Loads," *Research Report UHCE 83-19*, Department of Civil Engineering, University of Houston, Houston, Texas.

37. Kachedoorian, R. (1968). "Effects of Earthquake of March 27, 1964 on the Alaska Highway System," *Professional Paper 545-C*, U.S. Geological Survey, Department of Interior, Washington, D.C.

38. Elliot, A.L. and Nagai, I. (1973). "Earthquake Damage to Freeway Bridges," *San Fernando, California Earthquake of February 9, 1971*, Vol. II, National Oceanic and Atmospheric Administration, U.S. Department of Commerce, Washington, D.C.

39. Hideaki, K. (1980). "Damage of Reinforced Precast Piles During the Miyagi-Ken-Oki Earthquake of June 12, 1972" *Proceedings*, 7th World Conference on Earthquake Engineering, Vol. 9, Istanbul, Turkey.

40. Margason, E. and Holloway, D.M. (1977). "Pile Bending During Earthquakes," *Proceedings*, 6th World Conference on Earthquake Engineering, Vol. 4, New Delhi, India.

41. Banerjee, S., Stanton, J.F., and Hawkins, N.M. (1987). "Seismic Performance of Precast Prestressed Concrete Piles," *Journal of Structural Engineering*, ASCE, Vol. 113, No. 2, pp. 381-396.

BIBLIOGRAPHY

Andrejko, M. J., Fiene, F., and Cohen, A. D. (1983). "Comparison of ashing techniques for determination of the inorganic content of peats," *Testing of Peats and Organic Soils*, ASTM STP 820, 5-20.

Applied Technology Council (1984). "Tentative Provisions for the Development of Seismic Regulations for Buildings," Report ATC-3-06, Palo Alto, California, 599 pp.

Applied Technology Council (1986). "Seismic Design Guidelines for Highway Bridges," Report ATC-6, Redwood City, California, 204 pp.ASTM (1991). "Test for Moisture, Ash, and Organic Matter of Peat Materials," *Annual Book of ASTM Standards*, Part 19, pp.

Banerjee, S., Stanton, J.F., and Hawkins, N.M. (1987). "Seismic Performance of Precast Prestressed Concrete Piles," *Journal of Structural Engineering*, ASCE, Vol. 113, No. 2, pp. 381-396.

Blaney, G.W. and O'Neill, M.W. (1983). "Lateral Response of a Single Pile in Overconsolidated Clay to Relatively Low-Frequency Pile-Head Loads and Harmonic Ground Surface Loads," *Research Report UHCE 83-19*, Department of Civil Engineering, University of Houston, Houston, Texas.

Board of Inquiry (1990) "Competing Against Time," C. C. Thiel, ed., Office of Planning and Research, State of California, May, 264 pp.

Chan, C. K. (1982). "An Electropneumatic Cyclic Loading System," *Geotechnical Testing Journal*, ASTM, pp. 183-187.

Chan, C. K. and Mulilis, J. P. (1976). "Pneumatic Sinusoidal Loading System," *Journal of the Geotechnical Engineering Division*, ASCE, Vol. 102, No. GT3, pp. 277-282.

Crouse, C. B., Kramer, S. L., Mitchell, R. and Hushmand, B. (1991). "Dynamic tests of a pipe pile in saturated peat," submitted for review to *ASCE Journal of Geotechnical Engineering*, May.

Dobry, R. and Vucetic, M. (1987). "State-of-the-Art Report: Dynamic Properties and Response of Soft Clay Deposits," *Proceedings of the International Symposium on Geotechnical Engineering of Soft Soils*, Mexico City, Mexico, Vol. 2, pp. 51-87.

Dobry, R. and Vucetic, M. (1990). "Dynamic properties and seismic response of soft clay deposits," *Proc.*, Int. Symp. Geotech. Engrg. Soft Soils, Mexico City, 2, 51-87.

Dyvik, R. and Madshus, C. (1985). "Lab Measurements of G_{max} Using Bender Elements," Advances in the Art of Testing Soils Under Cyclic Conditions, ASCE, V. Khosla, ed., pp. 186-196.

Elliot, A.L. and Nagai, I. (1973). "Earthquake Damage to Freeway Bridges," *San Fernando, California Earthquake of February 9, 1971*, Vol. II, National Oceanic

and Atmospheric Administration, U.S. Department of Commerce, Washington, D.C.

Galster, R. W. and Laprade, W. T. (1991). "Geology of Seattle, Washington, United States of America," Bulletin of the Association of Engineering Geologists, Vol. 28, No. 3, pp. 235-302.

Gazetas, G. and Dobry, R. (1984). "Horizontal Response of Piles in Layered Soils," Journal of the Geotechnical Engineering Division, ASCE, Vol. 101, No. 1, pp. 20-40.

GeoEngineers, Inc. (1989). "Report of Geotechnical Services, EB-N/S Ramp and EBCD Widening, Bellevue Transit Access, SR-90, Bellevue, Washington," February, 36 pp.

GeoEngineers, Inc. (1989). "Report of Geotechnical Services, SB-HOV Ramp, WB Ramp Widening, and S-WB Ramp, Bellevue Transit Access, SR-90, Bellevue, Washington," July, 50 pp.

Hideaki, K. (1980). "Damage of Reinforced Precast Piles During the Miyagi-Ken-Oki Earthquake of June 12, 1972" *Proceedings*, 7th World Conference on Earthquake Engineering, Vol. 9, Istanbul, Turkey.

Idriss, I. M. (1991). *Personal communication.*

Idriss, I. M., Dobry, R., and Singh, R. D. (1978). "Nonlinear Behavior of Soft Clays During Cyclic Loading," *Journal of the Geotechnical Engineering Division*, ASCE, Vol. 104, No. GT2, pp. 1427-1447.

Kachedoorian, R. (1968). "Effects of Earthquake of March 27, 1964 on the Alaska Highway System," *Professional Paper 545-C*, U.S. Geological Survey, Department of Interior, Washington, D.C.

Kokoshu, T., Yoshida, Y. and Esashi, Y. (1982). "Dynamic properties of soft clay for wide strain range," *Soils and Found.*, 22(4), 1-18.

Kramer, S. L. (1991). "Behavior of Piles in Full-Scale, Field Lateral Loading Tests," Washington State Transportation Center, Seattle, Washington, October, 79 pp.

Kramer, S. L., Satari, R., and Kilian, A. P. (1990). "Evaluation of insitu strength of a peat deposit from laterally loaded pile test results," *Transportation Research Record No. 1278*, Transportation Research Board, Washington, D. C., 103-109.

Kramer, S. L., Von Laun, F.-Y., and Sivaneswaran, N. (1992). "Strain-controlled, variable frequency cyclic loading system for soft soils, " submitted for review to *ASTM Geotechnical Testing Journal*, July.

Landva, A. (1986). "In-Situ Testing of Peat," *Proceedings*, ASCE Conference on Use of In Situ Tests in Geotechnical Engineering, Blacksburg, Virginia, pp. 191-205.

Landva, A. and LaRochelle, P. (1983). "Compressibility and Shear Characteristics of Radforth Peats," ASTM STP 820, pp. 141-156.

Landva, A., Korpijaakko, E. O., and Pheeney, P. E. (1983). "Geotechnical classification of peats and organic soils," *Testing of Peat and Orgnaic Soils*, ASTM STP 820. 37-54.

Li, X. S., Chan, C. K., and Shen, C. K. (1988). "An Automated Triaxial Tesing System," Advanced Triaxial Testing of Soil and Rock, ASTM STP 977, pp. 95-106.

Margason, E. and Holloway, D.M. (1977). "Pile Bending During Earthquakes," *Proceedings*, 6th World Conference on Earthquake Engineering, Vol. 4, New Delhi, India.

Matlock, H. (1970). "Correlations for design of laterally pile in soft clays," *Paper No. OTC 1204*, Second Annual Offshore Technology Conference, Houston, Texas, Vol. 1, pp. 577-594.

Matlock, H. and Reeses, L.C. (1960). "Generalized Solution for Laterally Loaded Piles," *Journal of the Soil Mechanics and Foundations Division*, ASCE, Vol. 86, No. SM5, pp. 63-91.

Newman, D. E. (1983). "A 13,500 year pollen record from Mercer Slough, King County, Washington," M. S. Thesis, University of Washington.

Nogami, T. and Novak, M. (1977). "Resistance of Soil to a Horizontally Vibrating Pile," *Journal of Earthquake Engineering and Structural Dynamics*, Vol. 5, pp. 249-261.

Novak, M. (1991). "Piles Under Dynamic Loads," Proceedings, Second International Conference on Recent Advances in Geotechnical Engineering and Soil Dynamics, St. Louis, Missouri, Vol. III, pp. 247-273.

Rittenhouse-Zeman and Associates (1989). "Bellevue Transit Access, EBDC & WBCD Ramp Movement, SR-90, King County, Washington, " 40 pp.

Schnabel, P. B., Lysmen, J., and Seed, H. B. (1972). "SHAKE: A Computer Program for Earthquake Response Analysis of Horizontally Layered Sites," Earthquake Engineering Research Center Report No. EERC 72-12, December, 88 pp.

Scott, R. F. (1981). *Foundation Analysis*, Prentice Hall, Inc., Englewood Cliffs, N.J., 545 pp.

Seed, H. B. and Fead, J. W. (1959). "Apparatus for Repeated Load Tests on Soils," *Proceedings*, ASTM.

Seed, H. B. and Idriss, I. M. (1970). "Analyses of ground motions at Union Bay, Seattle during earthquakes and distant nuclear blasts, " *Bull. Seism. Soc. Am.*, 60(1), 125-136.

Seed, H. B. and Idriss, I. M. (1970). "Soil Moduli and Damping Factors for Dynamic Response Analysis," Report No. EERC 70-10, Earthquake Engineering, Research Center, University of California, Berkeley, California, September, 37 pp.

Shannon and Wilson (1967). "Thomson Way crossing of Union Bay, Seattle, Washington," *Foundation Engineering Report Technical Supplement*, November, 108 pp.

Shirley, D. J. and Hampton, A. L. (1975). "Acoustic and Engineering Properties of Sediments," Applied Research Laboratory, University of Texas at Austin, Report No. ARL-TR-75-58.

Thomann, T. G. and Hryciw, R. D. (1990). "Laboratory Measurement of Small Strain Shear Modulus Under K_0 Conditions," Geotechnical Testing Journal, ASTM, Vol. 13, No. 2, pp. 97-105.

Tsai, N.-C. (1969). "Influence of local geology on earthquake ground motion," Earthquak Engrg. Res. Lab., Calif. Inst. Tech.

Vucetic, M. and Dobry, R. (1991).. "Effect of soil plasticity on cyclic response," *J. Geotech. Engrg.*, ASCE, 117(1), 89-107.

APPENDIX A

STAGE 1 GROUND RESPONSE ANALYSES

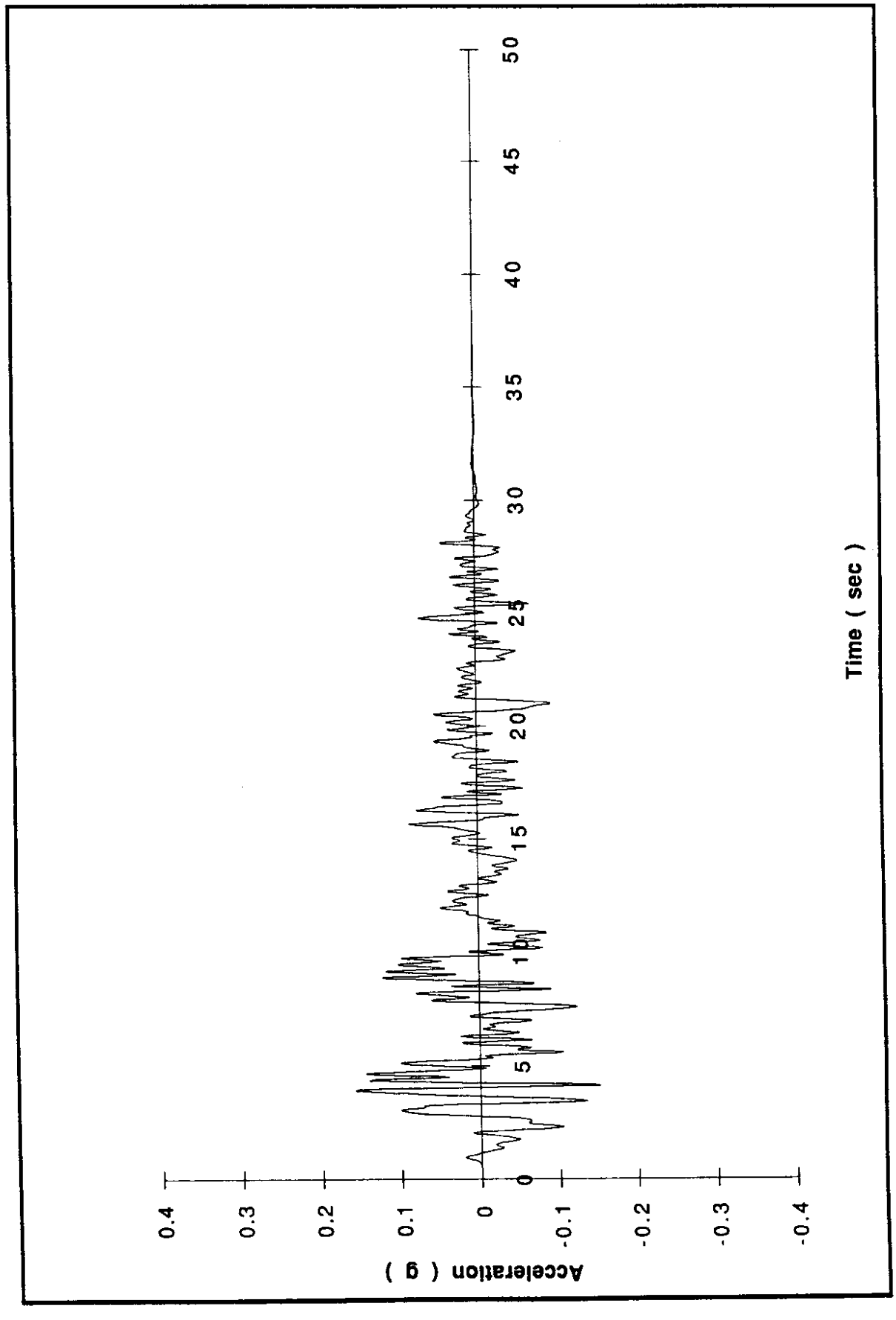

Figure A-1. Zone 1 — El Centro

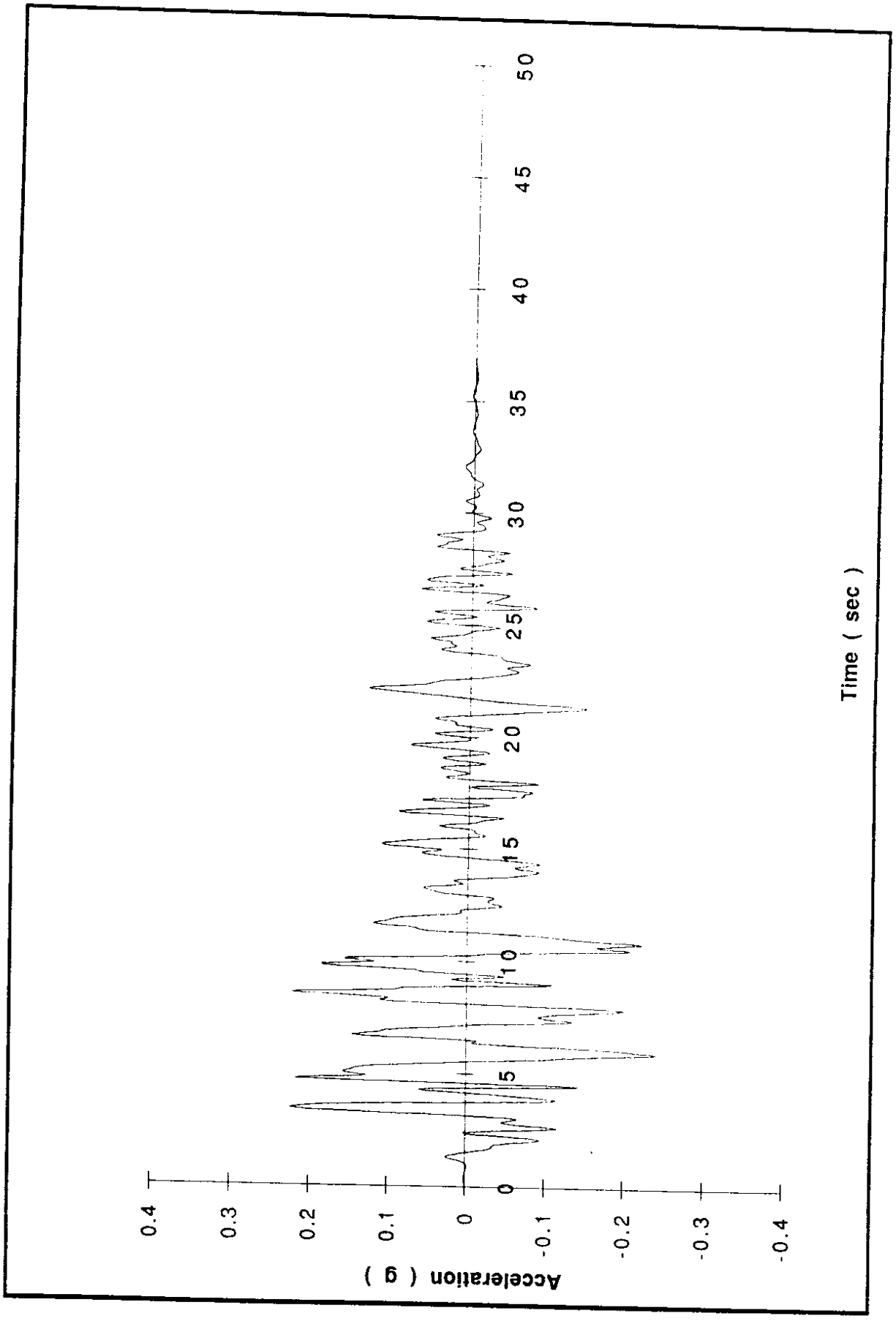

Figure A-2. Zone 2 — El Centro

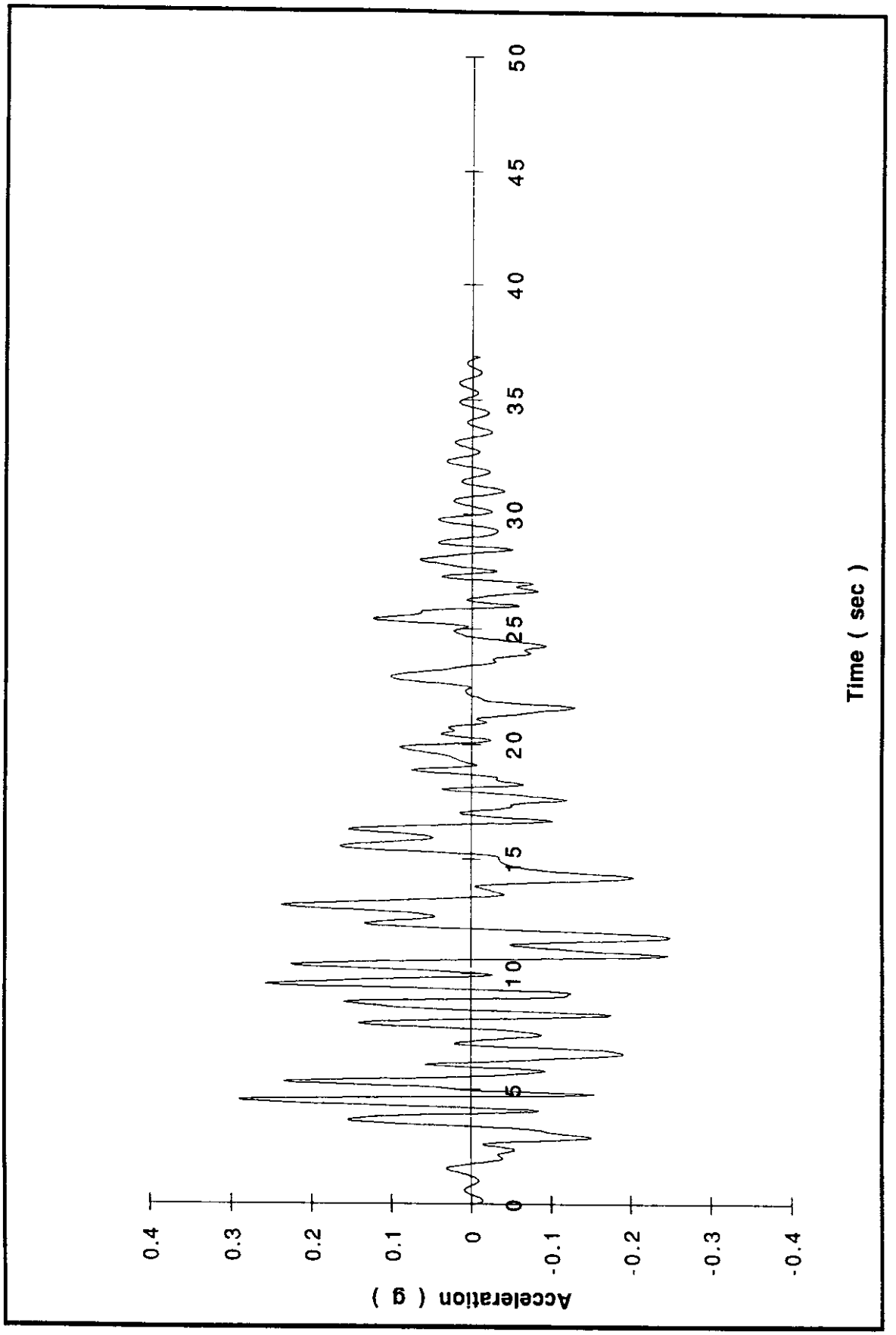

Figure A-3. Zone 3 — El Centro

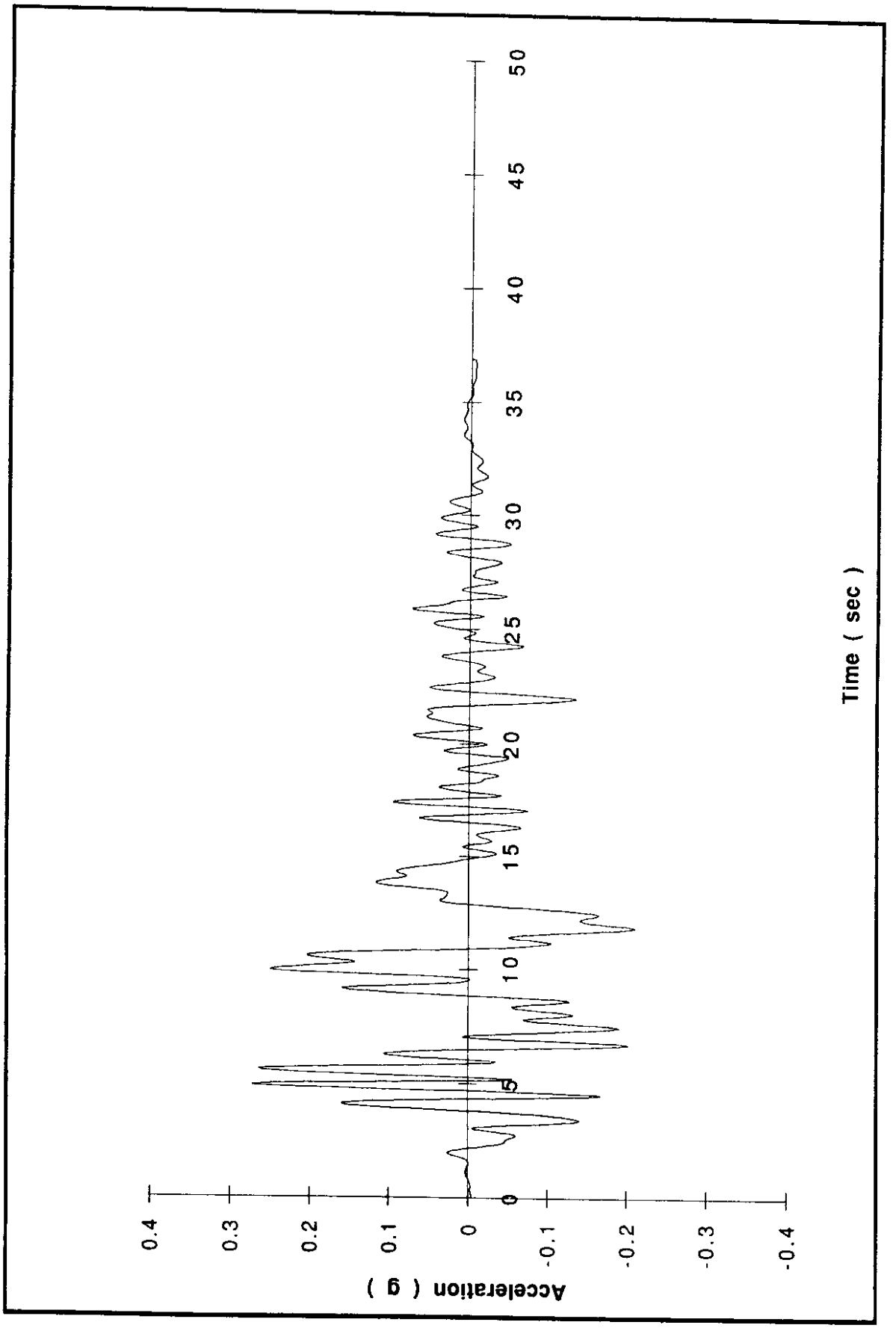

Figure A-4. Zone 4 — El Centro

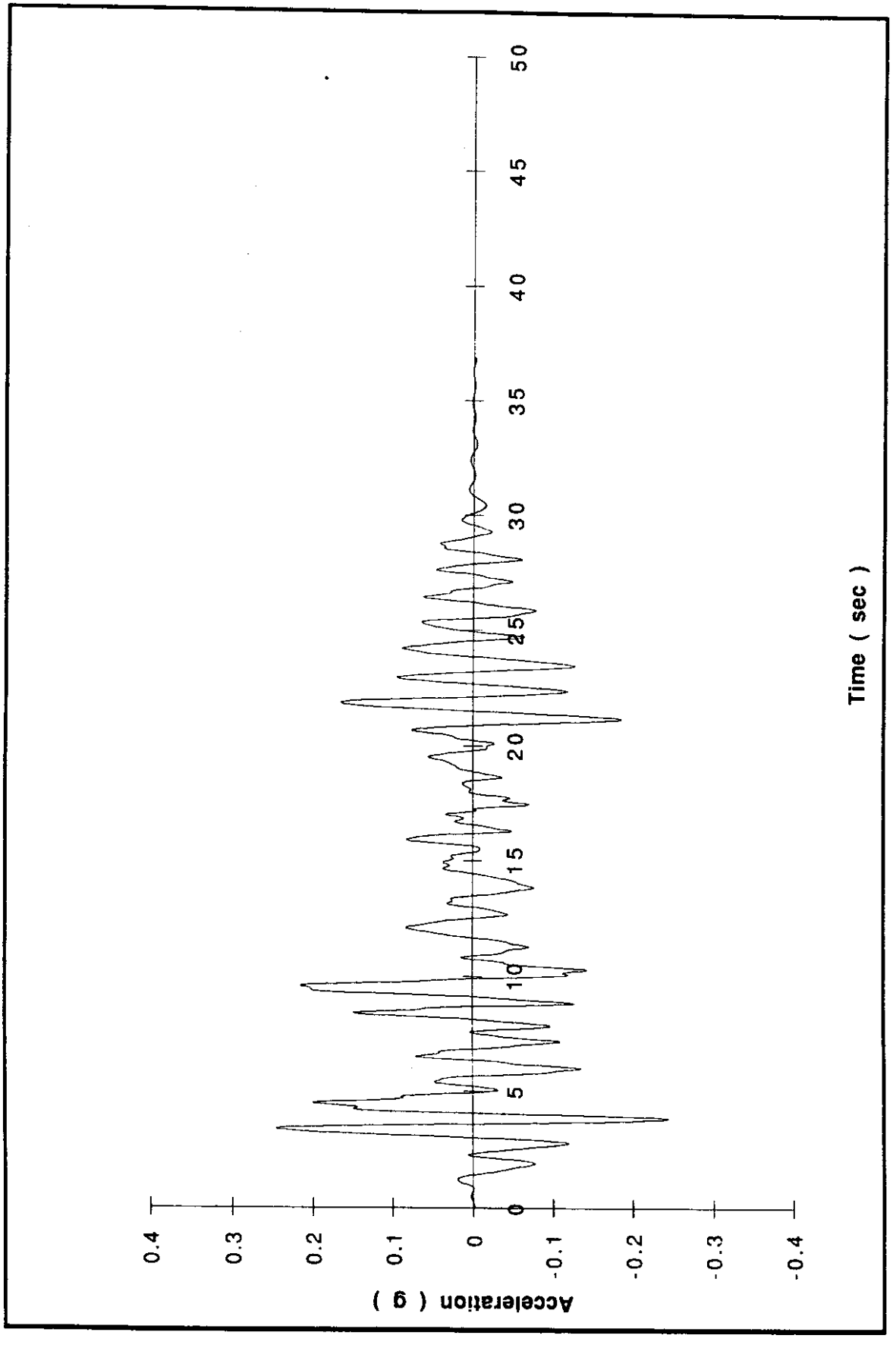

Figure A-5. Zone 5 — El Centro

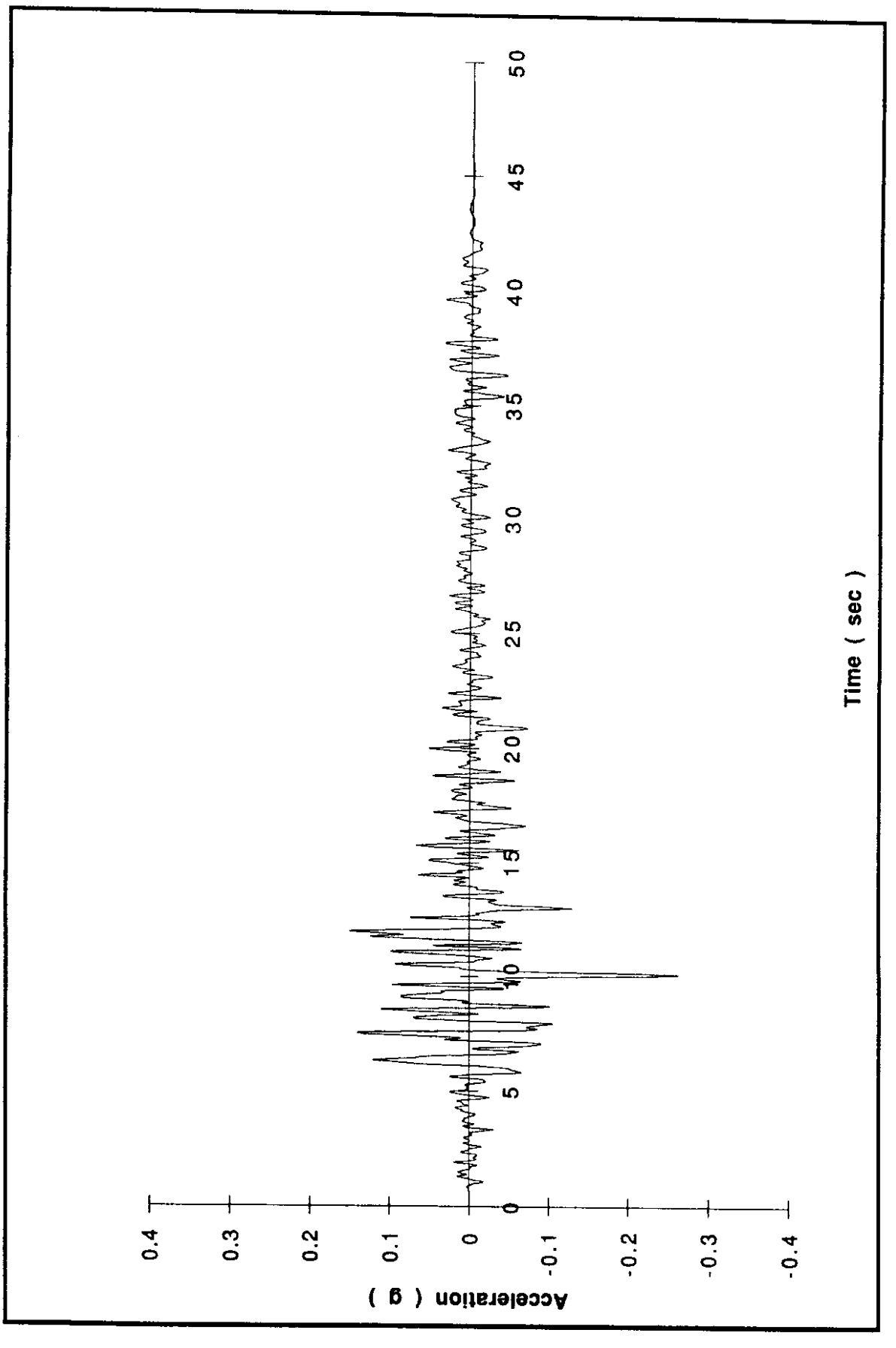

Figure A-6. Zone 1 — Lake Hughes

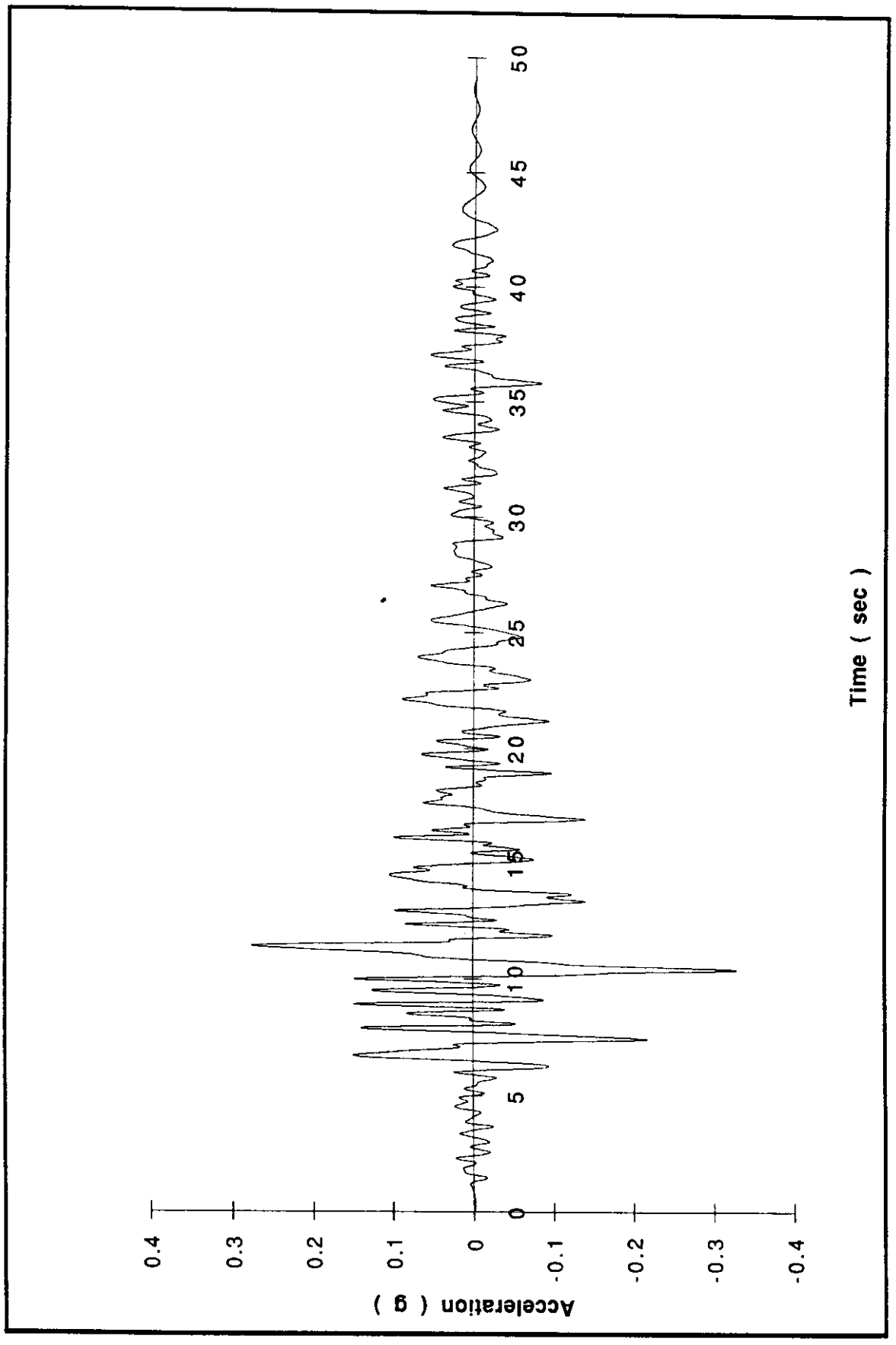

Figure A-7. Zone 2 — Lake Hughes

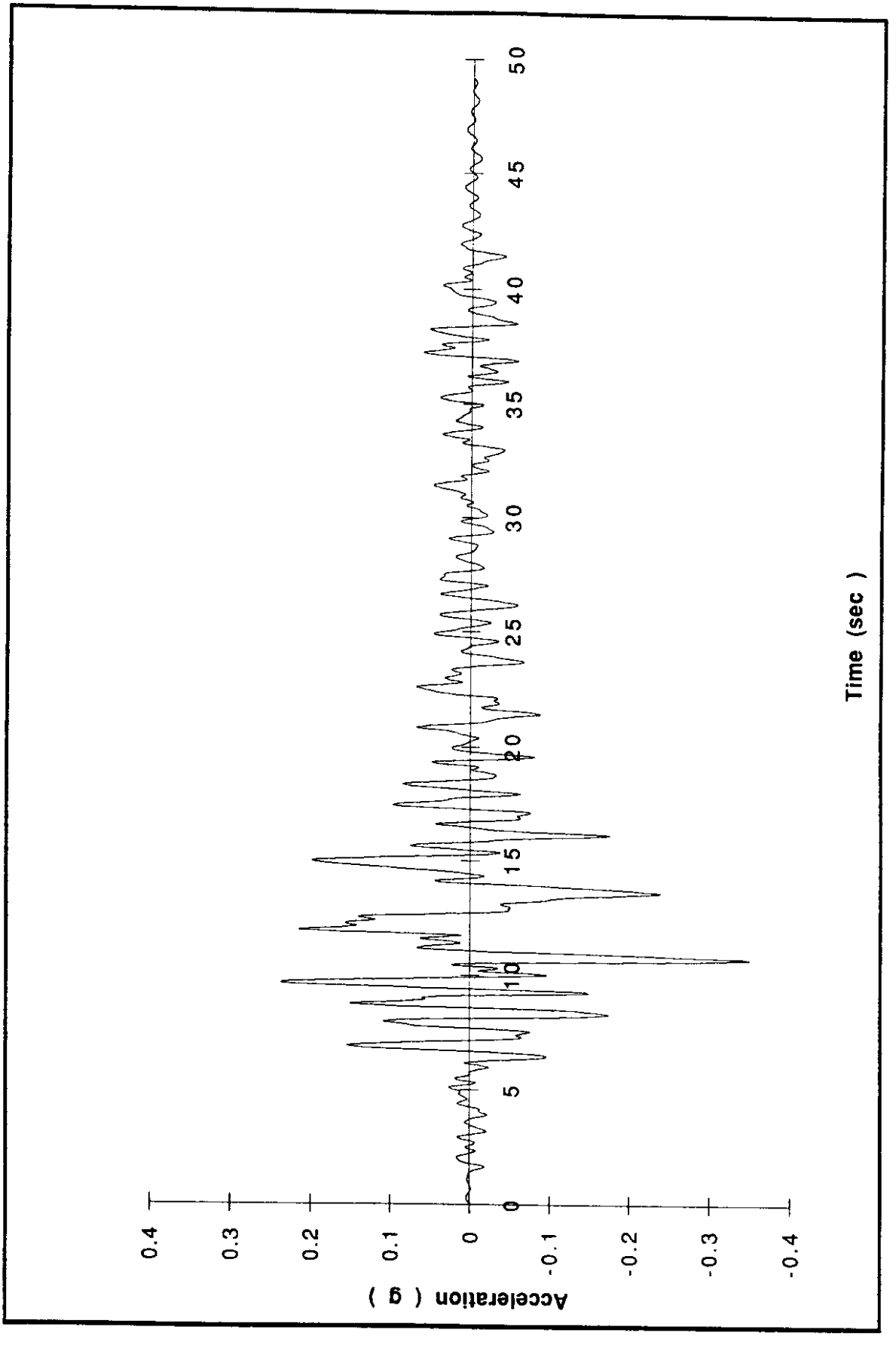

Figure A-8. Zone 3 — Lake Hughes

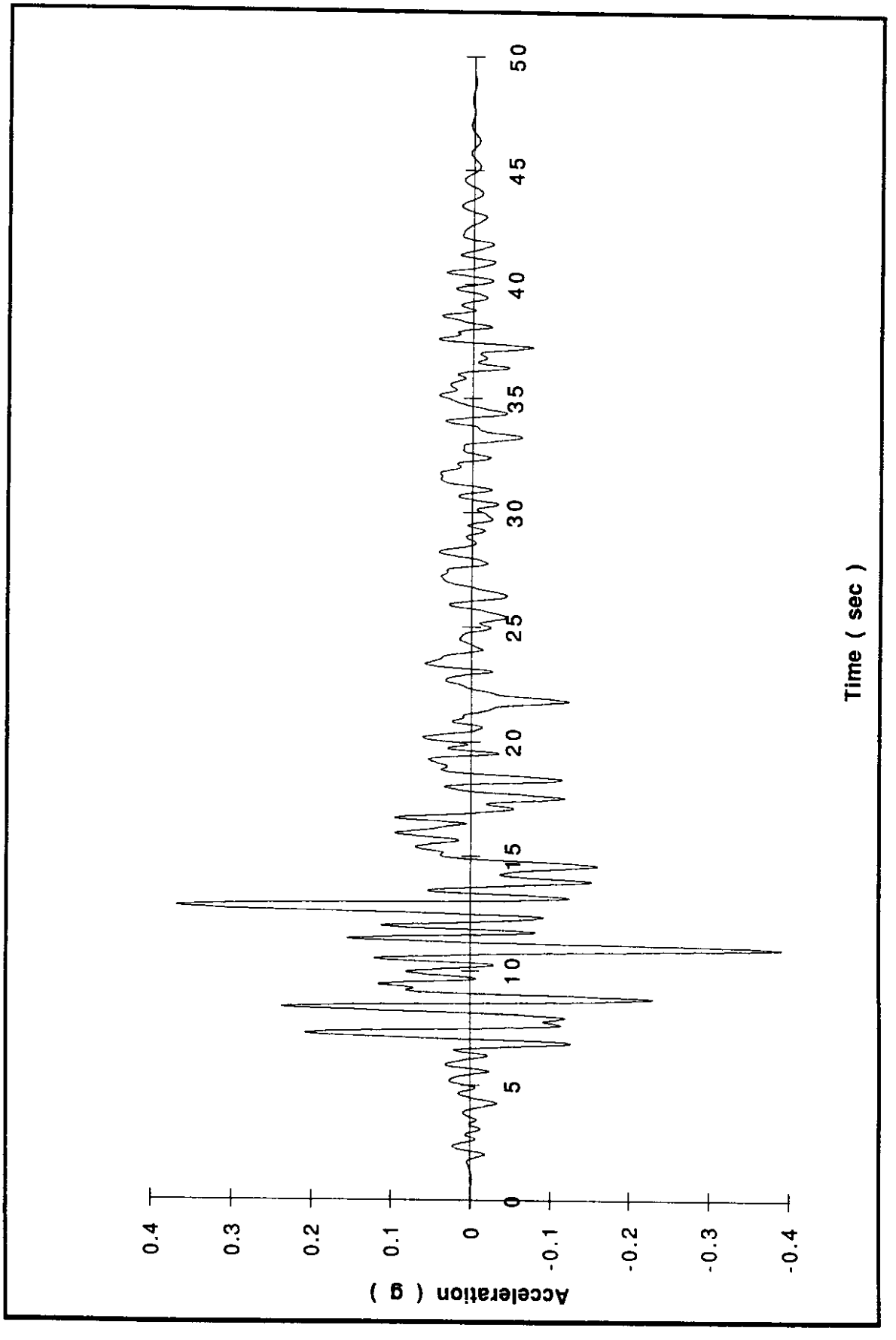

Figure A-9. Zone 4 — Lake Hughes

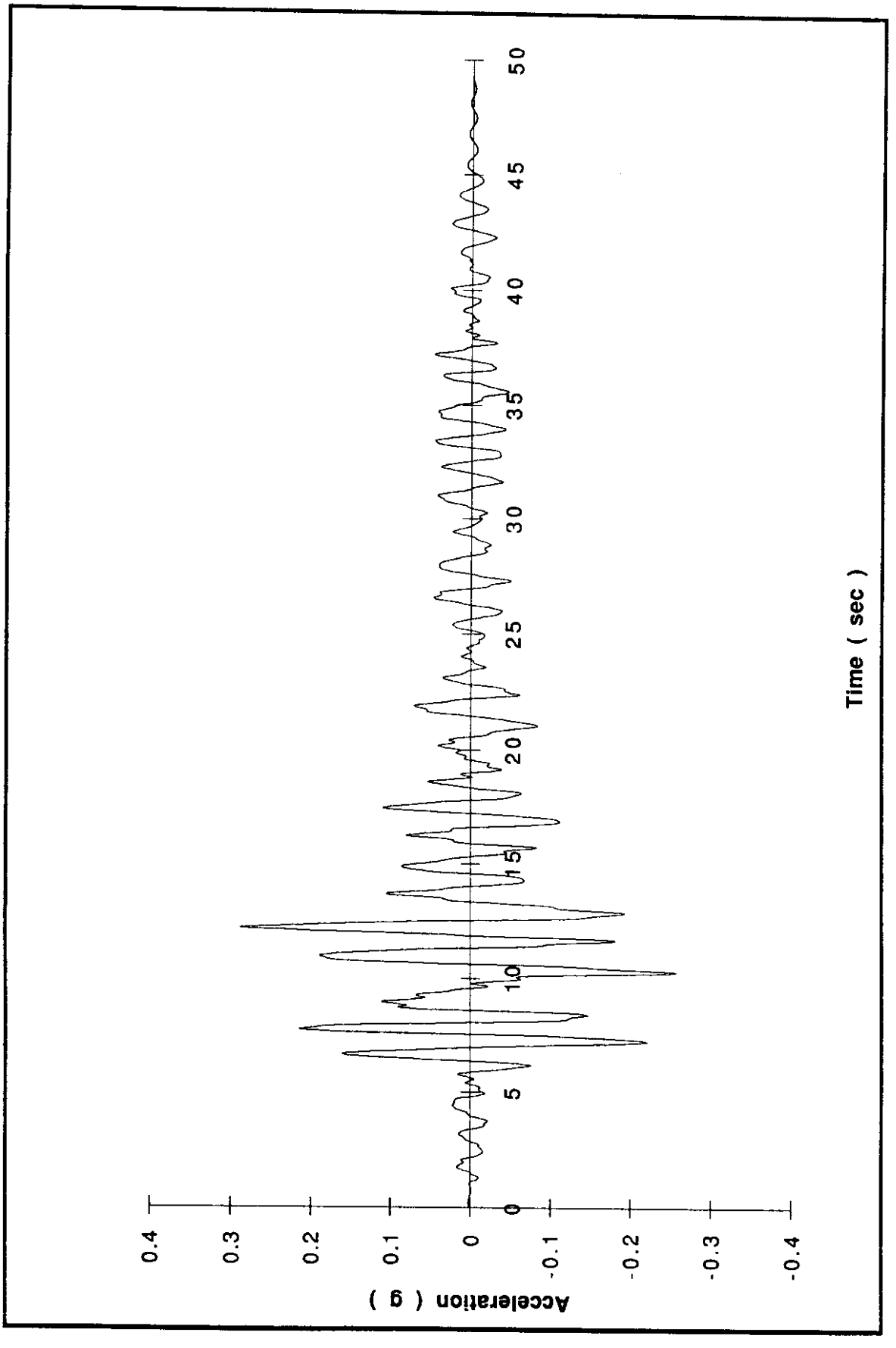

Figure A-10. Zone 5 — Lake Hughes

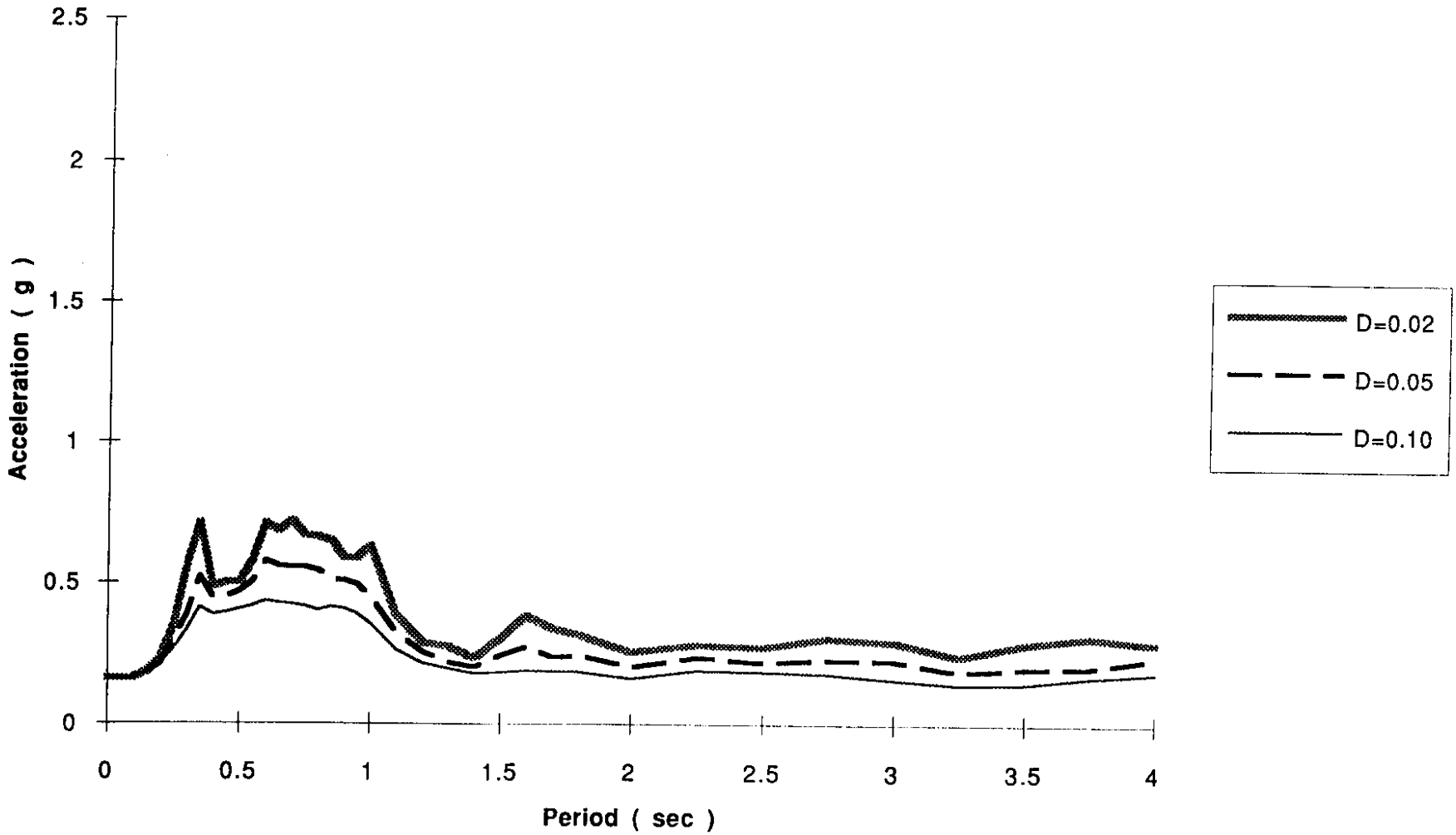

Figure A-11. Zone 1 — El Centro

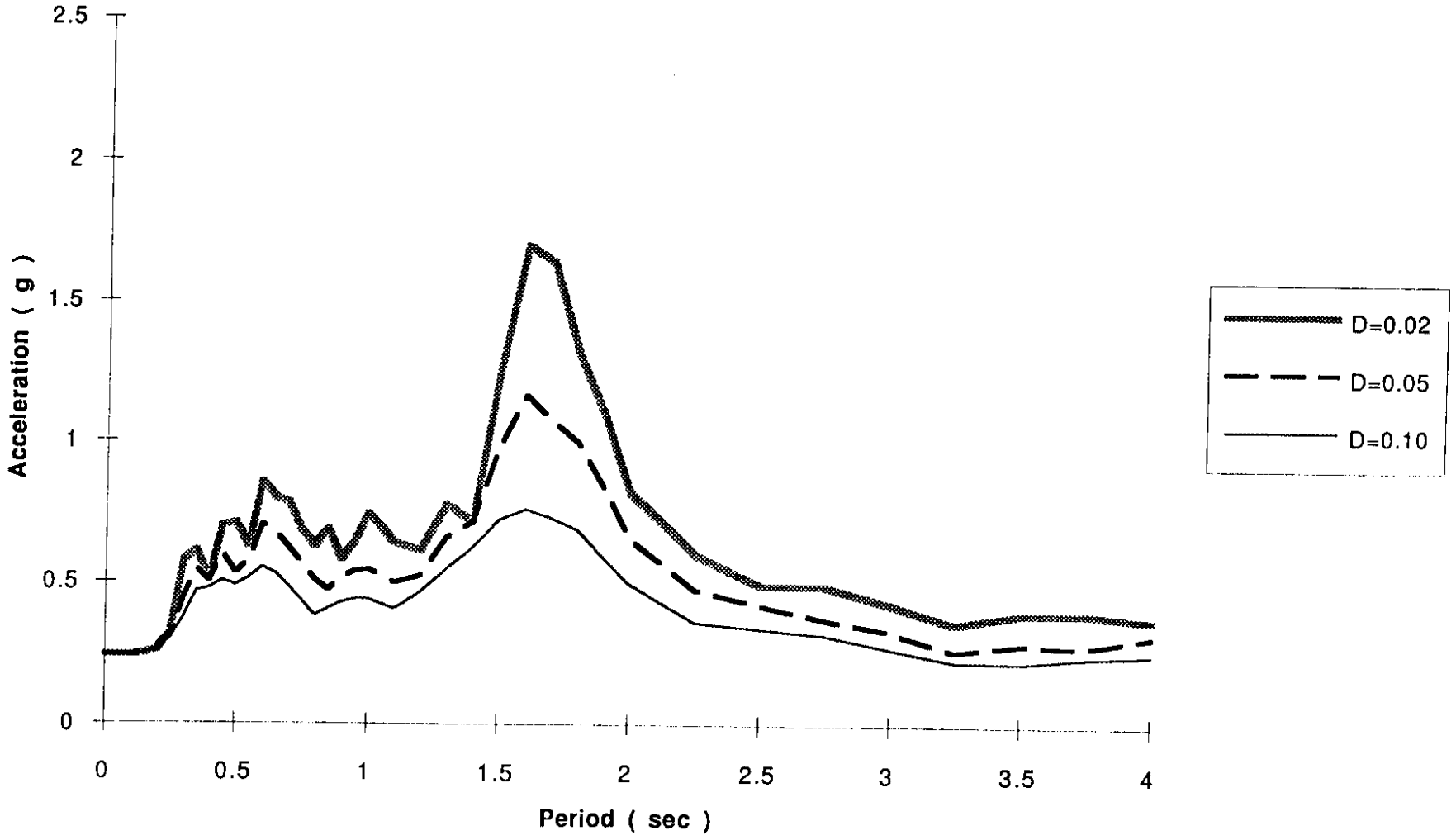

Figure A-12. Zone 2 — El Centro

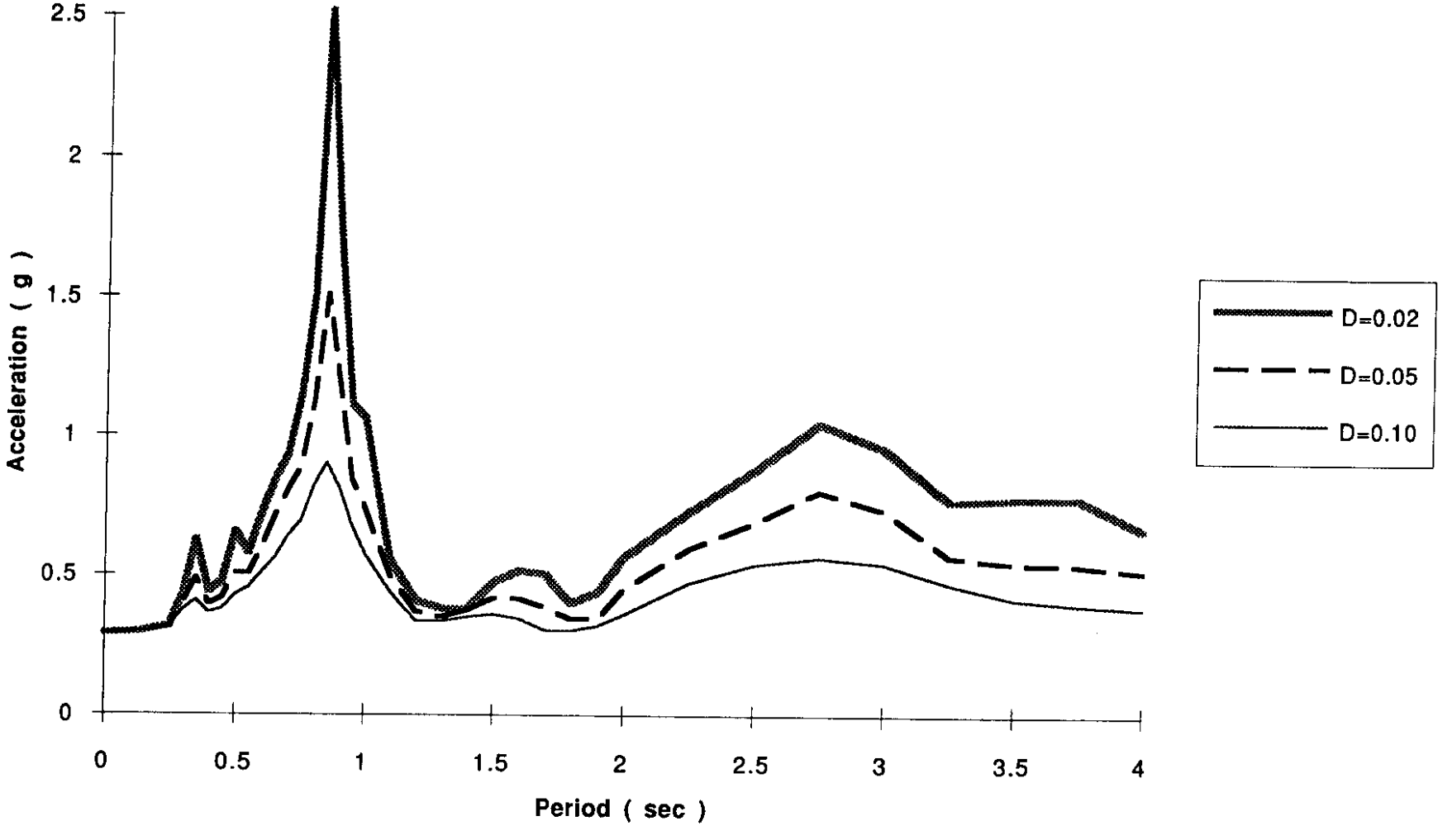

Figure A-13. Zone 3 — El Centro

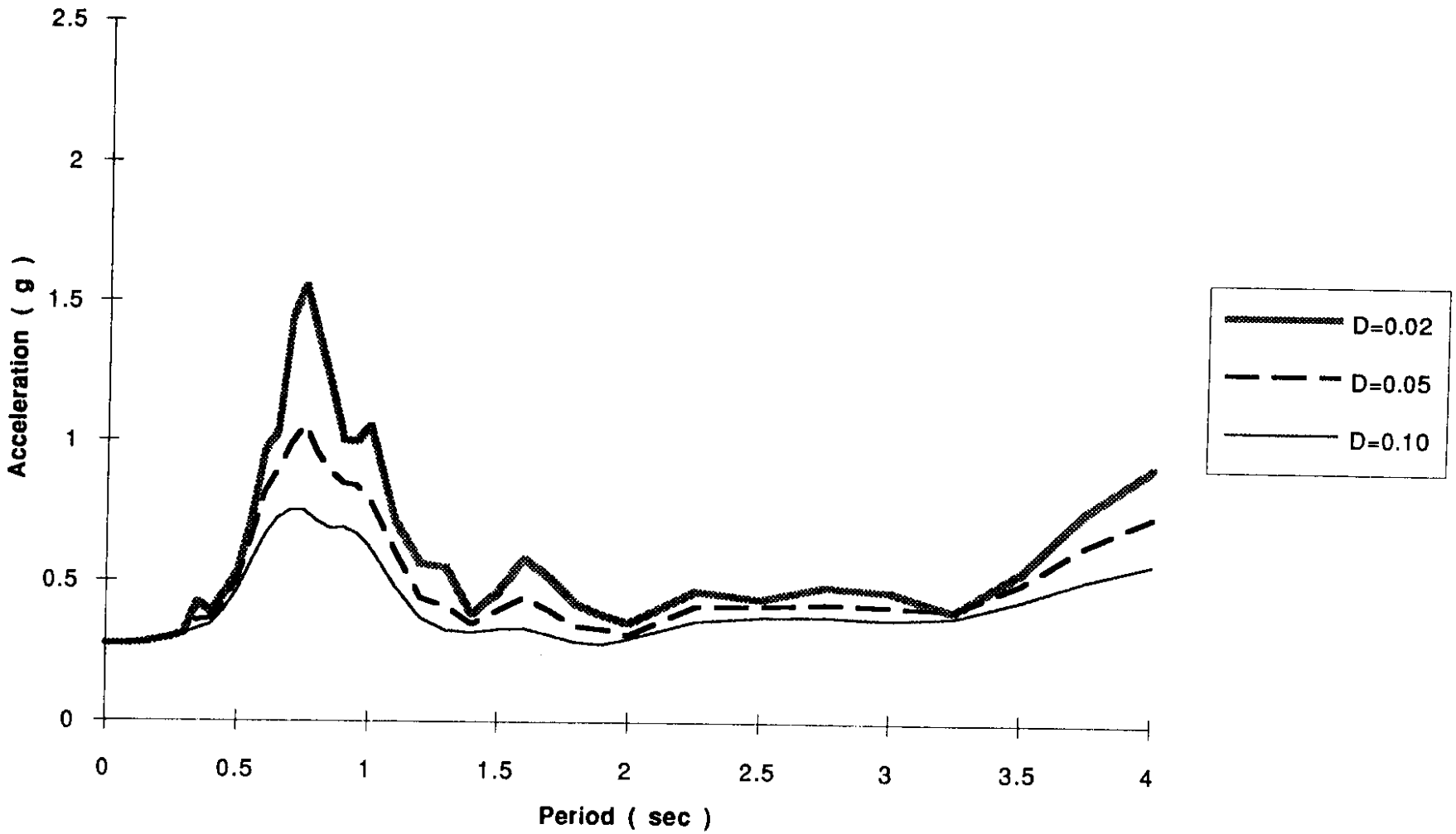

Figure A-14. Zone 4 — El Centro

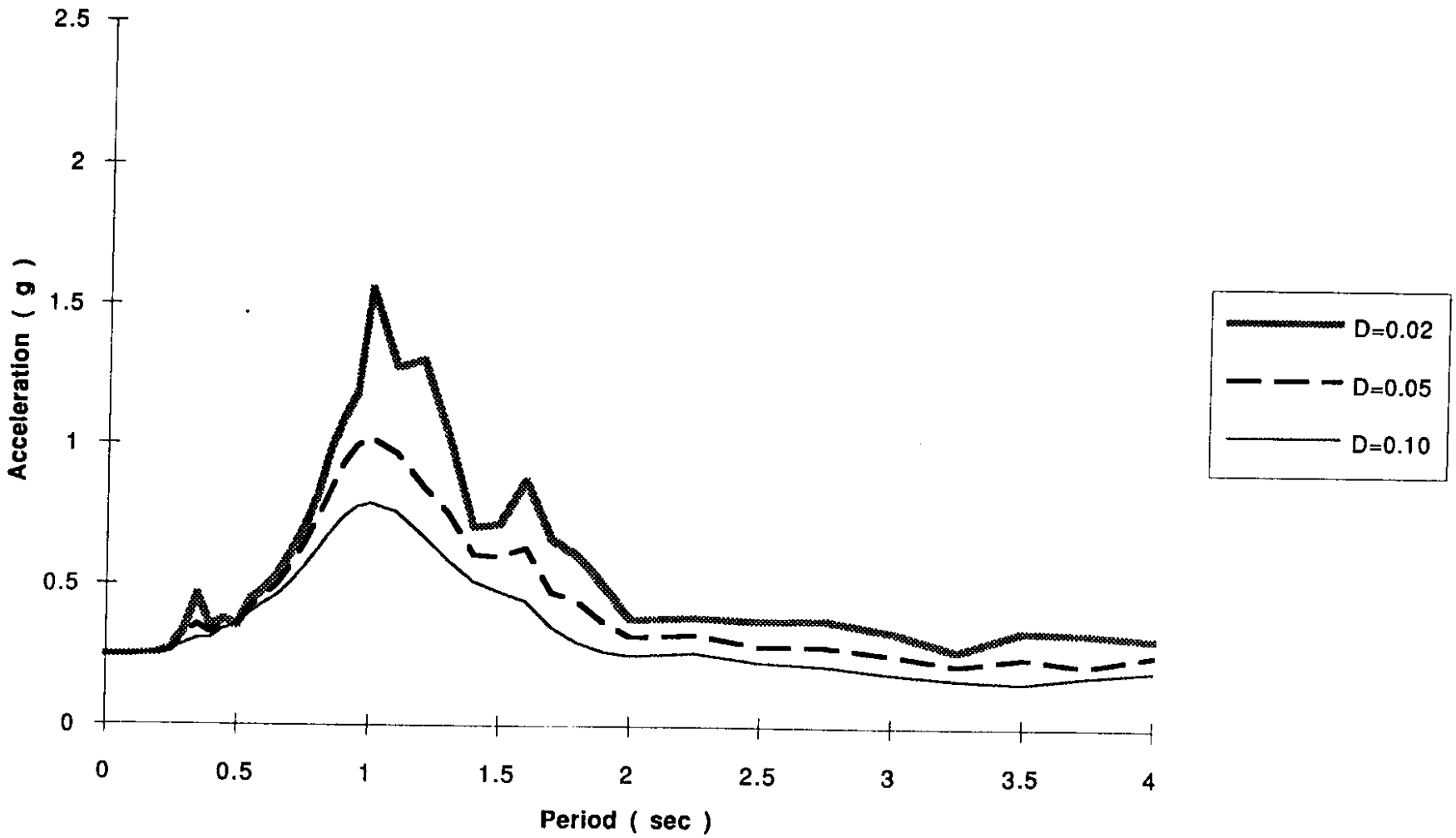

Figure A-15. Zone 5 — El Centro

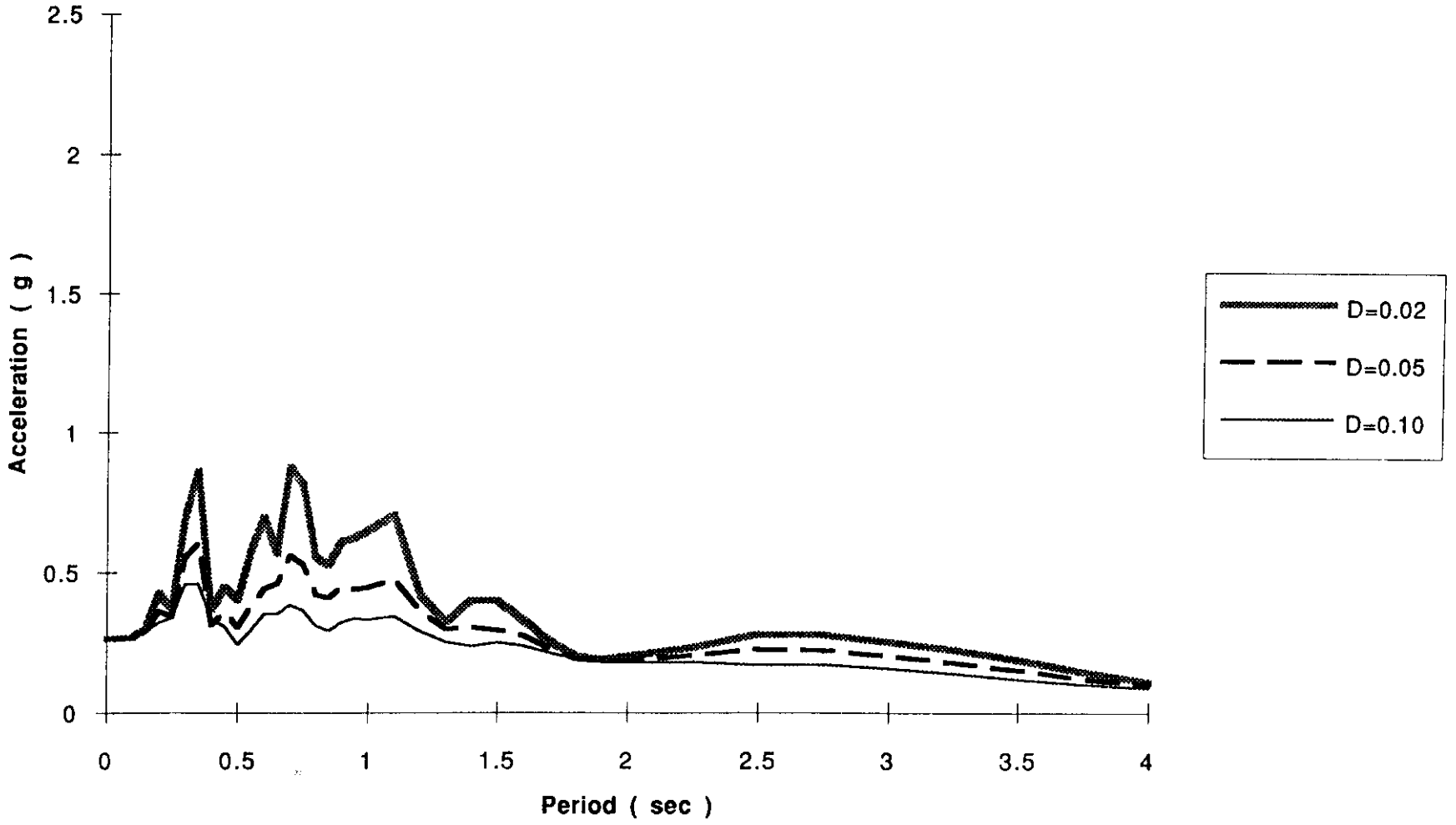

Figure A-16. Zone 1 — Lake Hughes

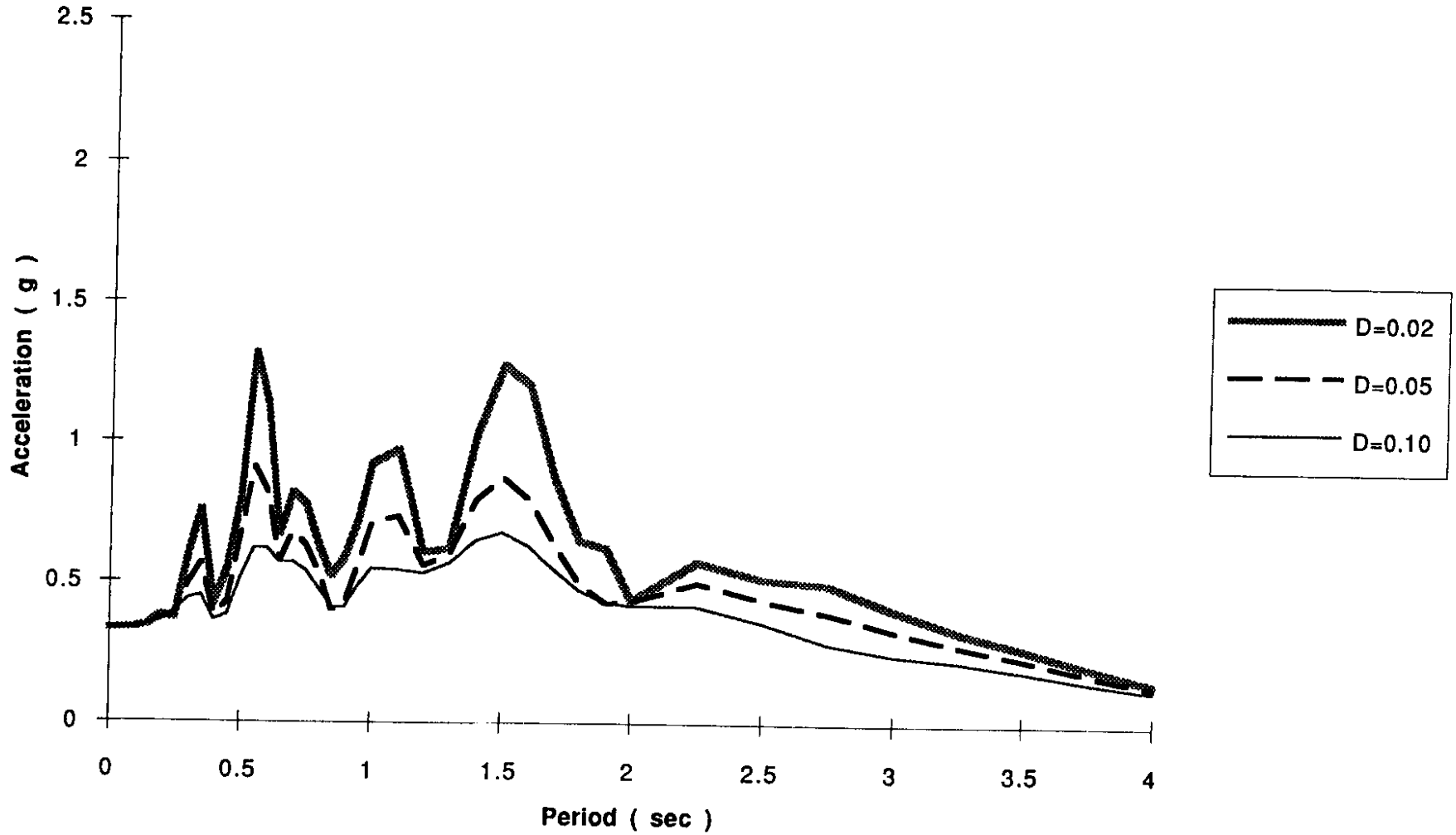

Figure A-17. Zone 2 — Lake Hughes

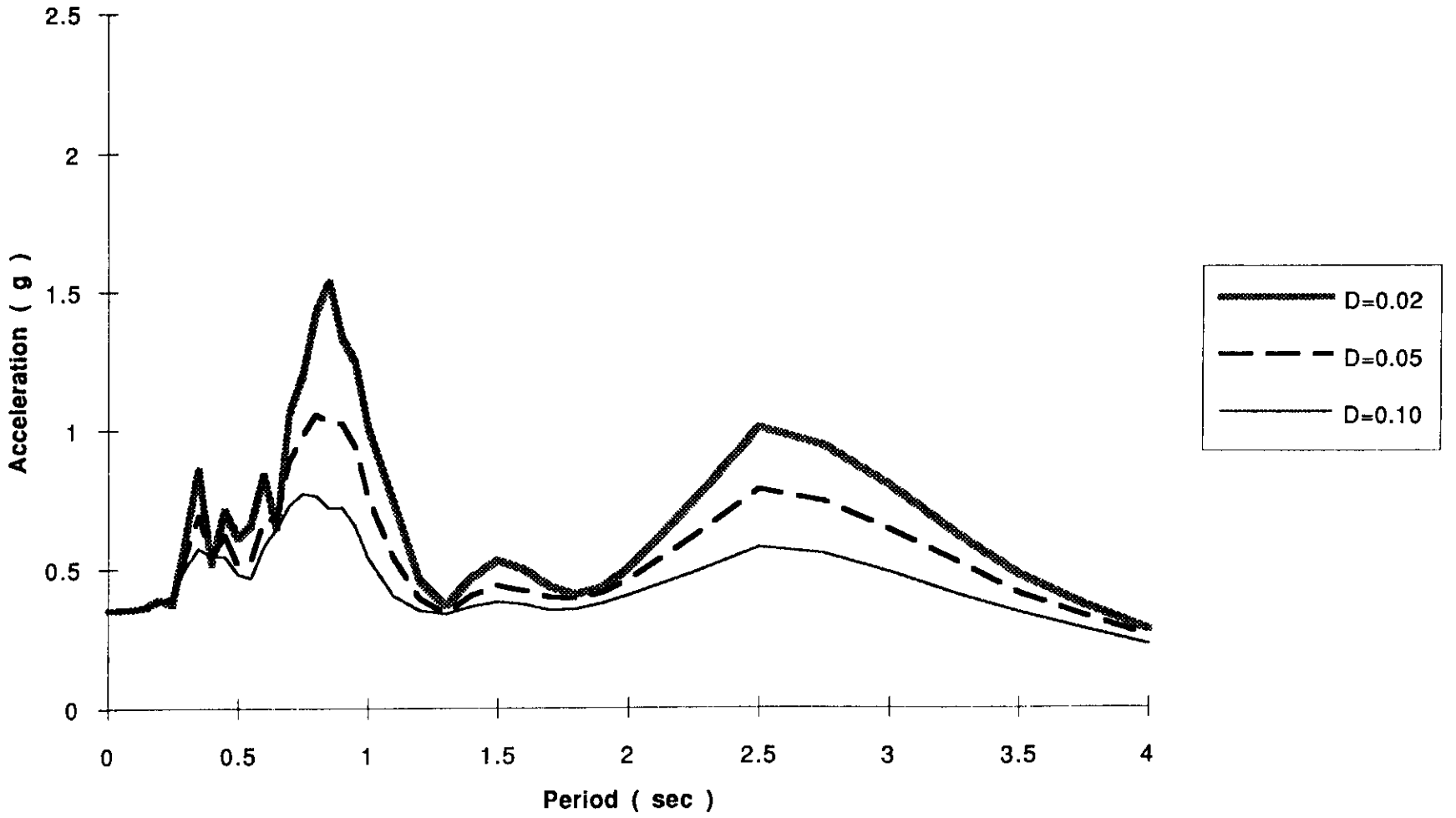

Figure A-18. Zone 3 — Lake Hughes

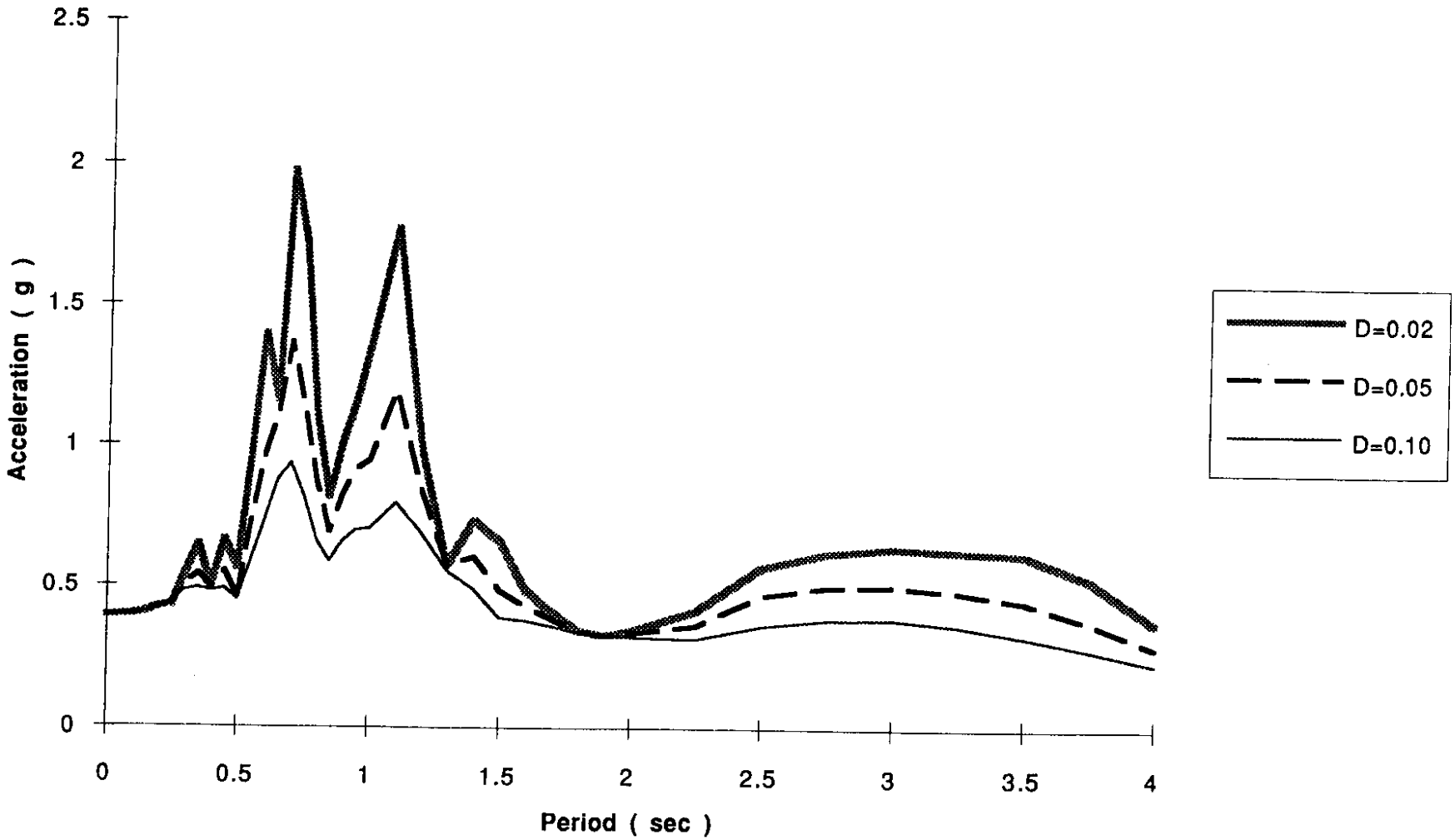

Figure A-19. Zone 4 — Lake Hughes

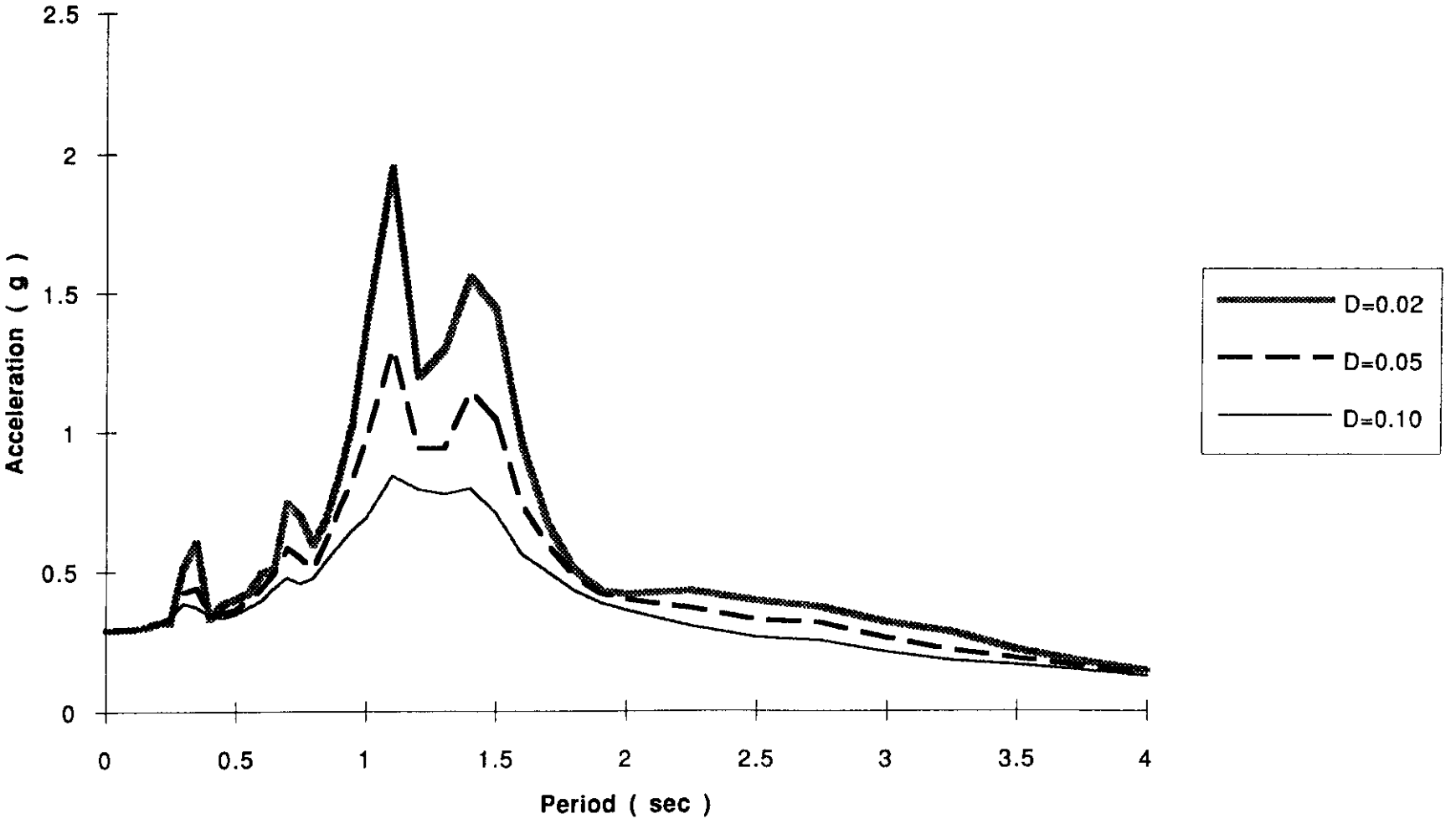

Figure A-20. Zone 5 — Lake Hughes

APPENDIX B

STAGE 2 GROUND RESPONSE ANALYSES

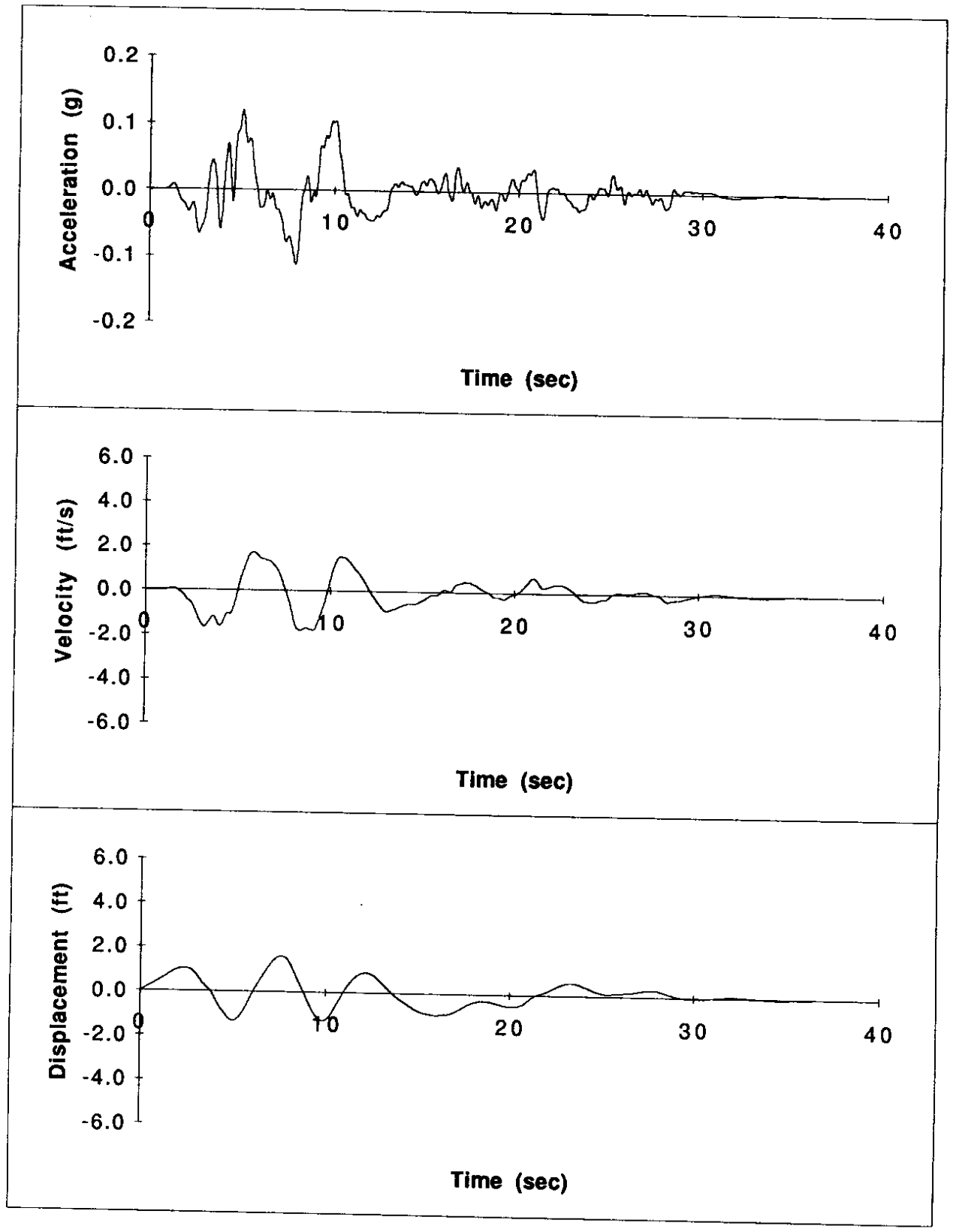

Figure B-1. Zone 1 — El Centro

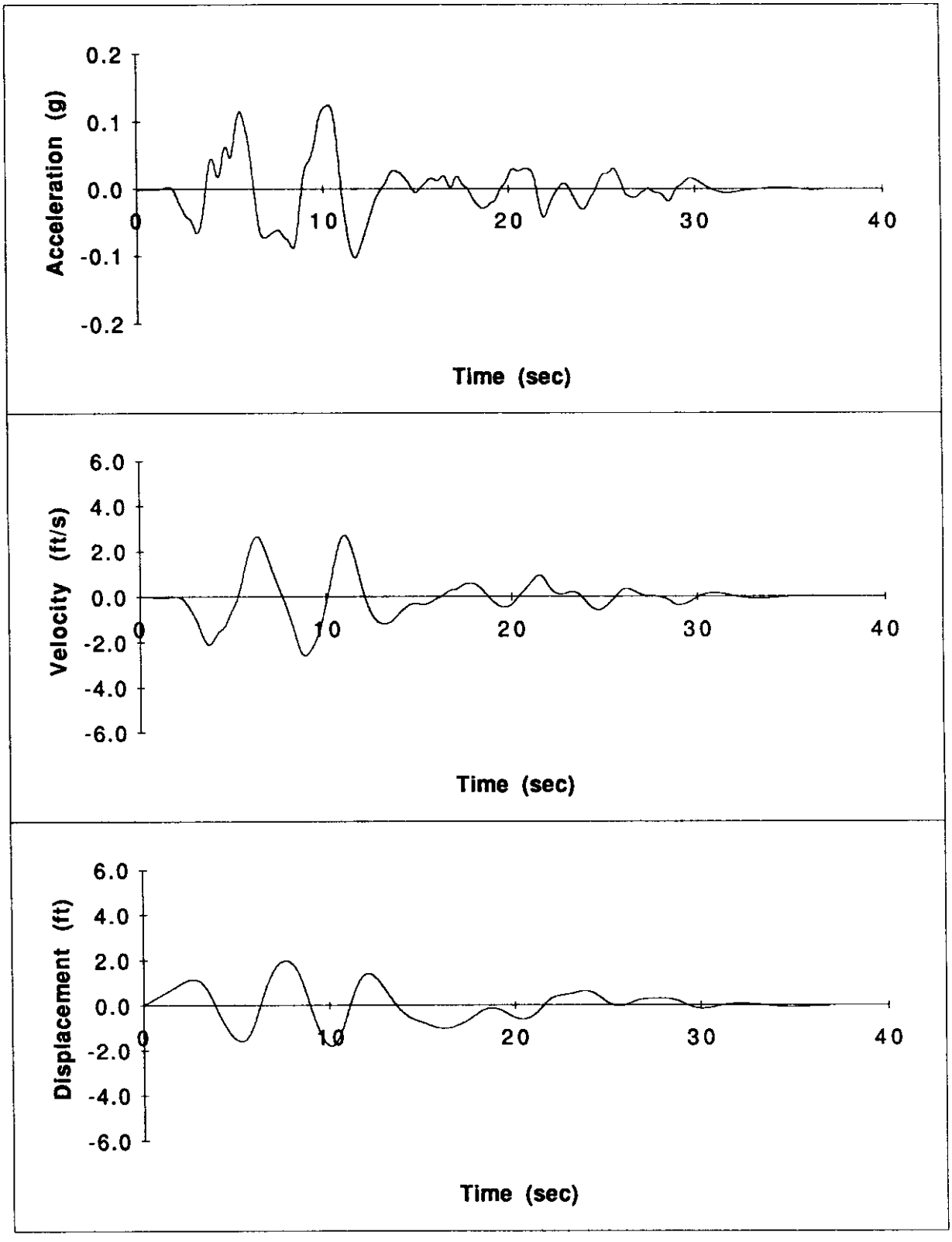

Figure B-2. Zone 2 — El Centro

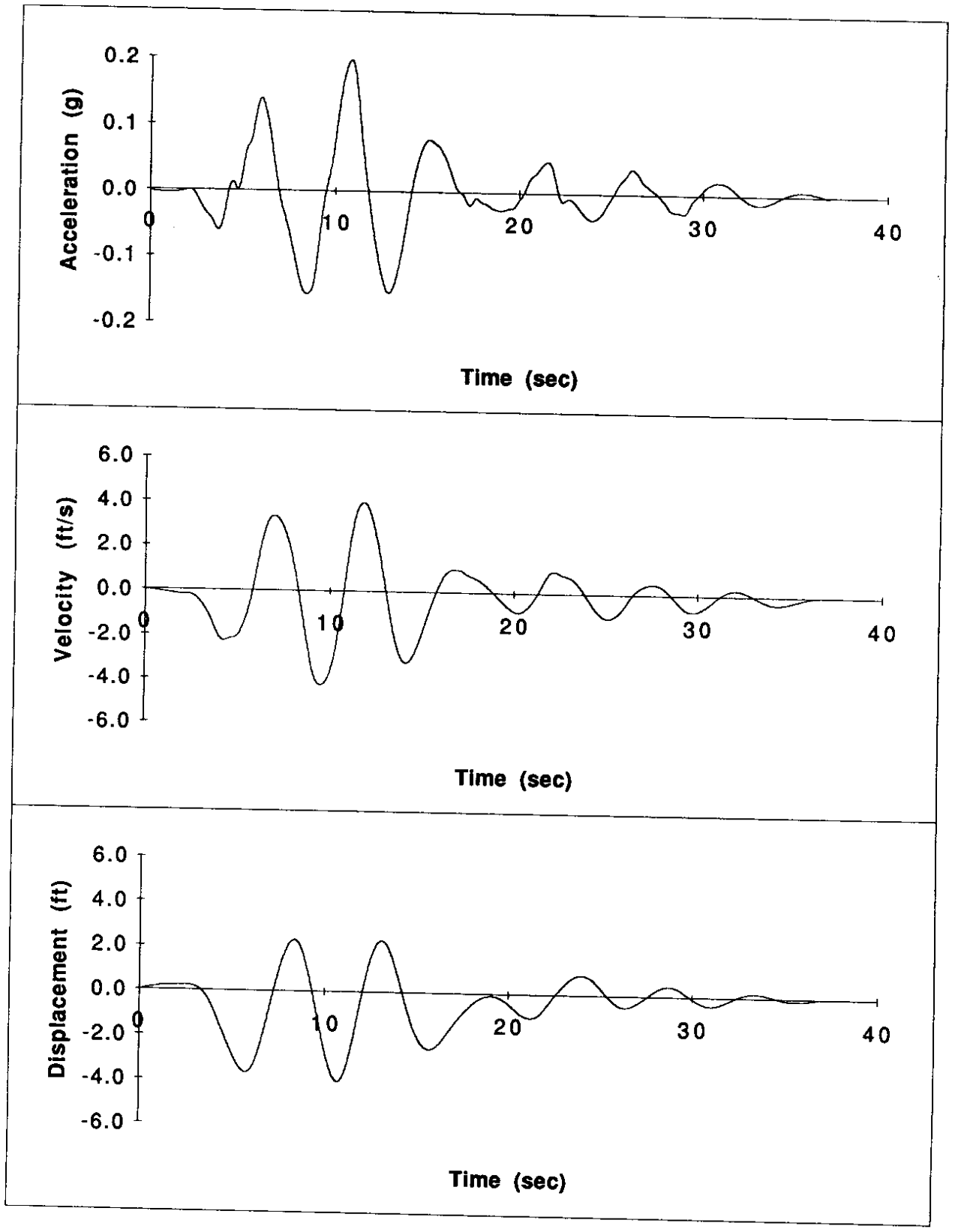

Figure B-3. Zone 3 — El Centro

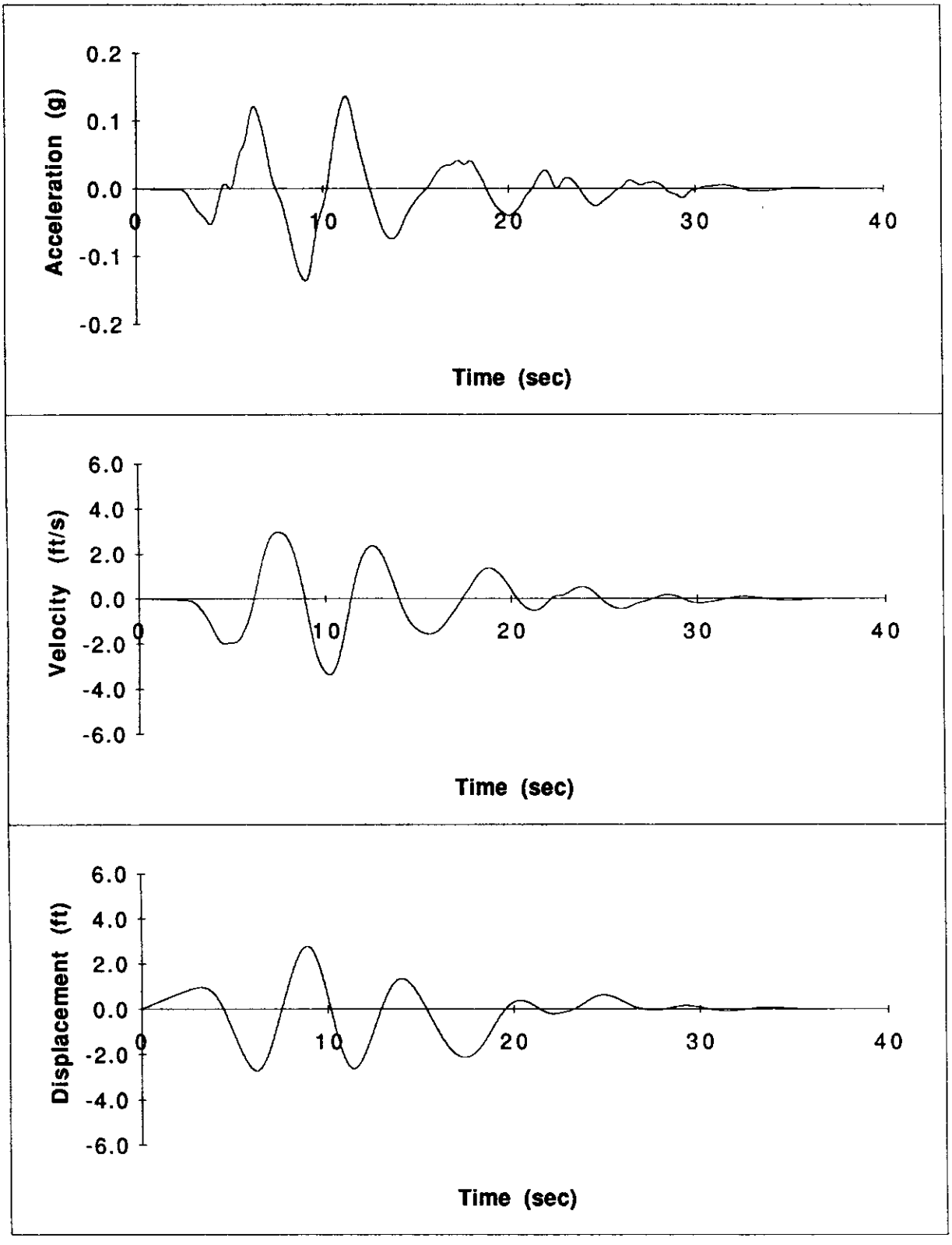

Figure B-4. Zone 4 — El Centro

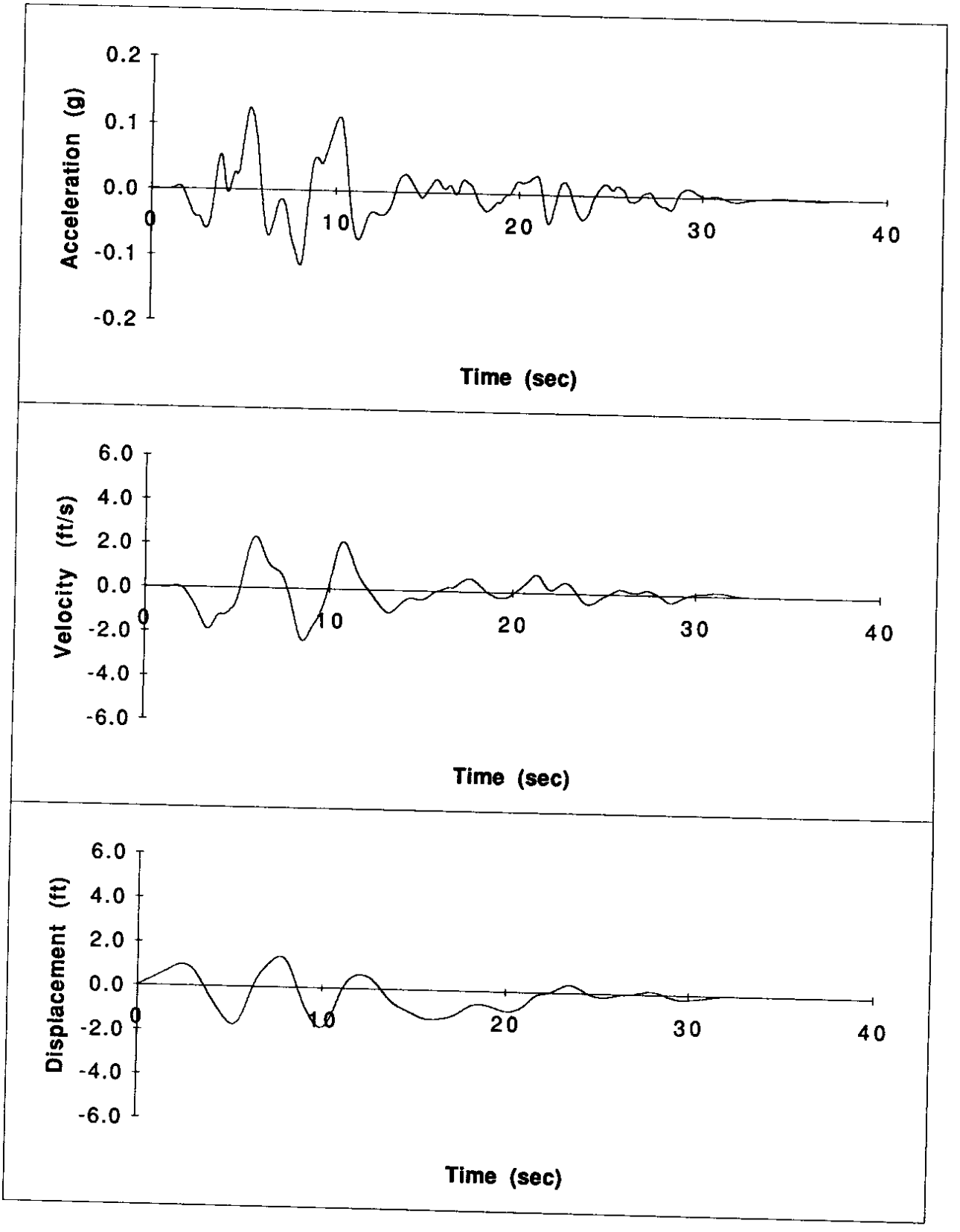

Figure B-5. Zone 5 — El Centro

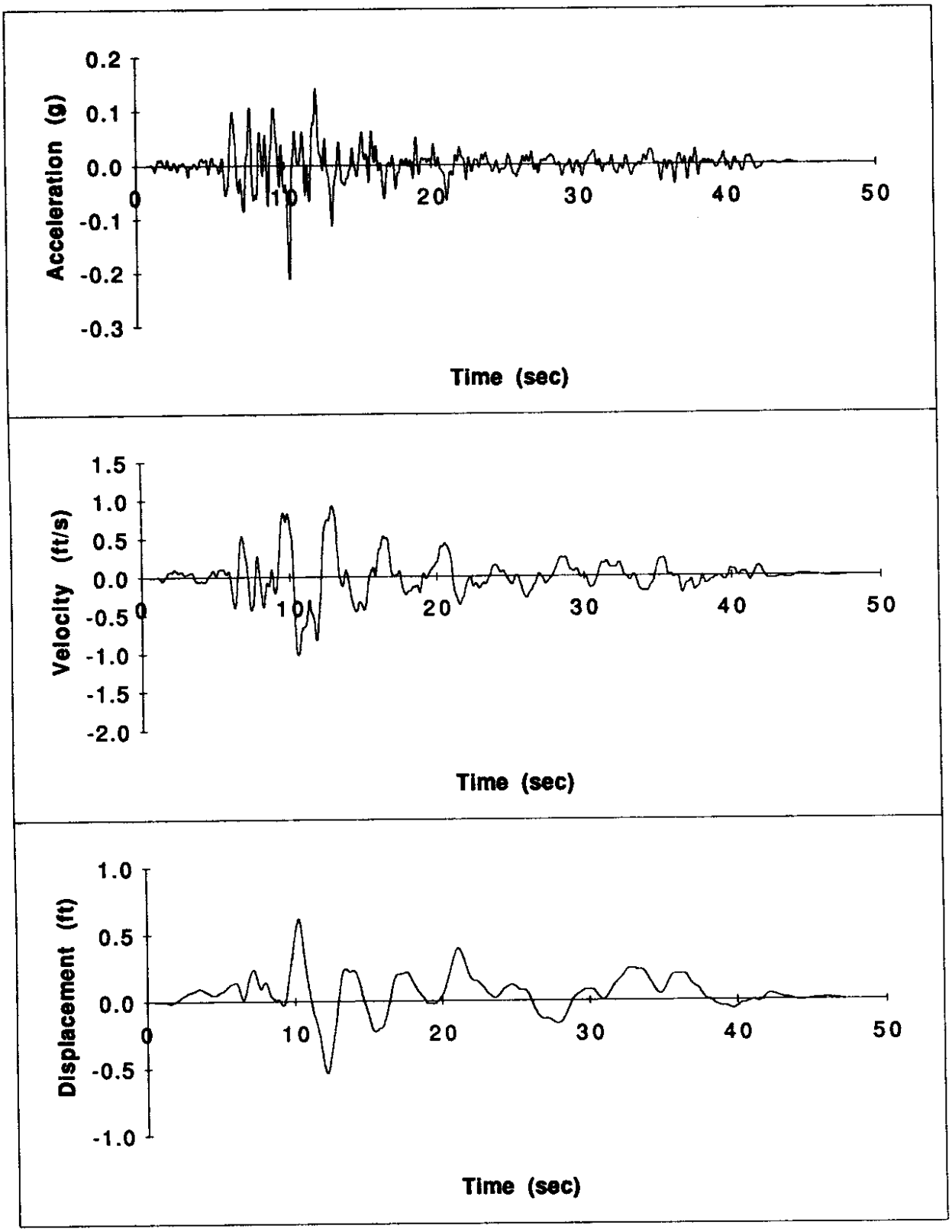

Figure B-6. Zone 1 — Lake Hughes

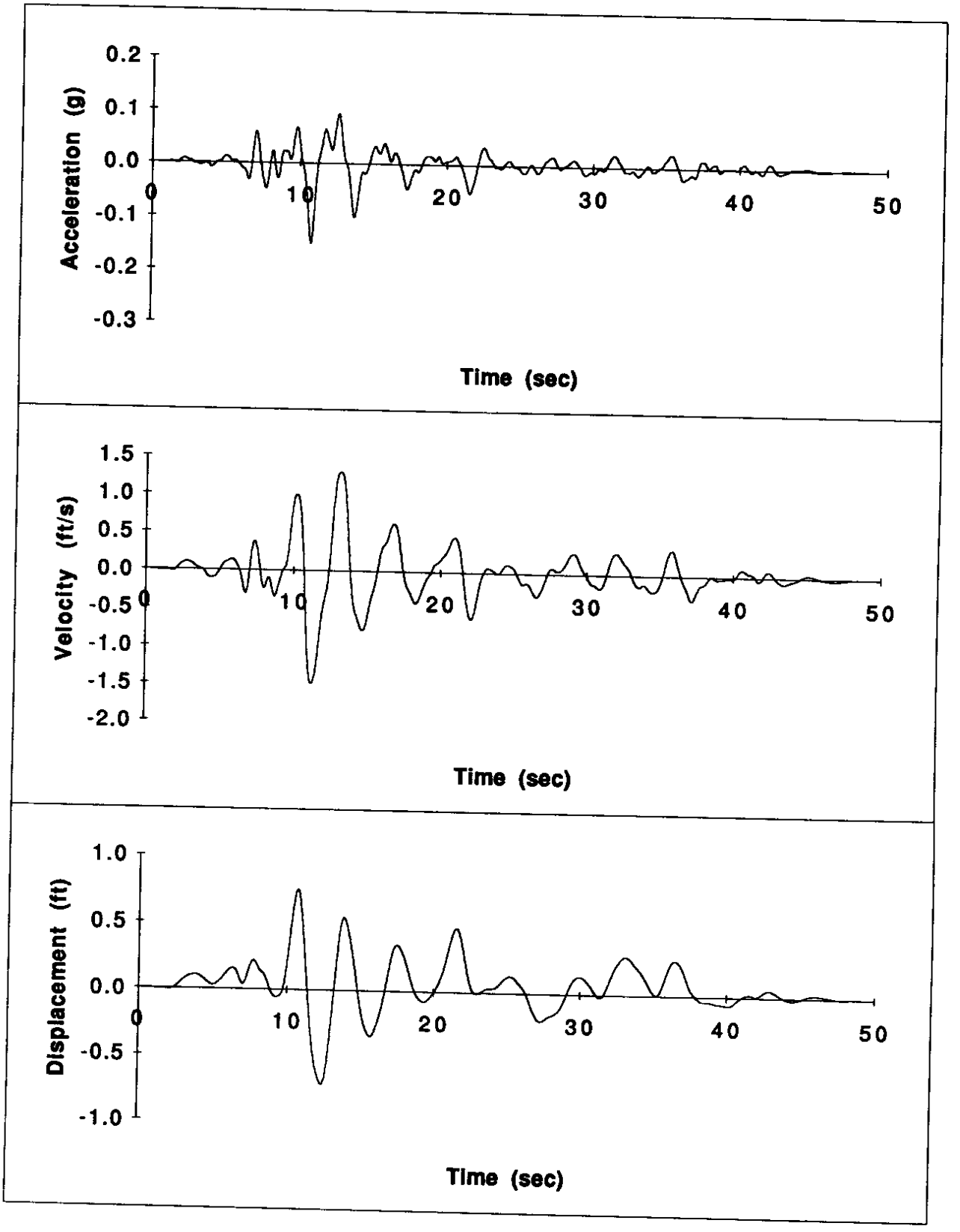

Figure B-7. Zone 2 — Lake Hughes

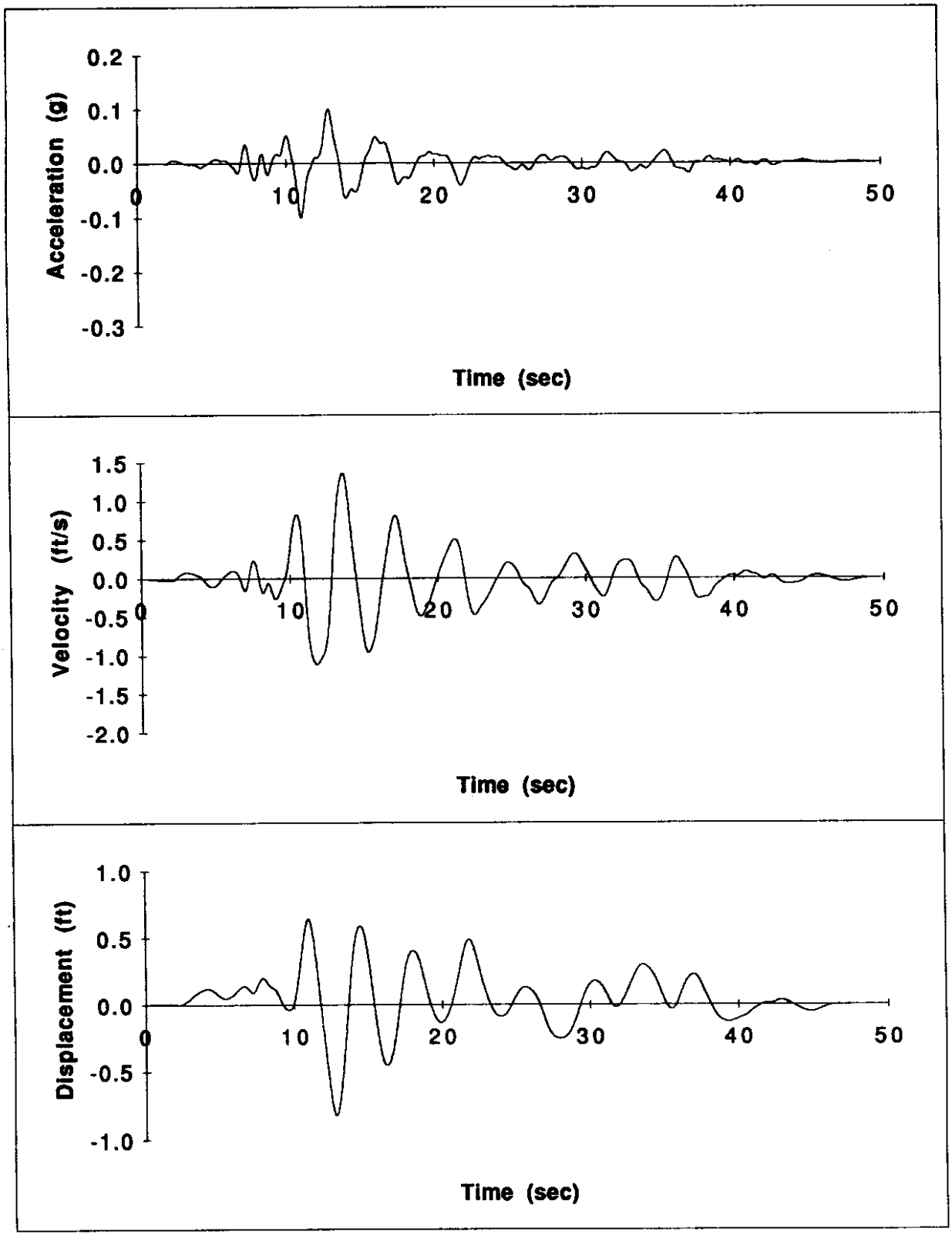

Figure B-8. Zone 3 — Lake Hughes

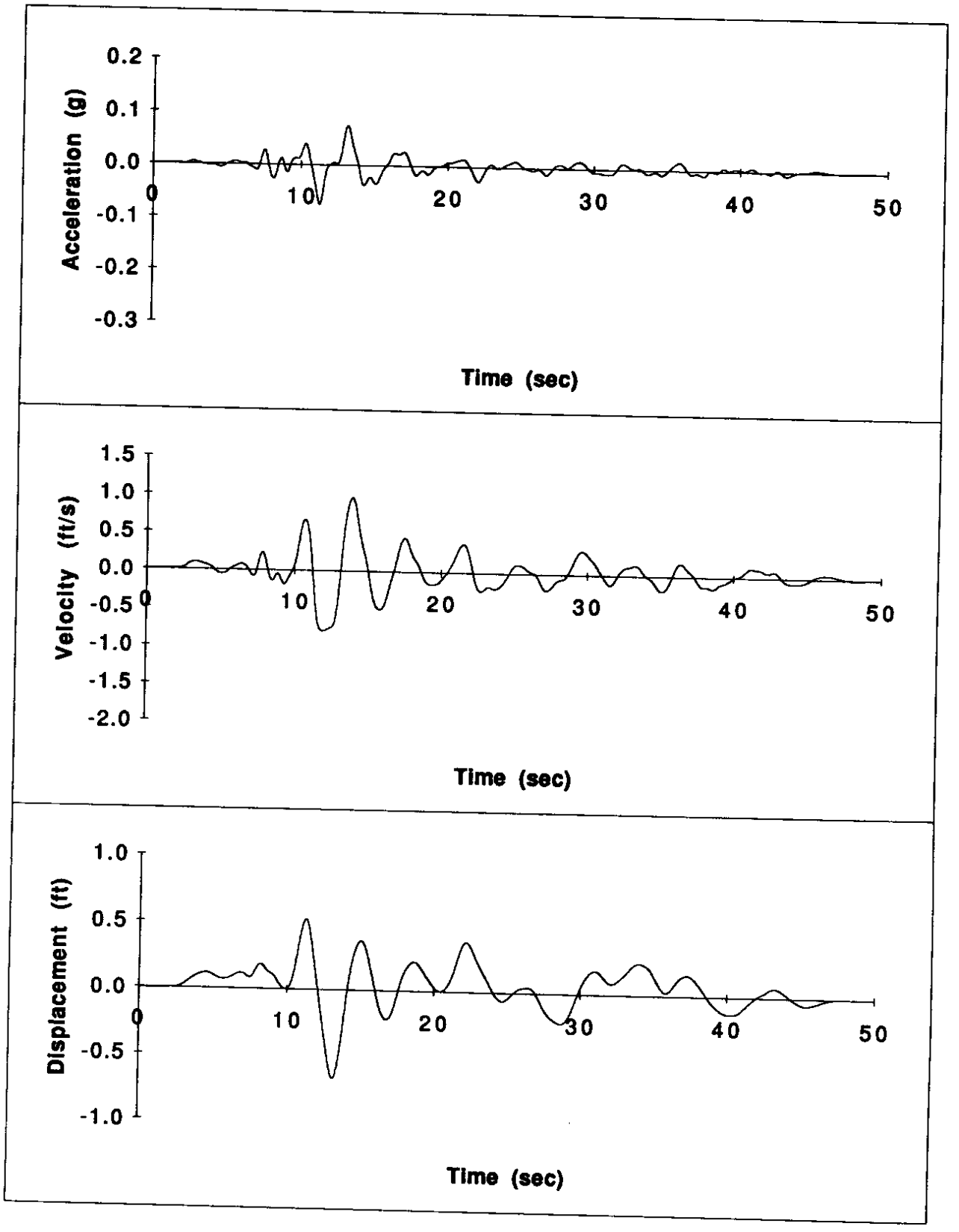

Figure B-9. Zone 4 — Lake Hughes

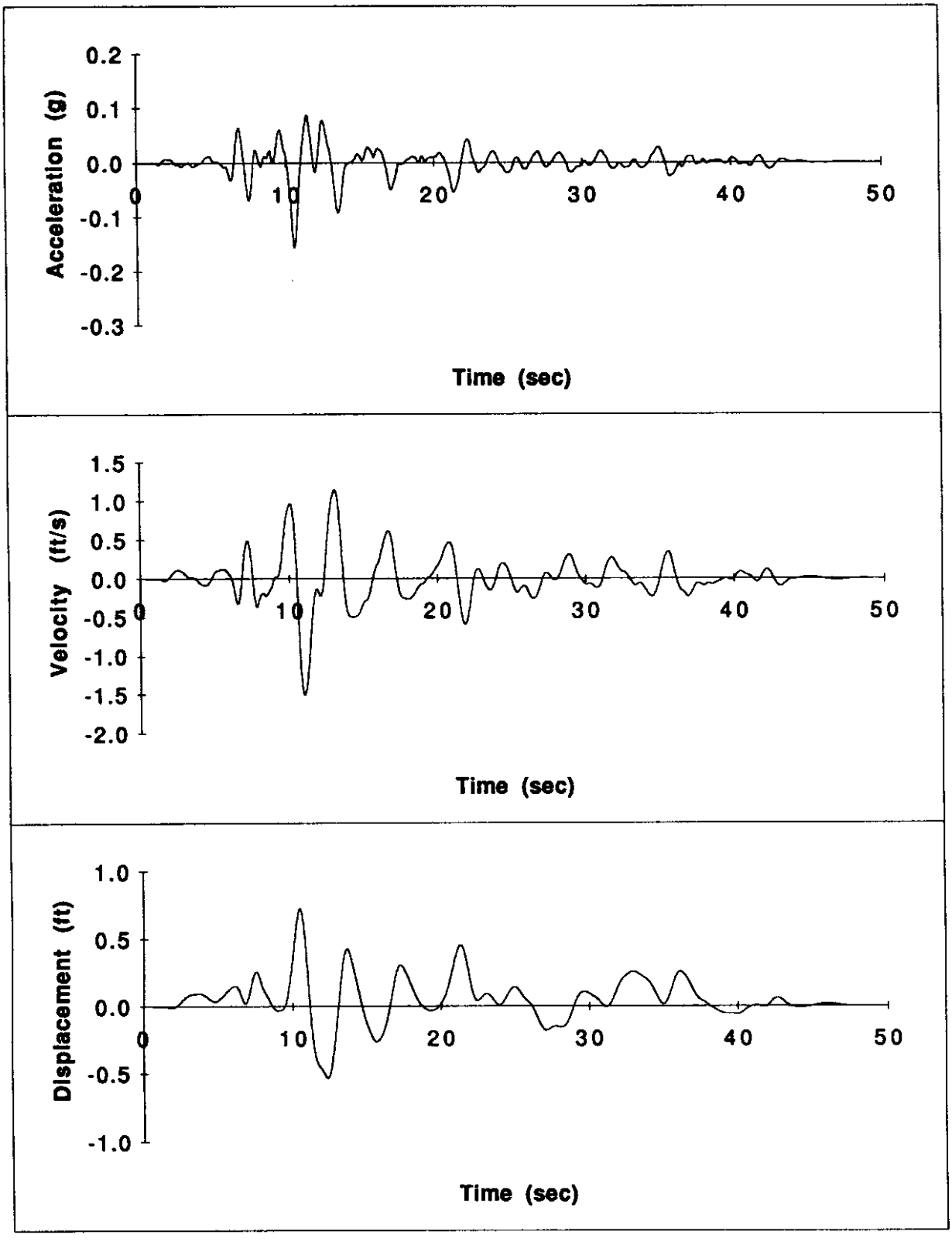

Figure B-10. Zone 5 — Lake Hughes

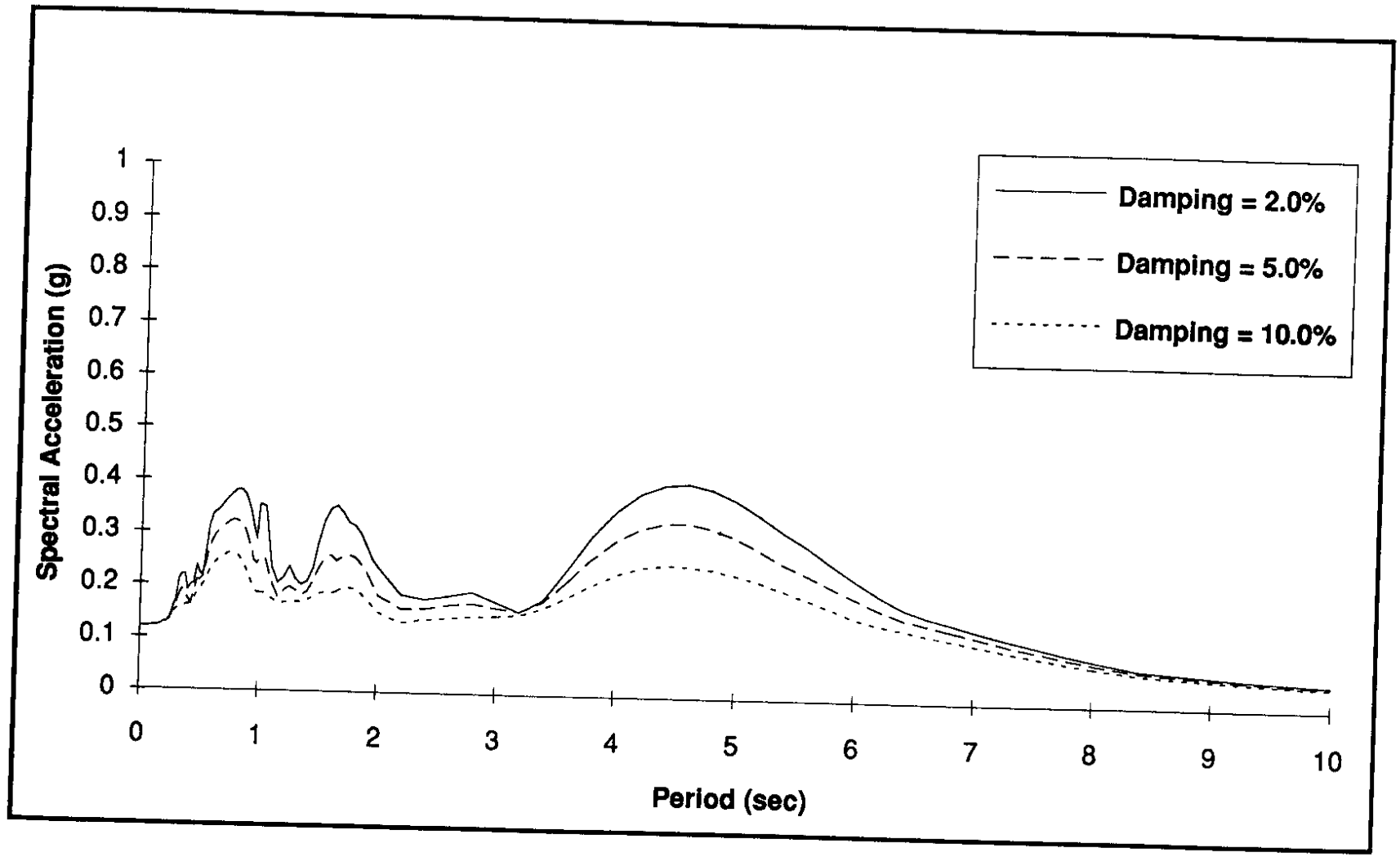

Figure B-11. Zone 1 — El Centro

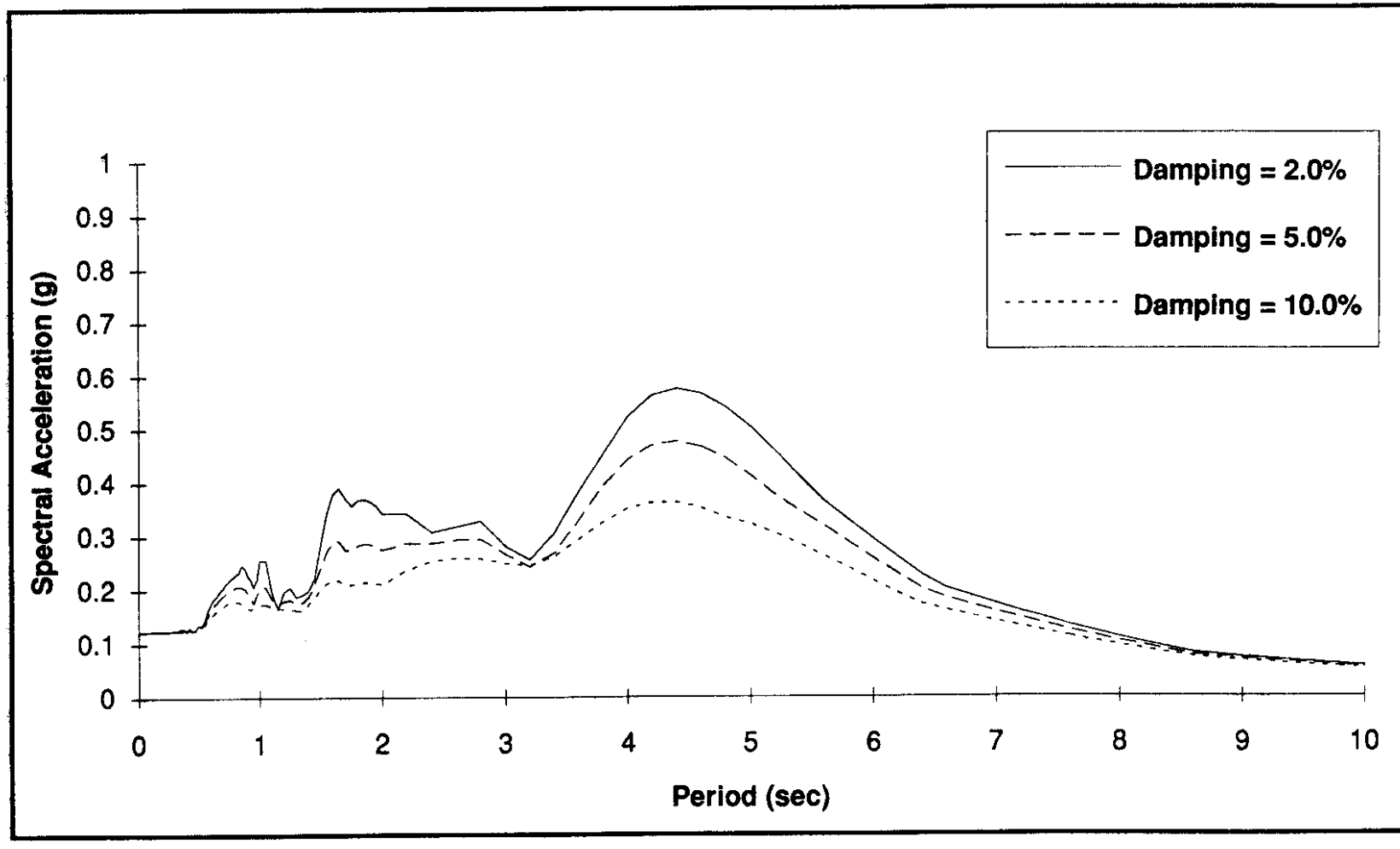

Figure B-12. Zone 2 — El Centro

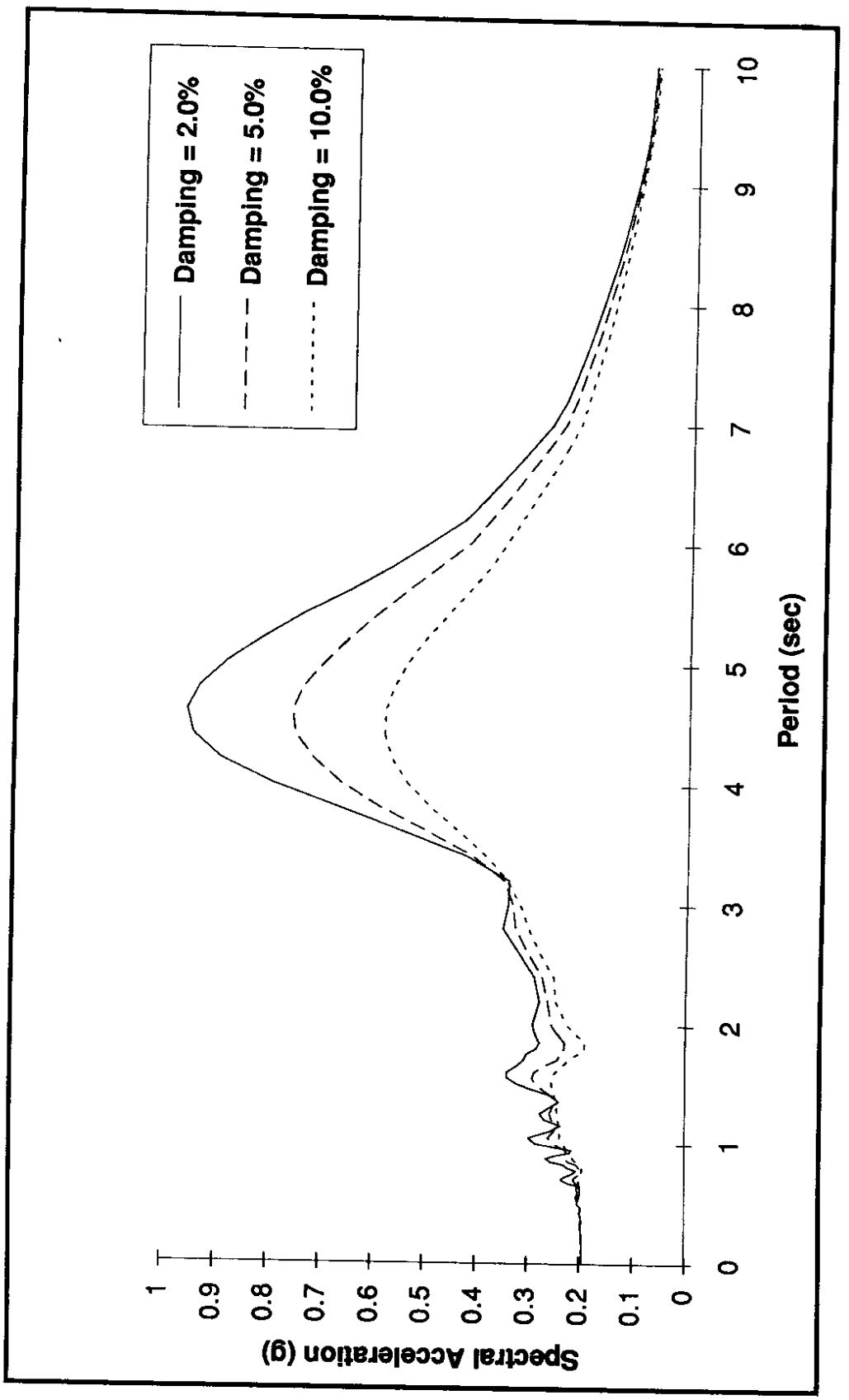

Figure B-13. Zone 3 — El Centro

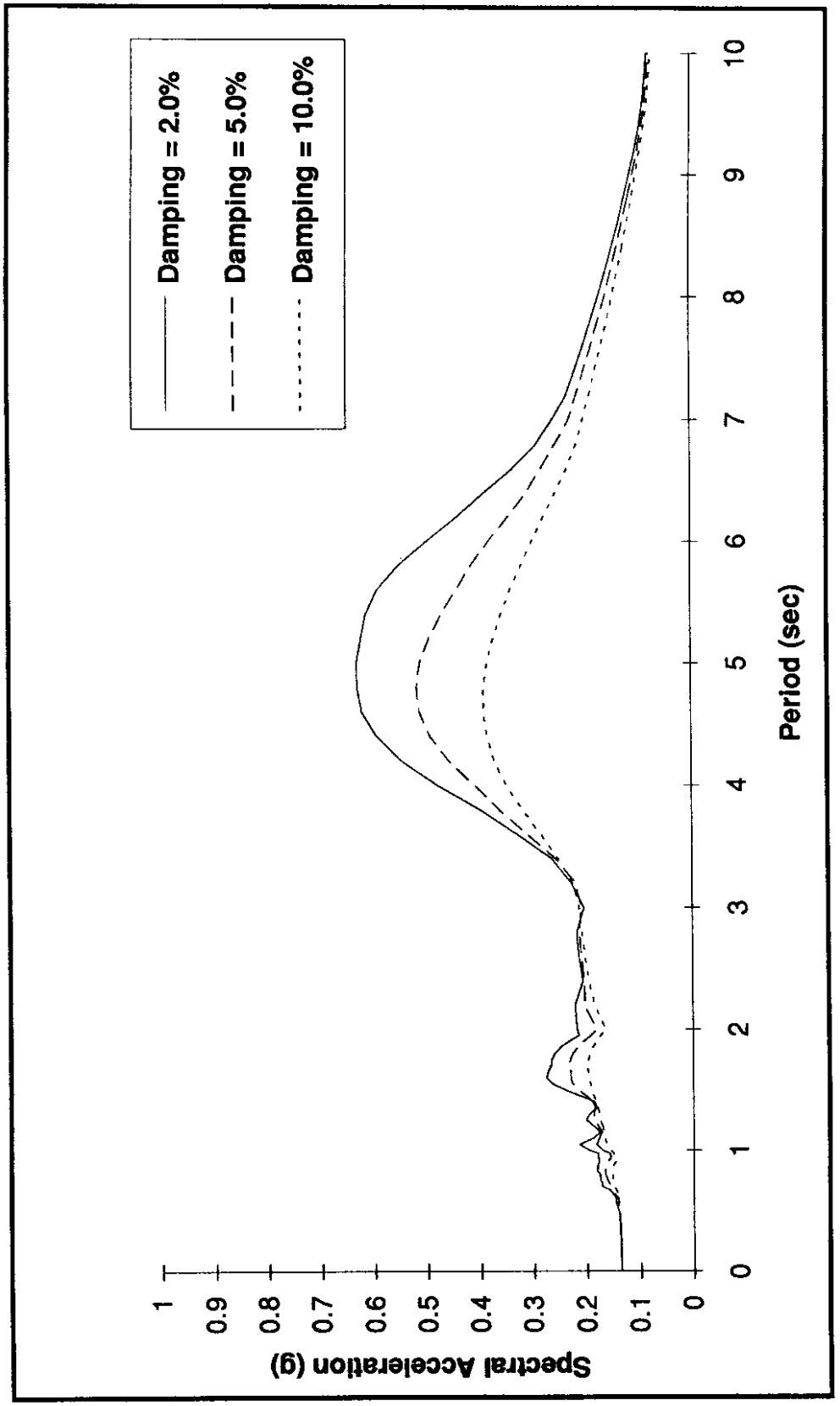

Figure B-14. Zone 4 — El Centro

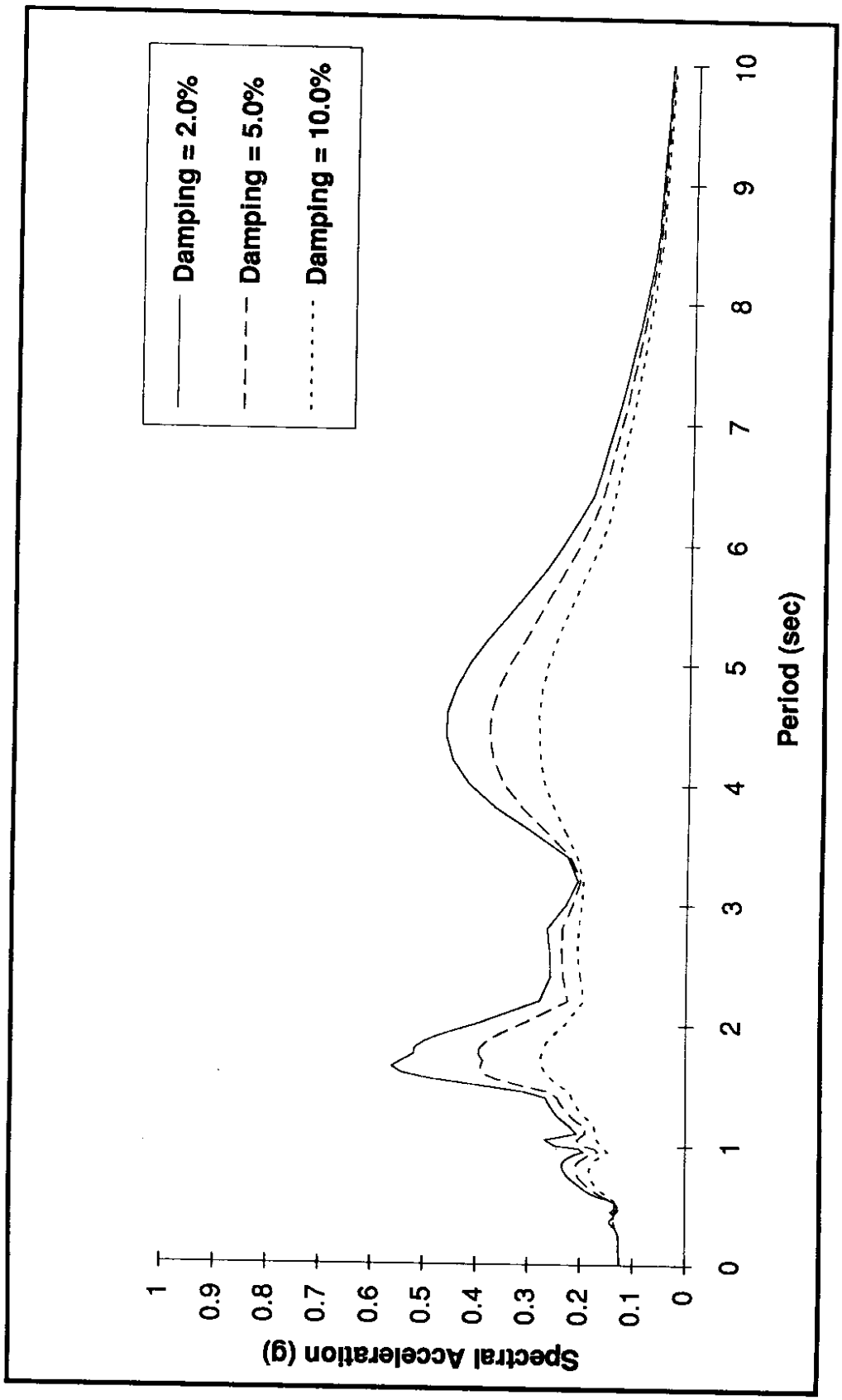

Figure B-15. Zone 5 — El Centro

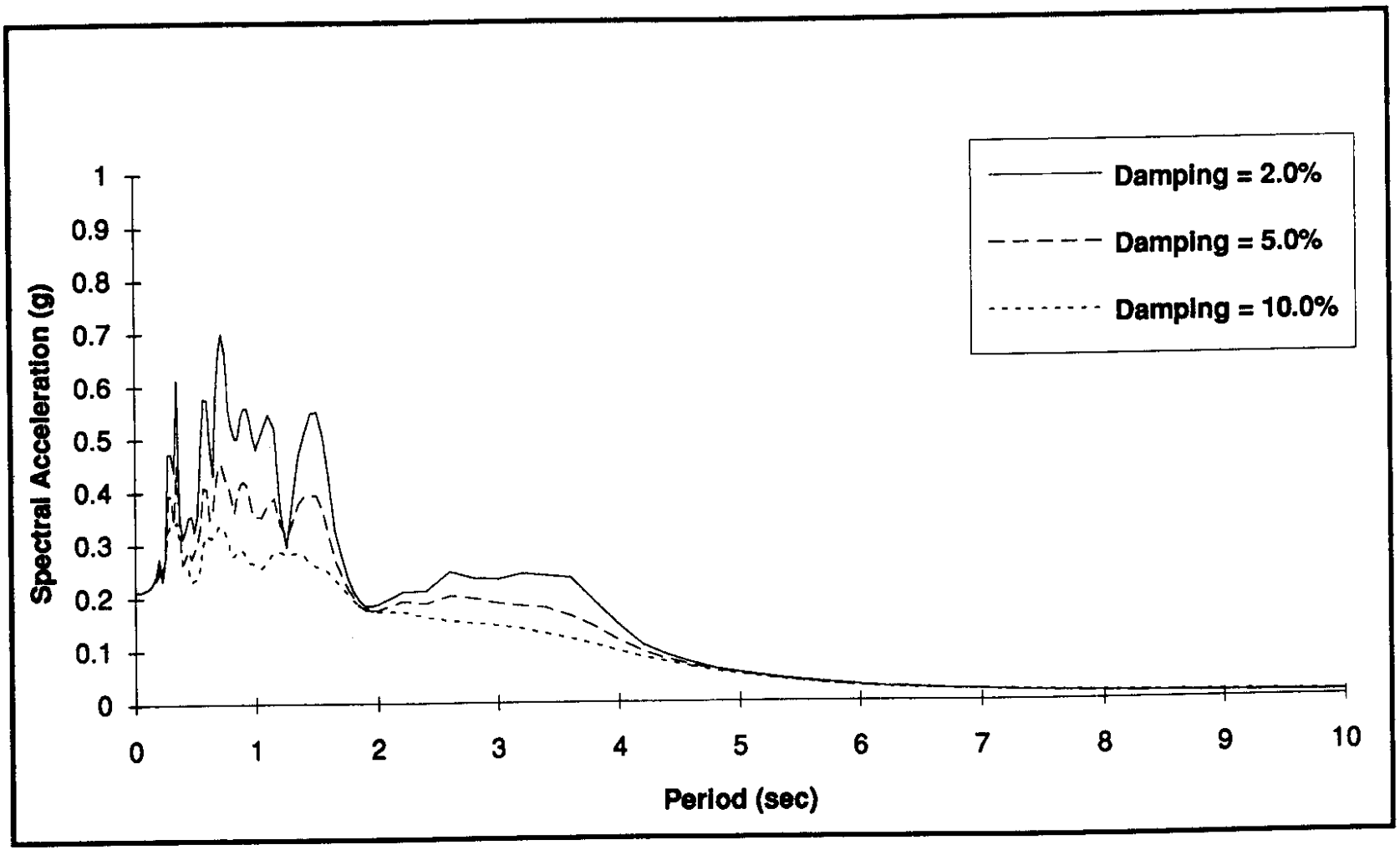

Figure B-16. Zone 1 — Lake Hughes

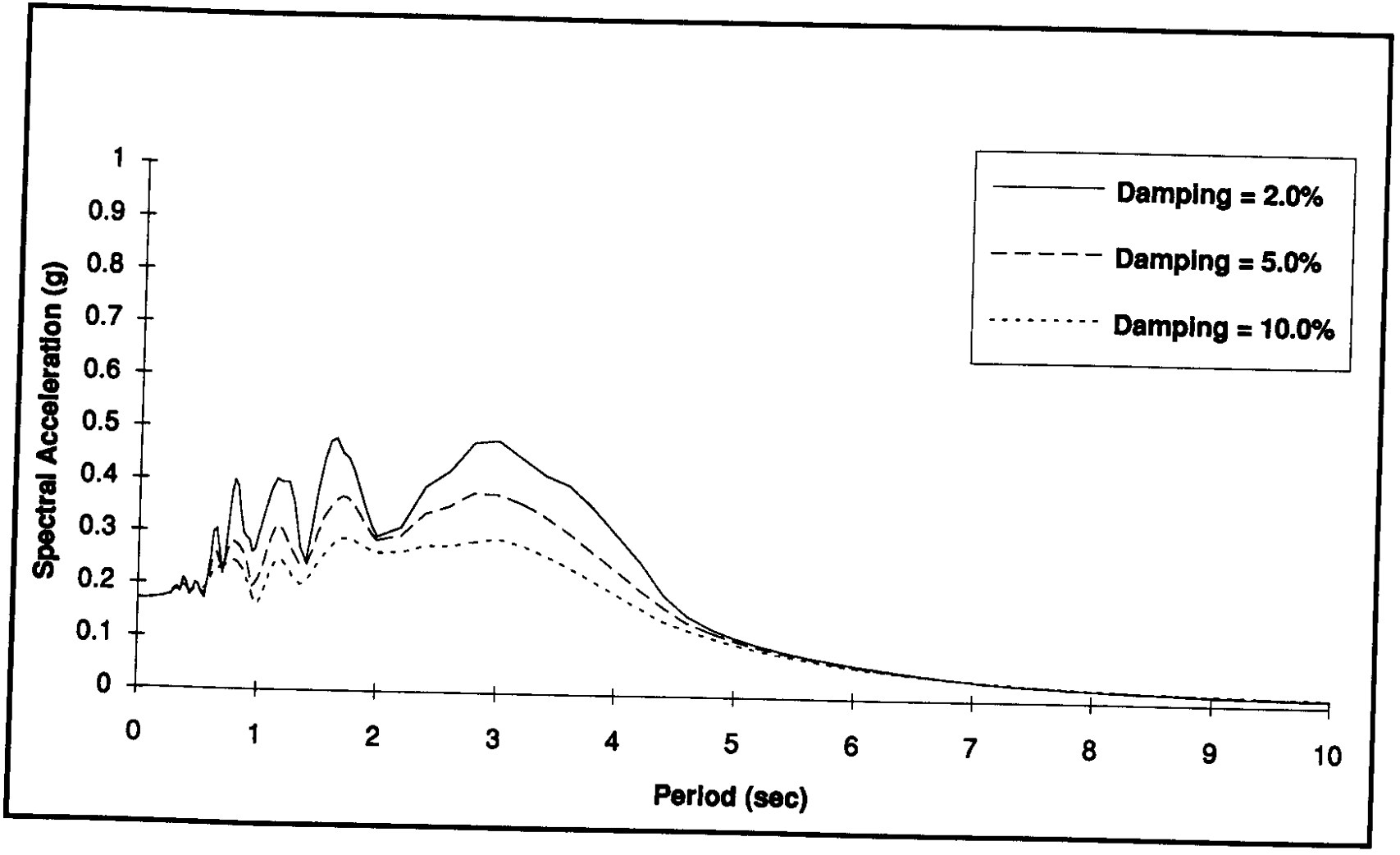

Figure B-17. Zone 2 — Lake Hughes

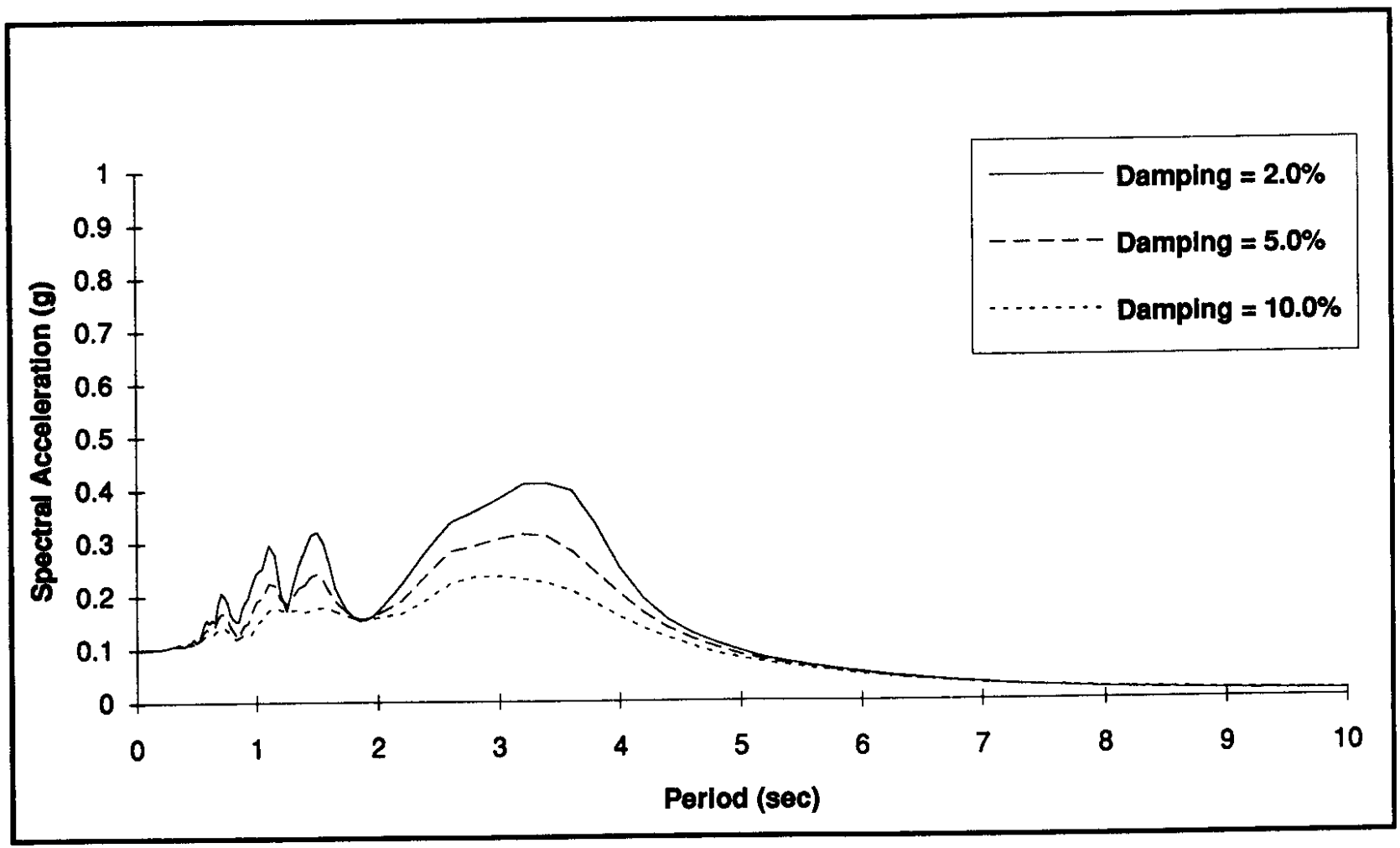

Figure B-18. Zone 3 — Lake Hughes

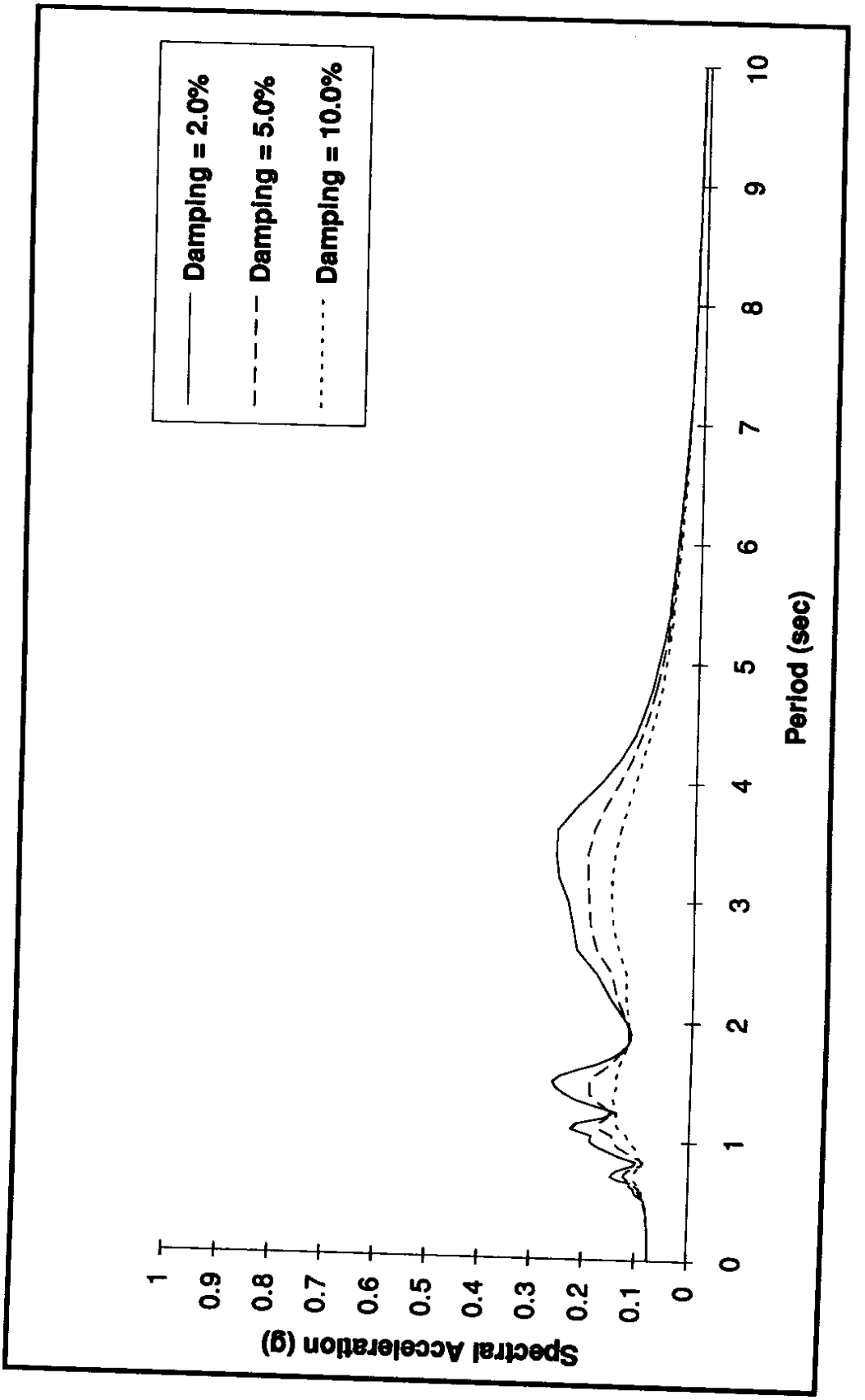

Figure B-19. Zone 4 — Lake Hughes

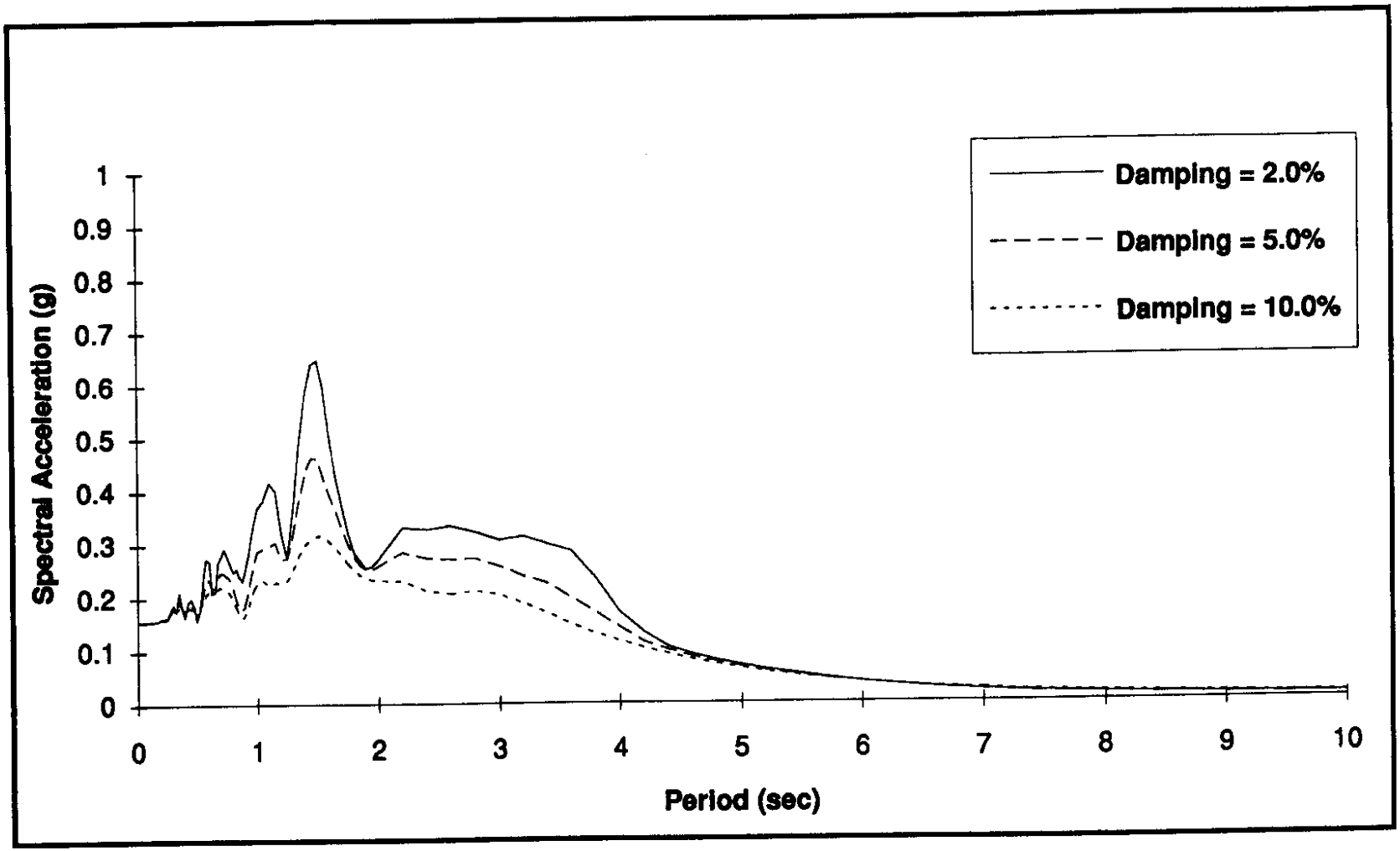

Figure B-20. Zone 5 — Lake Hughes